SYNTHESIS OF NITROGENOUS HETEROCYCLES VIA GROUP 3 METAL-CATALYZED HYDROAMINATION AND ZINC (II) MEDIATED METALLOAMINATION

by

Adrian Robert Smith

A dissertation submitted in partial fulfillment
of the requirements for the degree

of

Doctor of Philosophy

in

Chemistry

MONTANA STATE UNIVERSITY
Bozeman, Montana

April 2015

©COPYRIGHT

by

Adrian Robert Smith

2015

All Rights Reserved

To my wife, Lauren.

ACKNOWLEDGEMENTS

The completion of this thesis could not have been possible without the support and guidance of many people in my life.

Professor Tom Livinghouse has been a fantastic research advisor, giving his time, expertise, and even personal money towards furthering my research studies. Professors Paul Grieco, Mary Cloninger, Trevor Rainey, and Valerie Copie have been invaluable in helping me to grow intellectually through their teaching and guidance.

Fellow group members and coauthors Dr. Bryce Sunsdahl and Dr. Helena Lovick have been wonderful to work with in producing results for shared papers. I also need to thank all group members, especially Bryon Anderson, for esoteric discussions and arguments of advanced organic chemistry.

Most importantly, I need to thank my family and friends who have been supportive and understanding of the time and effort required for my studies. Their unwavering support has been a source of strength throughout my graduate career. I especially need to thank my wife Lauren, for her encouragement and endless love. This thesis is dedicated to her.

TABLE OF CONTENTS

1. INTRODUCTION 1

Hydroamination 1
Metalloamination 9
Organozinc Chemistry 13

2. RESULTS AND DISCUSSION 16

Chapter 1: Donor Ligand Effects in Group 3 Metal-catalyzed Hydroaminations 16
Chapter 2: Rapid and Efficient Procedure for the Synthesis of Group 3 Metal-Tris[bis(dimethylsilyl)amide] THF Complexes 26
Chapter 3: Intramolecular Hydroaminations of Secondary Aminoalkenes Catalyzed by New Group 3 Metal Trisamides 31
Chapter 4: Intramolecular Metalloaminations of *N*,*N*-Dimethylhydrazinoalkenes 39
Chapter 5: Bidentate Anionic Ligands in the Zinc Metalloamination Reaction 49

3. CONCLUSION 58

4. EXPERIMENTAL INFORMATION 59

Chapter 1 60
Chapter 2 62
Chapter 3 65
Chapter 4 72
General Procedure for CuCN Mediated Allylation of Metalloamination Intermediates 74
Synthesis of Cycles: General Procedure for Fukuyama Coupling of Metalloamination Cycles 77
Chapter 5 81

REFERENCES CITED 89

APPENDIX A: ^{1}H NMR / ^{13}C NMR Data 94

LIST OF TABLES

Table Page

1. Hydroamination of Aminoalkenes with Silylamide Precursors.....5

2. Additive Effects of Ethereal Ligands.....18

3. Effect of a Series of Donor Ligands on Y(III)-catalyzed Hydroaminations.....20

4. Additive-free Hydroamination Reactions.....22

5. Influence of Donor Ligands on Group 3 Metal Precatalysts.....23

6. Diastereoselectivity Effects of Ethereal Ligands and Alternative Solvents on the Hydroamination of **1b**.....24

7. Trials of Forming Group 3 Metal Complex **5b**.....28

8. Synthesis of Group 3 Metal Complexes **5a-5e**.....29

9. Hydroamination of Substrate **9a**.....35

10. Hydroamination of Substrate **9b**.....36

11. Hydroamination of Substrate **9c**.....37

12. Hydroamination of Substrate **9d**.....38

13. Metalloamination/allylation of Hydrazinoalkenes to Pyrrolidines.....43

14. Metalloamination/allylation of Hydrazinoalkenes.....44

15. Optimization of the Fukuyama Reaction from **13a**.....47

16. Metalloamination/acylation of Hydrazinoalkenes.....48

17. Screening of Miscellaneous Anionic Bidentate Ligands.....51

18. Results of 1,1,1-trifluoro-4-(amino)pent-3-en-2-one Ligands in Metalloamination.....53

19. Evaluation of 1,3-dicarbonyl Ligands **19a-19h**.....55

LIST OF TABLES – CONTINUED

Table Page

20. Metalloamination/allylation Utilizing Ligated Organozincs 57

LIST OF SCHEMES

Scheme Page

1. Group 3 Metal Hydroamination Mechanism 3

2. Group 3 Metal Precatalysts With Diastereoselectivity and Enantioselectivity.....6

3. Ligand Coordination via the "Silylamide Route" and "Extended Silylamide Route".....7

4. Ligation of a Chiral Binaphthyl Ligand from Trisamide **7f** 9

5. Mechanism of Metalloamination / Electrophile Trapping.....10

6. Heteroannulation of Titanium Imido Complex.....11

7. Application of Metalloamination Towards (±)-Ferruginine 12

8. Previous Examples of Zinc Metalloamination.....13

9. Products Made by sp^3 C-Zn Precursors 14

10. The Negishi Reaction in the Industrial-scale Synthesis of PDE472.....15

11. Fukuyama Coupling Towards (+)-Biotin 15

12. Simplified Mechanism of Yttrium-Catalyzed Intramolecular Hydroamination of **1b** 25

13. Previous Synthesis of Group 3 Metal Complex **5b** 26

14. Substitution of tritox-H from Group 3 Metal Trisamides.....30

15. Synthesis of New Group 3 Metal Trisamides **7b**, **7f** 32

16. Synthesis of Secondary Aminoalkenes **9a-9d** 33

17. Hydroamination Utilizing Diethylzinc and Activator.....39

18. Early Metalloamination Trials 40

19. Copper (I) Allylation of Intermediate **13a**.....41

LIST OF SCHEMES – CONTINUED

Scheme Page

20. *N*,*N*-Dimethylhydrazineamine Substrate Synthesis 42

21. Reversibility of Organozinc Intermediate **14d** 45

22. General Zinc Ligand Screening Scheme.....49

23. Synthesis of Aryl 1,1,1-Trifluoroacetylenamines.....52

24. Synthesis of *N*,*N*-disubstituted Acetoacetamide Ligands 54

LIST OF FIGURES

Figure Page

1. Hydrocodone.....1

2. Double Bond Isomerization Product.....21

3. Simple Group 3 Metal Precatalysts.....33

NOMENCLATURE

C_6D_6	Benzene-d_6
DCM	Dichloromethane
DMA	Dimethylacetamide
DME	1,2-Dimethoxyethane
HMPA	Hexamethylphosphoramide
MTBE	Methyl *t*-butyl ether
r.t.	Room Temperature (22-25 °C)
THF	Tetrahydrofuran
TMEDA	Tetramethylethylenediamine
tritox-H	tri-*t*-butyl-carbinol

ABSTRACT

Pyrrolidines and piperidines respresent a motif found in a wide array of bioactive compounds. Hydroamination, or the insertion of a carbon-nitrogen bond into a site of unsaturation, represents an atom economical method for accessing substituted pyrrolidines and piperidines. Synthesis of nitrogenous heterocycles through group 3 metal hydroamination and zinc(II) metalloamination has been achieved. The hydroamination of aminoalkenes has been thoroughly screened and has shown good tolerance for ethereal solvents, and solvent choice can result in improved rate and diastereoselectivity. The hydroamination of secondary amines with electron rich heteroatoms has also been realized utilizing a new group 3 metal trisamide developed in these labs.

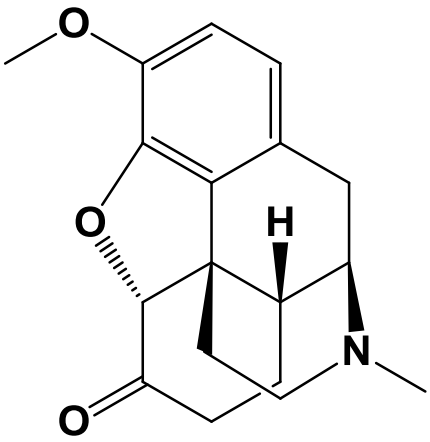
Additionally, zinc(II) metalloamination has been performed on *N*,*N*-dimethylhydrazinoalkenes and successfully resulted in the synchronous formation of a nitrogen-carbon bond to form a ring as well as carbon-zinc bond formation at the adjacent carbon. This carbon-zinc bond has been intercepted by different carbon electrophiles to synchronously form a nitrogen-carbon bond and carbon-carbon bond in situ. Ligand studies for these transformations suggest 1,1,1-trifluoroacetylenamines as well as acetoacetamides are promising motifs for future ligand scaffolds due to their ease of synthesis, low cost, and good reactivity with a range of *N*,*N*-dimethylhydrazinoalkene substrates.

INTRODUCTION

Hydroamination

Molecules containing the unsaturated nitrogenous heterocycles pyrrolidine (5 membered ring) and piperidine (6 membered ring) moieties include many biologically active compounds. The pyrrolidine and piperidine moiety can be found in a vast array of pharmaceuticals, and of the 70 most prescribed small molecule pharmaceuticals of 2012, ten contain at least one pyrrolidine or piperidine ring structure[55]. The piperidine ring system is frequently used in pharmaceutical synthesis as a linker or to improve the pharmacokinetic profile of a drug (such as by increased solubility under physiological conditions)[56]. Piperidine rings are also often used as a spacer, generally in the 1,4-substitution fashion. The most commonly prescribed opioid in the world, hydrocodone, possesses the piperidine moiety (**Figure 1**).

Figure 1: Hydrocodone



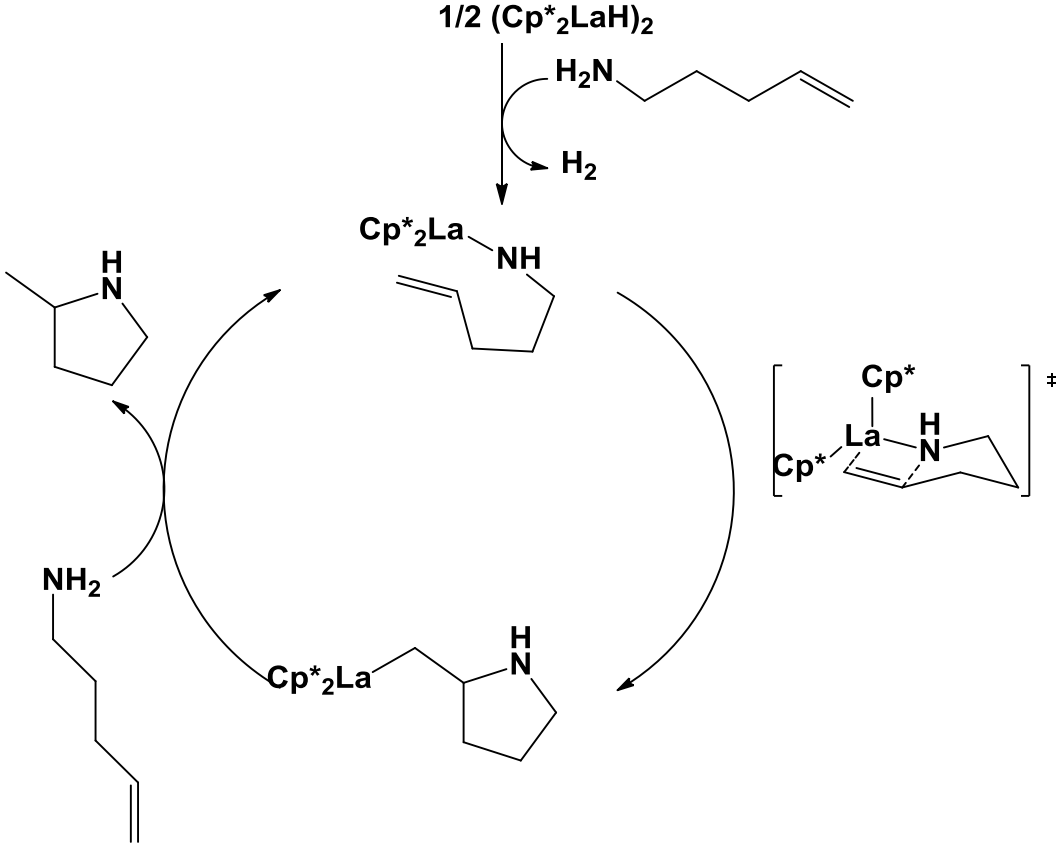
One of the best methods to synthesize these heterocycles is through the net addition of either a nitrogen-hydrogen bond into an alkene, alkyne, or allene (hereafter referred to as hydroamination), resulting in synchronous formation of a nitrogen-carbon and hydrogen-carbon bond. Hydroamination is rarely observed in the absence of a catalyst due in part to electrostatic repulsion of the nitrogen lone pair and the π bond of the electron rich alkene, alkyne, or allene[1]. A decrease in the electron richness of these carbon-carbon double or triple bonds can be achieved by the coordination of metal to the carbon-carbon π-bond, and many catalytic metal sources have been used to achieve hydroamination. Metals used for these processes span early transition metals in group 3-5, late transition metals in groups 8-10, as well as lanthanides and actinides[1].

The first metal-catalyzed intramolecular hydroaminations were reported by the Marks lab in 1989[2]. They utilized lanthanocenes derived from rare-earth metals such as lanthanum, lutetium, and samarium. The rates of these catalytic hydroaminations are inversely correlated to the ionic radius of the metal, with lanthanum being the fastest and largest. With regards to solvent, they found the reaction worked well in hydrocarbon solvent, while running the reaction in Lewis-basic THF resulted in a depressed hydroamination rate.

The proposed mechanism for the intramolecular hydroamination reaction from the Marks paper is outlined in **Scheme 1**[2]. Addition of the respective aminoalkene to the respective lanthanocene results in evolution of H_2 and formation of the metal-nitrogen bond. Through a chair-like transition state, the metal-nitrogen bond inserts into the carbon-carbon double bond, forming a new nitrogen-carbon bond in the form of a

heterocycle as well as a metal carbon bond. The complex undergoes protonolysis from an additional molecule of aminoalkene substrate, releasing the cyclized pyrrolidine and continuing the catalytic cycle. The requirement of the reaction to assume a chair-like transition state explains the increased reactivity of 2,2-disubstituted substrates through Thorpe-Ingold conformational activation[1].

Scheme 1: Group 3 Metal Hydroamination Mechanism[2]

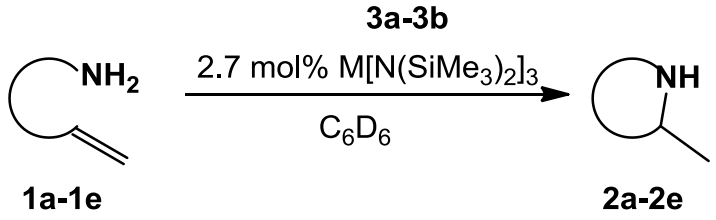


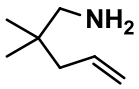
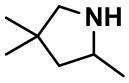
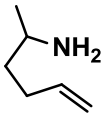
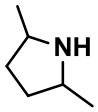
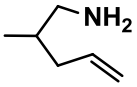
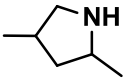
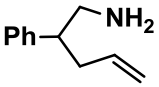
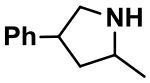
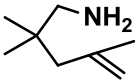
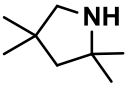
The hexamethyldisilylamide $[N(SiMe_3)_2]^-$ ligand has seen wide use in group 3 metal chemistry, including as a starting material for forming precatalysts for hydroamination. This very bulky ligand can be used to prepare low-coordinate

trisubstituted complexes of group 3 metals of type $Ln[N(SiMe_3)_2]_3$ in high yield from the respective anhydrous group 3 metal trichloride[3]. These silylamide ligands can be dissociated off by protic reagents and has been used to synthesize many new complexes in what's referred to as the "silylamide route". Purification of complexes following addition of protic reagents requires simple removal of the free bis(trimethylsilyl)amine under vacuum.

Research of hydroamination utilizing these easily accessible group 3 metal trisamides as precatalysts was initiated by the Livinghouse lab (**Table 1**)[4]. The research shows that for aminoalkenes **1a – 1e**, pyrrolidine products (**2a-2e**) can be isolated in high to quantitative yields. Hydroamination activity is rapid for 2,2-dimethyl substrate **1a**, going to >95% completion in less than 4 hours with the neodymium precatalyst. Notably, a single methyl at this 2-position (**1c**) was far more sluggish by comparison, requiring 7 days at 90 °C for the same neodymium precatalyst, and the products showing modest *cis/trans* selectivity. Methyl substitution at the α position gave preferentially *cis* products, and best selectivity was observed for the yttrium precatalyst. The reaction was also shown to work with disubstituted terminal alkenes (**1e**), requiring only slightly increased catalyst loading to proceed to completion.

Table 1: Hydroamination of Aminoalkenes with Silylamide Precursors

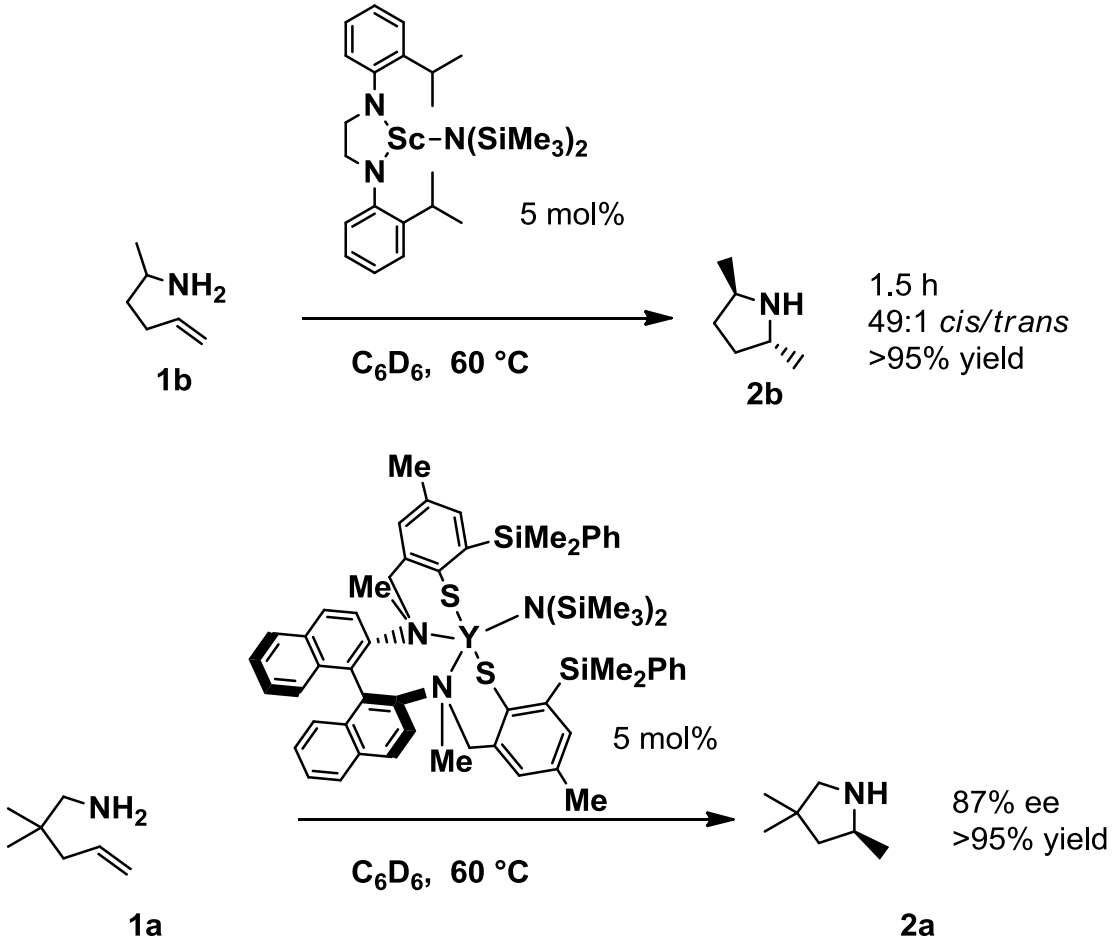


Aminoalkene	Metal	Conditions	Pyrrolidine	*cis:trans*	% Yield[b]
1a 	**3b** Y **3a** Nd	24 °C, 6 h 24 °C, 4 h	**2a** 	-----	>95
1b 	**3b** Y **3a** Nd	90 °C, 6 d 90 °C, 2 d	**2b** 	7:1 4:1	94
1c 	**3b** Y **3a** Nd	90 °C, 10 d 90 °C, 7 d	**2c** 	2:1 2:1	>95
1d 	**3b** Y **3a** Nd	90 °C, 1.5 h 90 °C, 1.5 h	**2d** 	1.7:1 2.2:1	95
1e 	**3b** Y	70 °C, 8 h	**2e** 	----	94[a]

[a] In this instance, 3 mol% of catalyst was used. [b]Isolated yield.

The Livinghouse group has extended these findings by investigation of precatalysts formed through this silylamide route, which were shown to be diastereoselective and enantioselective (**Scheme 2**)[5]. In the first example, the silylamide precatalyst converts **1b** into **2b** in a 49:1 *trans*/*cis* ratio[6a], a dramatic improvement in selectivity over the tris(silyl)amide used previously. In the second example, a chiral silylamide precatalyst is used on the prochiral substrate **1a** to give the indicated product in 87% enantiomeric excess (93.5 : 6.5 of the indicated product to its enantiomer)[6b].

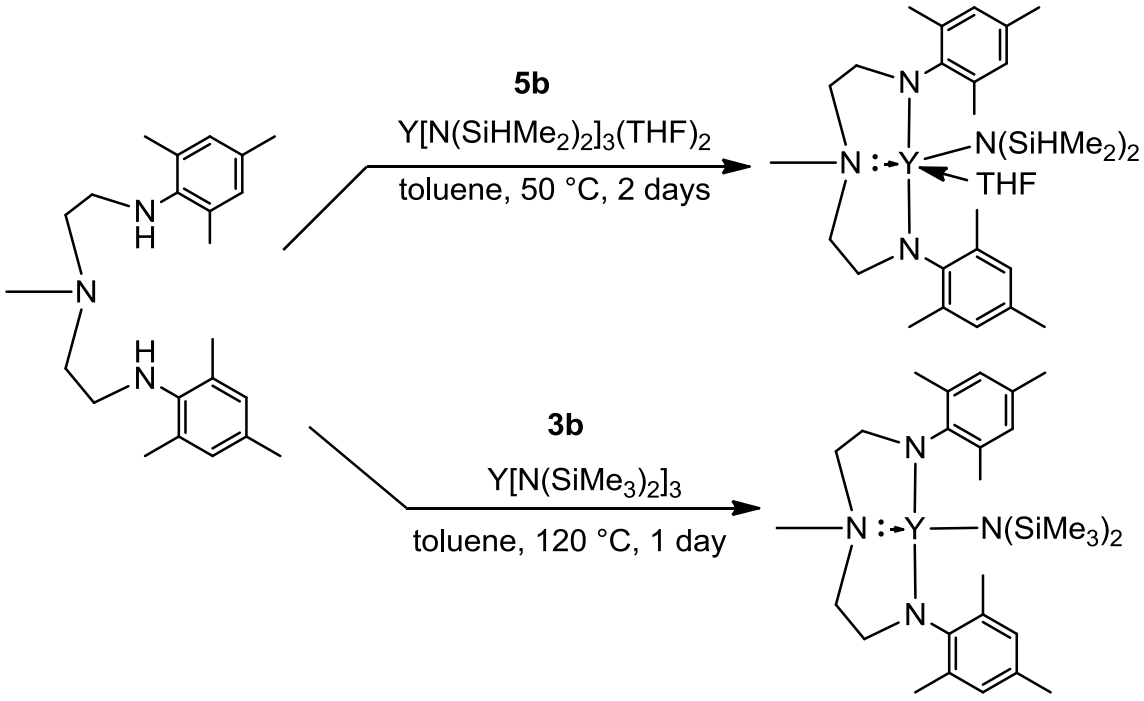
Scheme 2: Group 3 Metal Precatalysts With Diastereoselectivity and Enantioselectivity[6]



The steric bulk of the bis(trimethylsilyl)amide ligand is a limiting factor for its utility, and literature cites multiple examples of incomplete exchange and rearrangement with other similarly bulky ligands[7]. Previously published literature suggests the much smaller bis(dimethylsilyl)amide ligand coordinates bulky ligands more effectively and also other ligands at lower temperatures than the bis(trimethylsilyl)amide. Additionally, the presence of the Si-H bond of the amide presents a good spectroscopic probe via ^{1}H NMR.

Formation of complexes through this "extended silylamide route" have been employed in group 3 metal precatalysts. An example is presented below (**Scheme 3**) where the bis(dimethylsilyl)amide precatalyst **5b** required lower temperatures to form the ligated complex, while the respective bis(trimethylsisyl)amide analogue from **3b** requires more harsh conditions for conversion[8]. The reduced temperature, as well as the reduced possibility of rearrangement complexes, is attractive for the potential of coordinating temperature sensitive ligands to group 3 metal precatalysts.

Scheme 3: Ligand Coordination via the "Silylamide Route" and "Extended Silylamide Route"[8]

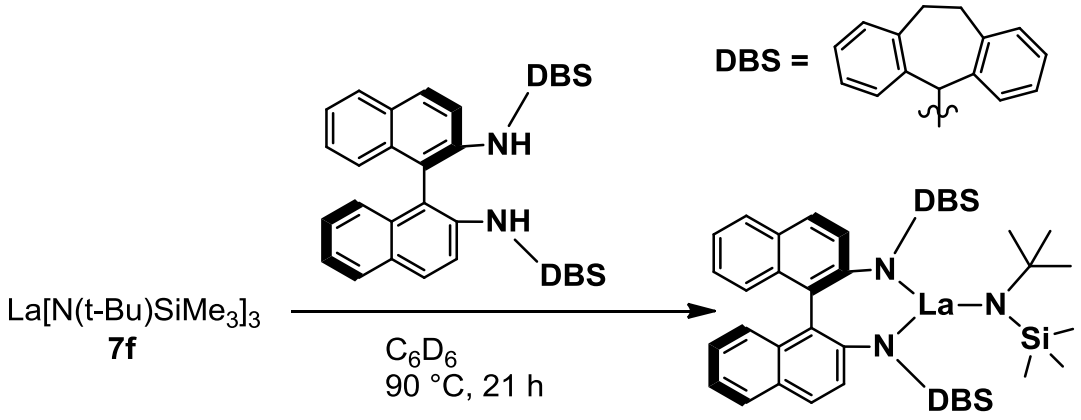


While the bis(dimethylsilyl)amide THF complexes require lowered temperatures to form precatalysts in select cases[8], their reactivity is limited by the lowered pK_a of the free ligand relative to bis(trimethylsilyl)amine. This lowered pK_a results in the above

bis(dimethylsilyl)amide THF complex being preferred to the catalytically active amido-species in the case of **1a**[8]. This represents a notable limitation to the utility of these complexes for hydroamination, and a group 3 metal trisamide precatalyst with good stability, increased basicity relative to bis(dimethylsilyl)amine, and decreased steric bulk relative to bis(trimethylsilyl)amide is a complex of great interest.

Improved group 3 trisamides of this type have been produced by the Livinghouse lab conforming to these properties utilizing the (*t*-butyl)trimethylsilyl amide ligand[9]. A recent publication by these labs demonstrates the utility of these complexes as starting material for hydroamination precatalysts (**Scheme 4**)[9]. While the group 3 metal complexes corresponding to $M[N(SiHMe_2)_2]_3(THF)_2$ and $M[N(SiMe_3)_2]_3$ did not successfully coordinate the chiral binaphthyl ligand even upon heating, the lanthanum complex **7f** neatly complexed this ligand over 21 h at 90 °C. This diamine complex was later reacted with primary aminoalkenes and exhibited high reactivity and enantioselectivity for the hydroamination reaction of aminoalkenes such as **1a**.

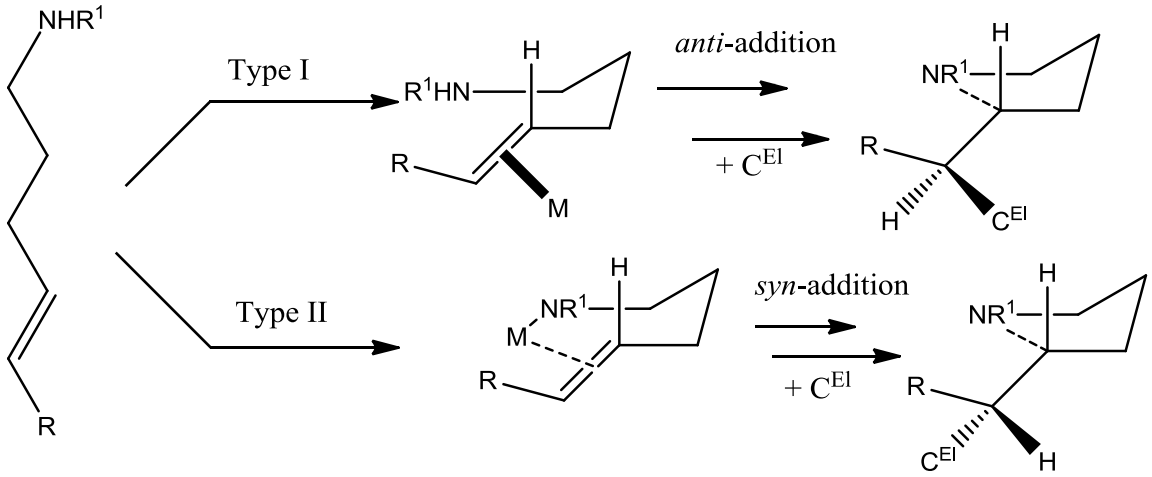
Scheme 4: Ligation of a Chiral Binaphthyl Ligand from Trisamide **7f**[9]



Metalloamination

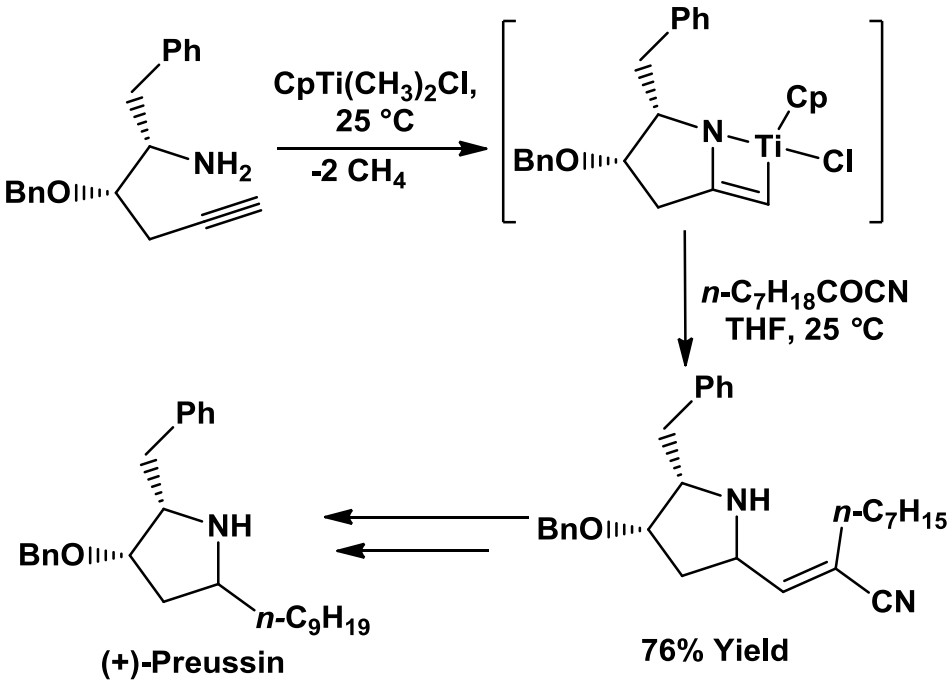
A more recent development in intramolecular formation of nitrogenous heterocyles is the intramolecular insertion of a nitrogen-metal bond into a site of unsaturation forming a nitrogen-carbon bond and metal-carbon bond simultaneously, henceforth referred to as metalloamination. The importance of this event is the metal-carbon bond can often be intercepted by a carbon-based electrophile, resulting in a dramatic increase in molecular complexity through creation of a carbon-carbon bond and a nitrogen-carbon bond in one pot. The mechanism for the intramolecular variant of the reaction can proceed in two different fashions (**Scheme 5**)[10]. In type I, a metal-alkene complex is formed followed by metalloamination resulting in *anti*-addition. In type II, a metal-amide complex is formed which then undergoes *syn*-addition. The fashion of addition either through a metal-alkene complex or a nitrogen-metal bond inserting into the alkene determines the preferred diastereomer of the reaction.

Scheme 5: Mechanism of Metalloamination / Electrophile Trapping[10]



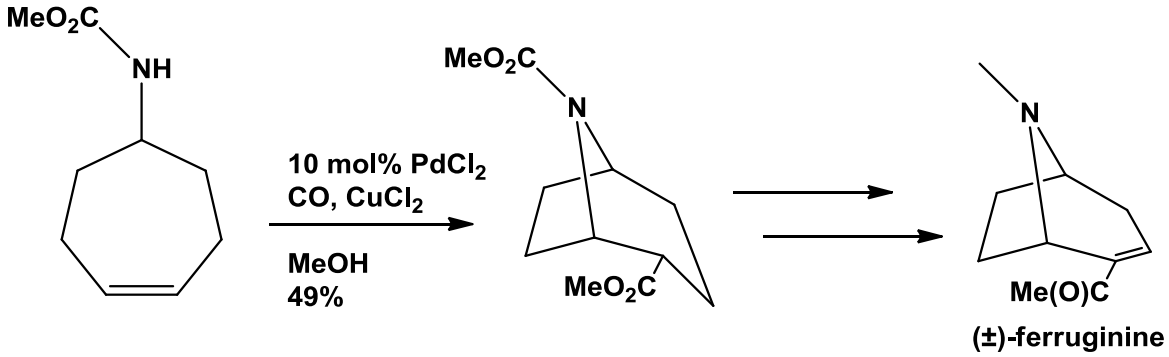
Previous work in the Livinghouse lab has been performed in the insertion of a titanium-nitrogen double bond into an alkyne in the fashion of a [2 + 2] cycloaddition[11]. The metallacyclic intermediate can undergo selective C or N functionalization by electrophilic substitution[11b]. This chemistry was used to good effect in the total synthesis of (+)-preussin (**Scheme 6**)[11c]. As outlined below, aminoalkyne reacts with $CpTi(CH_3)_2Cl$ at ambient temperature in a [2+2] fashion to eventually form the metallacyclic intermediate. Subsequent addition of octanoyl cyanide to this mixture results in the desired imine precursor to (+)-preussin in 76% yield.

Scheme 6: Heteroannulation of Titanium Imido Complex[11c]



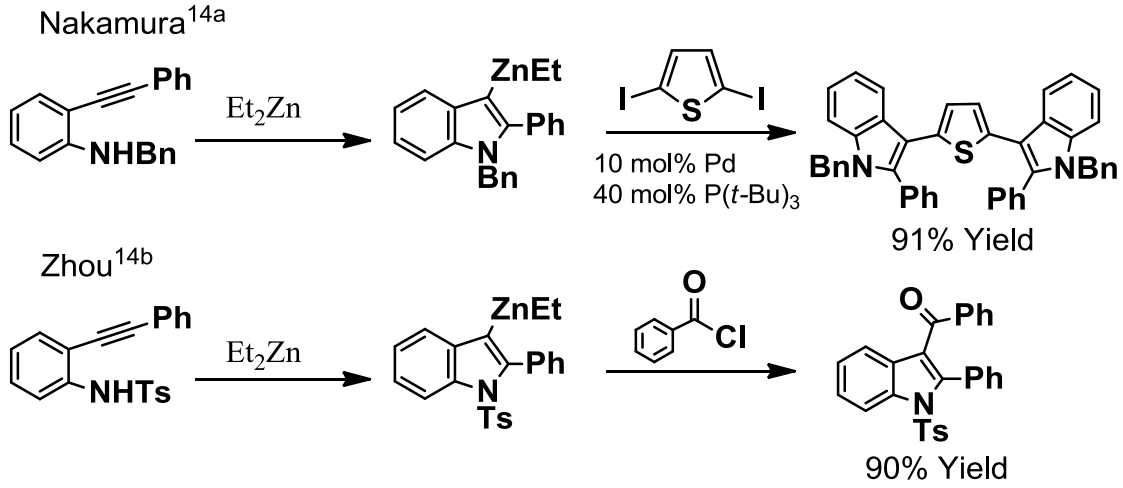
The most well-studied metal in the metalloamination-type reactions is palladium, with contributions coming largely from the groups of Waser and Wolf[10, 12]. Electrophile instertions into this palladium-carbon bond has resulted in reactions including arylation, alkenylation, alkynylation and carbonylation[10]. Palladium is advantageous for this type of reaction due to its broad functional group tolerance, however the high cost of the palladium catalyst ($PdCl_2$ costs $4600/mol) as well as generally high catalyst loading (5-20 mol%)[12] and the requirement in most cases of stoichiometric additives currently represent a limitation of the methodology. An application of Pd-catalyzed aminocarbonylation chemistry was used in the racemic synthesis of the tropane (±)-ferruginine (**Scheme 7**)[13].

Scheme 7: Application of Metalloamination Towards (±)-Ferruginine[13]



To date, the use of zinc in metalloamination/electrophile trapping reactions are limited. Research by the laboratory of Nakamura utilized *N*-benzylanilines with alkynes to cyclize to a 3-zincioindole, which is then trapped with aryl iodide and heteroaryl iodide electrophiles (**Scheme 8**)[14a]. The laboratory of Zhao developed a tandem cyclization/acylation reaction, providing high conversion of starting materials to 3-keto-*N*-benzylindoles[14b]. A limitation to the general applicability of both works is the requirement of an alkyne for insertion of the nitrogen-zinc bond, as well as conformational restriction from the aromatic backbone.

Scheme 8: Previous Examples of Zinc Metalloamination[14]

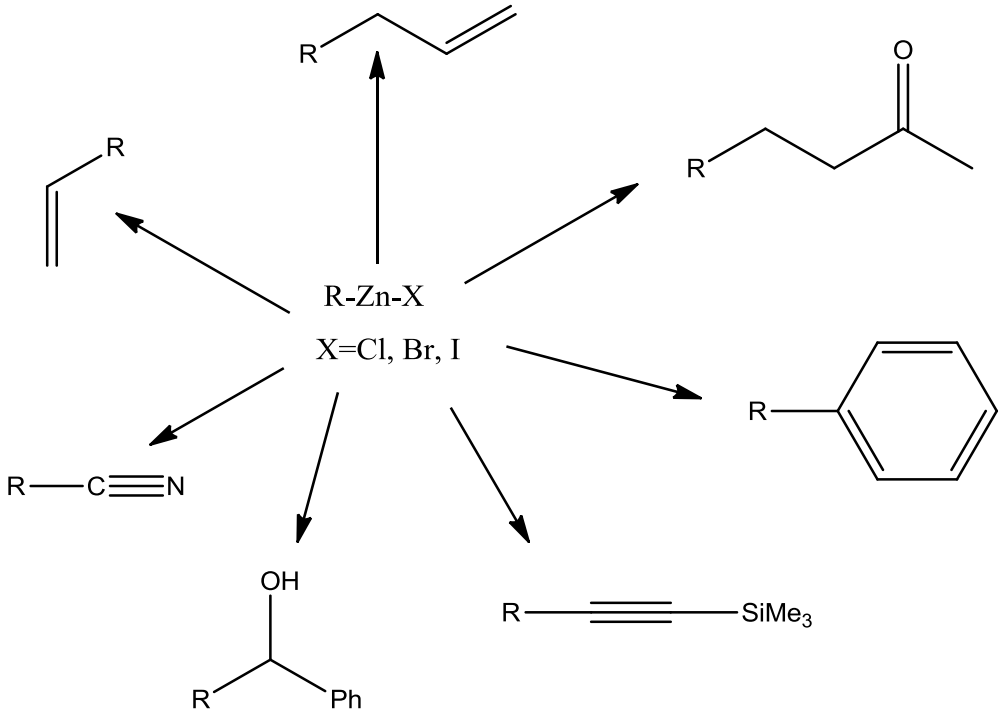


Organozinc Chemistry

A carbon-zinc bond is particularly attractive due to its well-developed carbon-carbon bond forming chemistry and improved stability relative to other metal-carbon bonds such as those of palladium and titanium. Zinc-carbon bonds are also easily transmetallated with copper or palladium to extend the utility of these bonds even further[15]. Reactions that can be performed on either zinc-carbon bonds or their transmetallated derivatives include allylation, arylation, acylation, and vinylation. A few of the substitutions obtained from organozinc intermediates are shown in **Scheme 9**[15].

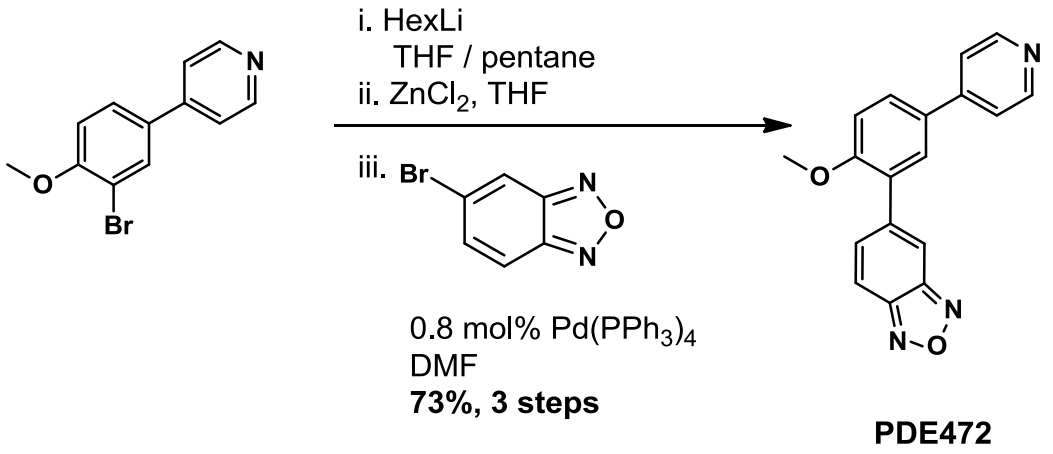
\

Scheme 9: Products Made by sp^3 C-Zn Precursors[15]



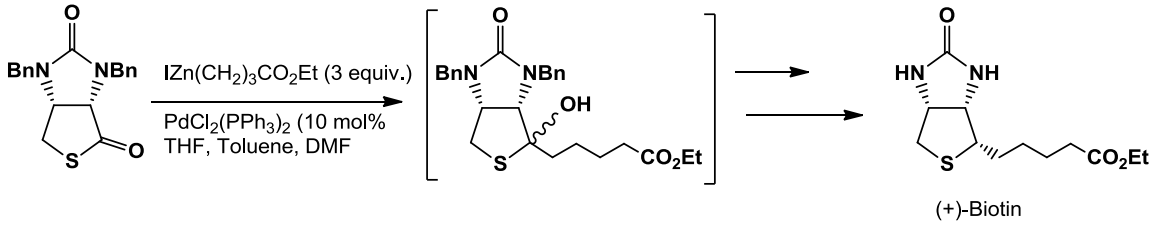
The most well known of these is the Nobel prize-winning Negishi coupling, which involves the cross-coupling of an organozinc halide to an aryl, allyl, vinyl, or benzyl halide catalyzed either by palladium (0) or nickel (0)[15]. The low cost of zinc reagents ($ZnCl_2$ is $24/mol) makes them a reasonable stoichiometric intermediate for industrial-scale syntheses. An example is the manufacturing of asthma drug target PDE472 by Novartis, which utilized the Negishi coupling in 73% yield (**Scheme 10**)[16].

Scheme 10: The Negishi Reaction in the Industrial-scale Synthesis of PDE472[16]



A more recently developed cross-coupling is that of a thioester and an organozinc halide in the presence of palladium catalyst known as the Fukuyama coupling[17]. Distinct advantages to this method of acylation include compatability with sensitive functional groups such as chlorides, ketones, acetates, sulfides and aldehydes. An interrupted version of this reaction was used in the total synthesis of (+)-biotin (**Scheme 11**)[18].

Scheme 11: Interrupted Fukuyama Coupling Towards (+)-Biotin[18]



Development of metalloaminations using zinc represents an important area of study, with the low cost of zinc combinded with the wide number of substitutions available for zinc-carbon bonds suggesting an inexpensive pathway to high molecular complexity in one pot

RESULTS AND DISCUSSION

Chapter 1: Donor Ligand Effects in Group 3 Metal-Catalyzed Hydroaminations[19]

Our aim in this research was to examine the effects of different donors upon the rate of group 3 metal intramolecular alkene hydroamination[19]. To date, the use of catalytic hydroamination utilizing group 3 metals has been limited outside of its methodology, largely due to concerns of reactivity in the presence of Lewis basic molecules. We sought to evaluate common bases and solvents used that could be of potential concern, to ascertain the total reaction inhibition of these groups, if any.

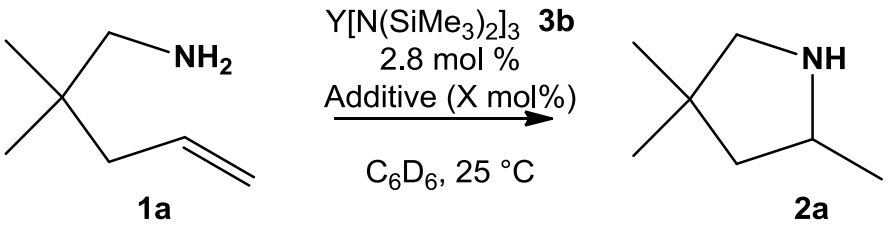
Mechanistically, hydroaminations in the presence of a Lewis base require dissociation of the base from the metal center to coordinate substrate[2]. For that reason, Lewis bases that coordinate strongest to the metal center will inhibit the hydroamination the most. As a result, anionic and/or chelating Lewis bases are expected to dramatically hinder the hydroamination reaction while neutral monodentate Lewis bases will only have a minor effect on rate.

We first evaluated the additive effects of ethereal solvents on the hydroamination of geminal-dimethyl aminoalkene **1a** with 2.8 mol% catalyst **3b** (**Table 2**). Ethereal solvents are known to slightly suppress catalytic activity of oxophilic metal complexes by coordinating to the metal centers though their lone pairs[2]. When 14 mol% of the listed ethereal additives are used (five equivalents per lanthanide metal center), minimal to no suppression of hydroamination is observed.

It is particularly notable that THF (entry 4), which forms coordination complexes with group 3 metals[3] shows minimal rate suppression at 14 mol% concentration. As shown in entries 4-7, increasing the equivalents of THF in the solution resulted in gradually slower catalyst turnover, with neat THF slowing the overall reaction time to 2 weeks. Results obtained at around 50% conversion show that there is a pronounced deceleration in neat THF.

Chelating ethereal ligands DME and 1,4-dioxane were also evaluated for their effects on rate (entries 8-11). DME is also known to form coordination complexes with group 3 metals[3], and shows some rate suppression at 14 mol% concentration (entry 8) and entirely suppresses the hydroamination when used as a neat solvent (entry 9). 1,4-dioxane shows minor rate suppression at 14 mol% concentration (entry 10), however when used as neat solvent is the least inhibitive ethereal ligand towards hydroamination evaluated as compared to THF and DME. 1,4-dioxane requires a boat conformation (35 kJ/mol higher in energy than the chair[57]) in order to be chelating, and it is likely that the energetic favorability of chelation due to coordination isn't great enough to favor chelation by 1,4-dioxane.

Table 2: Additive Effects of Ethereal Ligands



Entry	Additive	mol%	t(>50%)[a]	t(>95%)[b]
1	n/a	0	2.3 h	6 h
2	(*i*-Pr)$_2$O	14	--	6 h
3	MTBE	14	--	6 h
4	THF	14	--	6 h
5	THF	28	--	8 h
6	THF	56	--	9 h
7	THF	neat	24 h	336 h (2 weeks)
8	DME	14	--	7 h
9	DME	neat	No reaction observed	
10	1,4-dioxane	14	--	7 h
11	1,4-dioxane	neat	5.7 h	24 h

[a] 50% conversion, monitored by ^{1}H NMR spectroscopy.

[b] >95% conversion, monitored by ^{1}H NMR spectroscopy.

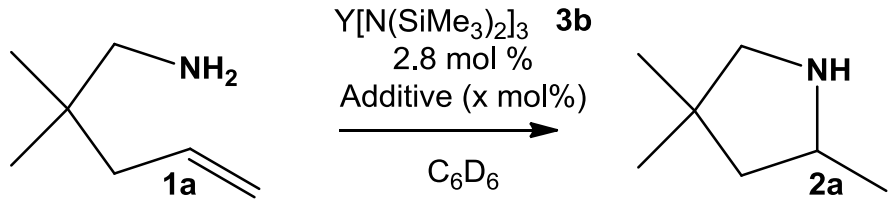
Following this analysis, other donor ligands were then screened in 14 mol% concentration for the same reaction (**Table 3**). With respect to the neutral ligands screened in this series, no inhibition was observed from tetrahydrothiophene (entry 1) while *N*-methylpyrrolidine (entry 2) only slightly slowed reaction progress. These additives generally don't coordinate very strongly to group 3 metal centers[2], so these results are as expected. In the presence of 14 mol% tetramethylurea, known to be a strong chelating ligand with group 3 metals, no conversion was observed at 22°C, suggesting complete inhibition of hydroamination. When the concentration of tetramethylurea was lowered to 2.8 mol%, the reaction was still very sluggish, proceeding to completion over

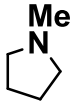
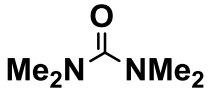
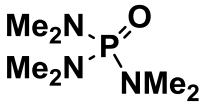
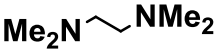
19 days (entry 3). Similarly, 14 mol% HMPA as an additive (entry 4) resulted in no conversion at room temperature, and required reduction to 2.8 mol% to proceed to completion over 4 days. In the case of the case of chelating ligand TMEDA (entry 5), only minor rate suppression was observed.

Thereafter we investigated the effects of anionic donor ligands on hydroamination (**Table 3**, entries 6-8). As a result of the significant rate suppression coming from these anionic compounds, the reaction temperature was raised to 60 °C and utilized only 2.8 mol% of additive. With lithium *tert*-butoxide (entry 6), the reaction took a total of four days while the sodium analogue (entry 7) took a total of nine days. The differences in reactivity are likely a result of the reduced association of sodium with oxygen relative to lithium with oxygen, resulting in a greater amount of negative charge surrounding the oxygen in the sodium analogue. It is well known that chloride anions coordinate strongly to lanthanide metals[3], with tetrabutylammonium chloride (entry 8) taking three days to completion.

It is noteworthy that in cases of HMPA, lithium *tert*-butoxide, and sodium *tert*-butoxide (entries 4, 8, and 9 respectively) that double bond isomerization to form **4** was observed (**Figure 2**). It deserves note that **4** was not formed when only the additive and substrate were present in reaction solution; only in cases where the catalyst **3b** was present along with these additives was isomerization observed.

Table 3: Effect of a Series of Donor Ligands on Y(III)-catalyzed Hydroaminations



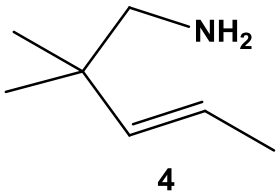
Entry	Additive	mol %	Temp (°C)	t(>50%)[a]	t(>95%)[b]
1		14	25	--	6 h
2		14	25	--	6.5 h
3		2.8	25	3.5 d	19 d
4		2.8	25	26 h	4 d[c]
5		14	25	--	6.5 h
6	*t*-BuOLi	2.8	60	25.3 h	4 d[c]
7	*t*-BuONa	2.8	60	28.5 h	9 d[c]
8	Bu_4N^+ Cl^-	2.8	60	24.7 h	3 d

[a] 50% conversion, monitored by ^{1}H NMR spectroscopy.

[b] >95% conversion, monitored by ^{1}H NMR spectroscopy.

[c] Double bond isomerization was observed inn the presence of these additives (HMPA <5%; *t*-BuOLi 15%, *t*-BuONa 21%)

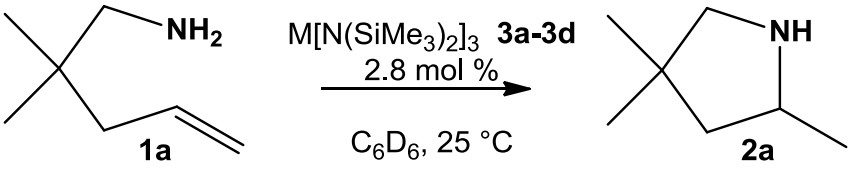
Figure 2: Double Bond Isomerization Product



4

As a result of the mild inhibition of the reaction of the ethereal donor ligands on the yttrium catalyst, we then sought to explore their effects on other group 3 metals. The hydroamination/cyclization of geminal-dimethyl substrate **1a** was initially carried out in the absence of any ethereal ligands for homoleptic bis(trimethylsilyl)amides **3a-3d** (**Table 4**). The rate of group 3 metal hydroamination reactions are positively correlated with the ionic radius of the metal center[1]. For that reason, the neodymium complex **3a** (Nd^{3+} ionic radius: 0.100 nm) most effectively catalyzed the reaction while the scandium complex **3d** (Sc^{3+} ionic radius: 0.081 nm) was the most sluggish even with additional catalyst loading[3,4]. By comparing the conversions after 50% cyclization to 95% cyclization, we observed the reactions are not first order with respect to the rate[20].

Table 4: Additive-free Hydroamination Reactions

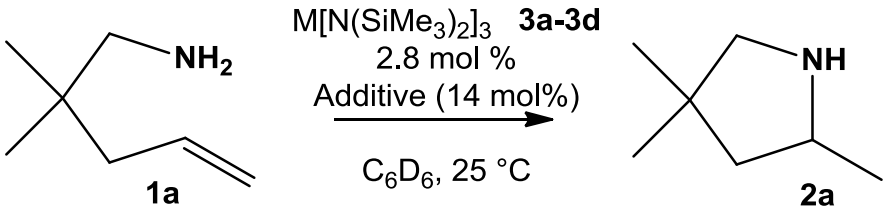


Entry	Catalyst	Metal	t(>50%)[a]	t(>95%)[b]
1	**3a**	Nd	0.7 h	4 h
2	**3b**	Y	2.3 h	6 h
3	**3c**	Lu	30.7 h	96 h
4	**3d**	Sc[c]	90.1 h	360 h

[a] 50% conversion, monitored by ^{1}H NMR spectroscopy.
[b] >95% conversion, monitored by ^{1}H NMR spectroscopy.
[c] 5 mol% of catalyst.

We next evaluated these catalysts for hydroamination rates in the presence of ethereal ligands. Similar to the trials carried out with yttrium catalyst **2b**, the small quantities of ethereal donor ligands had little influence on the hydroamination when neodymium catalyst **2a** was employed (**Table 5**, entries 1,2). However, when the lutetium and scandium analogues were used, these small quantities of THF and DME had an accelerating effect on the reaction. It is well known that scandium is quite oxophilic, so the rate increase upon addition of ethereal additives was notable. It is of particular interest that the times to 50% conversion were relatively similar in both the case of the **3c** and **3d** when compared to their additive-free reactions, however the times to full conversion in the presence of additive were roughly halved. This beneficial rate acceleration being confined to after t>50% may be a result of the ethereal groups coordination to the metal centers inhibiting complex aggregation and recoordination of cyclized product **2a** in these late stages of the reaction.

Table 5: Influence of Donor Ligands on Group 3 Metal Precatalysts



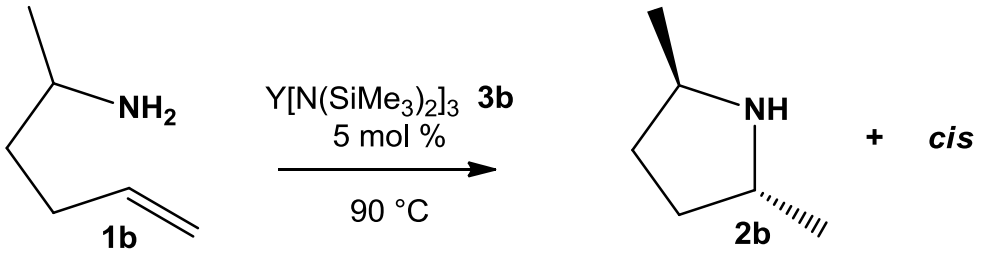
Entry	Catalyst	Metal	Additive	t(>50%)[a]	t(>95%)[b]
1	**3a**	Nd	THF	1.0 h	6.0 h
2	**3a**	Nd	DME	0.3 h	7.0 h
3	**3b**	Y	THF	---	6.0 h
4	**3b**	Y	DME	---	7.0 h
5	**3c**	Lu	THF	25.6 h	2.6 d
6	**3c**	Lu	DME	28.0 h	1.9 d
7	**3d**	Sc[c]	THF	96.0 h	8.0 d
8	**3d**	Sc[c]	DME	67.5 h	6.0 d

[a] 50% conversion, monitored by ^{1}H NMR spectroscopy.
[b] >95% conversion, monitored by ^{1}H NMR spectroscopy.
[c] 5 mol% of catalyst.

We were also interested in the effects of different solvents and additives on the rate and stereoselectivity of the hydroamination reaction (**Table 6**). We utilized substrate **1b** for this purpose, as it can close to either the *trans* or *cis* isomer and is known to have reasonable diastereoselectivity in C_6D_6[4]. A small amount of THF modestly increased the reaction rate (entry 2), while utilizing THF or 1,4-dioxane as the reaction solvent resulted in a rate suppression (entries 3 and 4). In the context of ethereal solvents, it is of interest that MTBE resulted in both a rate enhancement and increase in diastereoselectivity relative to hydrocarbon solvent. It's also noteworthy that chlorobenzene or benzotrifluoride solvents (entries 6 and 7) caused appreciably improved in reaction rate and diastereoselectivity. These aromatic molecules have an increased boiling point

relative to benzene, and may partially explain the increased rate of the hydroamination in this case.

Table 6: Diastereoselectivity Effects of Ethereal Ligands and Alternative Solvents on the Hydroamination of **1b**

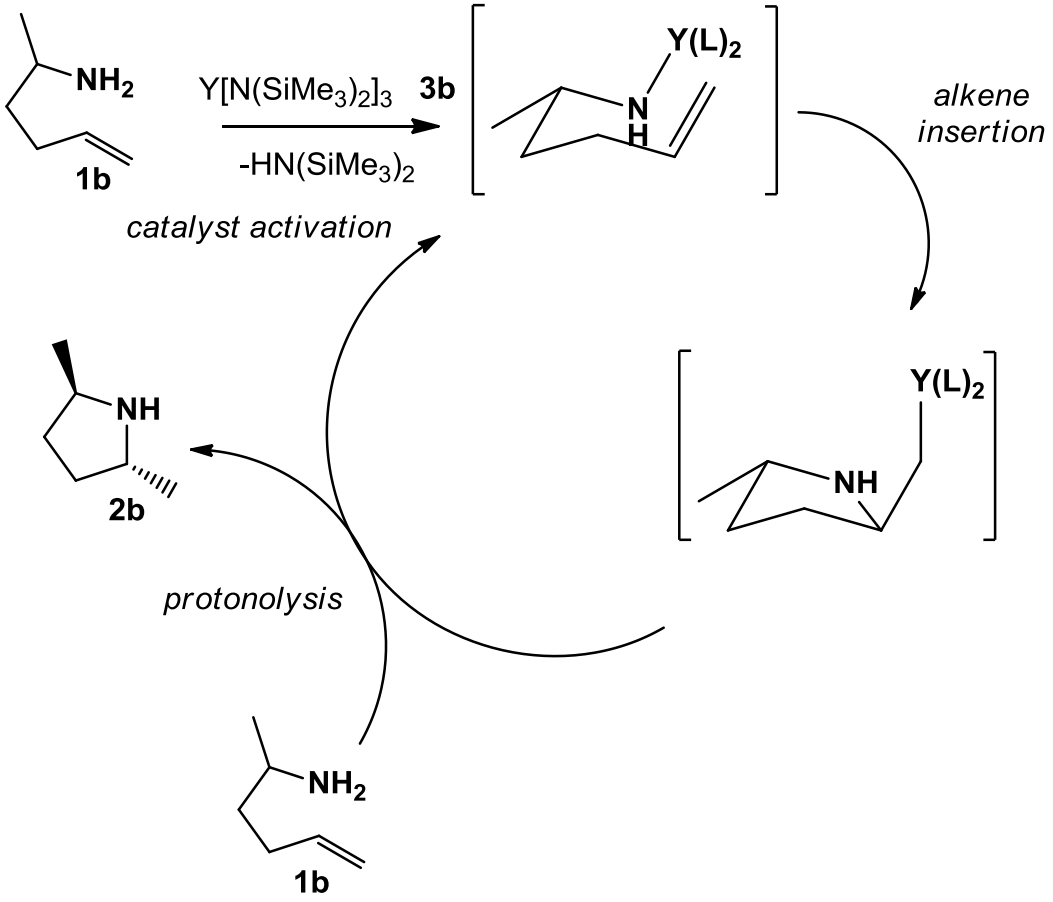


Entry	Solvent System	t(>95%)[a]	dr[b] (*t*/*c*)
1	C_6D_6	6.1 d	6:1
2	C_6D_6 + 14 mol% THF	5.0 d	9:1
3	THF	8.7 d	5:1
4	1,4-Dioxane	9.8 d	6:1
5	MTBE	4.4 d	9:1
6	C_6H_5Cl	3.2 d	9:1
7	$C_6H_5(CF_3)$	2.2 d	8:1

[a] >95% conversion, monitored by ^{1}H NMR spectroscopy.
[b] dr = diastereomeric ratio; *trans:cis*; determined by ^{1}H NMR spectroscopy

The mechanism of **1b**'s ring closure occurs through a chairlike transition state and helps to explain the preference for the *trans*-isomer (**Scheme 12**). The lower energy conformer of the transition state has both the methyl α to the amine and the alkene portion being equatorial, which produces the *trans* product. The *cis*-isomer's formation would require the methyl group be axial in this transition state, resulting in energetically unfavorable pseudo-1,3-diaxial interactions.

Scheme 12: Simplified Mechanism of Yttrium-Catalyzed Intramolecular Hydroamination of **1b**



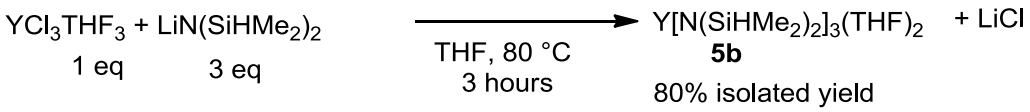
While select donor ligands have shown a substantial deleterious effect on the progress of these early transition metal-catalyzed hydroaminations[21], we have demonstrated the hydroamination reaction can tolerate certain ethereal ligands as neat solvent. Additionally, our results suggest while Lewis bases can slow and even prevent reaction progress, in most cases the hydroamination reaction proceeds to completion when the ratio of Lewis base to catalyst is 1:1. For some substrates, reactions are accelerated in the presence of small amounts of Lewis bases.

Chapter 2: Rapid and Efficient Procedure for the Synthesis of Group 3 Metal- Tris[bis(dimethylsilyl)amide] THF Complexes[22]

Encouraged by the reactivity of group 3 metal tris[bis(trimethylsilyl)amide]s **3a-d** towards hydroamination, we turned our attention to investigating the group 3 metal tris[bis(dimethylsilyl)amide] THF complexes to probe their reactivity in ligand exchange and hydroamination reactions[23]. In particular, the reduced temperatures required for ligation in certain cases as well as these complexes being able to successfully ligate certain bulky ligands is of particular interest[8].

An example of the procedure utilized by the Herrmann lab to access the group 3 metal tris[bis(dimethylsilyl)amide] THF complexes is outlined below (**Scheme 13**)[7]. In inert atmosphere, yttrium chloride THF complex and lithium bis(dimethylsilyl)amide are combined and stirred at 80 °C in THF for three hours. Following reaction completion, the solvent is removed in vacuo, and the residue is extracted with *n*-pentane to isolate the desired trisamide, and crystallized from the extracts in a -35 °C cooling bath to yield 80% of the desired product **5b**.

Scheme 13: Previous Synthesis of Group 3 Metal Complex **5b**[7]



The preparation of group 3 metal complexes of type **5** in this fashion is rather cumbersome. The lithium amide starting material is not commercially available and must be prepared in advance, and the LiCl salt formed in the reaction must be removed by

extracting product from the residue. These extracts must also be recrystallized at low temperature from pentane. Due to these difficulties, we sought to create a direct synthetic route to complexes of these types from commercially available reagents.

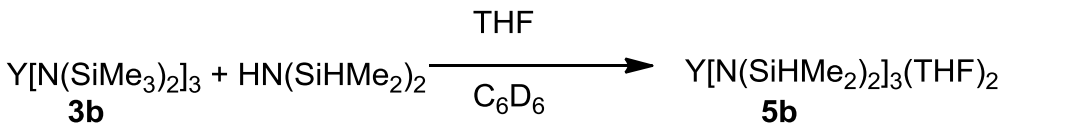
Our approach to synthesize this family of compounds was to exploit the pKa difference between $HN(SiMe_3)_2$ (pK_a =25.8) and $HN(SiHMe_2)_2$ (pK_a = 22.8) to favor the respective tris(dimethylsilyl)amide group 3 metal complex. The only side product of this reaction would be the free hexamethyldisilazane, which could easily be removed in vacuo.

Our initial efforts for synthesis was to synthesize the THF-free amide corresponding to the formula $Y[N(SiHMe_2)_2]_3$ by reacting $Y[N(SiMe_3)_2]_3$ **3b** in the presence of excess bis(dimethylsilyl)amine in benzene-d_6[24]. A thorough screening of temperature and bis(dimethylsilyl)amine only resulted in incomplete ligand exchange. A slight excess of THF, however, resulted in complete conversion to the THF adduct product (**Table 7**). These exchanges were tracked by ^{1}H NMR by comparing the integrations of the free bis(trimethylsilyl)amine -C$\underline{H}_3$ to the integrations of the ligated bis(dimethylsilyl)amide –C$\underline{H}_3$. Advantages of this method of reaction are bis(dimethylsilyl)amine and many group 3 metal tris[bis(trimethylsilyl)amide]s are commercially available[33], and purification requires only simple evacuation of volatiles to isolate the desired tris[bis(dimethylsilyl)amide] THF complexes in quantitative yield.

Following this result, we sought to optimize the reaction utilizing the yttrium tris(amide) **3b** (**Table 7**). While only slight excesses of THF and bis(dimethylsilyl)amine at room temperature were required for the reaction to go to completion in benzene,

adding extra equivalents of bis(dimethylsilyl)amine and heating resulted in dramatic rate acceleration. Slightly increased excesses of THF had no observed effect on ligand exchange. Attempts to perform the reaction in neat THF were rather lethargic, likely due to Lewis base competition for the empty coordination sphere hindering ligand exchange[1].

Table 7: Trials of Forming Group 3 Metal Complex **5b**



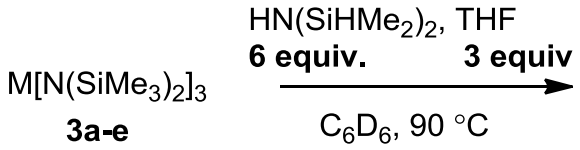
Temperature (°C)	Equiv. $HN(SiHMe_2)_2$	Equiv. THF	t (>95%)[a]
25	3.5	3	3.25 days
90	3.5	3	65 minutes
90	3.5	4	65 minutes
90	6	3	5 minutes
90	3.5	Neat	2.05 days

[a] Time to >95% conversion to desired product **5b** as observed by ^{1}H NMR.

Following optimization, we sought to investigate the applicability of this procedure to access other group 3 tris[bis(trimethylsilyl)amide]s (**Table 8**). The rates of these conversions correlates strongly with ionic radius of the metal, with trials forming **5a**, **5b**, **5e** each taking 5 minutes, while the group 3 metal with the smallest ionic radius, scandium, taking only 2.75 hours to >95% completion[3]. These reactions were amenable to scale, with **5b** being formed on 5 mmol scale replacing benzene-d_6 with toluene and extending reaction time to 30 minutes to compensate for the inability to monitor the

reaction in situ. For each of the complexes **5a-5e**, complexes were obtained in >95% isolated yield simply by removing volatiles at room temperature.

Table 8: Synthesis of Group 3 Metal Complexes **5a-5e**



$M[N(SiMe_3)_2]_3$ **3a-e** → $M[N(SiHMe_2)_2]_3(THF)_n$ **5a-e**

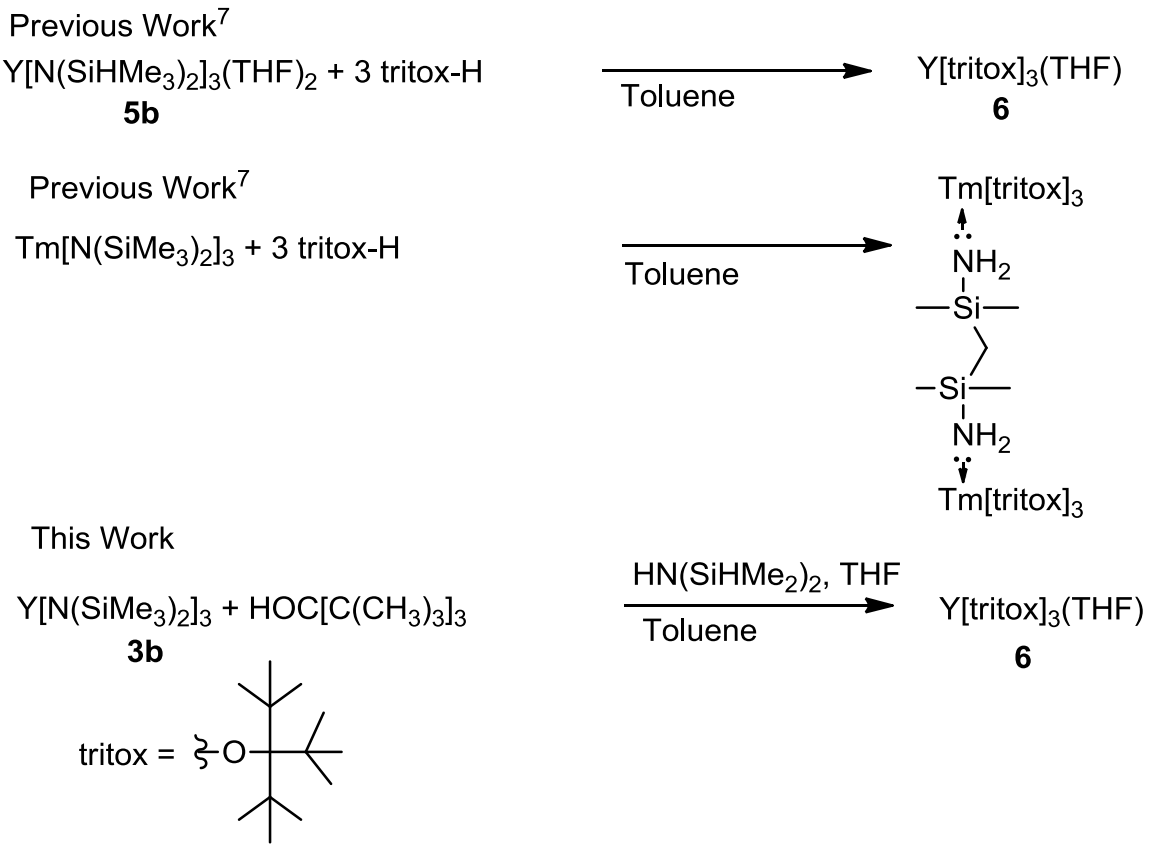
Complex	metal	product	$(THF)_n$	t (>95%)[a]
3a	Nd	**5a**	2	5 minutes
3b	Y	**5b**	2	5 minutes
3c	Lu	**5c**	2	1.67 hours
3d	Sc	**5d**	1	2.75 hours
3e	Sm	**5e**	2	5 minutes

[a] Time to >95% conversion to desired product as observed by ^{1}H NMR.

In a demonstration of the special reactivity of these group 3 metal trisamide THF complexes, the laboratory of Herrmann converted **5b** to tris(tritox) THF complex **6** when the respective alcohol was added at room temperature (**Scheme 14**). They noted that for thulium tris[bis(trimethylsilyl)amide] that direct treatment with tritox-H lead to the shown complex, and further heating caused rearrangement products to form. We confirmed that for complex **3b**, direct addition of tritox-H and a small amount of THF in toluene does not lead to **6**, and a highly complex ^{1}H NMR suggests rearrangement products. We attempted utilizing catalytic amounts of bis(dimethylsilyl)amine and a

slight excess of THF to access **6**, however these trials did not result in a clean conversion and a large amount of side products were visible by ^{1}H NMR. However, using six equivalents of bis(dimethylsilyl)amine and a slight excess of THF along with 3 equivalents of tritox-H results in full conversion to the desired complex **7** at room temperature, suggesting that future access to the reactivity from the "extended silylamide" route may be accessed by forming such complexes in situ.

Scheme 14: Substitution of tritox-H From Group 3 Metal Trisamides



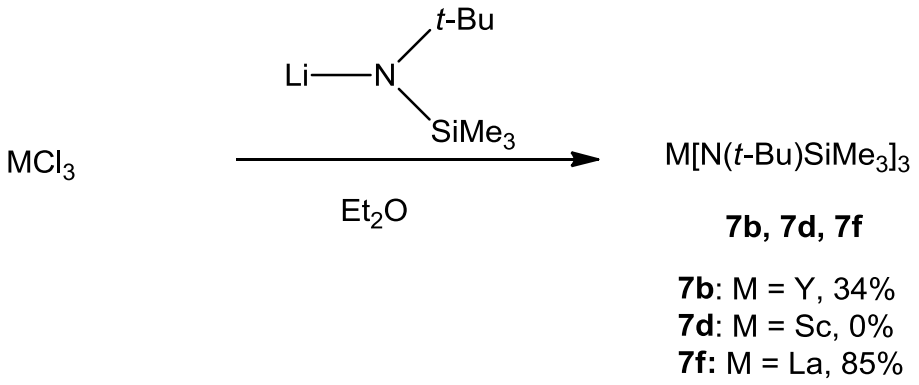
Chapter 3: Intramolecular Hydroaminations of Secondary Aminoalkenes Catalyzed by New Group 3 Metal Trisamides

Our attention turned towards the hydroamination of secondary aminoalkenes via easily accessible group 3 metal complexes. To date, research on secondary aminoalkene hydroamination catalyzed by group 3 metals has been limited to *N*-benzyl and *N*-methyl varieties[25]. For the vast majority of pharmaceuticals containing pyrrolidine and piperidine moieties, the nitrogen in the ring is trisubstituted, and for that reason the development of catalytic reactions for these substrates is of significant importance[55]. For the present study, we specifically investigated secondary aminoalkenes containing electron rich aromatic nuclei.

For this study, we additionally wanted to evaluate hydroamination capability of a new type of group 3 metal tris[*t*-butyltrimethylsilyl]amides **7b-7f** (**Scheme 15**). These new trisamides were shown in a related study to be more facile than their analogous group 3 metal tris[bis(trimethylsilyl)amide]s in secondary amine ligand coordination[9]. Synthesis of these new trisamides **7b**, **7d**, **7f** was attempted by reacting the respective group 3 metal chloride with three equivalents of lithium (*t*-butyl)trimethylsilylamide in diethyl ether stirred at room temperature for 2 days, followed by evacuation of volatiles and sublimation under high vacuum. Trials aimed at synthesizing the scandium variant **7d** were unsuccessful even when reaction time was extended to a week, and analysis of the reaction residue suggests incomplete ligand exchange and partial –ate complex formation[2]. The yttrium variant **7b** and lanthanum variant **7f** could successfully be

obtained by this protocol, and **7f** could also be made in similar yields from its lanthanum chloride THF adduct[3].

Scheme 15: Synthesis of New Group 3 Metal Trisamides **7b**, **7f**



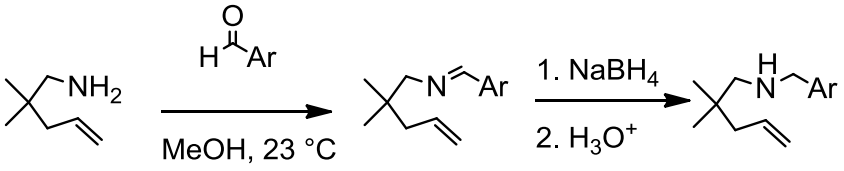
Along with these new group 3 metal trisamides, we also sought to investigate other simple group 3 precatalysts (**Figure 3**)[26]. The popular group 3 trisamides **3b-3f** were screened against these new trisamides **7b**, **7f** in order to assess differences in hydroamination reactivity with secondary aminoalkenes between the two. Further, group 3 tris(trimethylsilylmethyl) THF complexes **8b, 8d** were also screened due to the expectation that upon substrate addition the ligands around the metal center would immediately be displaced and form a trisamide correlating to the substrate[9]. The pK_as of the conjugate bases of the ligands range from 25.8 for hexamethyldisilazane, with *(t*-butyl)trimethylsilyl ether being ~35, and lastly tetramethylsilane being 50. These differences in pK_a were expected to correlate directly with the rate of exchange with the secondary aminoalkene substrates. In all cases, multiple metal centers were used to evaluate differences in reactivity, oxophilicity, and thiophilicity amongst the group 3 metals.

Figure 3: Simple Group 3 Metal Precatalysts

$M[N(SiMe_3)_2]_3$	$M[N(t\text{-}Bu)SiMe_3]_3$	$M[CH_2SiMe_3]_3(THF)_2$
3b-3f	**7b, 7f**	**8b, 8d**
3b: M = Y **3d:** M = Sc **3f:** M = La	**7b**: M = Y **7f:** M = La	**8b**: M = Y **8d:** M = Sc

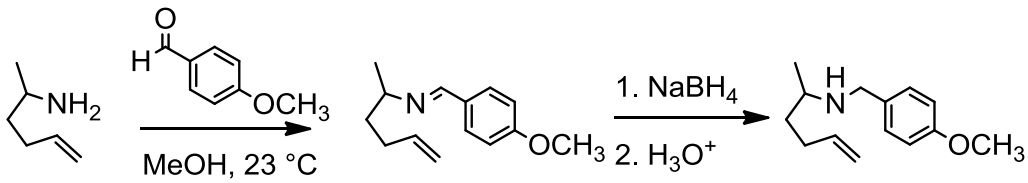
Synthesis of secondary aminoalkene substrates **9a-9d** was performed via a reductive amination from their primary aminoalkene precursor (**Scheme 16**)[27]. Combining the respective aldehyde with a slight excess of aminoalkene in methanol at room temperature created the imine in situ, which was followed by addition of sodium borohydride to efficiently provide the secondary aminoalkene in a single pot in good to excellent yields.

Scheme 16: Synthesis of Secondary Aminoalkenes **9a-9d**



1a **9a-9c**

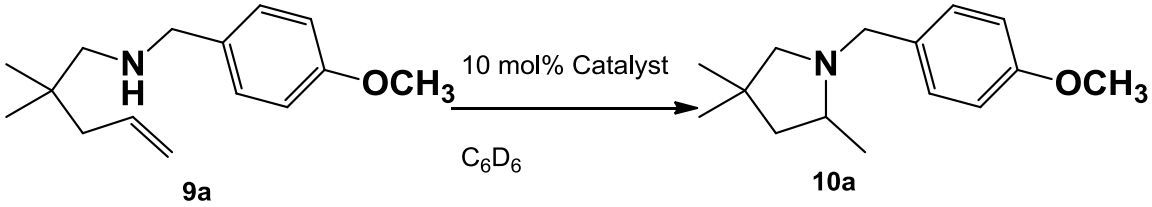
9a: Ar = 4-(methoxy)phenyl, 89%
9b: Ar = 2-furyl, 85%
9c: Ar = 2-thiophenyl, 83%



1b **9d**, 82%

We first sought to screen hydroamination of the secondary aminoalkene bearing a 4-methoxybenzyl group **9a**, as this *N*-substitution has been used as a protecting group for secondary amines in organic synthesis[28]. In the cases of tris[bis(trimethylsilyl)amide]s **3b-3f**, degradation of substrate was observed along with poor dissociation of bis(trimethylsilyl)amine (**Table 9**, entries 1-3). It bears note that these tris(bis(trimethylsilyl)amide) precatalysts have been known to form rearrangement products in certain cases upon attempts to coordinate bulky amines[7]. Notably, the tris(*t*-butyltrimethylsilylamide)s **7b, 7f** far more readily dissociate their ligands, and both successfully resulted in hydroamination of the substrate at only 60 °C, each in less than 2 hours (entries 4, 5). It bears note that precatalyst **8b**, which immediately dissociates its ligands in the presence of secondary amines[9], required over 2 hours at 90 °C to proceed to completion (entry 7). This suggests that coordination of as much substrate as possible to the metal center could hinder reaction progress, due to coordinative saturation from some combination of amide, alkene, and aryl coordination. While an earlier study in these labs suggests low concentration of THF with trisamide complexes should have little to no effect on their reactivity towards hydroamination[19], we cannot rule out THF as a source of reactivity inhibition.

Table 9: Hydroamination of Substrate **9a**



9a **10a**

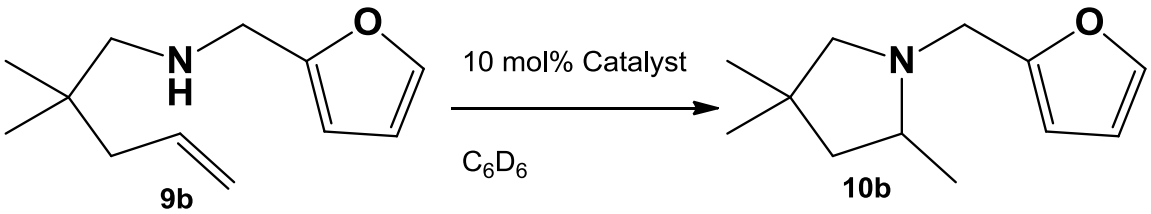
Entry		Catalyst	Temp (°C)	t(50%)[a]	t(90%)[b]
1	**3d**	$Sc[N(SiMe_3)_2]_3$	90	-----	-----
2	**3b**	$Y[N(SiMe_3)_2]_3$	90	-----	-----
3	**3f**	$La[N(SiMe_3)_2]_3$	90	-----	-----
4	**7b**	$Y[N(t\text{-}Bu)SiMe_3]_3$	60	-----	1.75 h
5	**7f**	$La[N(t\text{-}Bu)SiMe_3]_3$	60	0.50 h	1.00 h
6	**8d**	$Sc(CH_2SiMe_3)_3(THF)_2$	90	-----	-----
7	**8b**	$Y(CH_2SiMe_3)_3(THF)_2$	90	-----	2.25 h

[a] Time to 50% conversion as observed by ^{1}H NMR.
[b] Time to 90% conversion as observed by ^{1}H NMR.

We next sought to investigate the hydroamination of the benzylic 2-furyl aminoalkene **9b** (**Table 10**). The oxygen in the aromatic ring was expected to coordinate to the metal center, with strongest coordination toward the more oxophilic metals[3]. For silylamides **3b-3f**, the efficiency of hydroamination follows the trend La > Y > Sc, suggesting an inverse relationship between hydroamination efficiency and oxophilicity. Especially interesting is lanthanum precatalyst **3f** which required temperatures of only 60 °C to reach completion. In the case of the silylamide precatalysts **7b, 7f** the reaction did not proceed to completion, and the more oxophilic yttrium variant **7b** converted 63% of substrate versus the less oxophilic lanthanide species **7f**, which at the same temperature converted only 30% of substrate. Interestingly, running the reaction with **7f** at room temperature resulted in better conversion over the timespan, with hydroamination occurring to 42% of the substrate. In all screenings performed with **7b, 7f**, dissociation of

all the *t*-butyltrimethylsilylamine was associated with the cessation of substrate hydroamination. Curiously, **8d** both was more successful in hydroaminating substrate **9b** than **7b** in spite of immediately coordinating off all ligands when combined in solution, suggesting that THF coordination to the metal center may be beneficial to reducing coordinative saturation of the furan[19] .

Table 10: Hydroamination of Substrate **9b**



9b **10b**

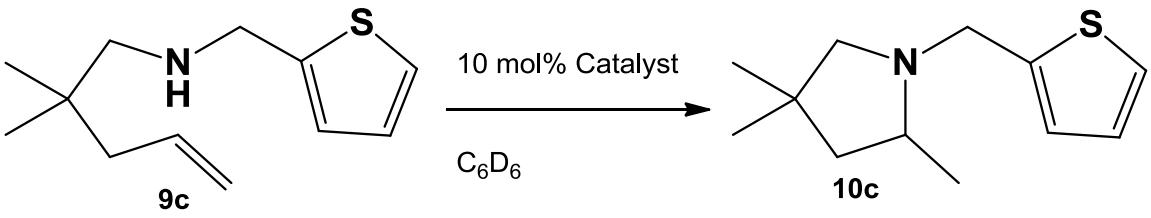
Entry		Catalyst	Temp (°C)	t(50%)[a]	t(final)[b]
1	**3d**	$Sc[N(SiMe_3)_2]_3$	90	-----	36 h
2	**3b**	$Y[N(SiMe_3)_2]_3$	90	-----	24 h
3	**3f**	$La[N(SiMe_3)_2]_3$	60	18.2 h	5.6 d
4	**7b**	$Y[N(t\text{-Bu})SiMe_3]_3$	60	-----	4.0 d (63%)
5	**7f**	$La[N(t\text{-Bu})SiMe_3]_3$	60	-----	2.0 d (30%)
6	**7f**	$La[N(t\text{-Bu})SiMe_3]_3$	25	-----	2.0 d (42%)
7	**8d**	$Sc(CH_2SiMe_3)_3(THF)_2$	90	7 d	14 d (69%)
8	**8b**	$Y(CH_2SiMe_3)_3(THF)_2$	90	16.4 h	14 d (85%)

[a] Time to 50% conversion as observed by ^{1}H NMR.
[b] Time to 90% conversion as observed by ^{1}H NMR, or greatest observed conversion if percentage is noted in parentheses.

In order to further evaluate the effect of aromatic lone pair donors, we evaluated the benzylic 2-thiophenyl substrate **9c** (**Table 11**). With respect to this substrate, we expect an inverse trend in hydroamination reactivity as compared to **9b** due to the thiophilicity of softer metals[3]. This indeed proved to be the case, as analogous silylamides **3b-3f** followed the rate trend Sc > Y > La (entries 1-3). Interestingly, **7b**, **7f**

both proceeded at room temperature, with yttrium variety **7b** going to completion in only 14.8 hours at room temperature (entries 6-7). Catalysts **8d, 8b** also share the reaction conversion trend of Sc > Y.

Table 11: Hydroamination of Substrate **9c**



9c **10c**

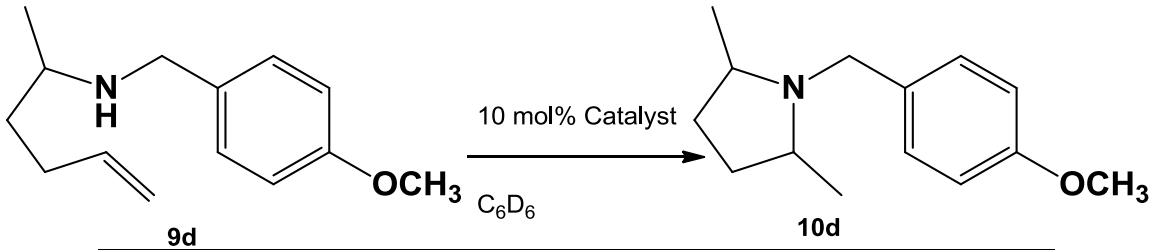
Entry		Catalyst	Temp (°C)	t(50%)[a]	t(final)[b]
1	**3d**	$Sc[N(SiMe_3)_2]_3$	90	-----	20.4 h
2	**3b**	$Y[N(SiMe_3)_2]_3$	90	-----	39 h
3	**3f**	$La[N(SiMe_3)_2]_3$	90	24 h	10.5 d
4	**7b**	$Y[N(t\text{-}Bu)SiMe_3]_3$	25	7.6 h	14.8 h
5	**7f**	$La[N(t\text{-}Bu)SiMe_3]_3$	25	22 h	7.0 d (84%)
6	**8d**	$Sc(CH_2SiMe_3)_3(THF)_2$	90	23 h	10 d (84%)
7	**8b**	$Y(CH_2SiMe_3)_3(THF)_2$	90	42.3 h	9 d (65%)

[a] Time to 50% conversion as observed by ^1H NMR.
[b] Time to 90% conversion as observed by ^1H NMR, or greatest observed conversion if percentage is noted in parentheses.

Following the hydroamination of geminal-dimethyl substituted substrates **9a-9c**, we sought to evaluate the diastereoselectivity of the hydroamination by screening substrate **9d** (**Table 12**). The silylamide precatalysts **3b**-**3f** were very poor at the hydroamination of this reaction, likely due in part to the steric bulk surrounding the group 3 metal center combined with steric hinderance from the α-methyl of **9d**. New silylamide precatalysts 7**b**, **7f** were again successful at lower reaction temperatures, and show great selectivity for the *cis* isomer **10d**, >19:1 *cis/trans* in the case of **7f**[29]. Trialkyl precatalysts

8d, **8b** proceeded entirely to completion, with ^{1}H NMR intergrations showing reasonable selectivity towards the *cis* isomer.

Table 12: Hydroamination of Substrate **9d**



9d **10d**

Entry		Catalyst	Temp (°C)	t(50%)[a]	t(final)[b]	dr (*c*/*t*)
1	**3d**	$Sc[N(SiMe_3)_2]_3$	90	-----	3 d (0%)	-----
2	**3b**	$Y[N(SiMe_3)_2]_3$	90	-----	3 d (34%)	-----
3	**3f**	$La[N(SiMe_3)_2]_3$	90	-----	3 d (34%)	-----
4	**7b**	$Y[N(t\text{-Bu})SiMe_3]_3$	60	-----	5 h	13:1
5	**7f**	$La[N(t\text{-Bu})SiMe_3]_3$	60	50 min	3.25 h	>19:1
6	**8d**	$Sc(CH_2SiMe_3)_3(THF)_2$	90	8.2 h	90.5 h	8:1
7	**8b**	$Y(CH_2SiMe_3)_3(THF)_2$	90	20 min	18 h	9:1

[a] Time to 50% conversion as observed by ^{1}H NMR.

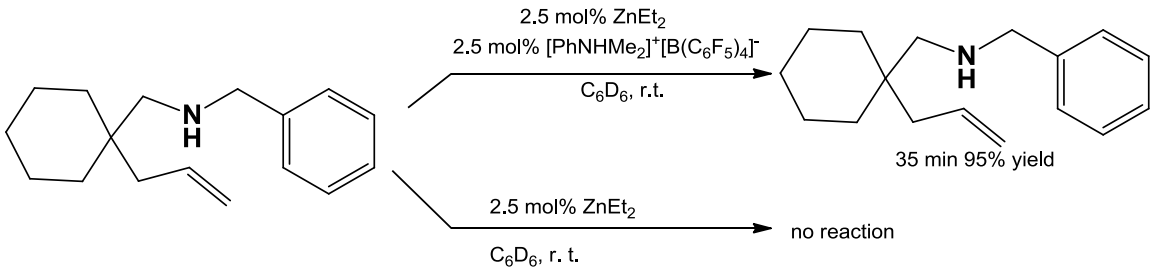
[b] Time to either 90% conversion as observed by ^{1}H NMR, or greatest conversion observed (conversion% in parentheses)

We have demonstrated that new silylamide precatalysts **7b-7f** show excellent reactivity as hydroamination catalysts for secondary aminoalkenes. Notably, these precatalysts reacted very quickly and diastereoselectively for substrates containing a *p*-methoxybenzylamine. The reduced temperatures required for these hydroamination reactions suggest facile hydroamination of thermally-sensitive substrates may be achieved.

Chapter 4: Intramolecular Metalloaminations of *N*,*N*-Dimethylhydrazinoalkenes[30]

In a recent publication from the labs of Roesky and Blechert, a cationic zinc hydroamination catalyst was generated by reacting diethylzinc with a dimethylanilinium tetrakis(pentaflurophenyl)borate as an activator (**Scheme 17**)[31]. In their reaction, they did not observe hydroamination in the absence of this activator. It has been demonstrated in the past that zinc amides can be obtained by simple mixing of secondary amines with diethylzinc[32], so presumably in the absence of the activator, only the zinc amide would be expected to form. Based on this information, we sought to investigate if certain zinc amides could insert into a site of carbon-carbon unsaturation, forming a nitrogen-carbon and carbon-zinc bond synchronously. A carbon-zinc bond is particularly attractive as it can be intercepted by a wide variety of carbon electrophiles in good yield[15].

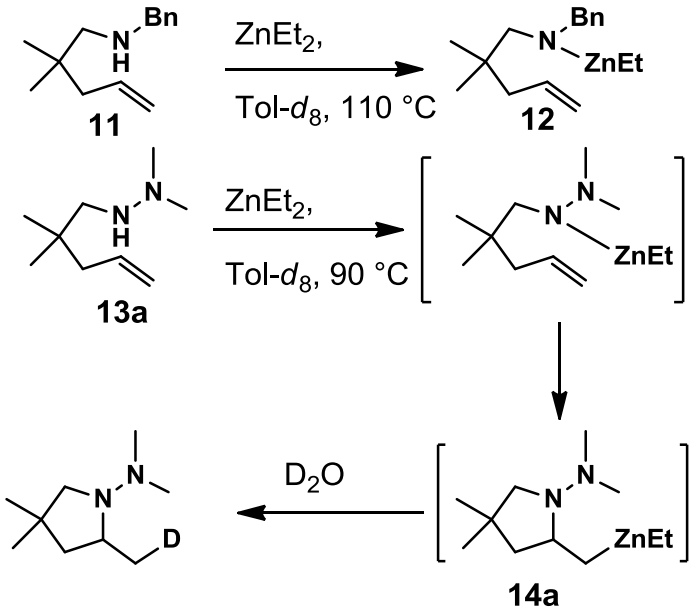
Scheme 17: Hydroamination Utilizing Diethylzinc and Activator[31]



In an initial trial, benzyl aminoalkene **11** was combined an equimolar amount of diethylzinc in toluene (**Scheme 18**). While we did observe the formation of amide **12** upon heating, no cyclization was observed, and continued heating at temperature resulted in the deposition of metallic zinc[32]. We next sought to investigate intermediate **13a** for

cyclization, based on the premise that the insertion of the nitrogen-zinc bond into the alkene would result in a internally coordinated zinc intermediate. This cyclization intermediate was indeed reached, with >95% conversion to the organozinc intermediate **14a** over 18 hours at 90 °C. Evidence of **14a** was confirmed by deuteration with D_2O exclusively at the indicated carbon.

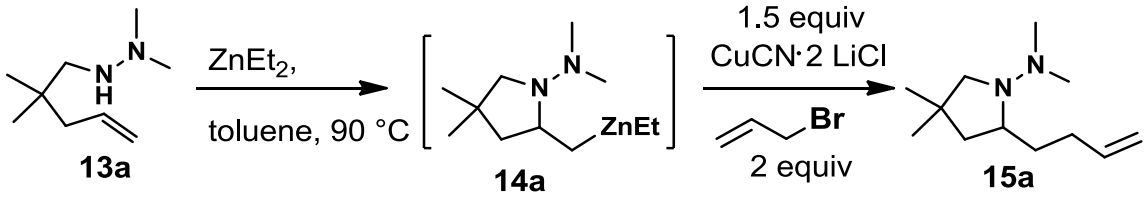
Scheme 18: Early Metalloamination Trials



Following successful deuteration of the intermediate, we sought to evaluate the utility of intermediate **14a** towards known organozinc carbon-carbon bond forming chemistry[15]. A well known and reliable functionalization reaction developed by the Knochel laboratory involves transmetallation of an organozinc to copper cyanide, followed by allylation in high yield. Adding two equivalents of allyl bromide and a 1.5 equivalents THF solution of CuCN • 2 LiCl to **14a** resulted in good conversion of the intermediate to the allylated product **15a** (R=H) (**Scheme 19**). Utilizing a procedure

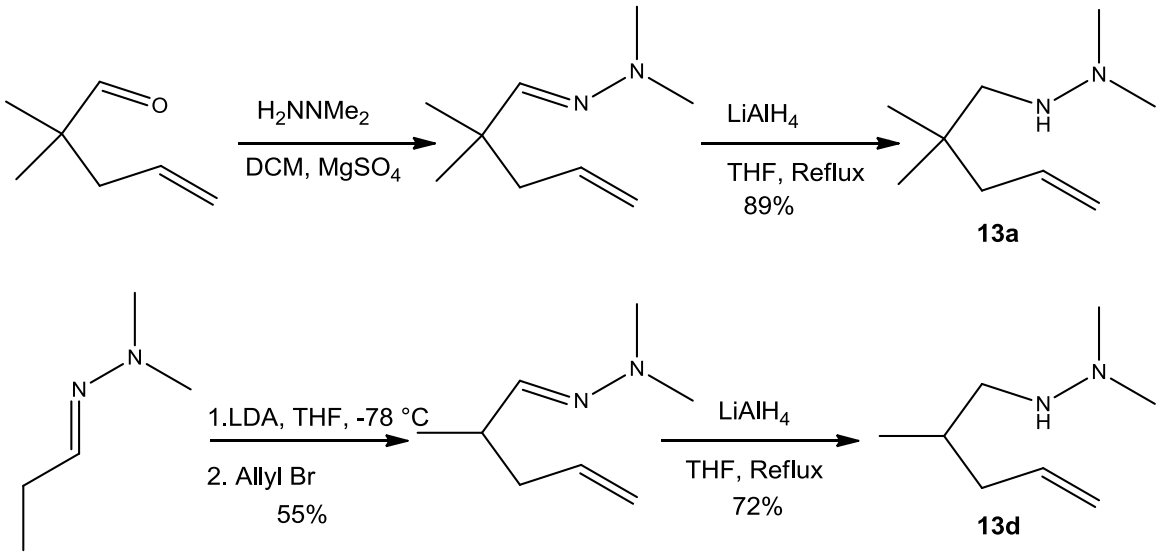
optimized by Dr. Sunsdahl for workup, 92% of the product from **13a** was obtained as its trifluoroacetate salt.

Scheme 19: Copper (I) Allylation of Intermediate **13a**



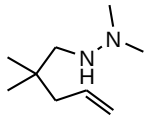
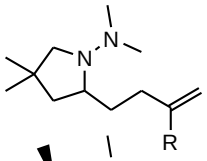
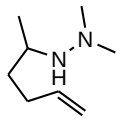
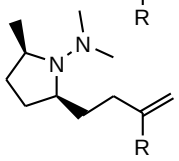
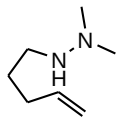
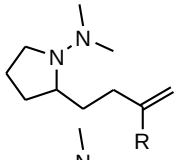
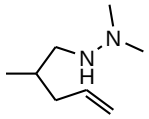
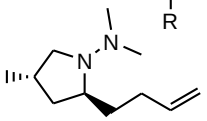
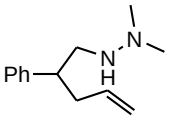
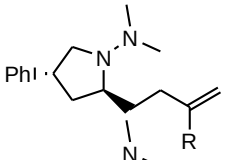
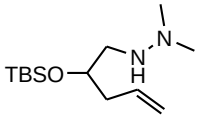
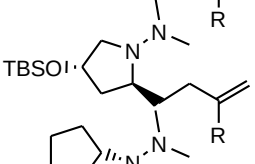
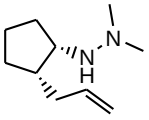
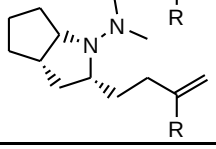
Encouraged by these early results, substrate synthesis was then carried out in generally good yields (**Scheme 20**). For the geminal dimethyl substrate **13a**, known aldehyde was obtained from the acid-catalyzed Claisen rearrangement from allyl alcohol and isobutyraldehyde[35]. Aldehyde **17** is then converted cleanly to the *N*,*N*-dimethylhydrazone via reaction with asymmetric dimethylhydrazine in CH_2Cl_2 and $MgSO_4$[36]. Reduction of this *N*,*N*-dimethylhydrazone with $LiAlH_4$ provides **13a**[31]. For substrate **13d**, the respective *N*,*N*-dimethylhydrazone precursor was allylated cleanly in LDA by the procedure of Corey and Enders[34], and the purified product was then reduced to form **13d**.

Scheme 20: *N*,*N*-Dimethylhydrazineamine Substrate Synthesis



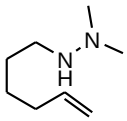
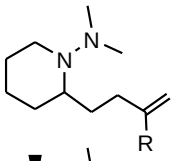
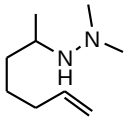
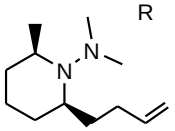
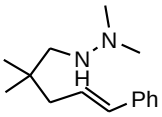
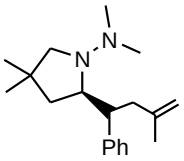
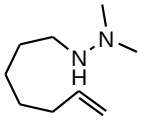
Following substrate synthesis, a screening of metalloamination/allylation reaction was carried out by Dr. Sunsdahl and myself on various substrates (**Table 13, Table 14**). Research by Dr. Sunsdahl shows that α-substituted hydrazinoalkenes (**13b**, **13g**, **13h**) gives products that favor *cis*-orientation in their products. Dr. Sunsdahl also demonstrated that unsubstituted pyrrolidine and piperidine rings can be formed by this reaction (**15c**, **15i**), and styryl alkenes (**13j**) are well tolerated. In these screenings, methallylation through the copper (I) intermediate was also shown to proceed with good yield.

Table 13: Metalloamination/allylation of Hydrazinoalkenes to Pyrrolidines

Hydrazinoalkene		Conversion [%][a]	d.r.	Product		Yield [%][e]
	**13a**	> 95 (18 h)[b]	---		**15a**	92 (R=H) 83 (R=Me)
	**13b**	> 95 (6 h)[b]	>20:1 (*c/t*)		**15b**	81 (R=H) 85 (R=Me)
	**13c**	90 (4 h)[b]	---		**15c**	80 (R=H) 76 (R=Me)
	**13d**	90 (15 h)[c]	1:6 (*c/t*)		**15d**	83
	**13e**	90 (24 h)[d]	1:15 (*c/t*)		**15e**	83
	**13f**	90 (8 h)[b]	1:2 (*c/t*)		**15f**	83
	**13g**	> 95 (16 h)[b]	>20:1 (*c/t*)		**15g**	87

[a] As calculated from ^{1}H NMR spectra utilizing *p*-xylene as an internal standard. [b] Reaction conducted on a 0.1 mmol scale in a 90 °C oil bath with toluene or (trifluoromethyl)benzene as solvent. [c] Reaction conducted at 10 °C. [d] Reaction conducted at 23 °C. [e] All products were isolated as TFA salts unless otherwise noted.

Table 14: Metalloamination/allylation of Hydrazinoalkenes

Hydrazinoalkene		Conversion [%][a]	d.r.	Product		Yield [%][e]
	**13h**	> 95 (3 h)[b]	---		**15h**	93 (R=H) 88 (R=Me)
	**13i**	70 (12 h)[b,]	9:1 (*c/t*)		**15i**	63
	**13j**	90 (24 h)[b]	---		**15j**	79
	**13k**	n.r. (3 d)	----	----		----

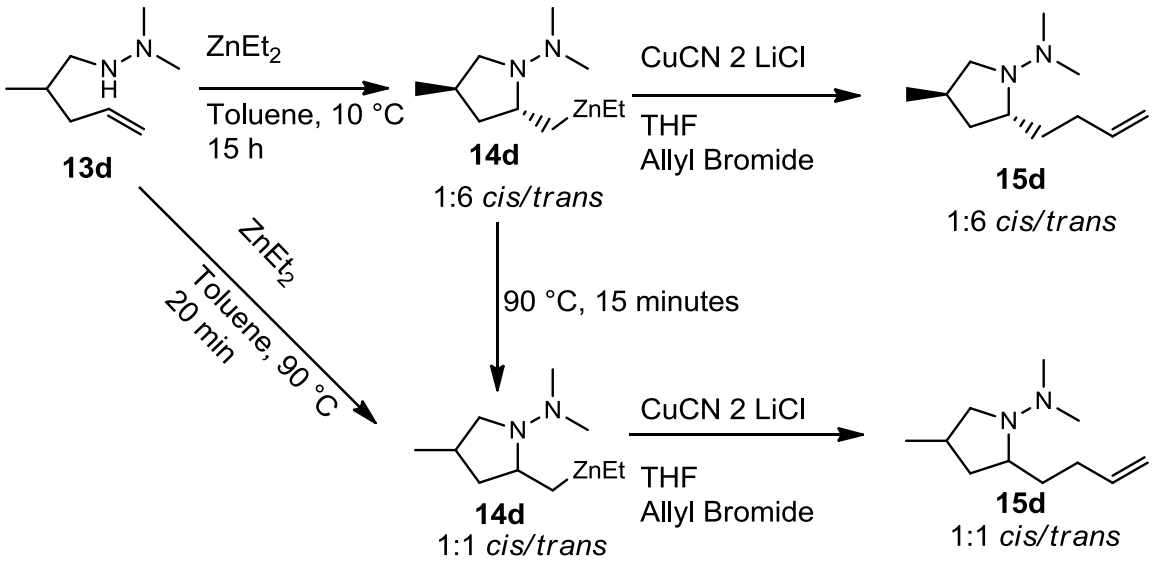
[a] As calculated from ^{1}H NMR spectra utilizing *p*-xylene as an internal standard. [b] Reaction conducted on a 0.1 mmol scale in a 90 C oil bath with toluene or (trifluoromethyl)benzene as solvent. [c] Required 2 equivalents of $ZnEt_2$ [d] Stereoselectivity is unoptimized. [e] All products were isolated as TFA salts unless otherwise noted.

The trial of substrate **13d** is of particular note. Upon heating the reaction mixture at 90 °C, the reaction converted to **14d** in a 1:1 *cis:trans* ratio after only 15 minutes. Comparison of this result to substrates **13a** and **13c** suggests that mono-substitution at this ß position rapidly accelerates the conversion of substrate to product. In many cases in group 3 metal hydroamination, Thorpe-Ingold activation (such as that in **1a**, **Table 1**) is required for rapid conversion of substrate to product; rate of conversion decreases with decreasing substitution at the ß-position[1]. It is therefore unusual that in conversion of substrate to the organozinc intermediate, the rate of conversion for substrate **13c** was dramatically faster than the rate of conversion of **13a**. Additionally, the mono-substituted

substrate **13d** proceeds at a greater rate at 90 °C than both the geminally disubstituted **13a** or unsubstituted **13c**.

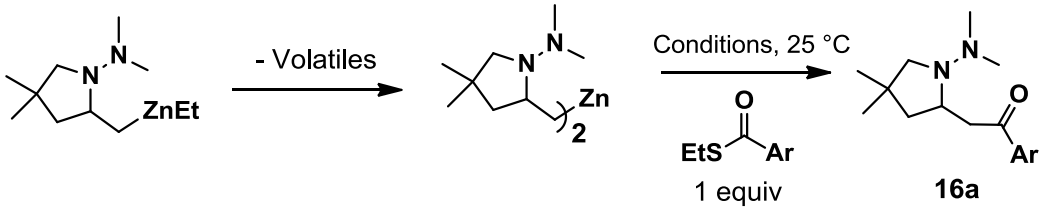
As a result of the conversion of substrate **13d** being so rapid at 90 °C, we ran a reaction at reduced temperature to see if we could favor kinetic control for the metalloamination (**Scheme 21**). To our delight, carrying out the reaction at 10 °C for 15 hours resulted in a 1:6 *cis*:*trans* ratio of cyclized intermediate **14d**[45] which can then be successfully allylated with preservation of stereochemistry. Heating of the stereoenriched organozinc intermediate **14d** made at 10°C may also be heated at 90 °C for 15 minutes to give a 1:1 *cis:trans* ratio, showing that this reaction is under equilibrium control. It bears note that stereocontrol of ß-monosubstituted substrates in ring closures is generally poor, and the good stereocontrol with a relatively small methyl group is of significant synthetic interest.

Scheme 21: Reversibility of Organozinc Intermediate **14d**



To further demonstrate electrophilic functionalization of the C-Zn bond, we sought to optimize conditions for acylation from organozinc intermediate **14a**. Our initial attempts at additive free or palladium(II)-catalyzed acylation with acid chlorides were met with failure[15], with ^{1}H NMR analysis shows no acylation at the desired carbon as well as ring opening of the organozinc intermediate. However, utilizing palladium(II) catalyst and aryl thioesters and the conditions of Fukuyama, azacyclic ketones were furnished[17]. Removal of volatiles prior to acylation was performed to remove excess diethylzinc from the solution and to minimize excess reagents, which results in simplified purification. Screening of various solvent systems and palladium sources previously used for these types of reactions resulted in the optimum conditions with the common $PdCl_2(PPh_3)_2$ catalyst in toluene (**Table 15**). Other sources of palladium resulted in lowered yields, particularly heterogeneous catalysts under their optimal mixed solvent systems[37]. The 67% conversion to the desired product is notable, as Fukuyama reactions regularly employ an excess of organozinc relative to the thioester to get good yields due to homocoupling of the organozinc being required to access Pd (0). As our system uses 10 mol% of $PdCl_2(PPh_3)_2$, at least 20%of the organozinc intermediate is lost before substitution in this fashion.

Table 15: Optimization of the Fukuyama Reaction from **13a**

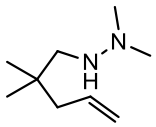
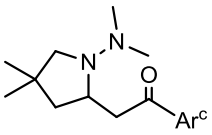
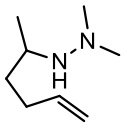
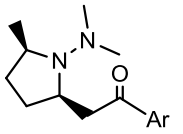
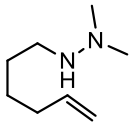
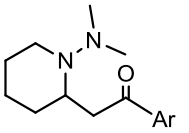


Solvent[a]	Catalyst	Mol% Cat.	t(>95%)[b]	% Yield[c]
THF	$PdCl_2(PPh_3)_2$	10	2.5 h	62%
Toluene	$PdCl_2(PPh_3)_2$	10	2.5 h	67%
Toluene/THF/DMA (62:34:4)	$PdCl_2(PPh_3)_2$	10	2.5 h	64%
Toluene/THF/DMA (62:34:4)	Pd/C, 5%	10	2.5 h	2%
Toluene/THF/DMA (62:34:4)	$PdCl_2$(dppf)•DCM	10	2.5 h	22%
Toluene/THF/DMA (62:34:4)	None	-	2.5 h	0%
Toluene/THF/DMA (62:34:4)	$PdCl_2$(dppf)•DCM, P(2-furyl)$_3$	10	2.5 h	0%
Toluene/THF/DMA (62:34:4)	$Pd_2(dba)_3$, 3 P(2-furyl)$_3$	5	2.5 h	1%

[a] 0.5 mL of solvent was used for each trial. [b] Percent loss of the organozinc intermediate as measured against the 4,4'-di-*t*-butyldiphenyl internal standard. [c] Percent yield calculated by comparison of 4,4'-di-*t*-butyldiphenyl internal standard peak against **16a** based on correction factors of the two purified separated compounds. [d] Ar = 4-*t*-BuPh

Following optimization of the Fukuyama procedure, a small substrate screening was carried out (**Table 16**). As in the case of the allylation, the *cis/trans* ratio of the organozinc intermediate was preserved upon acylation (**16b**). The reaction was also shown to work well to form piperidine **16f**. The formation of acylation product **16a** was also amenable to scale, giving a 63% yield in a 1 mmol scale reaction.

Table 16: Metalloamination/acylation of Hydrazinoalkenes

Hydrazinoalkene		Conversion [%][a]	d.r.	Product		Yield [%][d]
	**13a**	> 95 (18 h)[b]	---		**16a**	64
	**13b**	> 95 (6 h)[b]	>20:1 (*c/t*)		**16b**	61
	**13f**	> 95 (3 h)[b]	---		**16f**	61

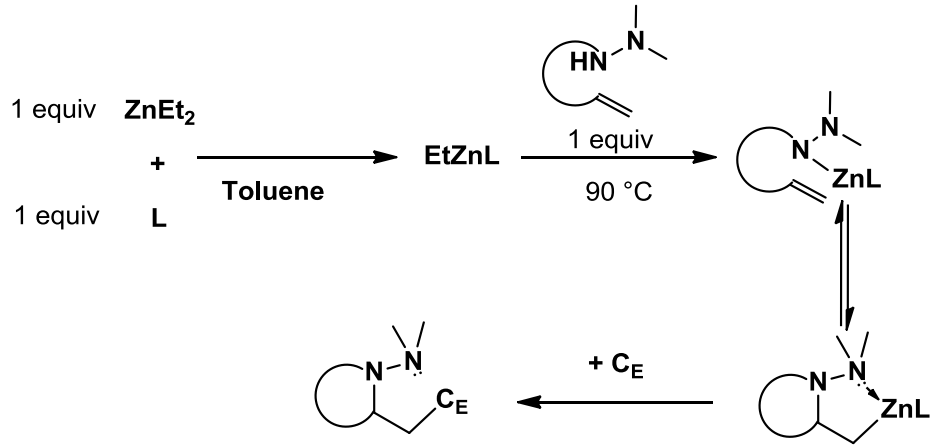
[a] As calculated from ^{1}H NMR spectra utilizing *p*-xylene as an internal standard. [b] All reactions conducted at a 0.1 mmol scale with toluene or (trifluoromethyl)benzene as solvent. [c] Ar = 4-*t*BuC_6H_4. [d] Isolated yield.

This research successfully demonstrates that commercially available diethylzinc can be used with hydrazinoalkenes to make organozinc pyrrolidine-type moieties. These zinc-pyrrolidine intermediates can successfully be either allylated or acylated to obtain formation of nitrogen-carbon bond in the formation of a heterocycle as well as a carbon-carbon bond formation in a single pot.

Chapter 5: Bidentate Anionic Ligands in the Zinc Metalloamination Reaction

Following our initial investigations in zinc metalloamination, our focus turned towards ligand design for the metalloamination reaction, with the intent of improving reactivity, diastereoselectivity, and inducing enantioselectivity through chiral ligands (**Scheme 22**). An ideal ligand for this reaction should be inexpensive and quickly accessible, due to its use being stoichiometric with zinc. The initial coordination of the ligand to diethylzinc should be rapid. The ligand should also allow the metalloamination ring closure for a wide variety of substrates, with the equilibrium should favor the ring closed organozinc over the zinc amide intermediate. Upon addition of an electrophile, the ligand shouldn't interfere with the substitution at the C-Zn bond, and subsequent workup of the product mixture should be trivial.

Scheme 22: General Zinc Ligand Screening Scheme

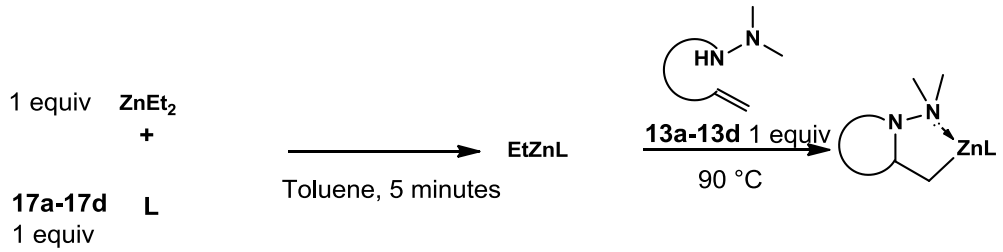


Following extensive ligand screenings, our attention became focused on anionic 1,3-dicarbonyl and ß-carbonyl-imine bidentate ligands (and their respective enol and

enamine tautomers). They satisfy many of the qualities of an ideal ligand for our system. Their coordination to diethylzinc is rapid (less than 5 minutes at room temperature to complete ligand complexation as observed by ^{1}H NMR), the compounds can be accessed by commercially available compounds in good yields, and their high polarity makes them easily separable by column chromatography from the far less polar cyclized products.

We initiated the study by evaluating ligands **17a-17d** (**Table 17**). The NAcNAc type ligand **17a** has seen regular use in organozinc chemistry[38], however for each of the substrates evaluated, the reaction was notably sluggish in its presence. ß-ketoenamine **17b** was better tolerated by comparison, with all substrates proceeding to at least 58% conversion. Amide-enamine **17c**, while sluggish, cyclized over 70% of each substrate. 1,3-bisamide **17d** was the fastest of these initial screenings, converting 84% of **13a** to a cyclized organozinc in just 57 hours.

Table 17: Screening of Miscellaneous Anionic Bidentate Ligands

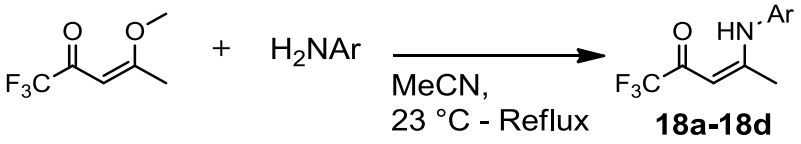


Substrates, t>90%[a] / Ligands	13a	13b	13d	13c
No Ligand	18 h	6 h	20 min	4 h
17a	96 h (14%)	96 h (16%)	96 h (32%)	96 h (57%)
17b	8.2 d (58%)	6.5 d (66%)	6.8 d	4.8 d (79%)
17c	9.5 d (73%)	7.6 d (70%)	7.7 d (74%)	4.8 d (87%)
17d	57 h (84%)	57 h (84%)	44 h (79%)	44 h (66%)

[a] Time to >90% conversion at 90 C as observed by ^{1}H NMR. For ligands that resulted in less than 90% conversion, the maximum obsered conversion percentage is listed in parentheses next to the time that percentage was observed.

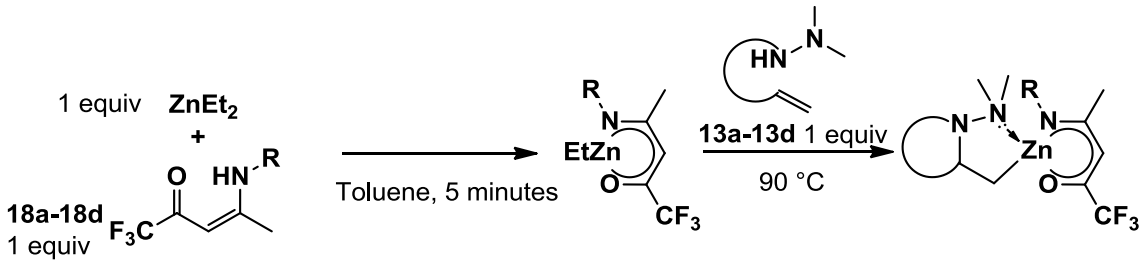
We next sought to evaluate aryl 1,1,1-trifluoroacetylenamines **18a-18d** for screening. These ligands can be accessed in high yields by combining the respective primary amine with 1,1,1-trifluoro-4-methoxypent-3-en-2-one in solvent, followed by recrystallization[39] (**Scheme 23**).

Scheme 23: Synthesis of Aryl 1,1,1-Trifluoroacetylenamines[39]



To our delight, **18a** showed good reactivity and substrate tolerance, with each substrate evaluated going nearly to completion (**Table 18**). Changing the electron-donating *para*-methyl of **18a** to the *para*-chloro of **18b** resulted in rate acceleration for substrates **13a** and **13b**, while rates for substrates **13c** and **13d** were slower by comparison. Substitution of chlorines in the *meta*-position of ligand **18c** resulted in good conversion overall, with t>90% rivaling the ligand free conditions for substrate **13c**. The sterically-constrained di*ortho*chloro-substituted **18d** was inferior to all other ligands screened of this type, with only substrate **13d** proceeding to at least 90% conversion.

Table 18: Results of 1,1,1-trifluoro-4-(amino)pent-3-en-2-one Ligands in Metalloamination



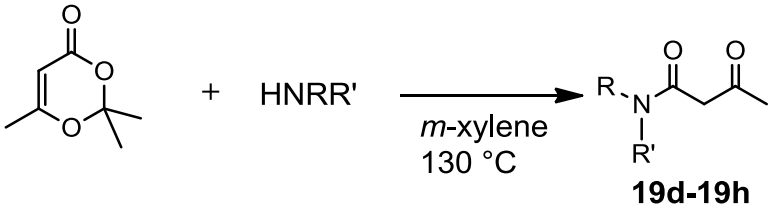
Ligands, R = \ Substrates, t>90%[a]	13a	13b	13d	13c
No Ligand	18 h	6 h	20 min	4 h
18a	144 h	40.4 h (86%)	5.6 h	5.4 h
18b	55.8 h	21 h	10.5 h	7.1 h
18c	88.5 h	11 h	7.1 h	5.1 h
18d	95 h (70%)	95 h (75%)	41.3 h	14.4 h (80%)

[a] Time to >90% conversion at 90 °C as observed by ^{1}H NMR. For ligands that resulted in less than 90% conversion, the maximum obsered percentage is listed in parentheses next to the time that percentage was observed.

In the course of our screenings, we also sought to evaluate 1,3-dicarbonyl type substrates starting with commercially available compounds **19a**-**19c** (**Table 19**). Neither acetylacetone **19a** nor 1,1,1-trifluoroacetylacetone **19b** resulted in any reasonable cyclization of substrate, however *N*,*N*-dimethylacetoacetamide **19c** had great utility as a

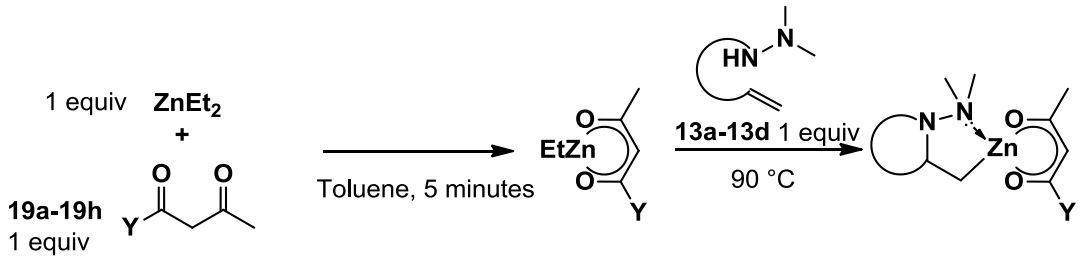
ligand, with good conversions of all substrates. Based on this result, we sought to further investigate *N*,*N*-disubstituted acetoacetamides leading us to synthesize **19d-19h**. Synthesis of these ligands required only the respective secondary alkene along with diketene acetone adduct in *m*-xylene at high temperature to obtain products in good yields following purification (**Scheme 24**).

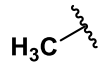
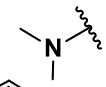
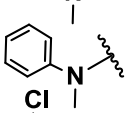
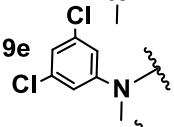
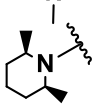
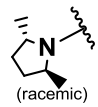
Scheme 24: Synthesis of *N*,*N*-disubstituted Acetoacetamide Ligands



N-methylphenyl substrate **19d** had very good reactivity, particularly having comparable metalloamination to the ligand-free system for substrates **13a** and **13b**. Adding electron-withdrawing groups to the aromatic ring, as in **19e**, resulted in significant rate suppression relative to **19d**. Piperidine and pyrrolidine-based ligands **19f** and **19g** were exceptional at cyclizing substrate **13a**, surpassing even the ligand-free trials. It bears note that **19g**'s requisite 2,5-*trans*-pyrrolidine can easily be accessed by group 3 metal hydroamination chemistry developed in these laboratories (**Scheme 2**)[6a], and addition of diketene acetone adduct to the crude reaction mixture following completion of hydroamination results in good yield of product and shows no presence of the 2,5-*cis* isomer by either ^{1}H NMR or GC analysis. **19g** may also be made chiral from chiral resolution, representing a potential chiral ligand for ring closure.

Table 19: Evaluation of 1,3-dicarbonyl Ligands **19a-19h**

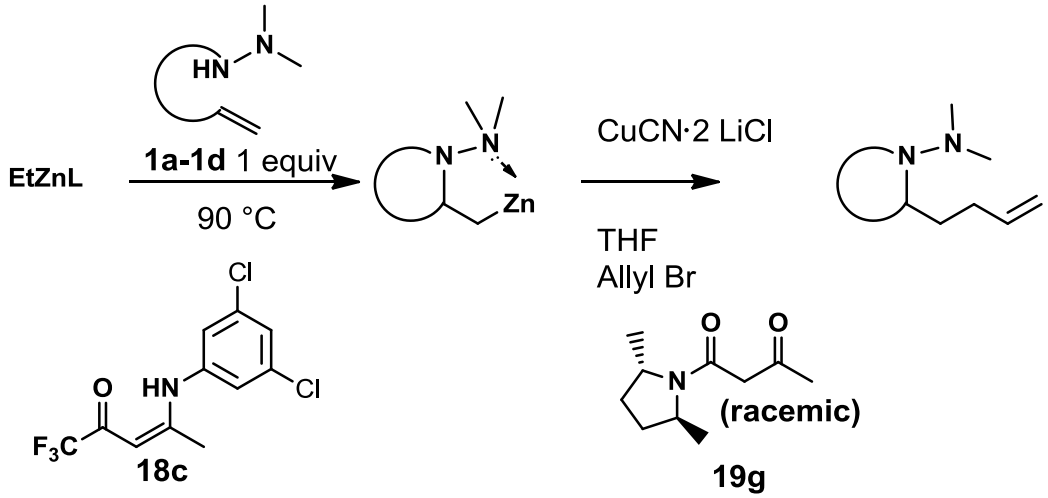


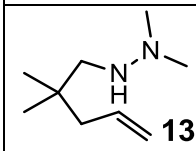
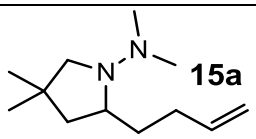
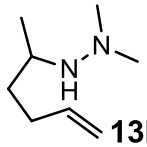
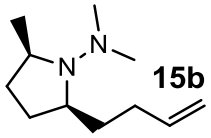
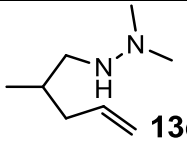
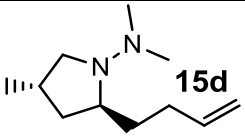
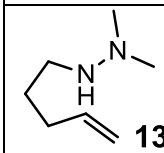
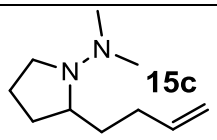
Ligands[b], Y =	Substrates, t>90%[a] 13a	13b	13d	13c
No Ligand	18 h	6 h	20 min	4 h
19a 	2 h (8%)	2 h (0%)	2 h (0%)	2 h (0%)
19b 	30 min (0%)	30 min (0%)	30 min (0%)	30 min (0%)
19c 	46 h	22 h	4.4 h	4.4 h (83%)
19d 	19.1 h	5.7 h	4.8 h	23 h (74%)
19e 	19 h (40%)	19 h (44%)	29 h (65%)	19 h (35%)
19f 	1.67 h	36 h (84%)	11.3 h	32.2 h (69%)
19g 	4.5 h	40 h (75%)	5.5 h (77%)	40 h (79%)
19h 	22.6 h	15.3 h (82%)	22.9 h	22.9 h (82%)

[a] Time to >90% conversion at 90 °C as observed by ^{1}H NMR. For ligands that resulted in less than 90% conversion, the maximum obsered conversion percentage is listed in parentheses next to the time that percentage was observed. [b] Ligands are represented in their keto form for ease of visualization, however most ligands exist as a mixture of keto and enol tautomers, with the keto form dominating.

Following these results, we sought to take representative examples from each the trifluoroaminopentenone series as well as the acetoacetamide series to verify that the organozincs can be intercepted by a carbon electrophile and the functionalized pyrrolidines isolated in comparative yields to those in the absence of ligands (**Table 20**). The workup for these reaction mixtures require slightly more manipulation than their ligand-free counterparts in that the product mixture must be pushed through silica (4:1 pentane:Et_2O) in order to separate the polar ligand from the nonpolar product. This filtrate is then subjected to standard conditions for formation of the TFA salt. The yields observed are reasonable, given the extra manipulation required to isolate the products as well as differing percent conversion in the case of the ligands.

Table 20: Metalloamination/allylation Utilizing Ligated Organozincs



Substrate	Product	No ligand	Ligand **18c**	Ligand **19g**
		Conversion: 18 h >95% Product Yield: 92%	Conversion: 88.5 h 90% Product Yield: 86%	Conversion: 4.5 h 90% Product Yield: 87%
		Conversion: 6 h >95% Product Yield: 81% >20:1 *t/c*	Conversion: 11 h 90% Product Yield: 76% 11:1 *t/c*	Conversion: 40 h 75% Product Yield: 58% 13:1 *t/c*
		Conversion: 20 min 90% Product Yield: 83% 1:1 *t/c*	Conversion: 7.1 h >90% Product Yield: 78% 1:1 *t/c*	Conversion: 5.5 h 77% Product Yield: 67% 1:1 *t/c*
		Conversion: 4 h >95% Product Yield: 80%	Conversion: 5.1 h 90% Product Yield: 75%	Conversion: 40 h 79% Product Yield: 65%

Conclusion

A thorough investigation into the formation of nitrogenous heterocycles through group 3 metal hydroamination and zinc (II) metalloamination has been performed. The hydroamination of primary aminoalkenes with group 3 metal trisamides tolerates ethereal solvents well, and in some cases these ethereal additives can even aid in accelerating the conversion to pyrrolidine products. New straightforward synthetic methods to access group 3 metal tris(bis(dimethylsilyl)amide) THF complexes as well as tris(*t*-butyltrimethylsilylamide)s have been developed. These new group 3 metal tris(*t*-butyltrimethylsilylamide)s show remarkable reactivity towards coordination of secondary amines and have been shown to be great catalysts for secondary aminoalkene hydroamination. The activity of these new amides is generally better than that of their respective group 3 metal tris(bis(trimethylsilyl)amide)s, and often show good catalytic activity at lowered temperatures.

Additionally, the zinc (II) metalloamination of hydrazinoalkenes has been carried out to form organozinc pyrrolidines and piperidines, which can then be allylated or acylated under optimized conditions by carbon electrophiles. Ligands for the zinc (II) metalloamination have also been developed that increase the rate of conversion for the reaction, and represent a future scaffold for diastereoselective and enantioselective ligands.

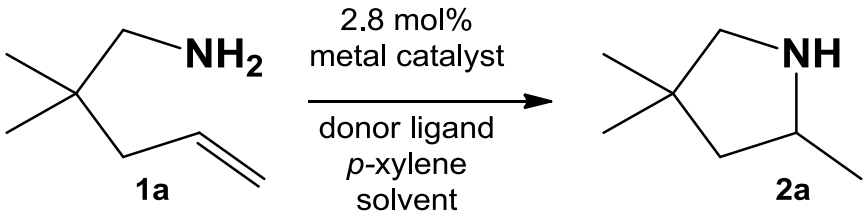
EXPERIMENTAL INFORMATION

Materials and Methods

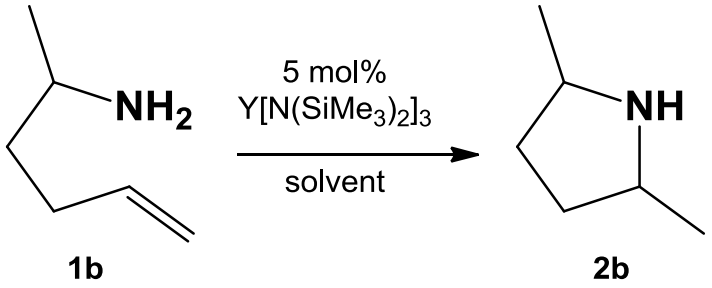
Reactions employed oven- or flame-dried glassware under nitrogen unless otherwise noted. J. Young NMR experiments were performed under an argon atmosphere, using standard Schlenk line techniques or in an argon-filled dry-box. THF and diethyl ether were distilled from sodium/benzophenone ketyl under nitrogen. Dichloromethane, diisopropylamine, trifluoromethylbenzene and toluene were distilled from CaH_2 under nitrogen. Benzene and *p*-xylene were distilled from potassium metal. 2,2-dimethyl-4-penten-1-amine **1a**[6a]**,** 1-methyl-4-penten-1-amine **1b**[6a], group 3 metal tris(bis(trimethylsilyl)amide)s **3a-3f**[46], group 3 metal tris(trimethylsilylmethyl) THF complexes **8b, 8d**[47], benzyl-(2,2-diemthyl-pent-4-enyl)-amine **11**[48], 2,2-dimethyl-4-pentenal[35], 2,2-dimethyl-4-pentenal-*N,N*-dimethylhydrazone[36], propionaldehyde-*N,N*-dimethylhydrazone[34], nacnac-*i*PrH **17a**[49], 4-(*N*-isopropylamino)pent-3-en-2-one **17b**[49], 1,3-di(piperidin-1-yl)propane-1,3-dione **17d**[50], 1,1,1-trifluoro-4-methoxy-3-penten-2-one[51], 1,1,1-trifluoro-4-(p-tolylamino)pent-3-en-2-one **18a**[39], 1,1,1-trifluoro-4-(p-chloroamino)pent-3-en-2-one **18b**[39], and *N,N*-diisopropyl-3-oxobutanamide **19h**[52] were prepared as previously reported. All other materials were used as received from commercial sources. Thin-layer chromatography (TLC) employed 0.25 mm glass silica gel plates with UV indicator and visualized with UV light (254 nm) or potassium permanganate staining. Flash chromatographic columns were packed with Merck silica gel 60 as a slurry in the initial elution solvent. Nuclear magnetic resonance (NMR) data

were obtained from Bruker DRX-300 (300 MHz) and Bruker DRX-500 (500 MHz). Infrared spectra (IR) were obtained from JASCO FTIR-4100. High-resolution mass spectra (HRMS) were obtained from Bruker MicroTOF with a Dart 100 – SVP 100 ion source (Ionsense Inc, Saugus, MA).

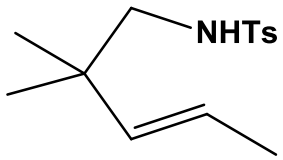
Chapter 1



Standard assay of 2,2-dimethyl-4-penten-1-amine (1a): In an argon-filled dry-box, $M[N(SiMe_3)_2]_3$ (0.009 mmol, 2.8 mol %) and solvent (0.5 mL) were combined in a J. Young NMR tube. *P*-xylene (17.0 mg, 0.16 mmol, 0.5 equiv.), donor ligand (0.045 mmol, 14 mol % or 0.009 mmol, 2.8 mol %), and **1a** (36 mg, 48 μL, 0.32 mmol) were then added. The resultant solution was held at temperature and monitored by ^1H NMR spectroscopy in the conversion to **2a**.



Diastereoselectivity Assay of 1-methyl-4-penten-1-amine (1b): In an argon-filled dry-box, $Y[N(SiMe_3)_2]_3$ **3b** (9.1 mg, 0.016 mmol), the appropriate solvent (0.5 mL), and 1-methyl-4-penten-1-amine **1b** (31.7 mg, 0.32 mmol) was added to a J. Young NMR tube. The tube was sealed, and the resulting solution was heated at 90°C and monitored by ^{1}H NMR spectroscopy. For the case where the solvent is methyl *t*-butyl ether, p-xylene (5.0 µL) was used as an internal standard. Percent conversions for hydroamination were calculated based on ^{1}H NMR integration of the vinyl peaks of **1b** relative to the aromatic resonance of the internal standard *p*-xylene. On reaction completion, the mixture in the J. Young NMR tube was poured into a 5 mL scintillation vial. Dichloromethane (1 mL) and trifluoroacetic acid (24.5 µL, 0.32 mmol) were added, and the mixture was stirred overnight. Volatiles were removed, and trans/cis selectivity of **2b•TFA** was measured via ^{1}H NMR.



***N*-(2,2-Dimethyl-pent-3-enyl)-p-toluenesulfonamide (4 Ts)** Following hydroamination in the presence of isomerizing additives (i.e. lithium *t*-butoxide, sodium *t*-butoxide, and hexamethylphosphoramide), the crude reaction mixture was diluted with dichloromethane (0.5 mL) and p-toluenesulfonyl chloride (61 mg, 0.32 mmol, 1.0 equiv.), and pyridine (31 µL, 0.38 mmol, 1.2 equiv.) were added. The yellow solution was stirred at 22 ºC for 2 h. The reaction mixture was diluted with dichloromethane (2 mL) and washed with 1 M HCl (2 mL). The aqueous layer was then extracted with

dichloromethane (2 X 2 mL). The organic layers were combined, dried over magnesium sulfate and concentrated. The residue was purified by column chromatography (silica gel, 5% ethyl acetate in hexanes for elution). **^{1}H NMR (300 MHz, $CDCl_3$)**, δ: 7.25 (d, 2 H, J = 7.8 Hz), 7.34 (d, 2 H, J = 8.1 Hz), 5.39 (dq, 1 H, J = 15.9, 6.6 Hz), 5.19 (d, 1 H, J = 15.9 Hz), 4.29 (t, 1 H, J = 6.0 Hz), 2.73 (d, 2 H, J = 6.0 Hz), 2.46 (s, 3 H), 1.67 (d, 3 H, J = 6.3 Hz), 0.99 (s, 6 H).**^{13}C NMR (125 MHz, $CDCl_3$),** δ: 143.3, 137.2, 136.9, 129.6, 127.08, 124.6, 53.0, 36.5, 25.07, 21.5, 18.1. **FTIR (neat),** cm-1: 3283, 2962, 2922, 2870, 2853, 1450, 1417, 1329, 1161, 1093, 1072, 971, 844, 815, 663, 552.

Chapter 2

$Nd[N(SiHMe_2)_2]_3(THF)_2$

Bis(tetrahydrofuran)-neodymium [III] tris[bis(dimethylsilyl)amide] (5a) 5a

In a glove box, $Nd[N(SiMe_3)_2]_3$ (10.0 mg, 0.016 mmol) was added to a J. Young NMR tube and dissolved in 0.5 mL of benzene-d_6. Tetrahydrofuran (3.46 mg, 0.048 mmol) and 1,1,3,3-tetramethyldisilazane (12.8 mg, 0.096 mmol) were then added, and the tube was sealed. The reactant mixture was placed in an oil bath maintained at 90°C and monitored by ^{1}H NMR. Upon completion of ligand exchange (5 minutes), the volatiles were removed on a Schlenk line (0.02 mmHg) to give **5a** (10.3 mg, 97%) as a light blue powder. The product was dissolved in benzene-d_6 to determine ^{1}H NMR data, which was identical to those described in the literature.

$Y[N(SiHMe_2)_2]_3(THF)_2$

Bis(tetrahydrfuran)-yttrium [III] tris[bis(dimethylsilyl)amide] (5b) 5b was synthesized in analogous fashion to **5a** utilizing $Y[N(SiMe_3)_2]_3$ (9.12 m g, 0.016 mmol) with ligand completion after 5 minutes to furnish **5b** (9.62 mg, 96%) as a white powder. ^{1}H NMR spectra were identical to those described in the literature. **Prep scale.** Tris(amide) $Y[N(SiMe_3)_2]_3$ (2.85 g, 5.0 mmol) was added to an oven-dried 100 mL Schlenk flask equipped with a magnetic stirring bar and an argon inlet. Toluene (35 mL), tetrahydrofuran (0.65 g, 50 mmol), and 1,1,3,3-tetramethyldisilazane (0.80 g, 30 mmol) were then added, and the flask was attached to a Schlenk line. The reactant mixture was heated at 90 °C under an argon atmosphere with stirring for 30 minutes and then cooled to -78 °C, whereupon the volatiles were removed under vacuum (0.02 mmHg) to give **5b** (3.05 g, 97%). ^{1}H NMR spectra were identical with those in the literature[7].

$Lu[N(SiHMe_2)_2]_3(THF)_2$

Bis(tetrahydrfuran)-lutetium [III] tris[bis(dimethylsilyl)amide] (5c) 5c was synthesized in analogous fashion to **5a** utilizing $Lu[N(SiMe_3)_2]_3$ (10.5 mg, 0.016 mmol) with ligand exchange complete after 1.67 hours at 90 °C to give **5c** (11.1 mg, 98%) as a white powder. ^{1}H NMR spectra were identical to those described in the literature[7].

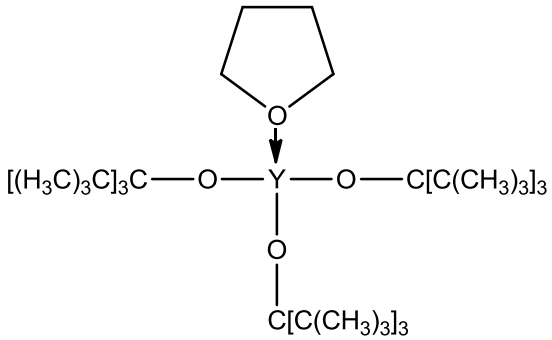
$Sc[N(SiHMe_2)_2]_3(THF)$

Tetrahydrfuran-scandium [III] tris[bis(dimethylsilyl)amide] (5d) 5d was synthesized in analogous fashion to **5a** utilizing $Sc[N(SiMe_3)_2]_3$ (9.12 mg, 0.016 mmol) with ligand exchange complete after 2.75 hours at 90 °C to give **5d** (7.9 mg, 96%) as a white powder. ^{1}H NMR spectra were identical to those described in the literature[7]. **^{1}H**

NMR (300 MHz, C_6D_6): δ 0.43 (36 H, m, –Si<u>C</u>H_3), 1.24 (4 H, m, THF), 3.93 (4 H, m, THF), 5.11 (6 H, h, Si<u>H</u>).

$$Sm[N(SiHMe_2)_2]_3(THF)_2$$

Bis(tetrahydrfuran)-samarium [III] tris[bis(dimethylsilyl)amide] (5e) 5e was synthesized in analogous fashion to **5a** utilizing $Sm[N(SiMe_3)_2]_3$ (10.1 mg, 0.016 mmol) with ligand exchange complete after 5 minutes at 90 °C to give **5e** (10.6 mg, 96%) as a white powder. ^{1}H NMR spectra were identical to those described in the literature. **1 mmol scale. 5e** was synthesized in a scaled-down analogous fashion to **5b** utilizing $Sm[N(SiMe_3)_2]_3$ (0.632g, 1.0 mmol) to furnish **5e** (0.676 g, 98%) as a light yellow powder. ^{1}H NMR spectra were identical to those described in the literature[7].



Tetrahydrofuran-tris[tri(*t*-butyl)methoxy]-yttrium [III] (6) In a glove box, $Y[N(SiMe_3)_2]_3$ (9.12 mg, 0016 mmol) and tri-*tert*-butylcarbinol (9.62 mg, 0.048 mmol) were dissolved in 0.5 mL of benzene-d_6. Tetrahydrofuran (3.46 mg, 0.048 mmol) and 1,1,3,3-tetramethyldisilazane (12.8 mg, 0.096 mmol) were then added. The reactant mixture was stored at ambient temperature and monitored by ^{1}H NMR, whereupon the formation of **6** was complete (38 h) and **6** was isolated in vacuo. The ^{1}H and ^{13}C NMR spectra were identical to those described in the literature[7]. **^{1}H NMR (C_6D_6):** δ 1.23 (4 H,

m, THF), 1.49 (81 H, s, CH_3), 4.11 (4 H, m, THF). **^{13}C NMR (C_6D_6):** δ 25.22 ppm (2 C, -CH_2-), 24.66 (27 C, -CH_3), 45.95 (9 C –$\underline{C}Me_3$), 73.36 (2 C, O-CH_2), 92.4 (3 C, O-C).

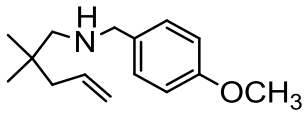
Chapter 3

$Y[N(t\text{-}Bu)SiMe_3]_3$

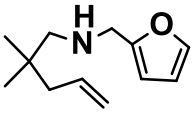
Yttrium [III] tris[*t*-butyltrimethylsilylamide] (7b) To a 25 mL Schlenk flask equipped with a stir bar in a glove box was added YCl_3 (0.195 g, 1.00 mmol) and lithium (*t*-butyl)trimethylsilylamide (0.454 g, 3.00 mmol). The flask was sealed with a Schlenk adapter and connected to a Schlenk line under argon. Through the sidearm under positive argon pressure was added diethyl ether (5 mL). The reaction was stirred for 18 h, then cooled to -78 °C via isopropanol / N_2 slush. The volatiles were evacuated overnight, and the solid residue was sublimed (0.001 mmHg, 110 °C) to obtain **7b** (0.176 g, 34%) as a white powder. **^{1}H NMR** (C_6D_6): δ 0.35 (27 H, SiCC$\underline{H}_3$), 1.44 (27 H, –CC$\underline{H}_3$). **^{13}C NMR** (126 MHz, C_6D_6): δ 54.41 , 35.91 , 4.64 .

$La[N(t\text{-}Bu)SiMe_3]_3$

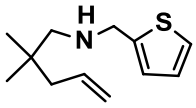
Lanthanum [III] tris[*t*-butyltrimethylsilylamide] (7f) The title compound was prepared in analogous fashion to **7b** utilizing $LaCl_3(THF)_{1.5}$ (1.06 g, 3.0 mmol), lithium (*t*-butyl)trimethylsilylamide (1.36 g, 9.0 mmol) and diethyl ether (5 mL) to obtain **7f** (1.44 g, 85%) as a white powder**. ^{1}H NMR** (300 MHz, C_6D_6) δ 1.39 (s, 27H, CC$\underline{H}_3$), 0.34 (s, 27H, SiCC$\underline{H}_3$). **^{13}C NMR** (126 MHz, C_6D_6) δ 54.40 , 35.29 , 4.52 .



***N*-(4-methoxybenzyl)-2,2-dimethylpent-4-en-1-amine (9a)** To a 25 mL round bottom flask equipped with a stir bar was added 2,2-dimethylpent-4-en-1-amine **1a** (0.50 g, 4.4 mmol), methanol (5 mL), and *p*-anisaldehyde (0.55 g, 4.0 mmol). The reaction was stirred at room temperature for 15 minutes, at which time the reaction was determined to be complete via GC. Sodium borohydride (0.16 g, 4.1 mmol) was added and the reaction was stirred overnight at room temperature. The reaction mixture was acidified with 3M HCl until a pH of 2, and extracted with ethyl acetate. The organic layer was dried ($MgSO_4$), concentrated in vacuo, and stored on calcium hydride overnight. Bulb-to-bulb distillation (110 °C, 0.5 mmHg) gave **9a** (0.83 g, 89%) as a clear oil. **^{1}H NMR** (300 MHz, $CDCl_3$) δ 7.25 (d, *J* = 8.5 Hz, 2H), 6.86 (d, *J* = 8.5 Hz, 2H), 5.97 – 5.67 (m, 1H), 5.24 – 4.85 (m, 2H), 3.80 (s, 3H), 3.72 (s, 2H), 2.35 (s, 2H), 2.02 (d, *J* = 7.4 Hz, 2H), 1.18 (s, 1H), 0.88 (s, 6H). **^{13}C NMR** (75 MHz, $CDCl_3$) δ 158.56 , 135.73 , 133.20 , 129.20 , 116.84 , 113.74 , 59.67 , 55.34 , 54.19 , 44.75 , 34.43 , 25.65 . **IR** (Film): 3331, 3072, 3000, 2954, 2906, 2869, 2833, 1638, 1612, 1585, 1512, 1465, 1441, 1363, 1301, 1247, 1173, 1107, 1038, 996, 913, 820, 576, 511, cm^{-1}. **HRMS** (ESI): Calcd for $C_{15}H_{23}NO$ $[M+H]^+$: 234.185o8, Found: 234.1940 .

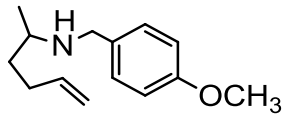


***N*-(furan-2-ylmethyl)-2,2-dimethylpent-4-en-1-amine (9b)** This compound was prepared in analogous fashion to **9a** utilizing 2,2-dimethylpent-4-en-1-amine **1a** (0.50 g, 4.4 mmol), methanol (5 mL), furfural (0.38 g, 4 mmol) , and sodium borohydride (0.16 g, 4.1 mmol) to furnish **9b** (0.61 g, 85%) as a clear oil. **^{1}H NMR** (300 MHz, Benzene-d_6) δ 7.14 (d, *J* = 10.8 Hz, 1H), 6.11 (dd, *J* = 3.1, 1.6 Hz, 1H), 6.02 (d, *J* = 3.1 Hz, 1H), 5.76 (ddt, *J* = 15.4, 10.8, 7.5 Hz, 1H), 5.18 – 4.84 (m, 2H), 3.61 (s, 2H), 2.22 (s, 2H), 1.95 (d, *J* = 7.5 Hz, 2H), 0.90 (s, 1H), 0.80 (s, 6H). ^{13}C NMR (75 MHz, Chloroform-*d*) δ 155.52 , 141.60 , 135.93 , 128.38 , 128.06 , 127.74 , 116.93 , 110.42 , 106.58 , 59.56 , 47.54 , 44.76 , 34.53 , 25.53 .**IR** (Film): 3074, 2956, 2822, 1638, 1506, 1469, 1387, 1363, 1147, 1112, 1077, 1009, 914, 884, 805, 733, cm^{-1}. **HRMS** (ESI): Calcd for $C_{12}H_{19}NO$ $[M+H]^+$: 194.1545 , Found: 194.1633 .

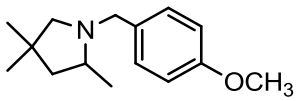


2,2-dimethyl-*N*-(thiophen-2-ylmethyl)pent-4-en-1-amine (9c) This compound was prepared in analogous fashion to **9a** utilizing 2,2-dimethylpent-4-en-1-amine **1a** (0.50 g, 4.4 mmol), methanol (5 mL), thiophene 2-carboxaldehyde (0.45 g, 4 mmol) , and sodium borohydride (0.16 g, 4.1 mmol) to give **9c** (0.65 g, 83%) as a clear oil. **^{1}H NMR** (300 MHz, Chloroform-*d*) δ 7.21 (dd, *J* = 4.7, 2.0 Hz, 1H), 6.95 (dd, *J* = 4.7, 3.0 Hz, 2H), 5.97 – 5.68 (m, 1H), 5.16 – 4.95 (m, 2H), 4.01 (s, 2H), 2.41 (s, 2H), 2.11 – 1.96 (m, 2H), 1.67 (br s, 1H), 0.90 (s, 6H). **^{13}C NMR** (126 MHz, Chloroform-*d*) δ 145.15 , 135.54 , 126.51 , 124.44 , 124.17 , 116.90 , 59.40 , 49.32 , 44.65 , 34.35 , 25.54 . **IR** (Film): 3072,

2955, 2870, 2817, 1638, 1468, 1438, 1388, 1363, 1163, 1109, 996, 913, 852, 823, 756, 696, cm^{-1}. **HRMS** (ESI): Calcd for $C_{12}H_{19}NS$ $[M+H]^+$: 210.1316 , Found: 210.1401 .



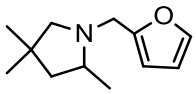
***N*-(4-methoxybenzyl)hex-5-en-2-amine (9d)** This compound was prepared in analogous fashion to **1a** utilizing 2-methylhex-5-en-2-amine **1b** (0.44g, 4.4 mmol), methanol (5 mL), *p*-anisaldehyde (0.55 g, 4.0 mmol), and sodium borohydride (0.16 g, 4.1 mmol) to furnish **9d** (0.72 g, 83%) as a light yellow oil. **^{1}H NMR** (500 MHz, $CDCl_3$) δ 7.26 (m, 2H), 7.01 – 6.68 (m, 2H), 5.80 (ddt, *J* = 16.8, 10.1, 6.5 Hz, 1H), 5.25 – 4.83 (m, 2H), 3.78 (s, 2H), 3.69 (d, *J* = 12.8 Hz, 2H), 2.71 (q, *J* = 6.5 Hz, 1H), 2.10 (dq, *J* = 16.5, 8.0 Hz, 2H), 1.61 (s, 1H), 1.45 (s, 1H), 1.11 (dd, *J* = 6.5, 2.5 Hz, 3H). ^{13}C NMR (126 MHz, Chloroform-*d*) δ 158.62 , 138.63 , 135.54 , 129.36 , 114.44 , 113.79 , 55.25 , 51.92 , 50.53 , 35.92 , 30.23 , 20.01 . **IR** (Film): 3074, 2958, 2930, 2833, 1640, 1612, 1585, 1512, 1464, 1442, 1301, 1247, 1173, 1038, 995, 910, 825, 750, 569, cm^{-1}. **HRMS** (ESI): Calcd for $C_{14}H_{21}NO$ $[M+H]^+$: 220.1701, found: 220.1763.



1-(4-methoxybenzyl)-2,4,4-trimethylpyrrolidine (10a) In a glove box, **9a** (23.3 mg, 0.1 mmol), catalyst (0.01 mmol, 10 mol%), and benzene-d_6 (0.5 mL) are added to a J. Young tube. The tube is sealed, and held at temperature until the reaction was determined

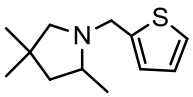
to be complete via ^{1}H NMR. The reaction mixture is diluted with diethyl ether, filtered through Celite, and concentrated in vacuo. Column chromatography (20% Ethyl acetate/Hexanes) gave the title compound as a clear oil. For the trial utilizing catalyst **7f**, 21.4 mg, 92%. **^{1}H NMR** (500 MHz, Chloroform-*d*) δ 7.22 (d, *J* = 7.6 Hz, 2H), 6.82 (d, *J* = 8.2 Hz, 2H), 3.93 (d, *J* = 12.8 Hz, 1H), 3.78 (s, 3H), 3.04 (d, *J* = 13.0 Hz, 1H), 2.59 (d, *J* = 7.5 Hz, 1H), 2.50 (s, 1H), 1.91 (d, *J* = 7.8 Hz, 1H), 1.69 (dd, *J* = 12.0, 7.2 Hz, 1H), 1.29 (s, 1H), 1.13 (s, 3H), 1.04 (s, 3H), 0.95 (s, 3H). **^{13}C NMR** (126 MHz, Chloroform-*d*) δ 158.34 , 132.00 , 129.78 , 113.40 , 76.74 , 68.23 , 59.58 , 57.24 , 55.20 , 49.12 , 35.26 , 30.58 , 29.25 , 19.40 . **IR** (Film): 3418, 2996, 2955, 931, 2866, 2834, 2777, 1613, 1585, 1512, 1464, 1373, 1300, 1248, 1179, 1171, 1119, 1100, 1039, 849, 822, 799, 750, 707, 687, 548, cm^{-1}. **HRMS** (ESI): Calcd for $C_{15}H_{23}NO$ $[M+H]^{+}$: 234.1858, Found: 234.1932

.



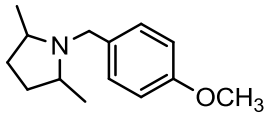
1-(furan-2-ylmethyl)-2,4,4-trimethylpyrrolidine (10b) In a glove box, **9b** (0.1 mmol), catalyst (0.01 mmol, 10 mol%), and benzene-d_6 (0.5 mL) are added to a J. Young tube. The tube is sealed, and held at temperature until the reaction was determined to be complete via ^{1}H NMR. The reaction mixture is diluted with diethyl ether, filtered through Celite, and cooled to 0 C. TFA (12 μL, 0.15 mmol) was added dropwise, and the mixture was stirred at room temperature for 1 hour, then concentrated in vacuo. The crude oil was purified by silica gel chromatography (100% EtOAc) to afford the TFA salt of pyrrolidine **10b** as a light yellow oil. For the trial with catalyst **3f**, the isolated yield was 25.9 mg (84%).**^{1}H NMR** (300 MHz, Chloroform-*d*) δ 12.90 (s, 1H), 7.48 (s, 1H), 6.56 (s,

1H), 6.43 (s, 1H), 4.33 (d, *J* = 15.1 Hz, 1H), 4.25 (d, *J* = 15.1 Hz, 1H), 3.53 (d, *J* = 11.5 Hz, 1H), 3.36 (s, 1H), 2.82 (d, *J* = 11.5 Hz, 1H), 1.85 (d, *J* = 9.0 Hz, 2H), 1.46 (d, *J* = 6.4 Hz, 3H), 1.18 (s, 4H), 0.93 (s, 3H). **^{13}C NMR** (75 MHz, Chloroform-*d*) δ 144.82 , 143.62 , 114.98 , 111.46 , 63.45 , 60.68 , 46.83 , 45.82 , 36.13 , 28.91 , 28.28 , 14.90 . **IR** (Film): 3437, 310, 2966, 2876, 2532, 1673, 1500, 1468, 1452, 1415, 1395, 1375, 1200, 1179, 1131, 1087, 1080, 1015, 935, 917, 830, 799, 751, 719, 600, cm^{-1}. **HRMS** (ESI): Calcd for $C_{12}H_{19}NO$ $[M+H]^+$: 194.1545 , Found: 194.1552 .



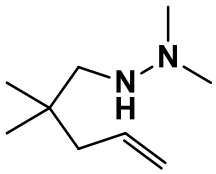
2,4,4-trimethyl-1-(thiophen-2-ylmethyl)pyrrolidine (10c) In a glove box, **9c** (20.9 mg, 0.1 mmol), catalyst (0.01 mmol, 10 mol%), and benzene-d_6 are added to a J. Young tube. The tube is sealed, and held at temperature until the reaction was determined to be complete via ^{1}H NMR. The reaction mixture is diluted with diethyl ether, filtered through Celite, and cooled to 0 C. TFA (12 μL, 0.15 mmol) was added dropwise, and the mixture was stirred at room temperature for 1 hour, then concentrated in vacuo. The crude oil was purified by silica gel chromatography (100% EtOAc) to afford the TFA salt of pyrrolidine **10c** as a light yellow oil. For the trial with catalyst **3d**, the isolated yield was 25.3 mg (79%). **^{1}H NMR** (300 MHz, Chloroform-*d*) δ 13.01 (s, 1H), 7.44 (d, *J* = 5.2 Hz, 1H), 7.21 (d, *J* = 3.7 Hz, 1H), 7.15 – 7.04 (m, 1H), 4.57 (d, *J* = 14.8 Hz, 1H), 4.40 (d, *J* = 14.8 Hz, 1H), 3.54 (d, *J* = 11.6 Hz, 1H), 3.41 (m, 1H), 2.82 (d, *J* = 11.6 Hz, 1H), 1.92 (s, 2H), 1.49 (d, *J* = 6.3 Hz, 3H), 1.23 (s, 3H), 0.99 (s, 3H). **^{13}C NMR** (75 MHz,

Chloroform-*d*) δ 132.48 , 129.16 , 128.92 , 128.09 , 63.31 , 60.44 , 48.06 , 46.87 , 35.99 , 29.07 , 28.33 , 15.20 . **IR** (Film): 3384, 3025, 2964, 2875, 1671, 1456, 1431, 1395, 1374, 1200, 1132, 1038, 912, 1038, 798, 719, 668, 649, cm^{-1}. **HRMS** (ESI): Calcd for $C_{12}H_{19}NS$ $[M+H]^+$: 210.1316 , Found: 210.1333 .

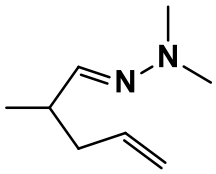


1-(4-methoxybenzyl)-2,5-dimethylpyrrolidine (10d) In a glove box, **9d** (21.9 mg, 0.1 mmol), catalyst (0.01 mmol, 10 mol%), and benzene-d_6 (0.5 mL) are added to a J. Young tube. The tube is sealed, and held at temperature until the reaction was determined to be complete via ^{1}H NMR. The reaction mixture is diluted with diethyl ether, filtered through Celite, and concentrated in vacuo. The crude oil was purified by silica gel chromatography (30% EtOAc/hexanes) to afford pyrrolidine **10d** as a light yellow oil. For the trial with catalyst **7f**, the isolated yield was 19.5 mg (89%). NMR data is shown for the *trans* isomer[45]. **^{1}H NMR** (300 MHz, Chloroform-*d*) δ 7.18 (d, *J* = 8.1 Hz, 2H), 6.82 (d, *J* = 8.1 Hz, 2H), 3.78 (s, 3H), 3.70 (s, 2H), 2.53 (m, *J* = 5.9 Hz, 2H), 1.74 (br s, 2H), 1.35 (br s, 2H), 1.06 (d, *J* = 5.9 Hz, 6H). **^{13}C NMR** (75 MHz, Chloroform-*d*) δ 165.16, 158.61 , 130.66 , 113.43 , 76.82 , 59.05 , 55.35 , 53.91 , 31.29 , 20.56 . **IR** (Film): 3063, 0958, 2928, 2868, 2833, 2808, 2065, 1511, 1458, 1371, 139, 1300, 1247, 1207, 1179, 1171, 1146, 1101, 1308, 948, 926, 820, 765, 749, cm^{-1}. **HRMS** (ESI): Calcd for $C_{14}H_{21}NO$ $[M+H]^+$: 220.1701 , Found: 220.1738 .

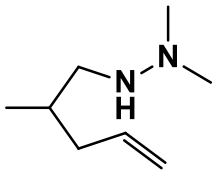
Chapter 4



2-(2,2-Dimethylpent-4-en-1-yl)-1,1-dimethylhydrazine (1a). A 100-mL, round-bottomed flask equipped with a magnetic stirring bar, an N_2 inlet and fitted with a reflux condenser was charged with $LiAlH_4$ (1.03 g, 27.1 mmol) and THF (40 mL) was subsequently added. The reactant mixture was cooled to 0 ^oC and a solution of 2,2-dimethyl-4-pentenal-*N*,*N*-dimethylhydrazone (2.79 g, 18.1 mmol) in THF (10 mL) was added dropwise. The reactant mixture was allowed to warm to room temperature and stirred for 30 min, followed by warming to a gentle reflux for 12 h. The resulting mixture was diluted with diethyl ether (25 mL) and cooled to 0 ^oC. Aqueous sodium hydroxide (15% w/v, 3.09 mL) was carefully added dropwise over 10 min with stirring, followed by warming to room temperature for 3 h. The white slurry was dried with $MgSO_4$ and filtered through a pad of Celite. After concentration the crude product was dried with CaH_2 and distilled in vacuo (23 ^oC, 0.5 torr) to afford 2.53g (89%) of the title compound as a clear liquid. **^{1}H-NMR** (500 MHz; C_6H_6): δ 6.01-5.95 (m, 1H), 5.18-5.15 (m, 2H), 2.62 (s, 2H), 2.35 (s, 6H), 2.16 (d, *J* = 7.5 Hz, 2H), 1.74 (d, *J* = 0.4 Hz, 1H), 1.02 (s, 6H). **^{13}C-NMR** (126 MHz; $CDCl_3$): δ 136.3, 117.0, 59.1, 47.9, 45.2, 34.5, 26.05, 26.01, 25.3 **IR** (Film): 3075, 2952, 2906, 2869, 2836, 2807, 2765, 1638, 1474, 1448, 912, cm^{-1} **HRMS** (ESI): Calcd for $C_9H_{20}N_2$ $[M+H]^+$: 157.1705, found: 157.1631.



2-(2-methylpent-4-enyl)-1,1-dimethylhydrazone (SI-1). The title compound was prepared following the procedure of Corey and Enders[34]. To a 100 mL flask equipped with a stir bar was added diisoproylamine (3.40 mL, 24.0 mmol) and tetrahydrofuran (35 mL). The flask was cooled to -78 °C, then *n*-butyllithium in hexanes (5.6 mL, 3.9 M), was added dropwise. The mixture was stirred for 5 minutes at -78 °C, then propionaldehyde *N*,*N*-dimethylhydrazone (2.00 g, 20.0 mmol) was added dropwise. The mixture was stirred for 2 hours at -78 °C, then allyl bromide (1.90 mL, 22.0 mmol) was rapidly added.. The mixture was stirred at -78 °C for 30 minutes, then warmed to 0 °C and stirred for 2 hours. The reaction mixture was Purification of the crude mixture was performed via flash chromatography in 15% ethyl acetate / hexanes (R_f = 0.35) to furnish the title compound (1.55 g, 55%) as a clear liquid. **^{1}H-NMR** (500 MHz, $CDCl_3$): δ 6.52 (d, *J* = 6.0 Hz, 1H), 5.84-5.75 (m, 1H), 5.06-5.00 (m, 2H), 2.76-2.67 (m, 6H), 2.44 (dt, *J* = 13.4, 6.7 Hz, 1H), 2.28-2.23 (m, 1H), 2.14-2.08 (m, 1H), 1.07 (dd, *J* =6.9, 1.4 Hz, 3H). **^{13}C-NMR** (126 MHz, $CDCl_3$): δ 136.67, 116.29, 43.55, 39.95, 25.09, 18.53. **IR** (Film): 3076, 2956, 2927, 2853, 2821, 2783, 1640, 1469, 1443, 1255, 1139, 1009, 911, 819 cm^{-1}. **HRMS** (ESI): Calcd for $C_8H_{16}N_2$ $[M+H]^+$: 197.2018, found 197.2058.

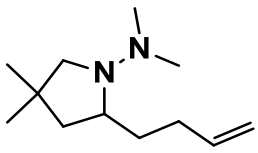


2-(2-methylpent-4-enyl)-1,1-dimethylhydrazine (13d). The title compound was prepared by the general procedure described for compound **13a** employing **SI-1** (1.16 g, 8.3 mmol) and $LiAlH_4$ (0.32 g, 8.3 mmol) to furnish the title compound (0.85 g, 72%) as a clear liquid. **^{1}H-NMR** (500 MHz, $CDCl_3$): δ 5.80 (ddt, *J* = 17.1, 10.0, 7.1 Hz, 1H), 5.04-4.99 (m, 2H), 2.71 (dd, *J* = 11.3, 5.9 Hz, 1H), 2.57 (dd, *J* = 11.3, 7.1 Hz, 1H), 2.19 (dt, *J* = 13.4, 6.9 Hz, 2H), 1.92 (dt, *J* = 14.2, 6.9 Hz, 1H), 1.76-1.69 (m, 1H), 0.93 (d, *J* = 6.7 Hz, 3H). **^{13}C-NMR** (126 MHz, $CDCl_3$): δ 139.39, 116.03, 54.85, 47.95, 39.66, 32.32, 18.24. **IR** (Film): 3076, 2976, 2838, 2809, 2765, 1640, 1484, 915, cm^{-1}. **HRMS** (ESI): Calcd for $C_8H_{18}N_2$ $[M+H]^+$: 143.1548, found 143.1517.

General Procedure for CuCN Mediated
Allylation of Metalloamination Intermediates:

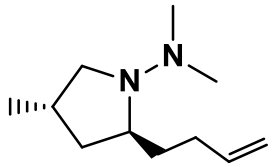
In an argon-filled glove box, $ZnEt_2$ in *p*-xylene (50 μL, 2.0 M, 0.10 mmol) and toluene or (trifluoromethyl)benzene (0.5 mL) were introduced into a J. Young NMR tube equipped with a Teflon screw cap, and hydrazinoalkene (**13a-13k**) (0.10 mmol) was subsequently added. The reactant mixture was heated in a 90 ^oC oil bath until metalloamination was complete (≥ 90% by ^{1}H NMR, *p*-xylene as internal standard). The volatiles were removed in vacuo and THF (0.5 mL) was introduced to the J. Young tube in an argon-filled dry box followed by the addition of a solution of CuCN•2LiCl in THF[7] (150 μL, 1.0 M, 0.15 mmol). After 5 min, allyl bromide (14.5 mg, 0.12 mmol) [or

methallyl chloride (10.9 mg, 0.12 mmol)] was added and the reactant mixture was kept at 23 ^{o}C for 2 h (or until the reaction was complete ≥95% ^{1}H NMR). The Teflon screw cap was removed and the reactant mixture transferred to a 10 mL test tube, diluted with diethyl ether (2.0 mL) and an aqueous solution of $NH_4Cl_{(sat)}$ and NH_3/H_2O (1:1 v/v, 2 mL) was subsequently added. The resulting suspension was vigorously stirred for 10 min until the aqueous layer developed a deep blue color. The organic layer was removed and washed with a second portion of NH_4Cl and NH_3/H_2O (1:1 v/v, 2 mL), followed by brine (2 mL) and dried with $MgSO_4$. The ether solution was then transferred to a 10-mL round-bottomed flask equipped with a magnetic stirring bar and a N_2 inlet and cooled to 0 ^{o}C. Trifluoroacetic acid (13.7 mg, 0.12 mmol) was added dropwise via gas-tight syringe and the reactant mixture was allowed to stir for 1 h. The volatiles were removed in vacuo and the resultant viscous oil was triturated with pentane (3 x 1 mL) to afford the trifluoroacetate salts **15a-15j**.



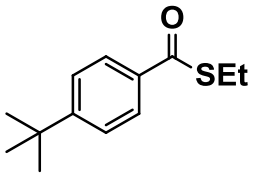
2-(But-3-en-1-yl)-*N*,*N*,4,4-tetramethylpyrrolidin-1-amine (15a R=H). The title compound was isolated as a light yellow oil, which slowly solidified upon storage. 28.6 mg (92%) **^{1}H-NMR** (500 MHz, C_6H_6): δ 5.77 (ddt, *J* = 17.0, 10.3, 6.7 Hz, 1H), 5.10-5.05 (m, 2H), 3.45 (tdd, *J* = 10.3, 6.8, 3.4 Hz, 1H), 3.37 (d, *J* = 10.8 Hz, 1H), 2.98 (d, *J* = 10.8 Hz, 1H), 2.75 (s, 6H), 2.23 (td, *J* = 13.5, 6.0 Hz, 1H), 2.18-2.11 (m, 1H), 2.04 (td, *J* = 14.4, 7.3 Hz, 1H), 1.96 (dd, *J* = 13.2, 6.7 Hz, 1H), 1.84-1.78 (m, 1H), 1.74 (dd, *J* =

13.0, 10.7 Hz, 1H), 1.24 (s, 3H), 1.20 (s, 3H). **^{13}C-NMR** (126 MHz, $CDCl_3$): δ 161.47, 161.16, 160.85, 160.54, 136.79, 116.59, 64.13, 56.11, 43.13, 41.04, 35.59, 30.59, 29.70, 29.43, 28.73. **IR** (Film): 3448 (b), 2968, 2875, 1674, 1463, 1409, 1197, 1132, cm^{-1}. **HRMS** (ESI): Calcd for $C_{12}H_{24}N_2$ $[M+H]^+$: 197.2018, found: 197.2058.



2-(But-3-en-1-yl)-*N*,*N*,4-trimethylpyrrolidin-1-amine (15d). The title compound was isolated as a mixture of diastereomers. Spectroscopic data is from a reaction conducted at 10 °C for 15 h to give a 6:1 *trans/cis* mixture of diastereomers[45]. Identification of the signals formally being *cis/trans* was by analogy from the similar ß-phenyl substituent **15e**'s nOe experiments. The title compound was isolated as a light yellow oil. 24.5 mg (83%). The reaction was also run on a 1 mmol scale at 10 °C for 15 h to give a 5.6:1 *trans/cis* mixture of diastereomers (251 mg, 85%). **^{1}H-NMR** (500 MHz, $CDCl_3$) δ 5.76 (ddt, J = 17.1, 10.6, 5.4 Hz, 1H, $CH_2C\underline{H}=CH_2$), 5.29 – 4.87 (m, 2H, $CH=C\underline{H_2}$), 3.48 – 3.34 (m, 2H), 3.34 – 3.22 (m, 1H), 2.75 (s, 6H, $N(CH_3)_2$ *trans isomer*), 2.68 (s, 6H, $N(CH_3)_2$ *cis isomer*), 2.35 – 2.14 (m, 4H), 2.07 (dt, J = 12.9, 6.7 Hz, 1H), 2.00 – 1.89 (m, 1H), 1.54 (q, J = 10.6 Hz, 1H), 1.16 (d, J = 6.1 Hz, 3H, $CHC\underline{H_3}$ *cis isomer*), 1.12 (d, J = 6.7 Hz, 3H, $CHC\underline{H_3}$ *trans isomer*)**.** **^{13}C NMR** (126 MHz, $CDCl_3$) δ 136.44 , 116.46 , 66.82 , 66.14 , 64.02 , 52.68 , 50.36 , 46.65 , 41.52 , 40.94 , 37.49 , 35.87 , 31.52 , 30.68 , 30.39 , 29.59 , 28.93 , 18.42 , 17.46 , 15.02. **IR** (Film): 3420 (b), 2974, 2936, 2882,

2524, 1780, 1673, 1461, 1200, 921, 798, 722, 705, cm^{-1}. **HRMS** (ESI): Calcd for $C_{11}H_{22}N_2$ $[M+H]^+$: 183.1861, found: 183.1778.

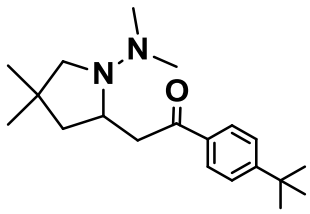


S-Ethyl 4-tert-butylbenzothioate (**SI-2**). The title compound was prepared following the procedure of Meshram and coworkers.[40] A 100-mL round-bottomed flask equipped with a magnetic stirring bar and an N_2 inlet was charged with zinc powder (0.654 g, 10 mmol), 4-tert-butyl-benzoyl chloride (1.8 mL, 10 mmol), toluene (40 mL), and ethanethiol (0.72 mL, 10 mmol). The reaction was stirred at 23 ^oC for 30 minutes, after which the mixture was filtered through Celite. The filtrate was washed with diethyl ether (2 x 5 mL) and concentrated in vacuo. The crude compound was purified by bulb to bulb distillation (85°C, 0.05 torr) to yield 2.05g (93%) of the title compound as a clear oil. **^{1}H-NMR** (300 MHz, C_6D_6): δ 8.12 (d, J = 8.7 Hz, 2H, ArH), 7.20 (d, J = 8.7 Hz, 2H, ArH), 2.97 (q, J = 7.4 Hz, 2H, $SC\underline{H}_2CH_3$), 1.21-1.14 (t, J = 7.4 Hz, 3H, $CH_2C\underline{H}_3$), 1.13 (s, 9H, $C(C\underline{H}_3)_3$). **^{13}C-NMR** (126 MHz, C_6D_6): δ 190.87, 156.77, 135.43, 125.82, 34.95, 31.01, 23.50, 15.06 . **IR** (Film): 2965, 1665, 1603, 1220, 1181, 1108, 917, 843, 731, 653 cm^{-1}. **HRMS** (ESI): Calcd for $C_{13}H_{18}OS$ $[M+H]^+$: 223.1157, found: 223.1125.

Synthesis of Cycles: General Procedure for
Fukuyama Coupling of Metalloamination Cycles

In an argon-filled glove box, $ZnEt_2$ in *p*-xylene (50 μL, 2.0 M, 0.10 mmol) and toluene or (trifluoromethyl)benzene (0.5 mL) were introduced into a J. Young NMR tube

equipped with a Teflon screw cap, and the indicated hydrazinoalkene **13a-13f** (0.10 mmol) was subsequently added. The reactant mixture was heated in a 90 ^{o}C oil bath until cyclization was complete (≥ 90% by ^{1}H NMR, *p*-xylene as internal standard). The volatiles were removed in vacuo and a THF/Toluene/dimethylacetamide mixture (0.5 mL 32:62:4 v/v/v) was introduced to the J. Young tube in an argon-filled dry box followed by bis(triphenylphosphine)palladium(II) dichloride (7.02 mg, 0.01 mmol) and S-ethyl 4-tert-butylbenzothioate **SI-2** (22.2 mg, 0.1 mmol). The reactant mixture was kept at 23 $^{\circ}$C until the reaction was judged complete by ^{1}H NMR. The Teflon screw cap was removed and the reactant mixture transferred with ethyl acetate to a scintillation vial, washed with saturated aqueous potassium carbonate (2 mL) and extracted with ethyl acetate (3 x 1 mL). The organic layer was dried with magnesium sulfate, filtered, and concentrated in vacuo. The crude residue was purified by silica gel chromatography (10% EtOAc/hexanes) to afford ketones **16a-16f**.



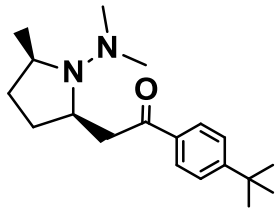
1-(4-(*tert*-Butyl)phenyl)-2-(1-(dimethylamino)-4,4-dimethylpyrrolidin-2-yl)ethanone (**16a)**. The title compound was prepared via the standard protocol of Fukuyama coupling to give a yellow oil. 20.2 mg (64%) . **^{1}H-NMR** (500 MHz, $CDCl_3$): δ 7.89 (d, *J* = 8.2 Hz, 2H, ArH), 7.45 (d, *J* = 8.2 Hz, 2H, ArH), 3.47 (dd, *J* = 15.4, 5.3 Hz, 1H, CHC<u>H</u>HC=O), 3.34 (t, *J* = 7.3 Hz, 1H, $CH_2C\underline{H}(N)CH_2$), 2.69 (dd, *J* = 15.4, 7.3 Hz,

1H, CHCH<u>H</u>C=O), 2.57 (d, *J* = 8.2 Hz, 1H, CC<u>H</u>HN), 2.36 (d, *J* = 8.2 Hz, 1H, CCH<u>H</u>N), 2.21 (s, 6H, N(C<u>H</u>$_3$)$_2$), 1.73 (dd, *J* = 12.6, 7.3 Hz, 1H, CCH<u>H</u>CH), 1.34 (s, 9H, C(C<u>H</u>$_3$)$_3$), 1.23 (dd, *J* = 12.6, 9.0 Hz, 1H, CCH<u>H</u>CH), 1.10 (s, 3H, CC<u>H</u>$_3$), 1.03 (s, 3H CC<u>H</u>$_3$). **^{13}C-NMR** (126 MHz, $CDCl_3$): δ 200.18, 156.12, 135.69, 128.18, 125.44, 58.15, 53.27, 44.54, 44.44, 39.84, 35.24, 34.53, 31.36, 31.00, 29.61. **IR** (Film): 2957, 2867, 1679, 1300, 1107, 1018, 800 cm^{-1}. **HRMS** (ESI): Calcd for $C_{20}H_{32}N_2O$ $[M+H]^+$: 317.2593, found: 317.2499.

1-(4-(*tert*-Butyl)phenyl)-2-(1-(dimethylamino)-4,4-dimethylpyrrolidin-2-yl)ethanone (16a) (1 mmol scale).

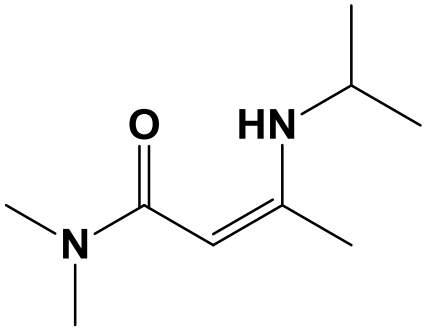
In an argon-filled glove box, a 10-mL Schlenk flask equipped with a magnetic stirring bar was charged with $ZnEt_2$ in *p*-xylene (0.50 mL, 2.0 M, 1.0 mmol), (trifluoromethyl)benzene (4 mL) and 2-(2,2-dimethylpent-4-en-1-yl)-1,1-dimethylhydrazine **13a** (156.2 mg, 1.0 mmol) was subsequently added. The reactant mixture was removed from the dry box, fitted with an N_2 inlet and placed in a 90 ^{o}C oil bath for 16 h. The volatiles were removed in vacuo, and the apparatus was pumped into an argon-filled glove box. To the reaction mixture was added a THF/Toluene/dimethylacetamide mixture (4.0 mL, 32:62:4 v/v/v) followed by bis(triphenylphosphine)palladium(II) dichloride (70.2 mg, 0.1 mmol) and **SI-2** (222 mg, 1.0 mmol). The reactant mixture was kept at 23 $^{\circ}$C overnight. The reactant mixture was transferred with ethyl acetate (10 mL) to a separatory funnel and washed with saturated aqueous potassium carbonate (2 x 10 mL) and the aqueous layer back-extracted with ethyl acetate (10 mL). The organic layer was dried with magnesium sulfate, concentrated,

and filtered in vacuo. The crude residue was purified by silica gel chromatography (10% EtOAc/hexanes) to afford **22 (**0.200 g, 63%) as a yellow oil. Spectral data was identical with that previously reported (vide supra).

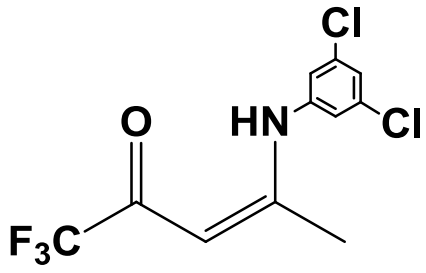


1-(4-(*tert*-Butyl)phenyl)-2-(1-(dimethylamino)-5-methylpyrrolidin-2-yl)ethanone (**16b)**. The title compound was prepared via the standard protocol of Fukuyama coupling to give a yellow oil. 18.6 mg (61%).**^{1}H NMR** (500 MHz, $CDCl_3$) δ 7.88 (d, *J* = 8.0 Hz, 2H, ArH), 7.45 (d, *J* = 8.0 Hz, 2H, ArH), 3.37 (d, *J* = 10.5 Hz, 2H, C(O)C$\underline{H}_2$CH), 3.17 – 2.91 (m, 1H, $CH_2C\underline{H}(CH_3)N$), 2.77 (dd, *J* = 15.7, 7.7 Hz, 1H, $CH_2C\underline{H}(CH_3)N$), 2.34 (s, 6H, $N(C\underline{H}_3)_2$), 1.83 (dd, *J* = 38.5, 8.6 Hz, 2H, 2 CHC$\underline{H}$HCH$_2$), 1.33 (s, 11H, $C(C\underline{H}_3)_3$; 2 CHCH$\underline{H}$CH$_2$), 1.14 (d, *J* = 4.8 Hz, 3H, CHC$\underline{H}_3$). **^{13}C-NMR** (126 MHz, $CDCl_3$): δ 199.70, 156.08, 135.52, 128.03, 125.42, 59.08, 52.51, 45.10, 40.52, 35.17, 31.28, 30.50, 27.45, 22.20. **IR** (Film): 2962, 2870, 1679, 1605, 1461, 1268, 1107, 1011, 822 cm^{-1}. **HRMS** (ESI): Calcd for $C_{19}H_{30}N_2O$ $[M+H]^+$: 303.2436, found: 303.2382.

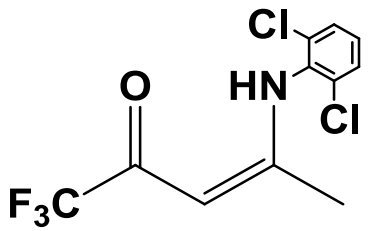
Chapter 5



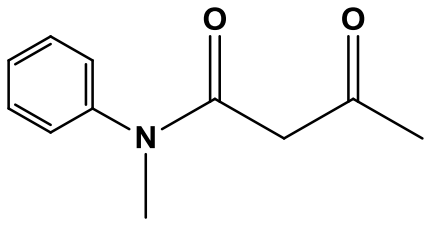
(Z)-3-(isopropylamino)-N,N-dimethylbut-2-enamide (17c) The title compound was prepared following the procedure of Nakamura et al[53]. A 25 mL flask equipped with a magnetic stirring bar and an N_2 inlet was charged with isopropylamine (0.75 mL, 8.3 mmol), hexanes (7.5 mL), *N*,*N*-dimethylacetoacetamide (0.93 mL, 7.5 mmol), and 4Å mol sieves (1.25 g). This mixture was stirred for 50 ^{o}C for 6 hours whereupon the reaction was determined complete by TLC. The mixture was cooled to room temperature, filtered through celite, and the celite was washed with ethyl acetate. The filtrate was concentrated in vacuo, then purified by bulb-to-bulb distillation (50 ^{o}C, 0.02 torr) to give **17c** (1.03 g, 81%) as a light yellow liquid entirely as the enamine tautomer. **^{1}H NMR** (500 MHz, Chloroform-*d*) δ 9.51 (s, 1H, N<u>H</u>), 4.49 (s, 1H, C(O)C<u>H</u>=C), 3.65 (sex, *J* = 6.3 Hz, 1H, NC<u>H</u>$(CH_3)_2$), 2.93 (s, 6H N$(C\underline{H_3})_2$), 1.95 (s, 3H, =C(N)-C<u>H_3</u>), 1.19 (d, *J* = 6.3 Hz, 6H). **^{13}C NMR** (126 MHz, Chloroform-*d*) δ 171.18 , 158.08 , 80.85 , 43.97 , 24.14 , 19.64 . **IR** (Film): 3123, 2967, 2927, 2873, 1611, 1583, 1513, 1442, 1380, 1364, 1308, 1148, 1012, 773, 690, 641, 557, cm^{-1} . **HRMS** (ESI): Calcd for $C_9H_{18}NO_2$ $[M+H]^+$: 171.1497, found: 171.1588.



(Z)-4-((3,5-dichlorophenyl)amino)-1,1,1-trifluoropent-3-en-2-one (18c) The title compound was prepared following the procedure of Patil [39]. To a 25 mL flask is added 1,1,1-trifluoro-4-methoxypent-3-en-2-one (0.88 g, 5.3 mmol), 3,5-dichloroaniline (0.81 g, 5.0 mmol) and acetonitrile (10 mL) The mixture was refluxed overnight, then the volatiles were removed in vacuo. Trituration with pentane followed by removal of filtrate gave **18c** (1.05 g, 88%) as a brown powder. **^{1}H NMR** (300 MHz, Chloroform-*d*) δ 12.47 (s, 1H, N<u>H</u>), 7.32 (s, 1H, Ar-H), 7.10 (s, 2H, Ar-H), 5.59 (s, 1H, C(O)C<u>H</u>=C), 2.16 (s, 3H, C<u>H</u>$_3$). **^{13}C NMR** (75 MHz, Chloroform-*d*) δ 177.79 (q, <u>C</u>F$_3$), 167.01 , 139.14 , 135.95 , 127.57 , 123.82 , 119.19 , 115.38 , 92.16 , 77.58 , 77.16 , 76.74 , 20.54 .**^{19}F NMR** (282 MHz, Chloroform-*d*) δ -76.91. **IR** (Film): 3079, 3004, 2967, 1621, 1584, 1566, 1442, 1384, 1360, 1301, 1243, 1191, 1142, 1112, 1014, 989, 879, 847, 805, 781, 735, 657, 583, cm^{-1} **HRMS** (ESI): Calcd for $C_{11}H_8Cl_2F_3NO$ $[M+H]^+$: 298.0013, found: 298.0045.

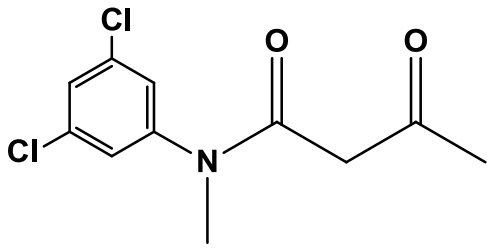


(Z)-4-((2,6-dichlorophenyl)amino)-1,1,1-trifluoropent-3-en-2-one (18d) The title compound was prepared in analogous fashion to **18c** using 1,1,1-trifluoro-4-methoxypent-3-en-2-one (0.88 g, 5.3 mmol), 2,6-dichloroaniline (0.81 g, 5.0 mmol) and acetonitrile (10 mL) and requiring overnight reflux. Recrystallization from ethanol gave **18d** (0.95 g, 64%) as yellow crystals. **^{1}H NMR** (300 MHz, Chloroform-*d*) δ 12.03 (s, 1H, NH), 7.45 (d, *J* = 8.0 Hz, 2H, Ar H), 7.31 (d, *J* = 8.0 Hz, 1H, Ar H), 5.64 (s, 1H, C(O)CH=C), 1.92 (s, 3H, CH_3). **^{13}C NMR** (75 MHz, Chloroform-*d*) δ 178.00 (q, CF_3) , 169.41 , 134.54 , 133.05 , 130.07 , 128.93 , 119.33 , 91.00 , 19.81 . **^{19}F NMR** (282 MHz, Chloroform-*d*) δ -76.79. **IR** (Film): 3130, 3018, 1625, 1578, 1562, 1521, 1440, 1295, 1234, 1189, 1135, 1118, 1066, 950, 780, 721, 586, cm^{-1} **HRMS** (ESI): Calcd for $C_{11}H_8Cl_2F_3NO$ $[M+H]^+$: 298.0013, found: 297.9999.



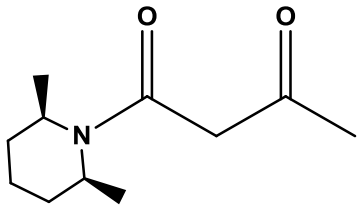
***N*-methyl-3-oxo-*N*-phenylbutanamide (19d)**: The title compound was prepared following the procedure of Pérez[54]. To a 25 mL round bottom flask equipped with a stir bar and a N_2 inlet was added *N*-methylaniline (0.75 g, 7.0 mmol) and *p*-xylene (5 mL).

The reaction is heated to 120 °C, then diketene acetone adduct (1.00 g, 7.0 mmol) was added dropwise. The reaction was kept at 120 °C for 90 minutes, then cooled to room temperature. The solvent was removed in vacuo, and the crude residue was distilled via bulb-to-bulb distillation (80 °C, 0.02 Torr) to give **19d** (1.07 g, 81%) as a yellow oil. Dilute in chloroform-*d* (15 mg **19d** in 0.5 mL $CDCl_3$), the compound exists entirely as its keto tautomer, while in high concentration in chloroform-*d* (150 mg **19d** in 0.5 mL $CDCl_3$), the compound exhibits a 76:24 keto:enol ratio. Signals specific either to the keto or enol tautomer are noted in spectra. **^{1}H NMR** (500 MHz, Chloroform-*d*) 14.2 (s, 1H, O<u>H</u> enol), 7.38 (t, 2H, Ar<u>H</u>), 7.32 (t, 1H, Ar<u>H</u>), 7.16 (d, 2H, ArH), 4.63 (s, 1H, C(O)C<u>H</u>=C enol), 3.25 (overlapping s, 5H, NC<u>H$_3$</u> + C(O)C<u>H$_2$</u>C(O) keto), 2.05 (s, 3H, C<u>H$_3$</u> keto), 1.74 (s, 3H, C<u>H$_3$</u> enol). **^{13}C NMR** (126 MHz, Chloroform-*d*) δ 202.31 , 171.78 , 166.62 , 143.51 , 143.30 , 129.90 , 129.62 , 128.25 , 127.60 , 127.30 , 127.18 , 88.85 , 49.86 , 37.25 , 36.31 , 30.29 , 21.62 . **IR** (Film): 3061, 2922, 1721, 1656, 1594, 1496, 1379, 1341, 1300, 1190, 1162, 1124, 1074, 1026, 924, 776, 701, cm^{-1} **HRMS** (ESI): Calcd for $C_{11}H_{13}NO_2$ $[M+H]^+$: 192.1025, found: 192.1138.



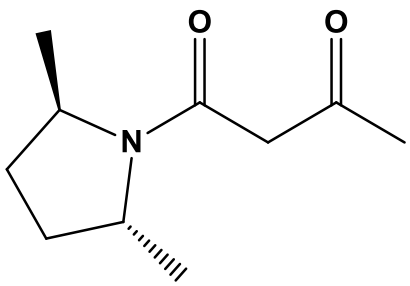
***N*-(3,5-dichlorophenyl)-*N*-methyl-3-oxobutanamide (19e**): The title compound was prepared in analogous fashion to **19d** utilizing *N*-(3,5-dichloromethyl)-*N*-methylamine (1.00 g, 5.7 mmol), *p*-xylene (5 mL), and diketene acetone adduct (0.81 g,

5.7 mmol). The crude residue was purified by flash chromatography in 25% ethyl acetate / hexanes (R_f = 0.35 of major spot, 0.05 of minor spot) to give **19e** (1.00 g, 68%) as an off-white crystalline solid. At high concentration in chloroform-*d* (100 mg in 0.5 mL $CDCl_3$), the compound exhibits a 49:21:30 keto:enol A: enol B ratio. At an alternative concentration (50 mg in 0.5 mL $CDCl_3$), the compound exhibits a 48:16:36 keto:enol A: enol B ratio by ^{1}H NMR; each spectra were used in tandem to associate signals with each compound. Signals specific either to the keto or enol tautomers are noted below. **^{1}H NMR** (300 MHz, Chloroform-*d*) δ 16.63 (s, 1H, O<u>H</u>, enol A), 14.02 (s, 1H, O<u>H</u>, enol B), 7.31 (overlapping s, 1H, Ar<u>H</u>), 7.10 (s, 2H, Ar<u>H</u>), 5.89 (s, 1H, C(O)C<u>H</u>=C, enol A), 4.68 (s, 1H, C(O)C<u>H</u>=C, enol B), 3.29 (s, 1H, C(O)C<u>H$_2$</u>C(O), keto), 3.22 (s, 3H, NC<u>H$_3$</u>, keto and enol B), 2.58 (s, 3H, NC<u>H$_3$</u>, enol A), 2.22 (s, 3H, C<u>H$_3$</u>, enol A), 2.12 (s, 3H, C<u>H$_3$</u>, keto), 1.81 (s, 3H, C<u>H$_3$</u>, enol B). **^{13}C NMR** (126 MHz, Chloroform-*d*) δ 201.87 , 181.12 , 175.34 , 171.56 , 169.16 , 166.16 , 145.39 , 145.28 , 136.04 , 135.68 , 128.71 , 127.92 , 126.22 , 126.17 , 101.49 , 88.45 , 77.38 , 49.78 , 37.34 , 36.45 , 30.57 , 30.11 , 21.84 , 20.75 . **IR** (Film): 3074, 2923, 1723, 1664, 1636, 1569, 1474, 1439, 1334, 1294, 1145, 1108, 995, 929, 858, 803, 776, 725, 693, cm^{-1} **HRMS** (ESI): Calcd for $C_{11}H_8Cl_2NO_2$ $[M+H]^+$: 260.0245, found: 260.0413.



1-(2,6-*cis*-dimethylpiperidin-1-yl)butane-1,3-dione (19f): The title compound was prepared following the procedure of Pérez[54]. To a 25 mL round bottom flask equipped with a stir bar and a N_2 inlet was added 2,6-*cis*-dimethylpiperidine (0.650 g, 5.68 mmol) and *m*-xylene (5 mL). The reaction is heated to 120 °C, then diketene acetone adduct (0.81 g, 5.68 mmol) was added dropwise. The reaction was kept at 120 °C for 90 minutes, then cooled to room temperature. The solvent was removed in vacuo, and the crude residue was distilled via bulb-to-bulb distillation (72 °C, 0.02 Torr) to give **19f** (0.87 g, 78%) as a yellow oil. Dilute in chloroform-*d* (15 mg **19f** in 0.5 mL $CDCl_3$), the compound exists entirely as its keto tautomer, while in high concentration in chloroform-*d* (150 mg **19f** in 0.5 mL $CDCl_3$), the compound exhibits a 65:35 keto:enol ratio. Signals specific either to the keto or enol tautomer are noted below. **^{1}H NMR** (500 MHz, Chloroform-*d*) δ 15.23 (s, 1H, O<u>H</u>, enol), 5.11 (s, 1H, C(O)C<u>H</u>=C, enol), 4.75 (s, 1H, C(O)C<u>H</u>HC(O), keto), 4.00 (s, 1H, C(O)CH<u>H</u>C(O), keto), 3.50 (d, *J* = 27.3 Hz, 2H), 2.26 (s, 3H, C(O)C<u>H$_3$</u>, keto), 1.93 (s, 3H, =C(OH)C<u>H$_3$</u>, enol), 1.86 – 1.71 (m, 1H), 1.60 (q, *J* = 13.7, 10.4 Hz, 4H), 1.48 (dt, *J* = 13.7, 3.4 Hz, 1H), 1.22 (app dd, *J* = 10.4, 8.2 Hz, 6H, CHC<u>H$_3$</u>). **^{13}C NMR** (126 MHz, Chloroform-*d*) δ 203.23 , 175.19 , 171.58 , 166.00 , 87.09 , 50.42 , 48.59 , 44.14 , 30.31 , 29.89 , 22.32 , 21.79 , 21.13 , 20.61 , 13.98 , 13.85 . **IR** (Film): 3061, 2922, 1721, 1656, 1594, 1496, 1379, 1341, 1300, 1190, 1162, 1124, 1074,

1026, 924, 776, 701, cm^{-1} **HRMS** (ESI): Calcd for $C_{11}H_{13}NO_2$ $[M+H]^+$: 192.1025, found: 192.1138.



1-(*trans*-2,5-dimethylpyrrolidin-1-yl)butane-1,3-dione (19g): To a J. Young tube equipped with a Teflon screw cap was added scandium tris[bis(trimethylsilyl)amide] **3b** (52.6 mg, 0.05 mmol), N^1,N^2-bis(2-isopropylphenyl)ethane-1,2-diamine (29.6 mg, 0.05 mmol) and toluene (0.5 mL). The Teflon cap was sealed, and the mixture heated in a 150 °C oil bath for 3 hours until ligand exchange was judged complete by ^{1}H NMR. The tube was then cooled to room temperature, then 1-methylaminopent-4-ene **1b** (99.2 mg, 1.00 mmol) was added. The reaction mixture was kept in a 10 °C cooling bath until hydroamination of the aminoalkene was judged complete by ^{1}H NMR. This mixture was warmed to room temperature, then diketene acetone adduct (142 mg, 1.00 mmol) was added. The reaction was heated in a 120 °C bath until judged complete by ^{1}H NMR. The tube was cooled to room temperature, then the contents transferred into a flask with diethyl ether and the mixture was concentrated in vacuo. The crude residue was purified via column chromatography with 30% ethyl acetate / hexanes (R_f = 0.23) to give **19g** (117 mg, 64%) as a yellow oil. GC analysis suggests a >20:1 ratio of *trans/cis*. **^{1}H NMR** (500 MHz, Chloroform-*d*) δ 14.88 (s, 1H, O<u>H</u>, enol), 4.91 (s, 1H, C(O)C<u>H</u>=C, enol), 4.20

(m, 1H, C(O)C<u>H</u>HC(O) , keto; $CH_2C\underline{H}(CH_3)N$, enol), 3.91 (m, 1H, C(O)C<u>H</u>HC(O) , keto; $CH_2C\underline{H}(CH_3)N$, enol), 3.60 – 3.27 (m, 2H, $CH_2C\underline{H}(CH_3)N$, keto), 2.26 (s, 3H, $C(O)C\underline{H}_3$, keto), 2.22 – 1.99 (m, 2H,2 $CHC\underline{H}HCH_2$), 1.89 (s, 3H, $=C(OH)C\underline{H}_3$, enol), 1.54 (dd, *J* = 36.4, 8.2 Hz, 2H, 2 $CHCH\underline{H}CH_2$), 1.15 (s, 6H, $CHC\underline{H}_3$). **^{13}C NMR** (126 MHz, Chloroform-*d*) δ 203.11 , 174.00 , 170.22 , 164.95 , 89.83 , 77.16 , 54.28 , 53.47 , 53.09 , 52.67 , 51.22 , 30.86 , 30.55 , 30.43 , 29.20 , 29.12 , 21.96 , 21.91 , 20.95 , 19.46 , 18.94 . **IR** (Film): 2969, 2930, 2877, 1721, 1639, 1587, 1481, 1432, 1407, 1380, 1350, 1206, 1168, 1030, 779, 718, 549, cm^{-1}. **HRMS** (ESI): Calcd for $C_{10}H_{17}NO_2$ $[M+H]^+$: 184.1338, found: 184.1441.

REFERENCES CITED

1. Hultzsch, K. C. *Org. Biomol. Chem.* **2005**, *3*, 1819-1824.

2. Gagné, M. R.; Marks, T. J. *J. Am. Chem. Soc*. **1989**, *111*, 4108-4109.

3. Aspinall, H. C. Chemistry of the f-Block Elements. In *Advanced Chemistry Texts;* Phillips, D., Ed.; Gordon and Breach: Amsterdam, 2001: Vol. 5.

4. Kim, Y. K.; Livinghouse, T.; Bercaw, J. E. *Tetrahedron Lett.* **2001**, *42*, 2933-2935.

5. (a) Aillaud, I.; Collin, J.; Hannedouche, J.; Schulz, E. *Dalton Trans.* **2007**, 5105-5118. (b. Gribkov, D. V.; Hultzsch, K. C.; Hampel, F. *J. Am. Chem. Soc.* **2006**, *128*, 3748-3759.

6. (a) Kim, J. Y.; Livinghouse, T. *Org. Lett.* **2005**, *7*, 4391-4393. (b) Kim, J. Y.; Livinghouse, T. *Org. Lett.* **2005**, *7*, 1737-1739.

7. Herrmann, W. A.; Anwander, R.; Munck, F. C.; Scherer, W.; Defaud, V.; Huber, N.W.; Artus, G. R. J. *Naturforsch.* **1994**, *49b*, 1789-1797.

8. Hultzsch, K. C.; Hampel, F.; Wagner, T. *Organometallics* **2004**, *23*, 2601-2612.

9. Huynh, K.; Livinghouse, T.; Lovick, H. M. *Synlett* **2014**, *25*, 1721-1724.

10. Wolfe, J. P. *Eur. J. Org. Chem.* **2007**, 571-582 and references therein.

11. (a) McGrane, P. L.; Livinghouse, T. *J. Org. Chem.* **1992**, *57*, 1323-1324. (b) McGrane, P. L.; Jensen, M.; Livinghouse, T. *J. Am. Chem. Soc.* **1992**, *114*, 5459-5460. (c) McGrane, P. L.; Livinghouse, T. *J. Am. Chem. Soc.* **1993**, *115*, 11485-11489.

12. (a) Bertrand, M. B.; Neukom, J. D.; Wolfe, J. P. *J. Org. Chem.* **2008,** *73*, 8851-8860. (b) Lemen, G. S.; Giampietro, N. C.; Hay, M. B.; Wolfe, J. P. *J. Org. Chem.* **2009**, *74*, 2533-2540. (c) Rosen, B. R.; Ney, J. E.; Wolfe, J. P. *J. Org. Chem.* **2010**, *75*, 2756-2759. (d) Mai, D. N.; Wolfe, J. P. *J. Am. Chem. Soc.* **2010**, *132*, 12157-12159. (e) Ward, A. F.; Wolfe, J. P. *Org. Lett.* **2011**, *13*, 4728-4731. (f) Nicolai, S.; Piemontesi, C.; Waser, J. *Angew. Chem. Int. Ed.* **2011**, *50*, 4680-4683. (g) Nicolai, S.; Waser, J. *Org. Lett.* **2011**, *13*, 6324-6327. (h) Nicolai, S.; Sedigh-Zadeh, R.; Waser. J. *J. Org. Chem.* **2013**, *78*, 3783-3801.

13. Ham, W.-H.; Jung, Y. H.; Lee, K.; Oh, C.-Y.; Lee, K.-Y. *Tetrahedron Lett.* **1997**, *38*, 3247-3248.

14. (a) Nakamura, M.; Ilies, L.; Otsubo, S.; Nakamura, E. *Angew. Chem. Int. Ed.* **2006**, *45*, 944-947. (b) Yin, Y.; Ma, W.; Chai, Z.; Zhao, G. *J. Org. Chem.* **2007**, *72*, 5731-5736.

15. Knochel, P.; Leuser, H.; Gong, L.-Z.; Perrone, S.; Kneisel, F. F. "Functionalized organozinc compounds" in *The chemistry of organozinc compounds*, Rappoport, Z. (Ed.); Marek, I. (Ed.), John Wiley & Sons, Ltd **2006**, in press.

16. Torborg, C.; Beller, M. *Adv. Synth. Catal.* **2009**, *351*, 3027-3043.

17. Tokuyama, H.; Yokoshima, S.; Yamashita, T.; Fukuyama, T. *Tetrahedron Lett.* 1998, **39**, 3189–3192.

18. Shimizu, T.; Seki, M. *Tetrahedron Lett.* **2000**, *41*, 5099-5101.

19. Smith, A. R.; Lovick, H.M.; Livinghouse, T. *Tetrahedron Lett.* **2012**, *53*, 6358-6360.

20. For rate studies involving group 3 complexes, see: (a) Li, Y.; Marks, T. J. *J. Am. Chem Soc.* **1996**, *118*, 9295–9306; (b) Hong, S.; Kawaoka, A. M.; Marks, T. J. *J. Am. Chem. Soc.* **2003**, *125*, 15878–15892; (c) Ryu, J. S.; Li, G. Y.; Marks, T. J. *J. Am. Chem. Soc.* **2003**, *125*, 12584–12605; (d) Gribkov, D. V. L.; Hultzsch, K. C.; Hampel, F. *J. Am. Chem. Soc.* **2006**, *128*, 3748–3759; (e) Giardello, M. A.; Conticello, V. P.; Brard, L.; Gagné, M. R.; Marks, T. J. *J. Am. Chem. Soc.* **1994**, *116*, 10241–10254; For rate studies involving Zr(IV) catalysts, see: (f) Leitch, D. C.; Platel, R. H.; Schafer, L. L. *J. Am. Chem. Soc.* **2011**, *133*, 15453–15463; (g) Manna, K.; Xu, S.; Sadow, A. D. *Angew. Chem., Int. Ed.* **2011**, *50*, 1865–1868.

21. Motta, A.; Lanza, G.; Fragalà, I. L.; Marks, T. J. *Organometallics* **2004**, *23*, 4097– 4104.

22. Smith, A. R.; Livinghouse, T. *Organometallics* **2013**, *32*, 1528-1530.

23. For examples of rare-earth-based catalysts synthesized from the “extended silylamide route” precursors, see: (a) Zi, G.; Li, H.; Xie, Z. *Organometallics 2002*, **21**, 1136−1145. (b) O’Shaughnessy, P. N.; Knight, P. D.; Morton, C.; Gillespie, K. M.; Scott, P. *Chem. Commun.* **2003**, 1770−1771. (c) Kerton, F. M.; Whitwood, A. C.; Willans., C. E. *Dalton Trans.* **2004,** 2237−2244. (d) Hultzsch, K. C.; Hampel, F.; Wagner, T. *Organometallics* **2004**, *23*, 2601−2612. (e) Westmoreland, I.; Arnold, J. *Dalton Trans.* **2006**, 4155−4163. (f) Heck, R.; Schulz, E.; Collin, J.;

Carpantier, J. *J. Mol. Catal. A: Chem.* **2007**, *268*, 163−168. (g) Wu, B.; Gallucci, J. C.; Parquette, J. R.; RajanBabu, T. V. *Angew. Chem., Int. Ed.* **2008**, *48*, 1126−1129. (h) Li, G.; Lamberti, M.; Mazzeo, M.; Pappalardo, D.; Roviello, G.; Pellecchia, C. *Organometallics* **2012**, *31*, 1180−1188.

24. The THF free lanthanum tris(bis(dimethylsilyl)amide is known. Yuen, H. F.; Marks, T. J. *Organometallics* **2008**, *27*, 155-158.

25. (a) Hong, S.; Kawaoka, A. M.; Marks, T. J. *J. Am. Chem. Soc.* **2003**, *125*, 15878 – 15892. (b) Queffelec, C.; Boeda, F.; Pouilhès, A.; Meddour, A.; Kouklovsky, C.; Hannedouche, J.; Collin, J.; Schulz, E. *ChemCatChem* **2011**, *3*, 122-126.

26. Attempts at secondary aminoalkene hydroamination with group 3 metal tris[bis(dimethylsilyl)amide] THF complexes **5a-5e** were all unsuccessful and didn't show dissociation of the bis(dimethylsilyl)amide ligand.

27. Zotova, N.; Roberts, F. J.; Kelsall, G. H.; Jessiman, A. S.; Hellgardt, K.; Hii, K. K. M. *Green Chem.* **2012**, *14*, 226-232.

28. Greene, T. W.; Wuts, P. G. M. *Protecting Groups in Organic Synthesis*, 3rd ed; Wiley-Interscience: New York, 1999.

29. Assignments of *cis/trans* isomers based on the spectra of the relative *N*-benzyl pyrrolidine ^{1}H NMR of *cis*/*trans* diastereomers. Fujita, K.-I.; Fujii, T.; Yamaguchi, R. *Org. Lett.* **2004**, *6*, 3525-3528.

30. Sunsdahl, B.; Smith, A. R.; Livinghouse, T. *Angew. Chem. Int. Ed.* **2014**, *53*, 14352-14356.

31. Pissarek, J-W.; Schlesiger, D.; Roesky, P. W.; Blechert, S. *Adv. Synth. Catal.* **2009**, *351*, 2081-2085.

32. Malik, M. A.; O'Brien, P. *Polyhedron* **1997**, *16*, 3593-3599.

33. Sigma-Aldrich. Tris[N,N-bis(trimethylsilyl)amide]yttrium. http://www.sigmaaldrich.com/catalog/product/aldrich/524514?lang=en&region=US (accessed Mar 20, 2015).

34. Corey, E. J.; Enders, D. *Chem.Ber.* **1978**, *111*, 1137-1161.

35. Salomon, R.; Ghosh, S. *Org. Synth.* **1984**, *62*, 125.

36. Timberlake, J. W.; Xiao, Z. *Tetrahedron* **1998**, *54*, 12715-12720.

37. Fukuyama, T.; Tokuyama, H. *Aldrichimica Acta* **2004**, ***37,*** 87-96.

38. Stanford, M. J.; Dove, A. P. *Chem. Soc. Rev.* **2010**, *39*, 486-494.

39. Patil, S. A.; Medina, P. A.; Gonzalez-Flores, D.; Vohs, J. K.; Dever, S.; Pineda, L. W.; Montero, M. L.; Fahlman B. D. *Synth. Comm.* **2013**, *43*, 349-2364.

40. Meshram, H. M.; Reddy, G. S.; Bindu, K. H.; Yadav, J. S. *Synlett* **1998**, *8*, 877-878.

41. Yin, Y.; Ma, W.; Chai, Z.;Zhao, G. *J. Org. Chem.* **2007**, *72*, 5731–5736.

42. Hojo, M.; Masuda, R.; Okada, E. *Synthesis* **1986**, *12*, 1013-1014.

43. Ogawa A.; Curran, D. P. *J. Org. Chem.* **1997**, *62*, 450-451.

44. Patil, S. A.; Medina, P. A.; Gonzalez-Flores, D.; Vohs, J. K.; Dever, S.; Pineda, L. W.; Montero, M. L.; Fahlman B. D. *Synth. Comm.* **2013**, *43*, 2349-2364.

45. *Cis/trans* ration based on ^{1}H NMR of a similar 1,3-*trans* pyrrolidine. Musacchio, A. J.; Nguyen, L. Q,; Beard, G. H.; Knowles, R. R. *J. Am. Chem. Soc.* **2014**, *136*, 12217-12220.

46. (a) Ghotra, J. S.; Hart, F. A. *J. Chem. Soc. Dalton Trans.* **1973**, 1021-1023. (b) Alyea, E. C.; Bradley, D. C.; Copperthwaite, R. G. *J. Chem. Soc. Dalton Trans.* **1972**, 1580-1584.

47. Lappert, M. F.; Pearce, R. *J. Chem. Soc. Chem. Commun.* **1973**, 126.

48. Bender, C. F.; Widenhofer, R. A. *J. Am. Chem. Soc.* **2005**, *127*, 1070-1071.

49. El-Zoghbi, I.; Ased, A.; Oguadinma, P. O.; Tchirioua, E.; Schaper, F. *Can. J. Chem.* **2010**, *88*, 1040-1045.

50. Texier, F.; Marchand, E.; Carrie, R. *Tetrahedron* **1974**, *30*, 3185-3192.

51. Bonacorso, H. G.; Bortolotto, G. P.; Navarini, J.; Porte, L. M. F.; Wiethan, C. W.; Zanatta, N.; Martins, M. A. P.; Flores, A. F. C. *J. Fluorine Chem.* **2010**, *131*, 1297-1301.

52. Grohmann, M.; Maas, G. *Tetrahedron* **2007**, *63*, 12172-12178.

53. Nakamura, M.; Fujimoto, T.; Endo, K.; Nakamura, E. *Org. Lett.* **2004**, *6*, 4837-4840.

54. Pérez, J. P.; Vidal, L.; Grande, M. T.; Menéndez, J. C.; Avendaño, C. *Tetrahedron* **1994**, *50*, 7923-7932.

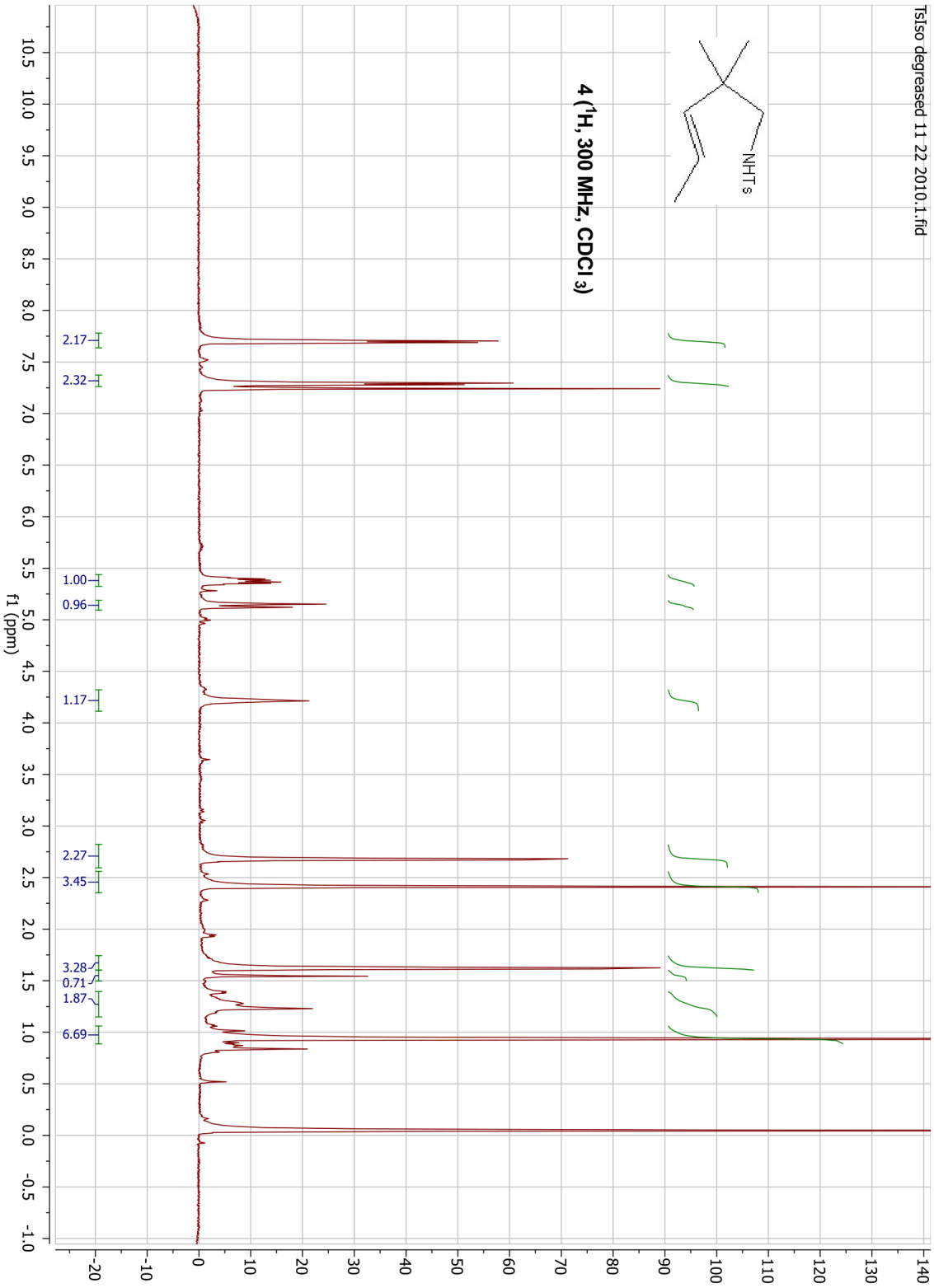
55. McGrath, N. A.; Brichacek, M.; Njardarson, J. T. *J. Chem. Educ.* **2010**, *87*, 1348-1349.

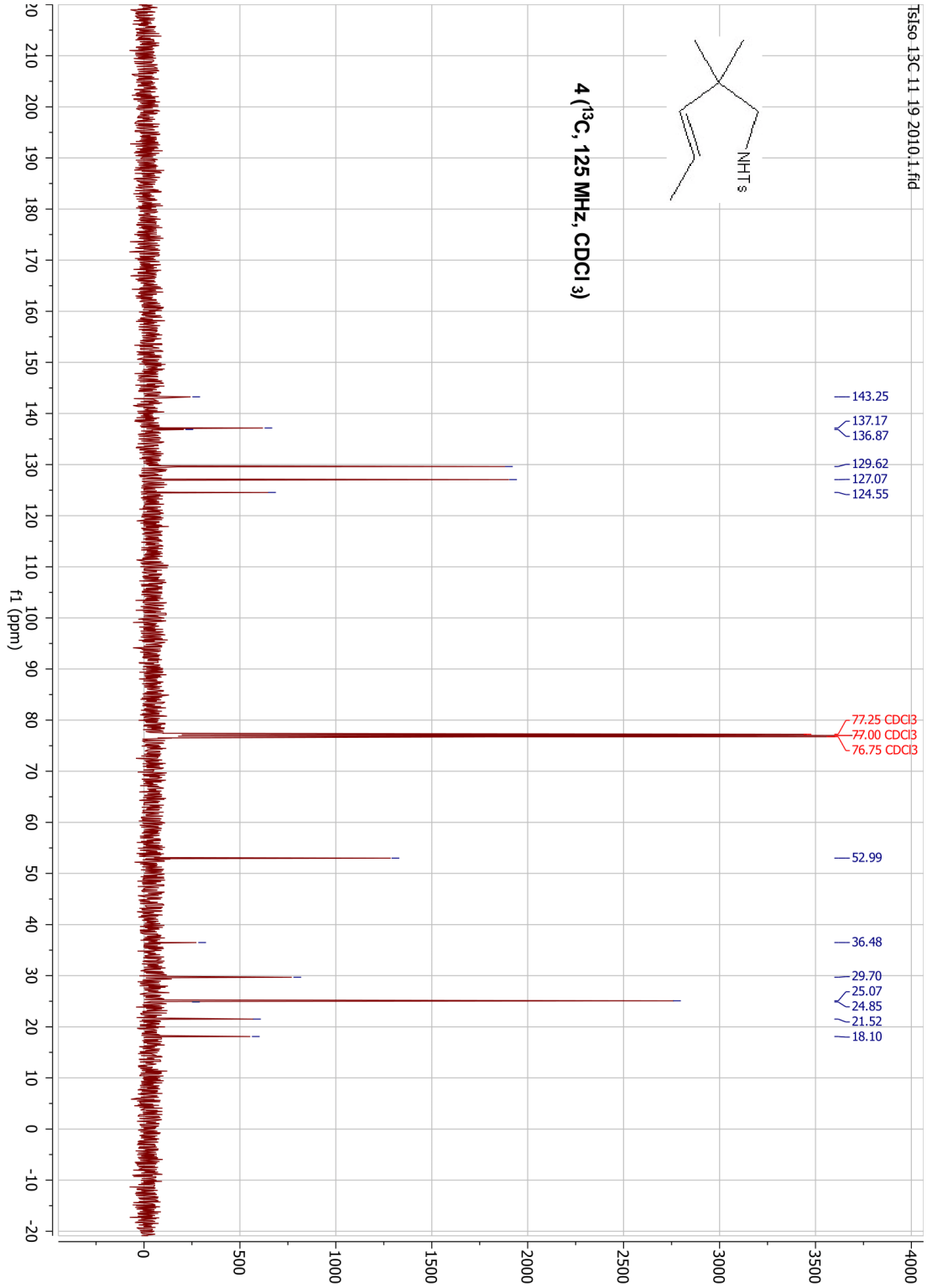
56. Baumann, M.; Baxendale, I. R. *Beilstein J. Org. Chem.* **2013**, *9*, 2265-2319.

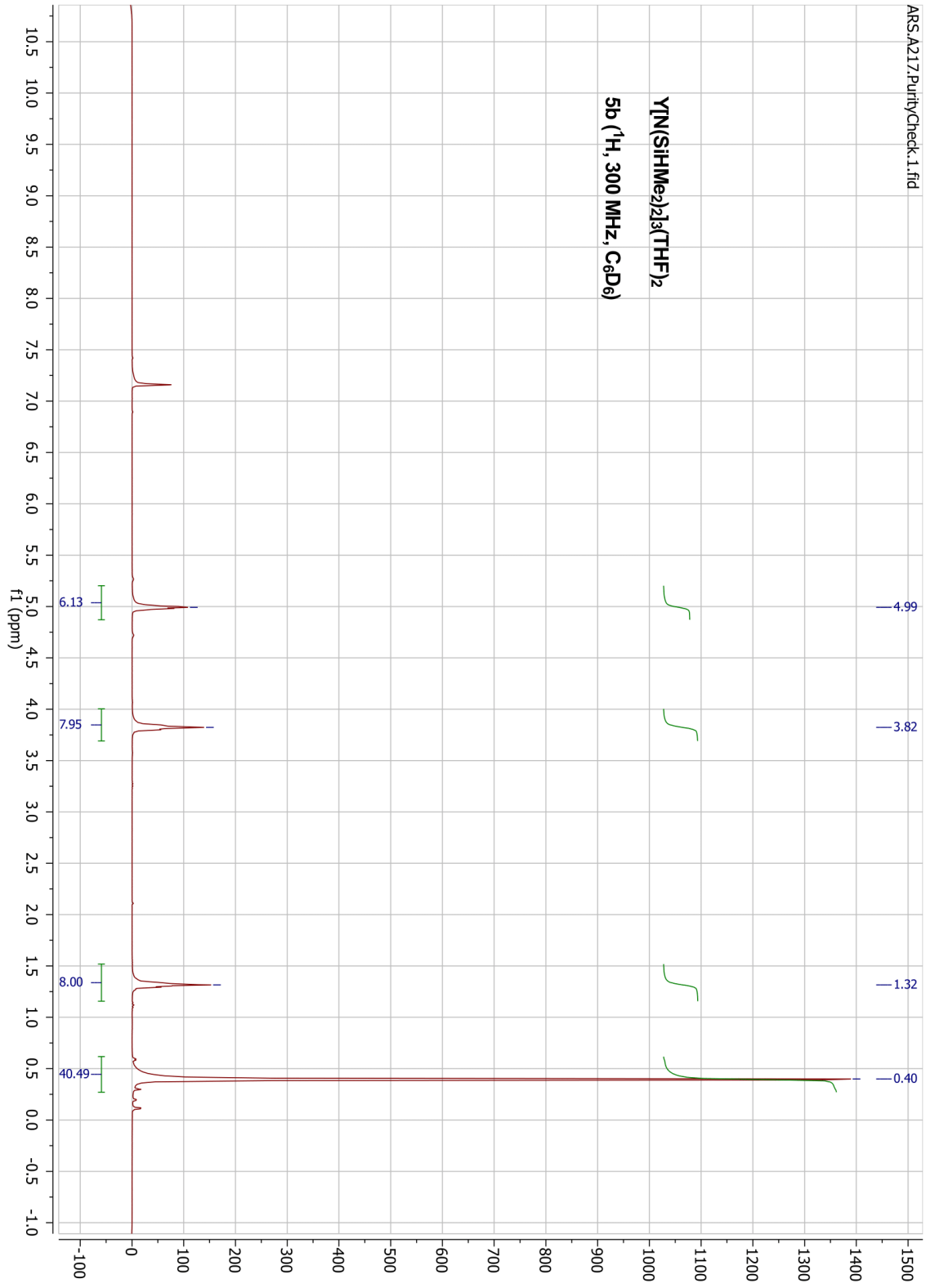
57. Chapman, D. M.; Hester, R. E. *J. Phys. Chem. A* **1997**, *101*, 3382-3387.

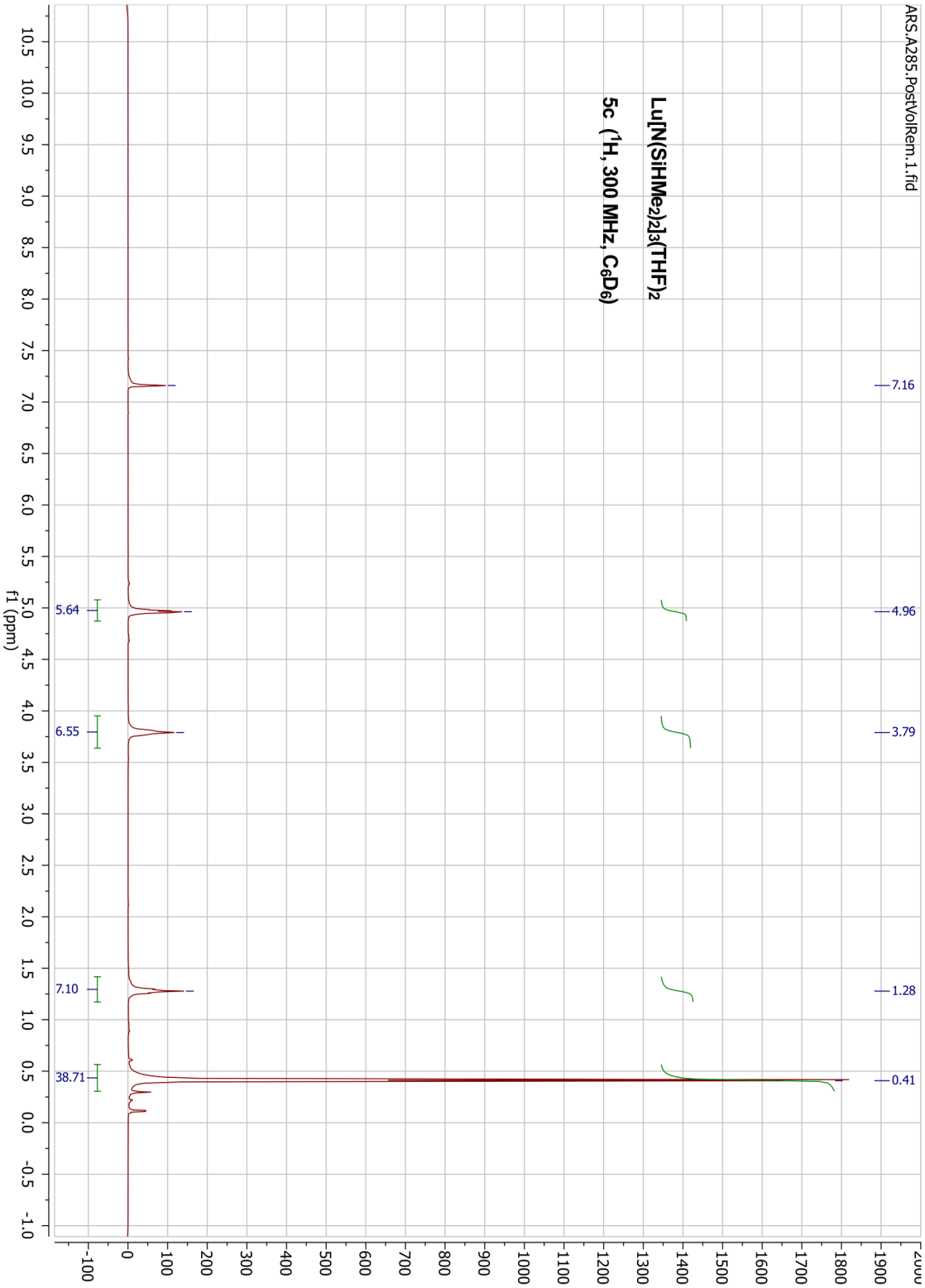
APPENDIX A

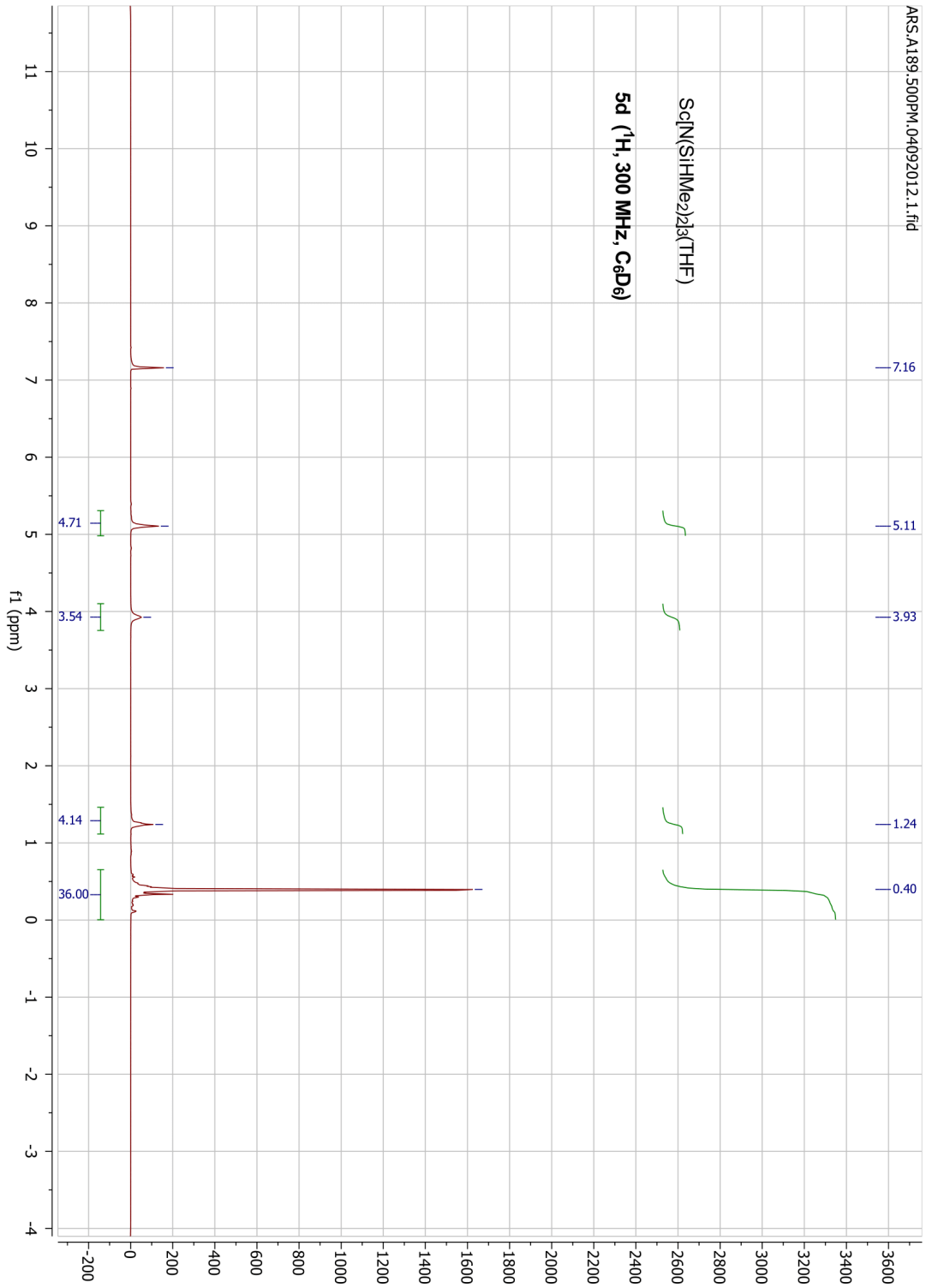
^{1}H NMR / ^{13}C NMR DATA

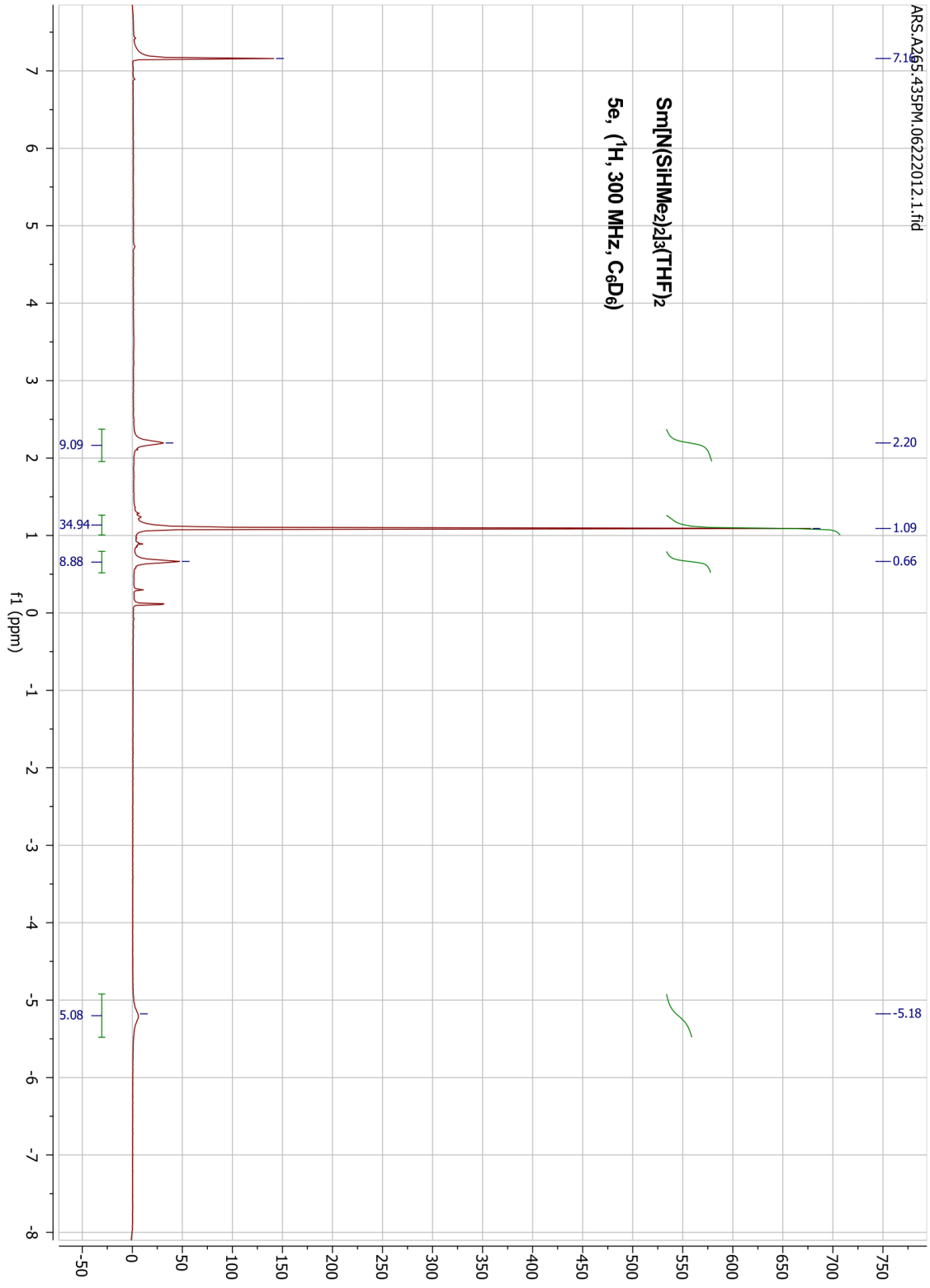

TsIso degreased 11 22 2010.1.fid
4 (1H, 300 MHz, CDCl 3)
NHTs
2.17
2.32
1.00
0.96
1.17
2.27
3.45
3.28
0.71
1.87
6.69
f1 (ppm)

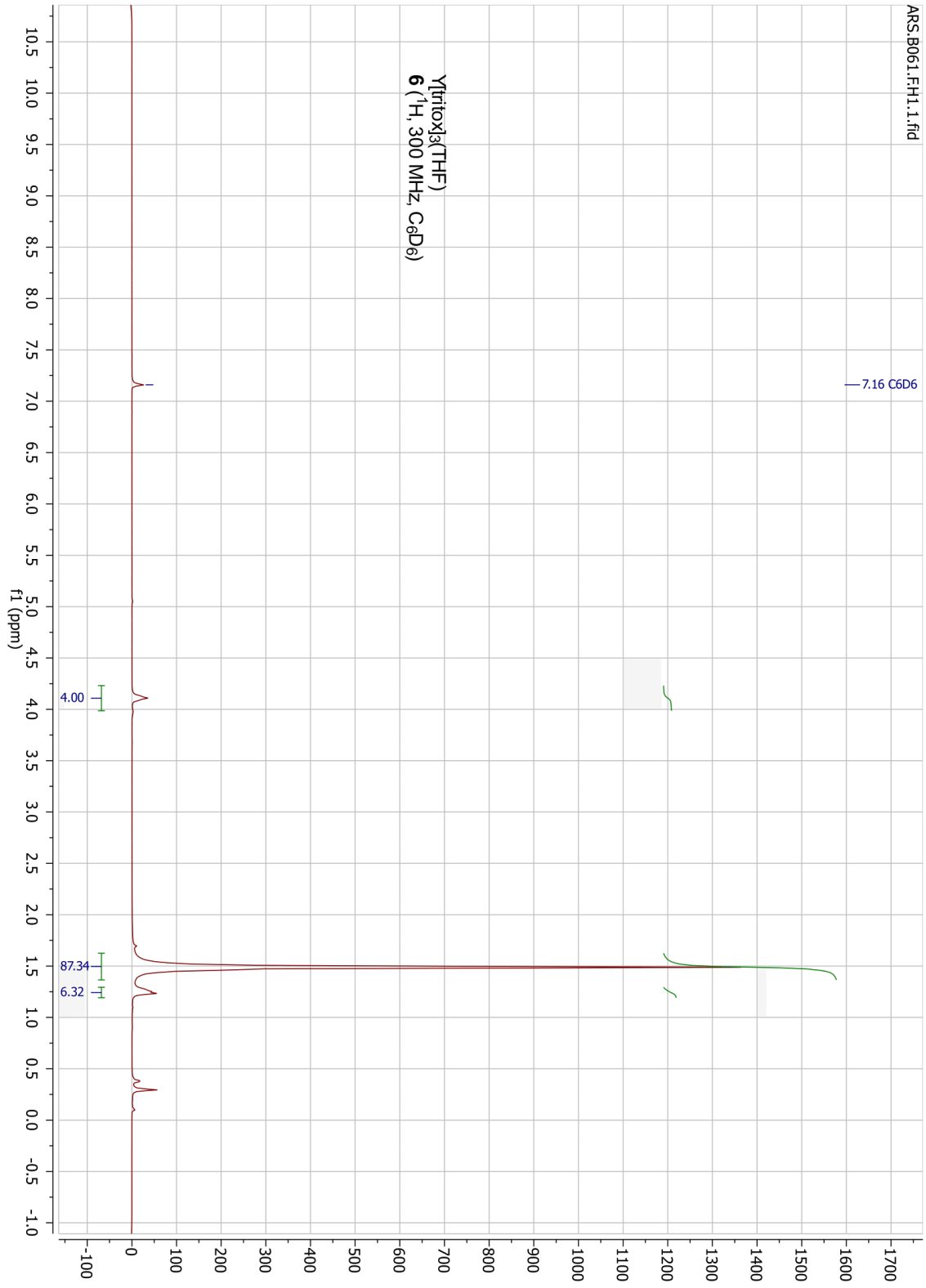

TsIso 13C 11 19 2010,1.fid
4 (^{13}C, 125 MHz, CDCl$_3$)
NHTs
143.25
137.17
136.87
129.62
127.07
124.55
77.25 CDCl3
77.00 CDCl3
76.75 CDCl3
52.99
36.48
29.70
25.07
24.85
21.52
18.10
f1 (ppm)

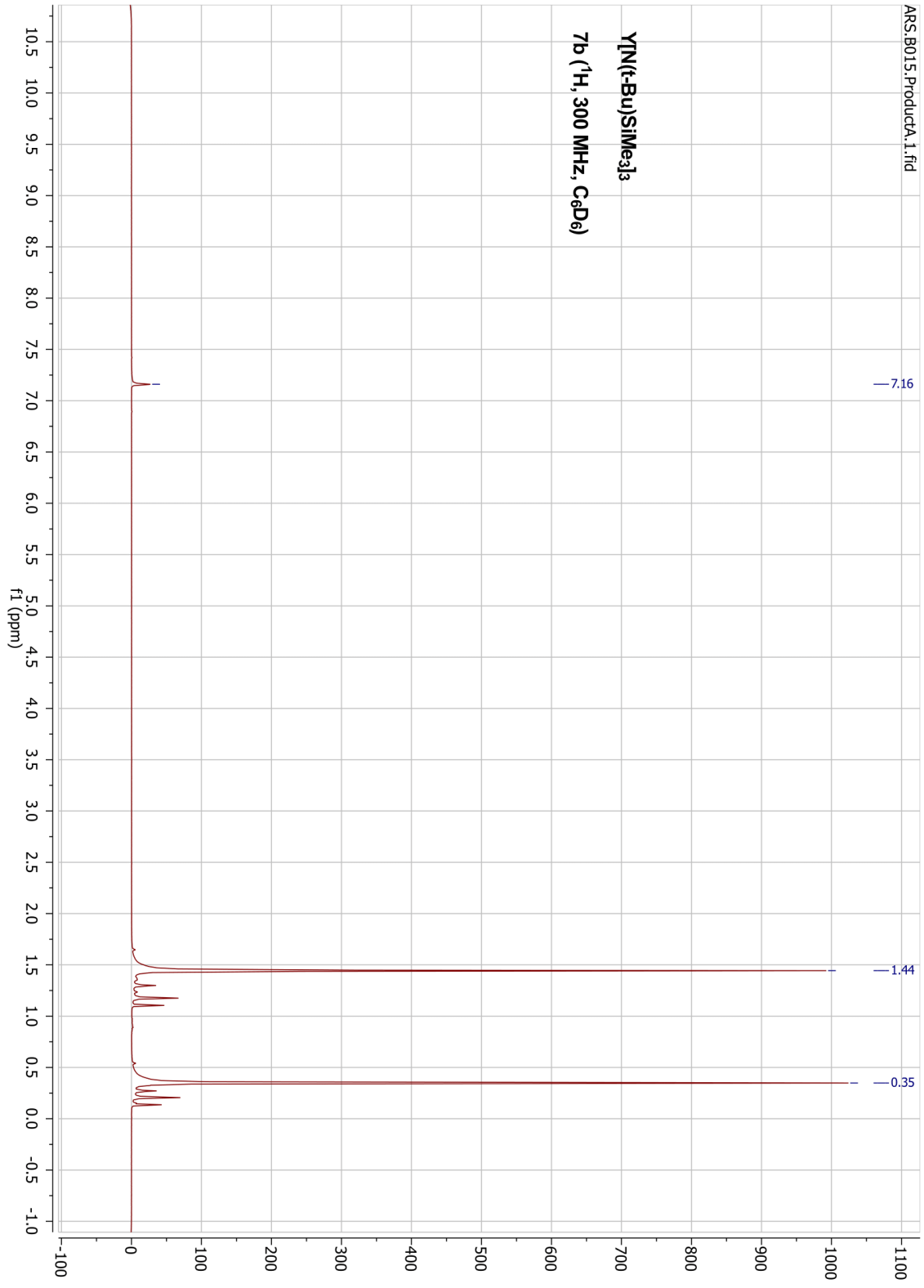

ARS.A217.PurityCheck.1.fid
Y[N(SiHMe2)2]3(THF)2
5b (1H, 300 MHz, C6D6)
f1 (ppm)
6.13
7.95
8.00
40.49
4.99
3.82
1.32
0.40

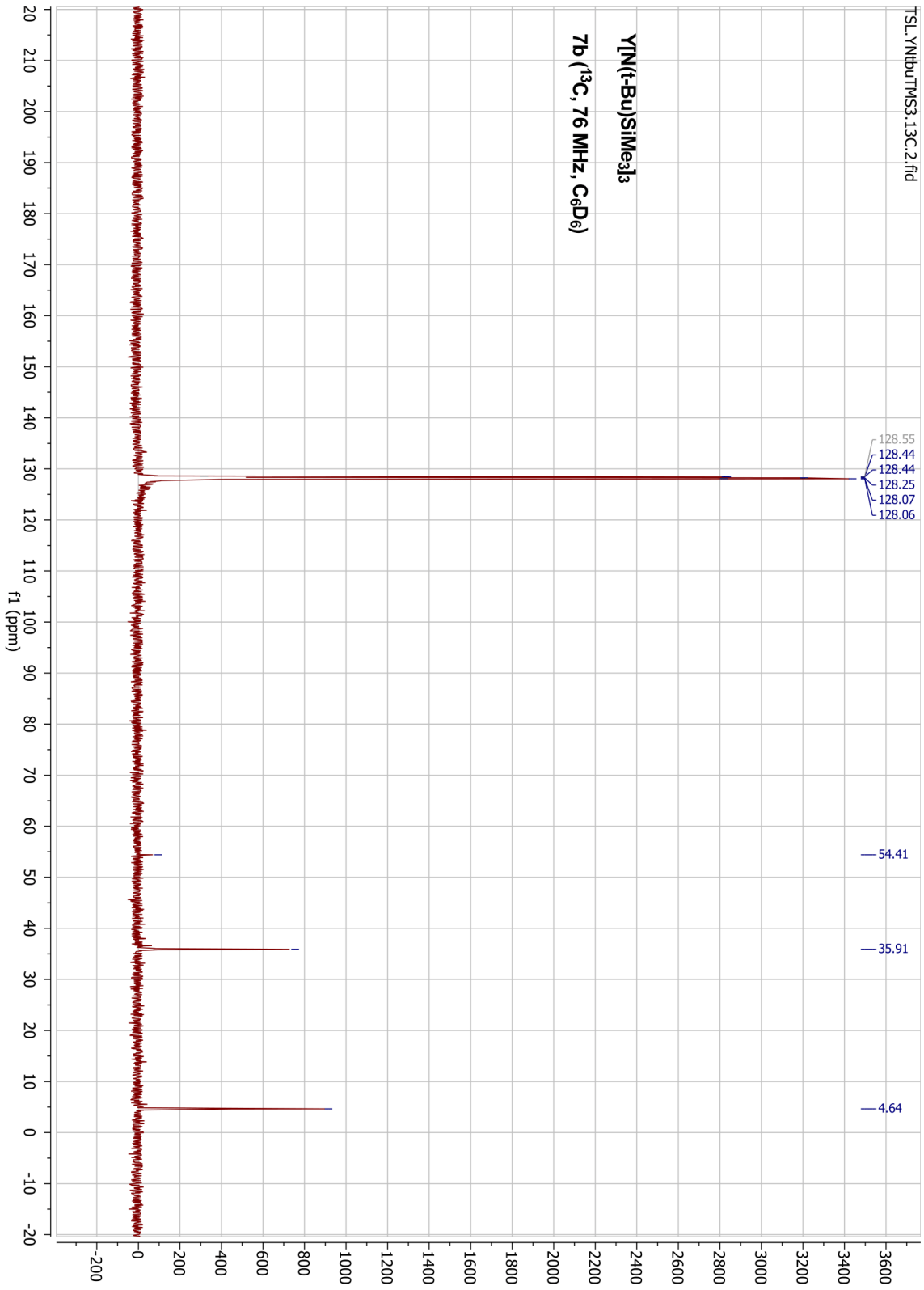

ARS.A285.PostVolRem.1.fid
Lu[N(SiHMe2)2]3(THF)2
5c (1H, 300 MHz, C6D6)
7.16
4.96
3.79
1.28
0.41
5.64
6.55
7.10
38.71
f1 (ppm)

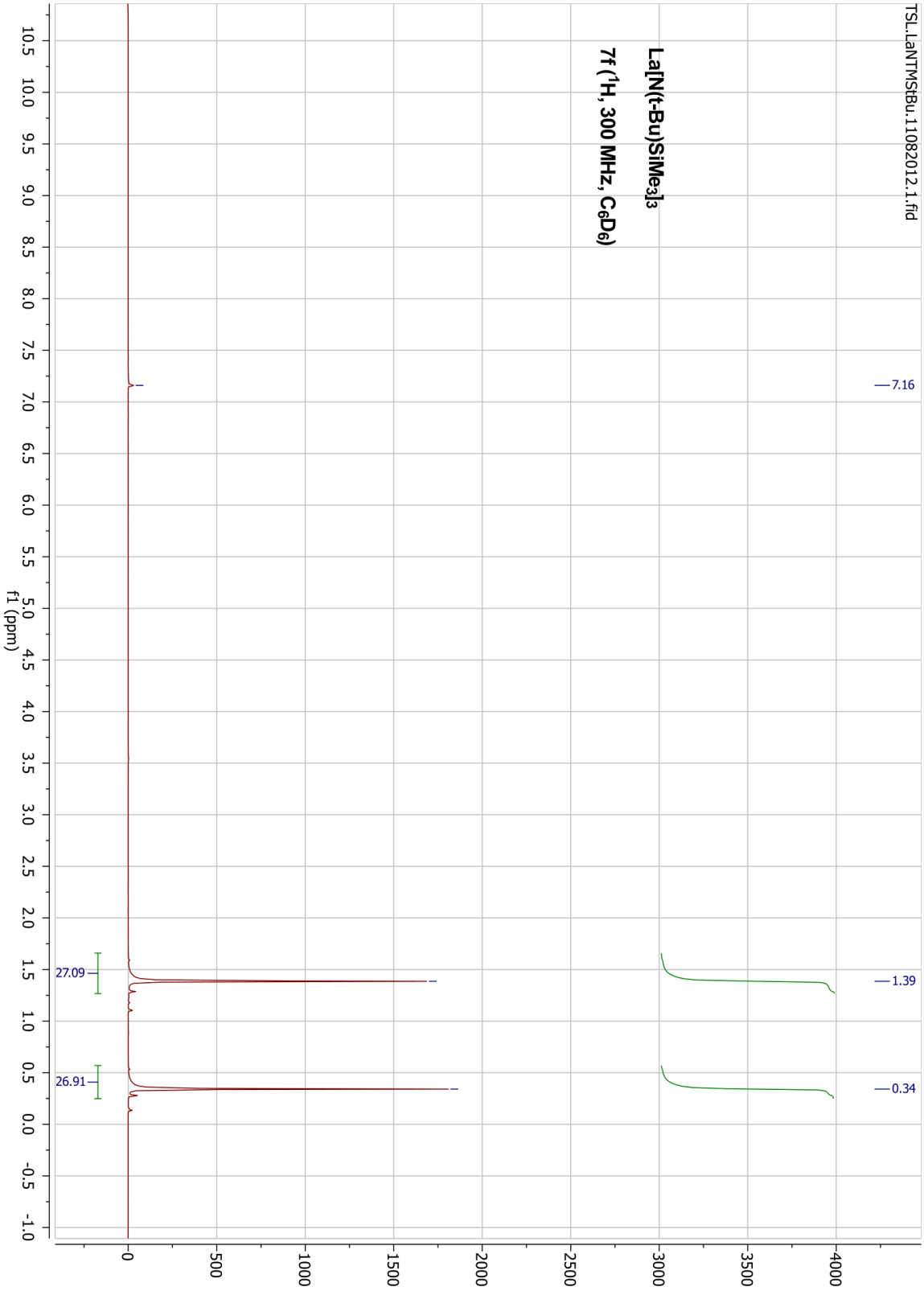

ARS.A189.500PM.04092012.1.fid
Sc[N(SiHMe2)2]3(THF)
5d (1H, 300 MHz, C6D6)
7.16
5.11
3.93
1.24
0.40
4.71
3.54
4.14
36.00
f1 (ppm)

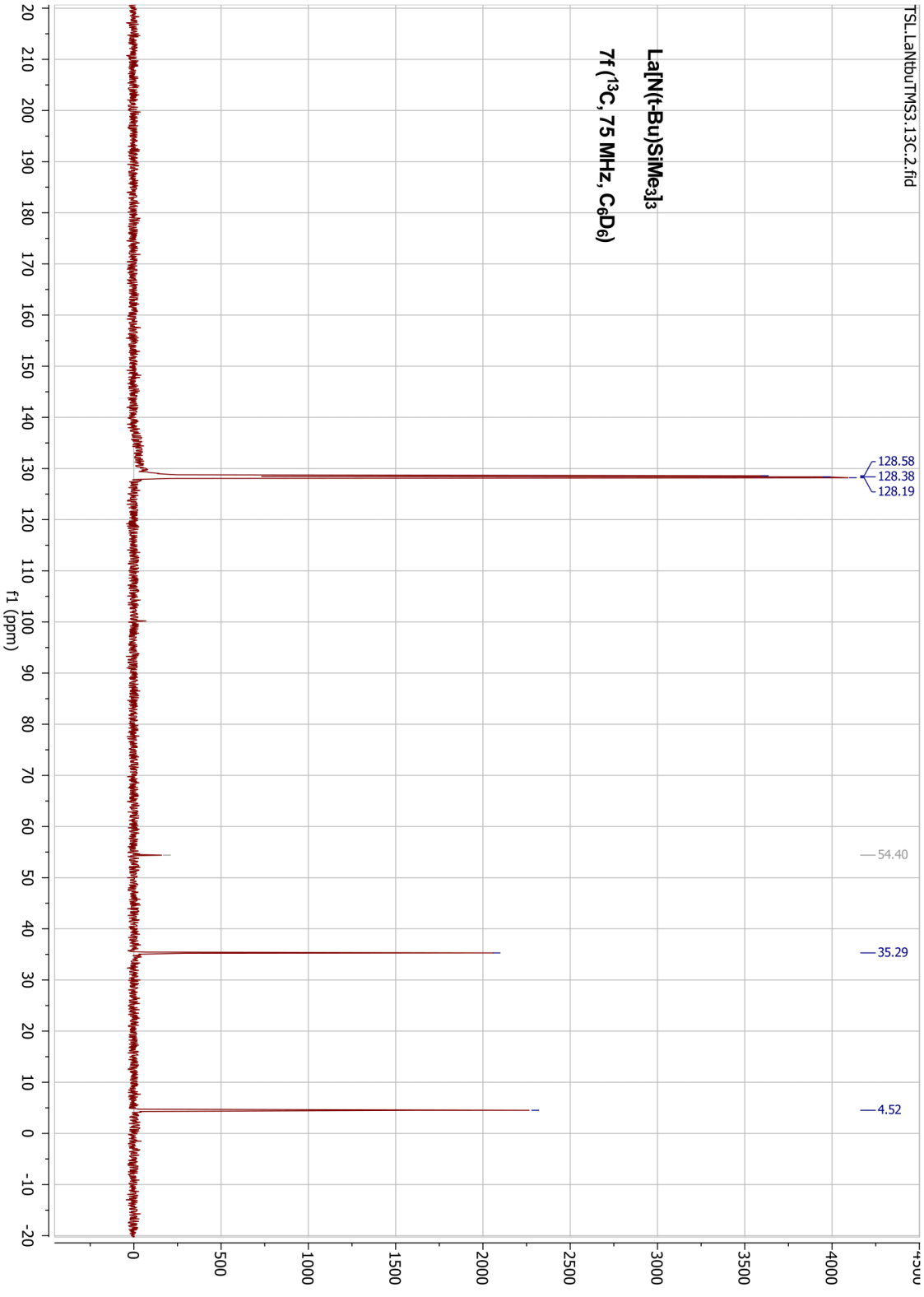

ARS.A265.435PM.06222012.1.fid
Sm[N(SiHMe2)2]3(THF)2
5e, (1H, 300 MHz, C6D6)
7.16
2.20
1.09
0.66
-5.18
9.09
34.94
8.88
5.08
f1 (ppm)

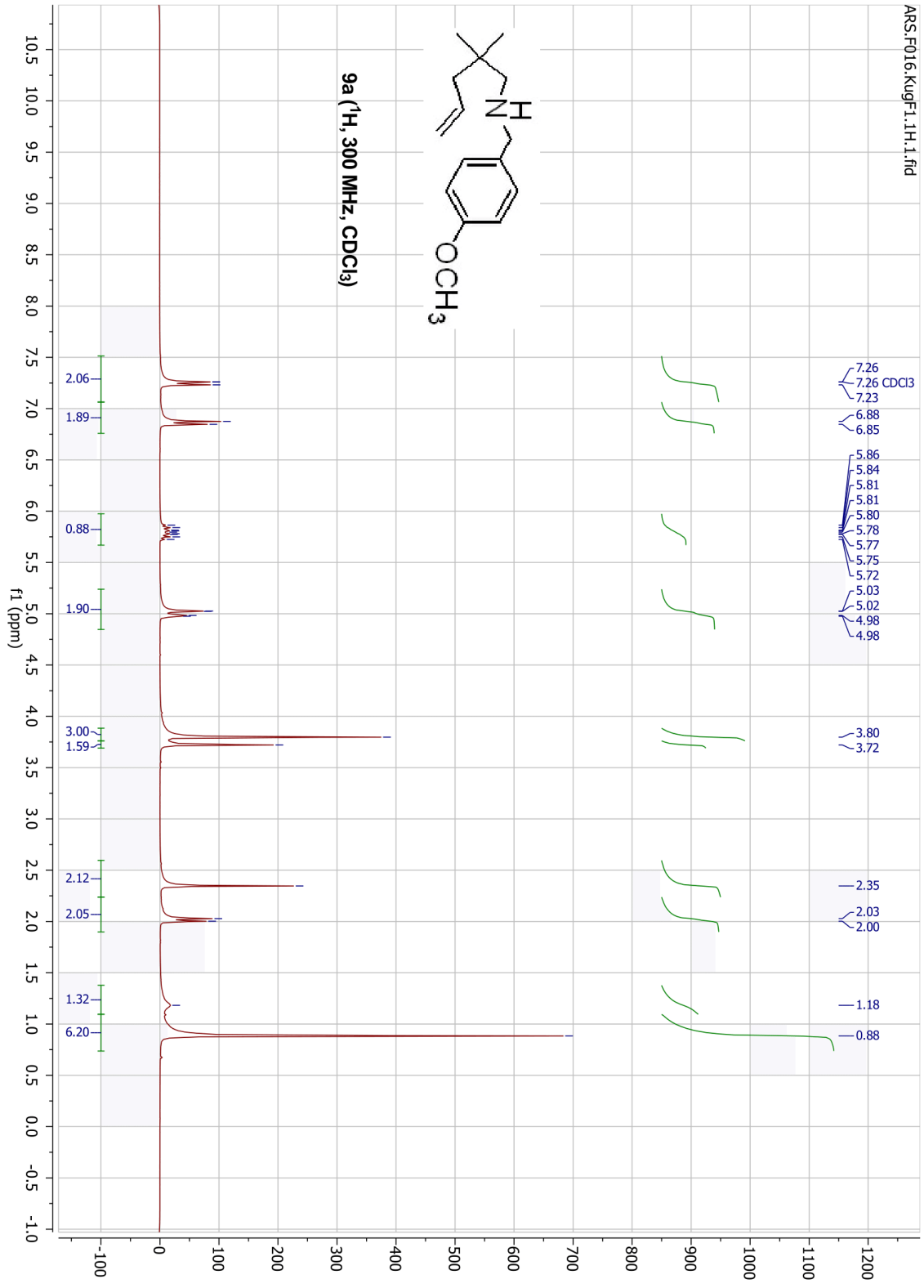

ARS.B061.F.H1.1.fid
Y[triox]3(THF)
6 (1H, 300 MHz, C6D6)
7.16 C6D6
4.00
87.34
6.32
f1 (ppm)

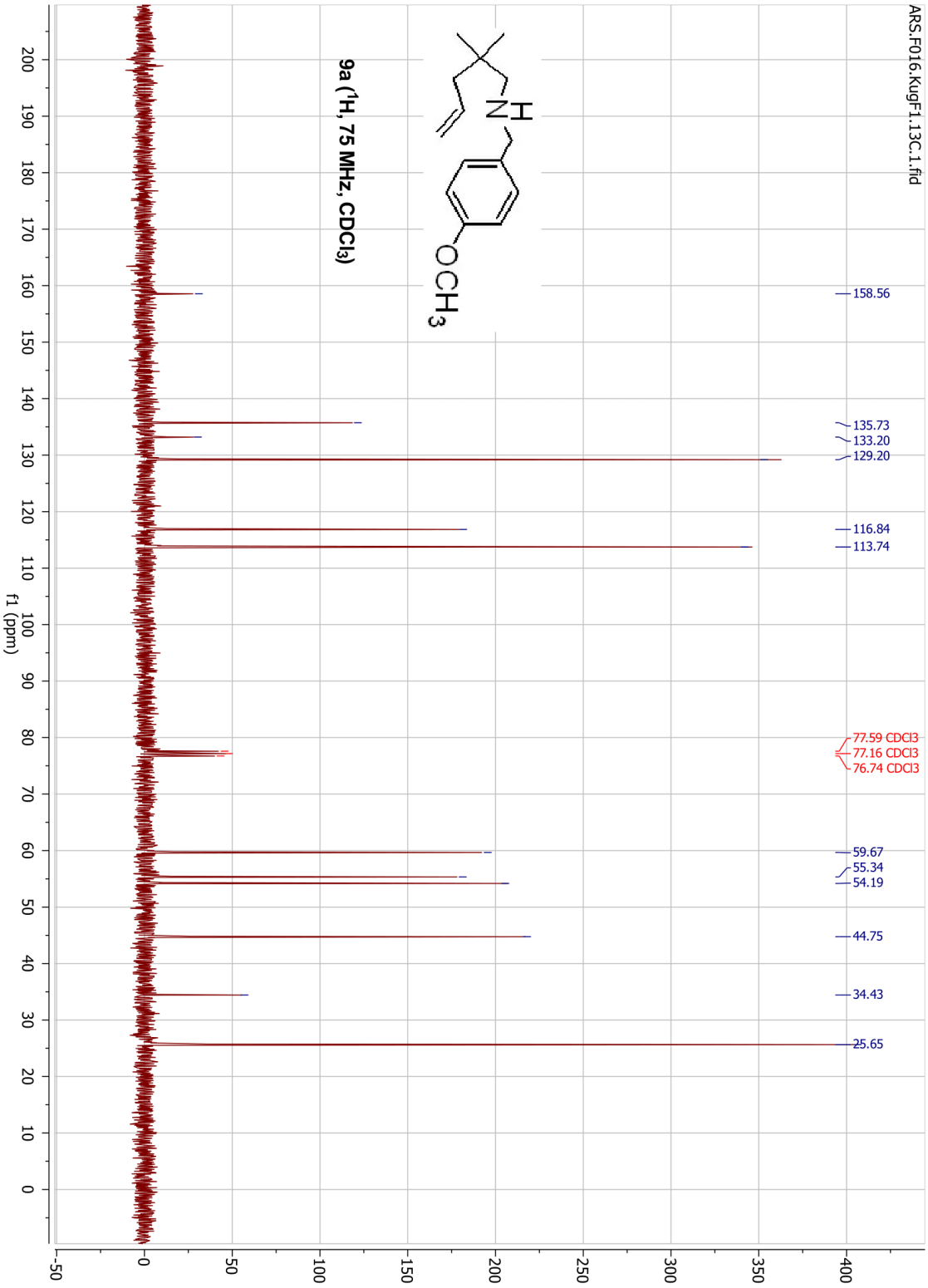

ARS.B015.ProductA.1.fid
Y[N(t-Bu)SiMe3]3
7b (1H, 300 MHz, C6D6)
7.16
1.44
0.35
f1 (ppm)

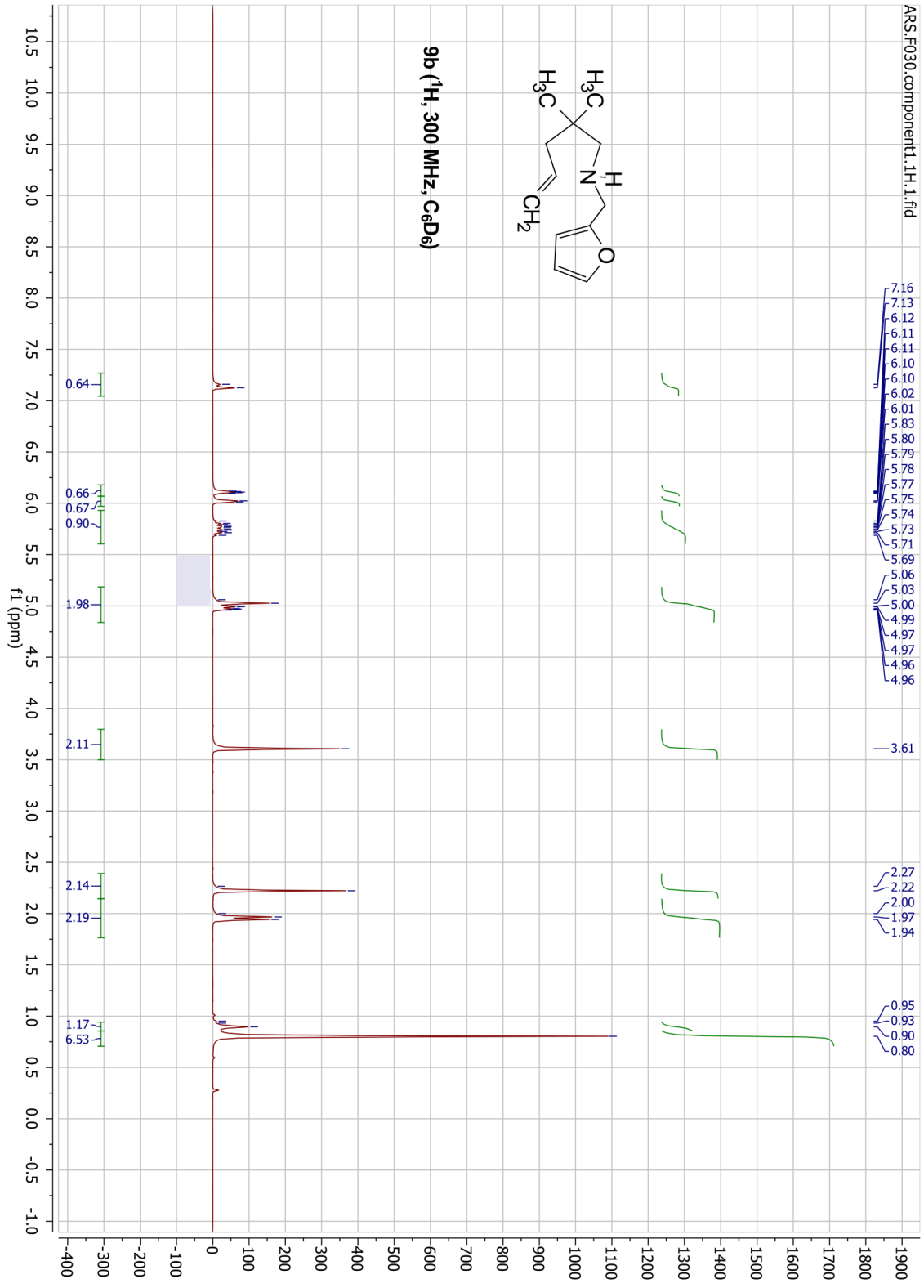

TSL.YNtbuTMS3.13C.2.fid
Y[N(t-Bu)SiMe3]3
7b (13C, 76 MHz, C6D6)
128.55
128.44
128.44
128.25
128.07
128.06
54.41
35.91
4.64
f1 (ppm)

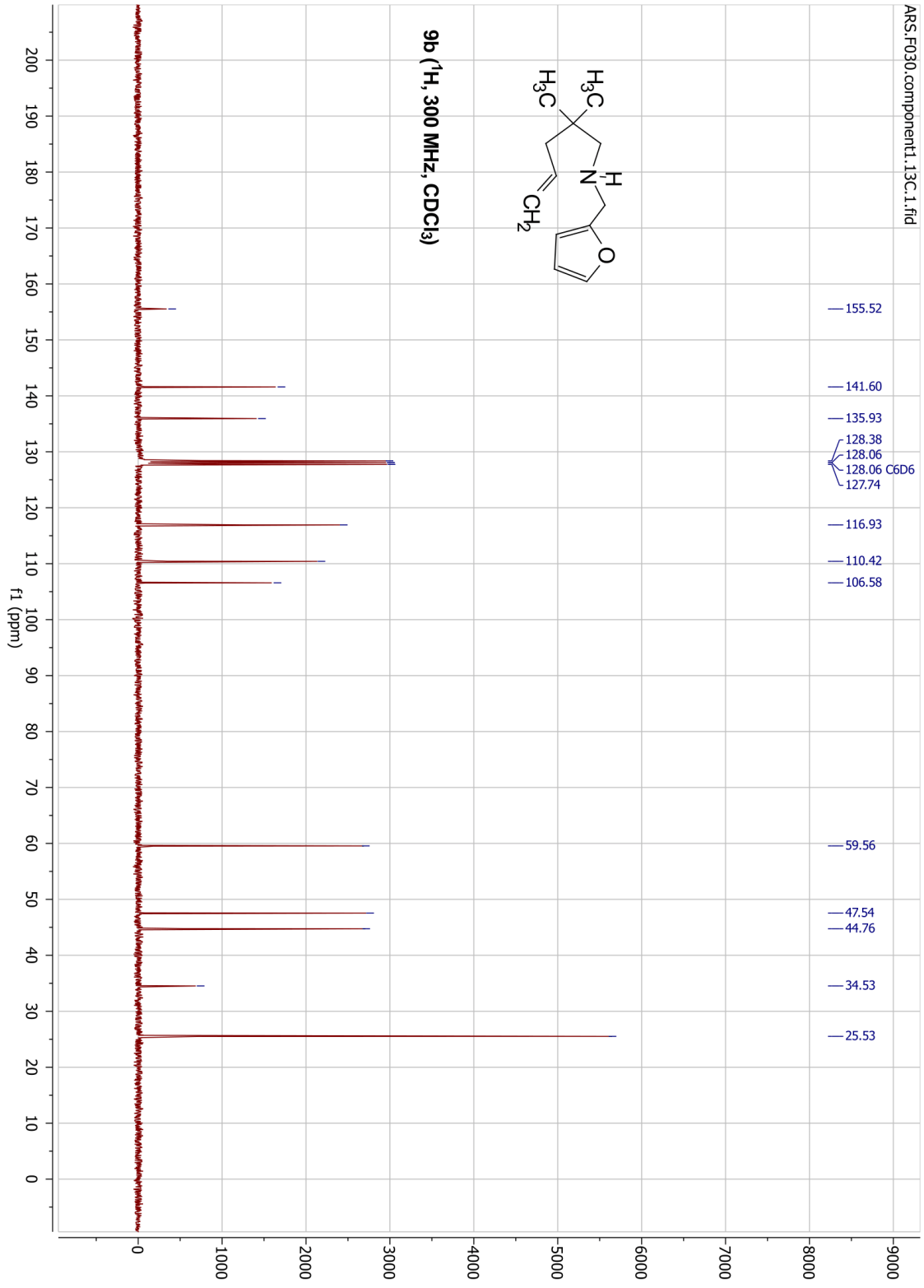

TSL.LaNTMStBu.11082012.1.fid
La[N(t-Bu)SiMe3]3
7f (1H, 300 MHz, C6D6)
7.16
1.39
0.34
27.09
26.91
f1 (ppm)

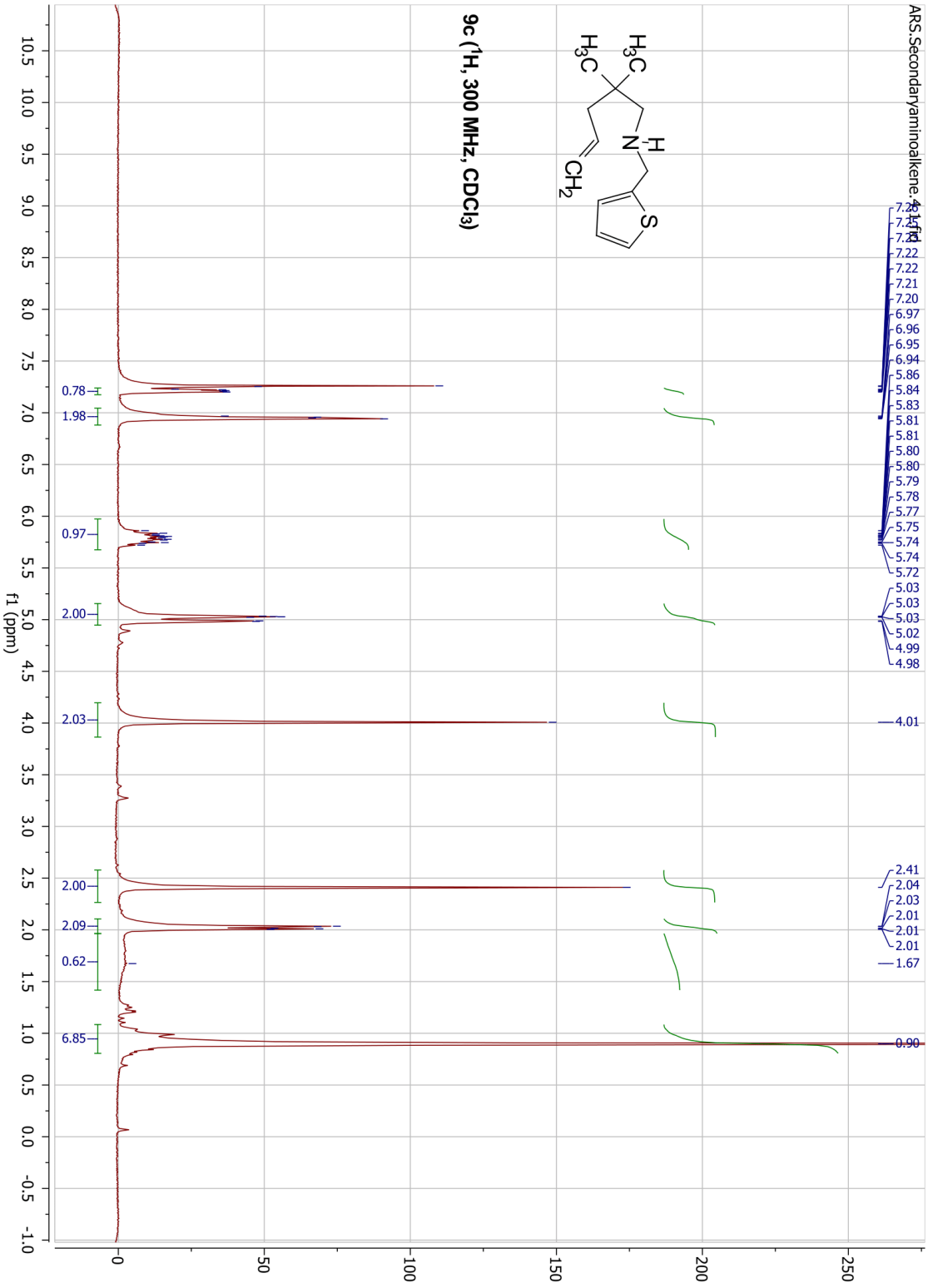

TSL.LaNtbuTMS3.13C.2.fid
La[N(t-Bu)SiMe3]3
7f (13C, 75 MHz, C6D6)
128.58
128.38
128.19
54.40
35.29
4.52
f1 (ppm)

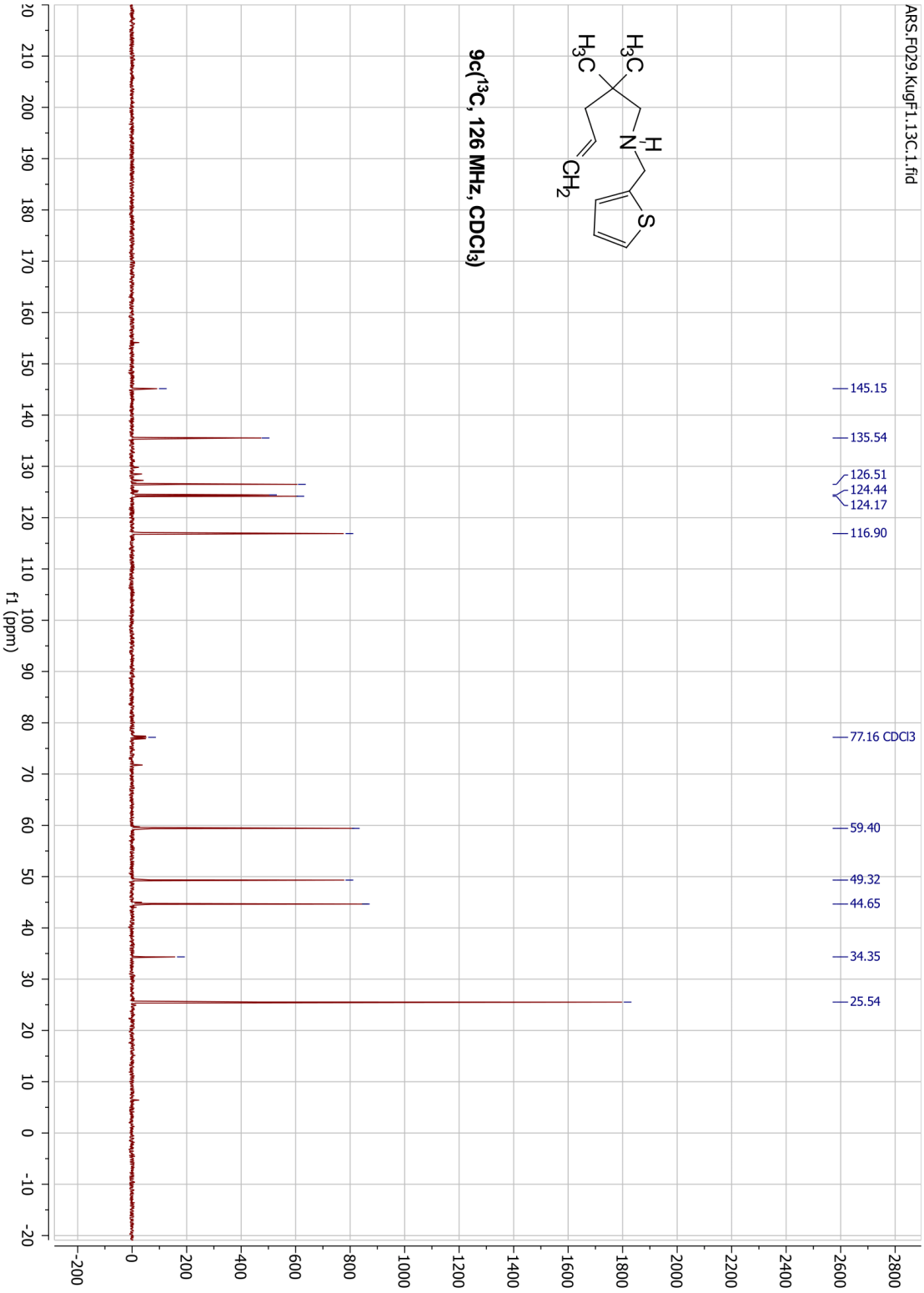

ARS.F016.KugF1.1H.1.fid
9a (^{1}H, 300 MHz, CDCl$_3$)
OCH$_3$
H
N
f1 (ppm)
2.06
1.89
0.88
1.90
3.00
1.59
2.12
2.05
1.32
6.20
7.26
7.26 CDCl3
7.23
6.88
6.85
5.86
5.84
5.81
5.81
5.80
5.78
5.77
5.75
5.72
5.03
5.02
4.98
4.98
3.80
3.72
2.35
2.03
2.00
1.18
0.88

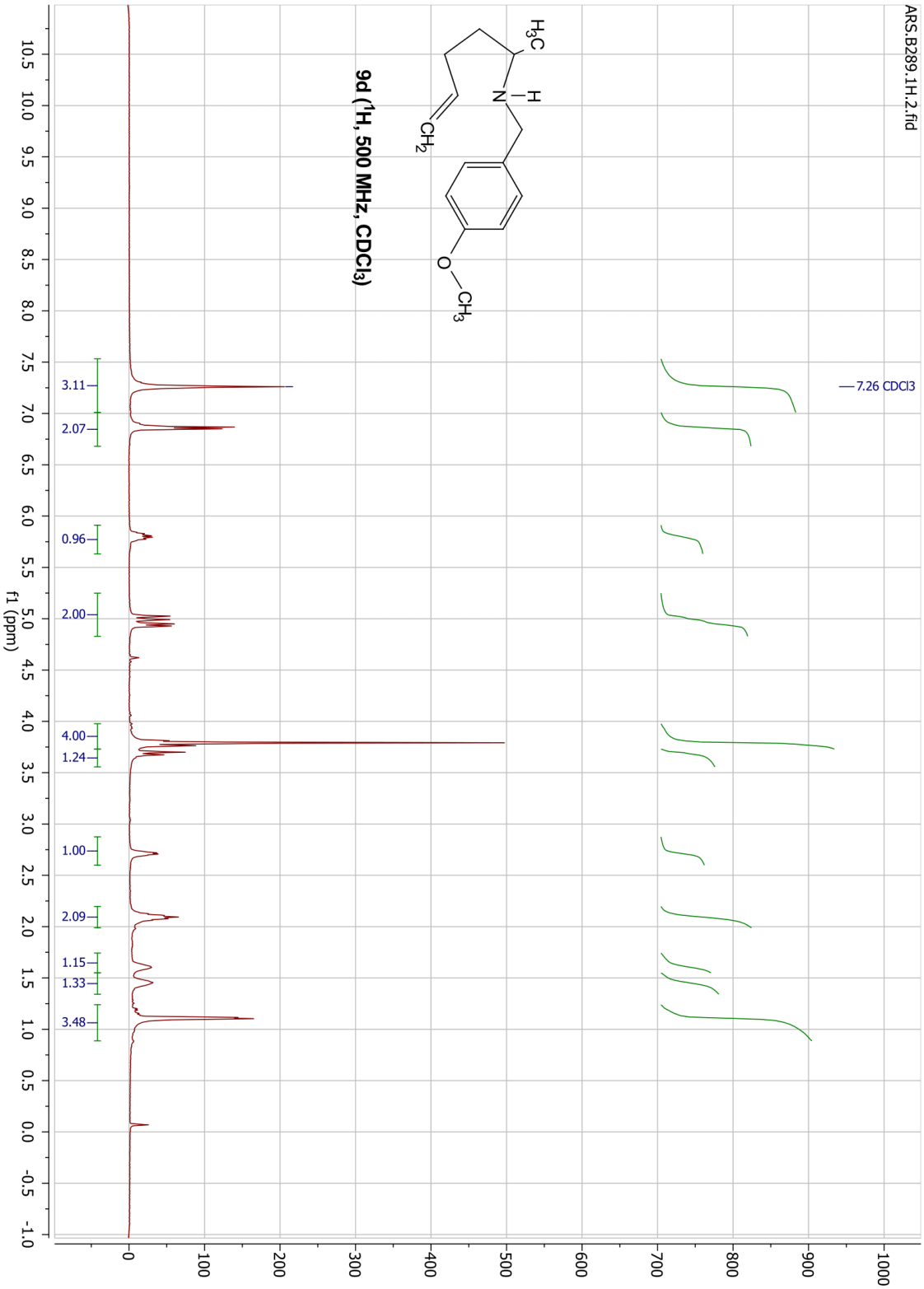

ARS.F016.KugF1.13C.1.fid
9a (^{1}H, 75 MHz, CDCl$_3$)
OCH$_3$
158.56
135.73
133.20
129.20
116.84
113.74
77.59 CDCl3
77.16 CDCl3
76.74 CDCl3
59.67
55.34
54.19
44.75
34.43
25.65
f1 (ppm)

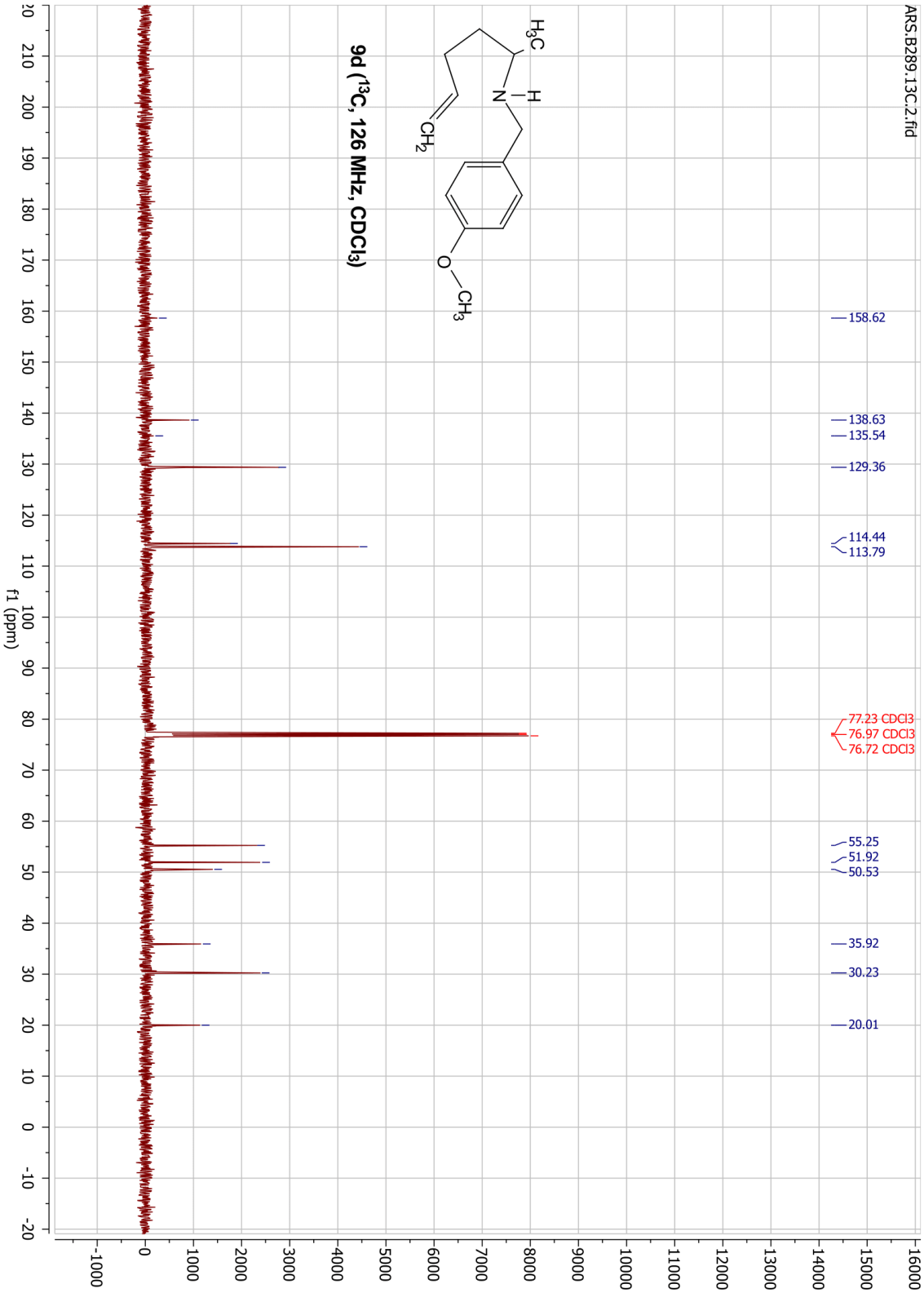

ARS.F030.component1.1H.1.fid
9b (1H, 300 MHz, C6D6)
H3C
H3C
N
H
CH2
O
7.16
7.13
6.12
6.11
6.11
6.10
6.10
6.02
6.01
5.83
5.80
5.79
5.78
5.77
5.75
5.74
5.73
5.71
5.69
5.06
5.03
5.00
4.99
4.97
4.97
4.96
4.96
3.61
2.27
2.22
2.00
1.97
1.94
0.95
0.93
0.90
0.80
0.64
0.66
0.67
0.90
1.98
2.11
2.14
2.19
1.17
6.53
f1 (ppm)

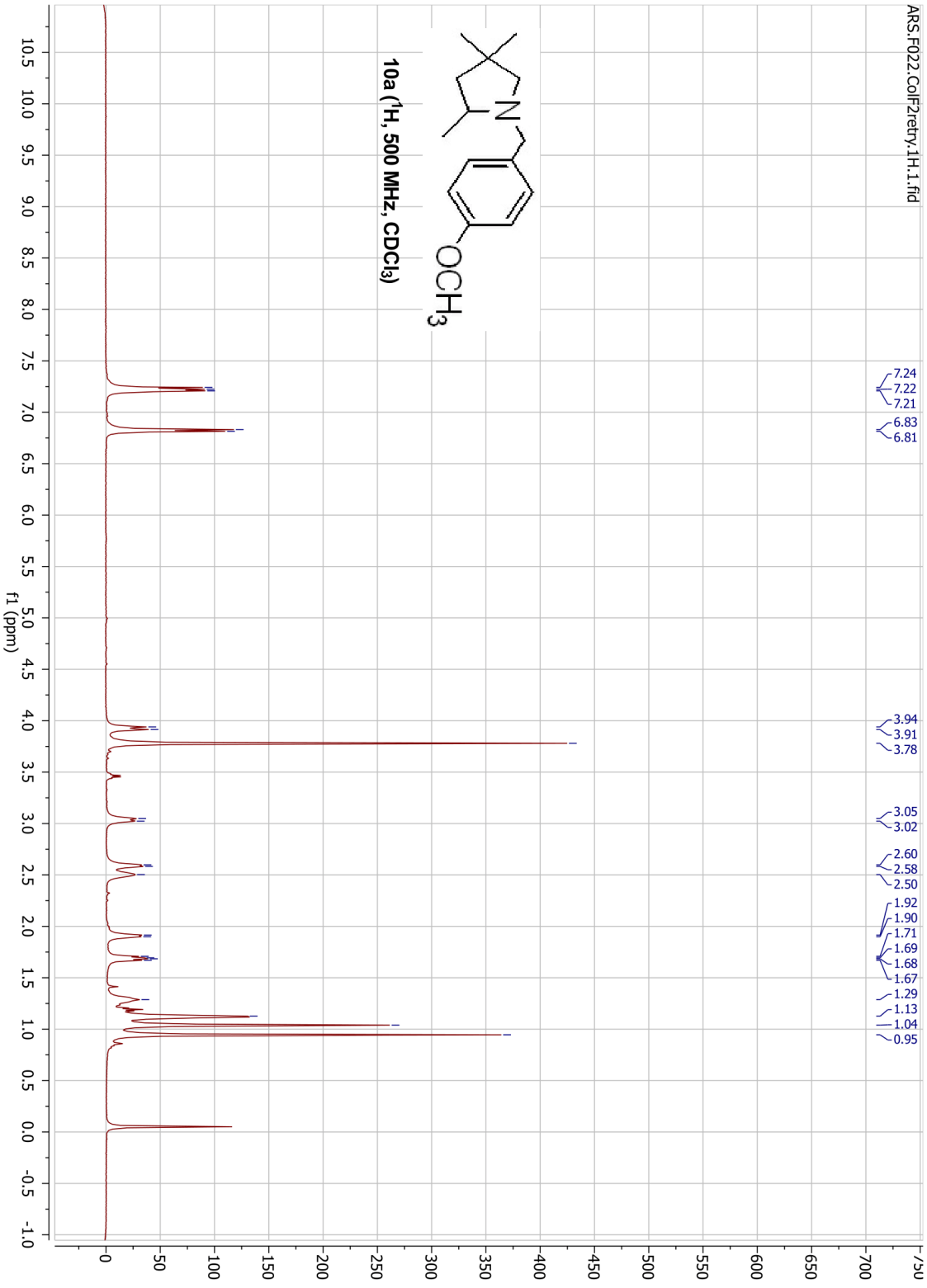

ARS.F030.component1.13C.1.fid
9b (^{1}H, 300 MHz, CDCl$_3$)
155.52
141.60
135.93
128.38
128.06
128.06 C6D6
127.74
116.93
110.42
106.58
59.56
47.54
44.76
34.53
25.53
f1 (ppm)

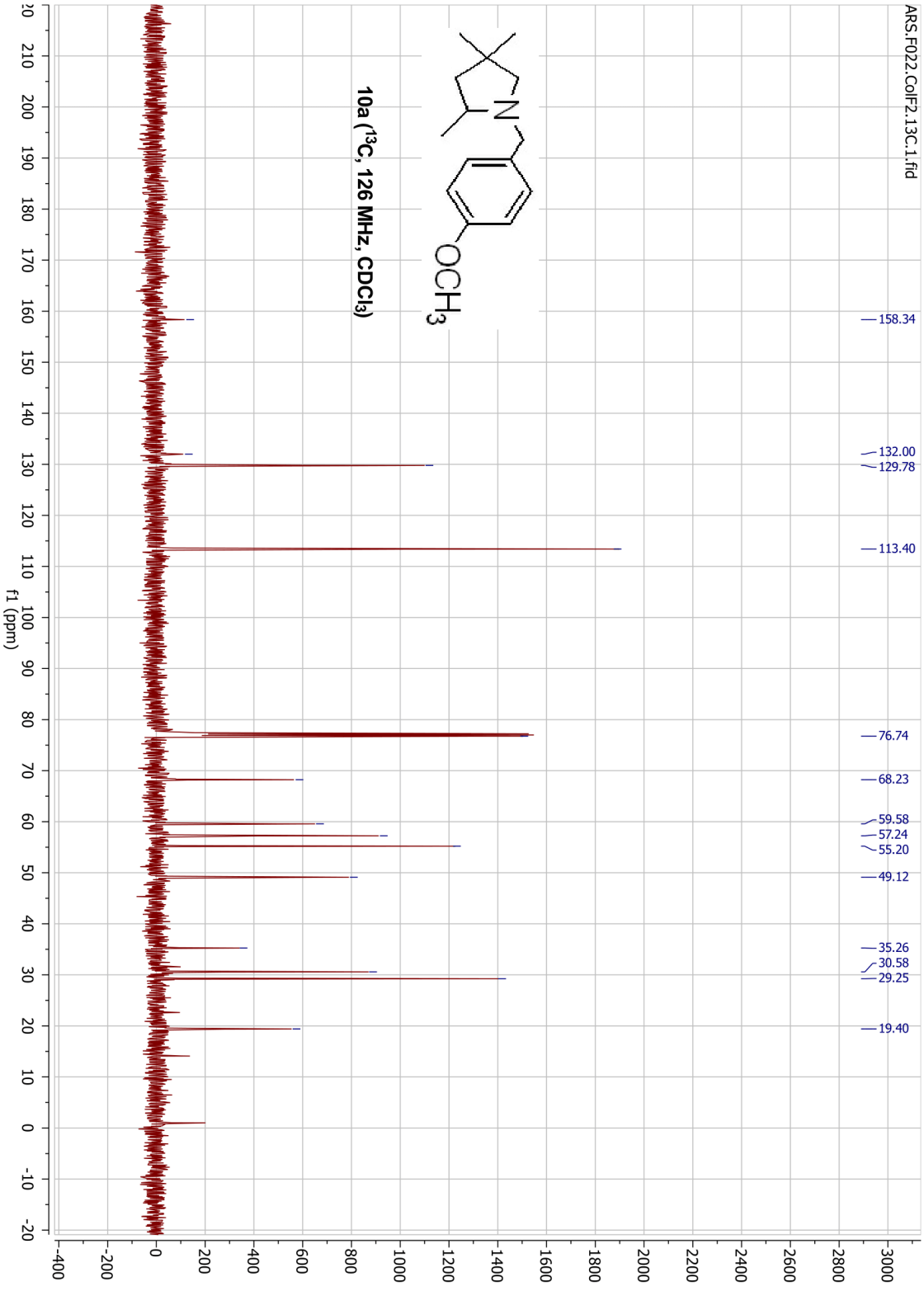

9c (1H, 300 MHz, CDCl3)
ARS.Secondaryaminoalkene.4.1.fid
f1 (ppm)
0.78
1.98
0.97
2.00
2.03
2.00
2.09
0.62
6.85
4.01
0.90

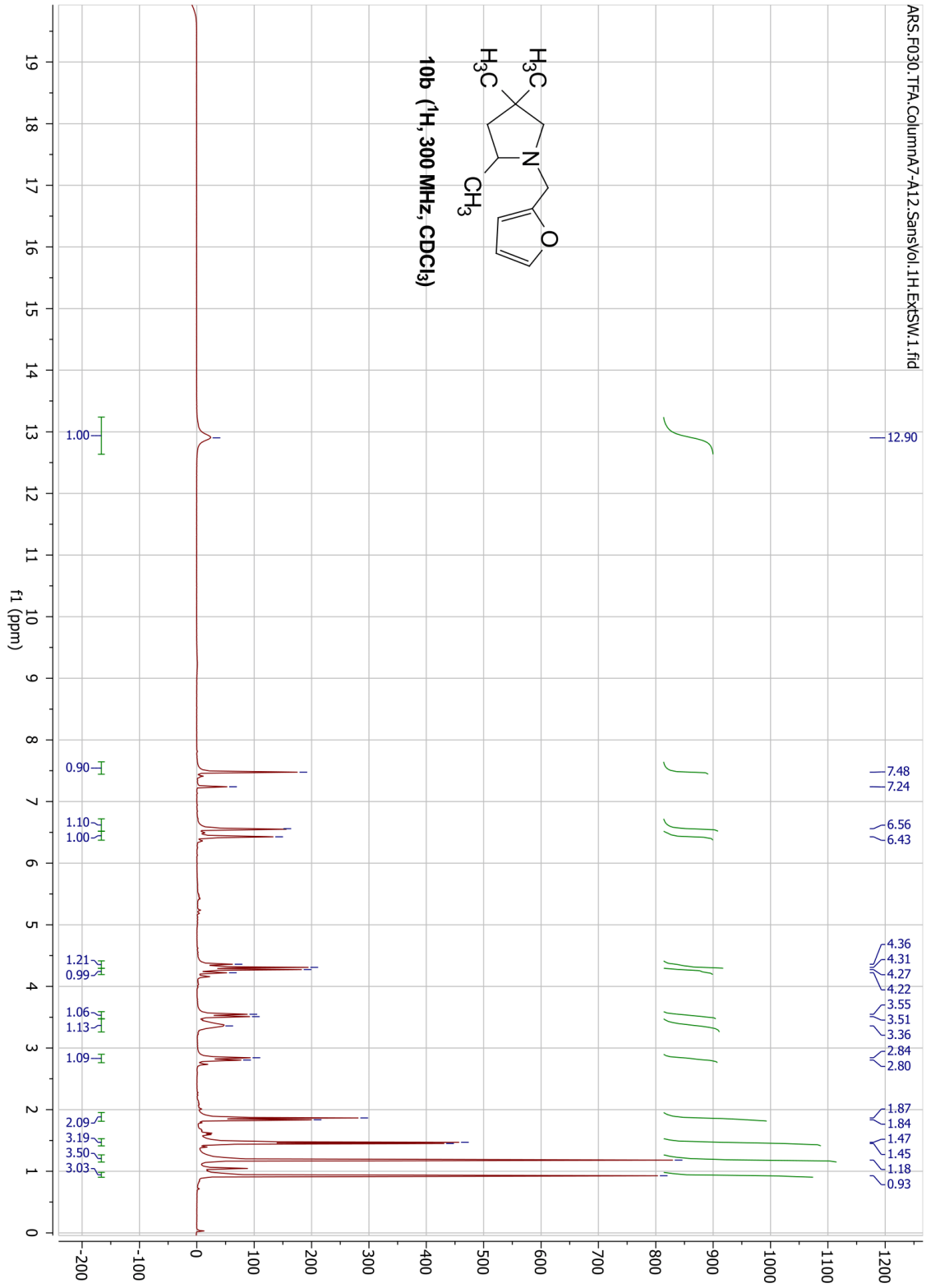

ARS.F029.KugF1.13C.1.fid
9c(13C, 126 MHz, CDCl3)
H3C
H3C
N
H
CH2
S
145.15
135.54
126.51
124.44
124.17
116.90
77.16 CDCl3
59.40
49.32
44.65
34.35
25.54
f1 (ppm)

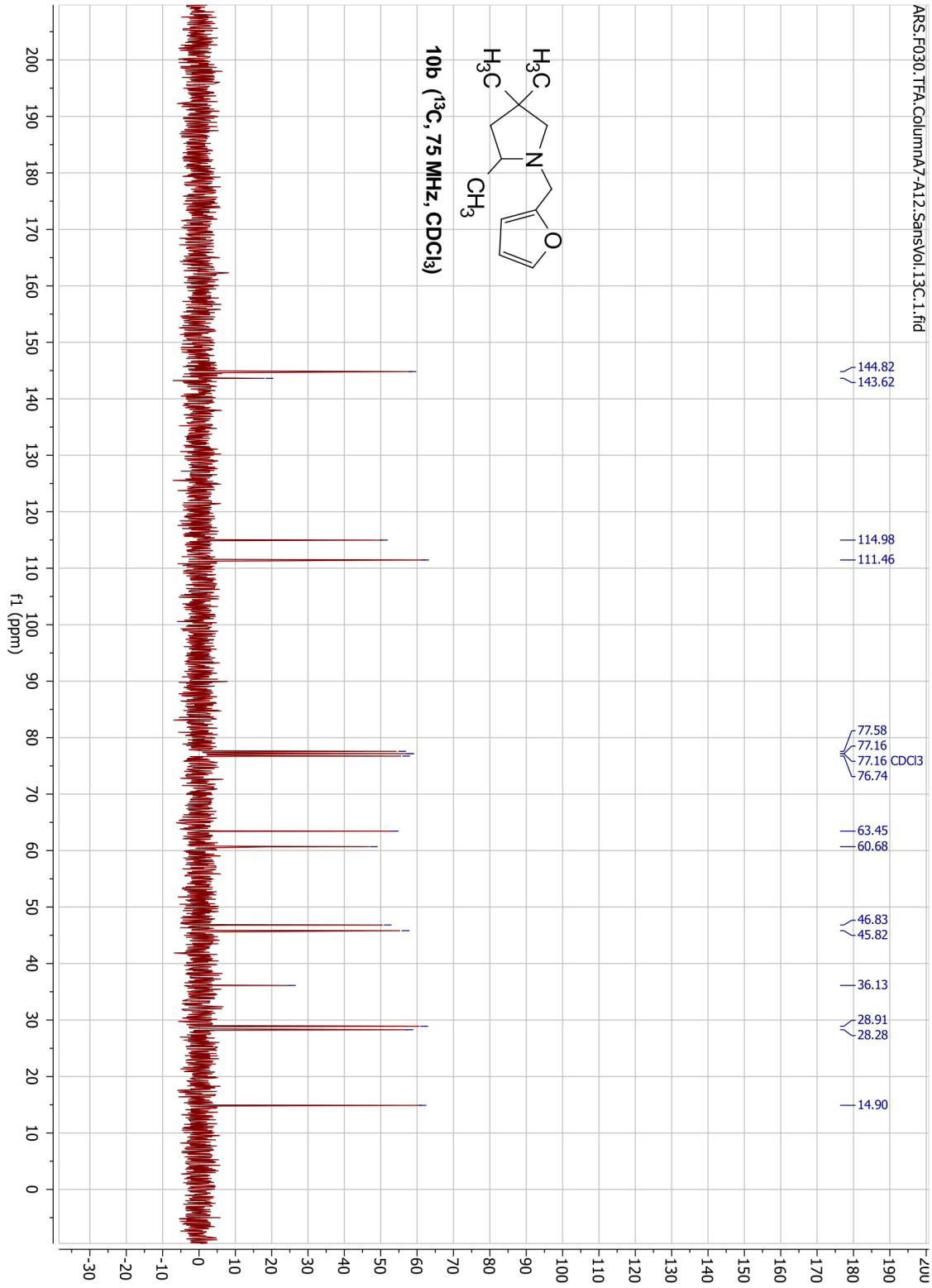

ARS.B289.1H.2.fid
9d (^{1}H, 500 MHz, CDCl$_3$)
7.26 CDCl3
3.11
2.07
0.96
2.00
4.00
1.24
1.00
2.09
1.15
1.33
3.48
f1 (ppm)

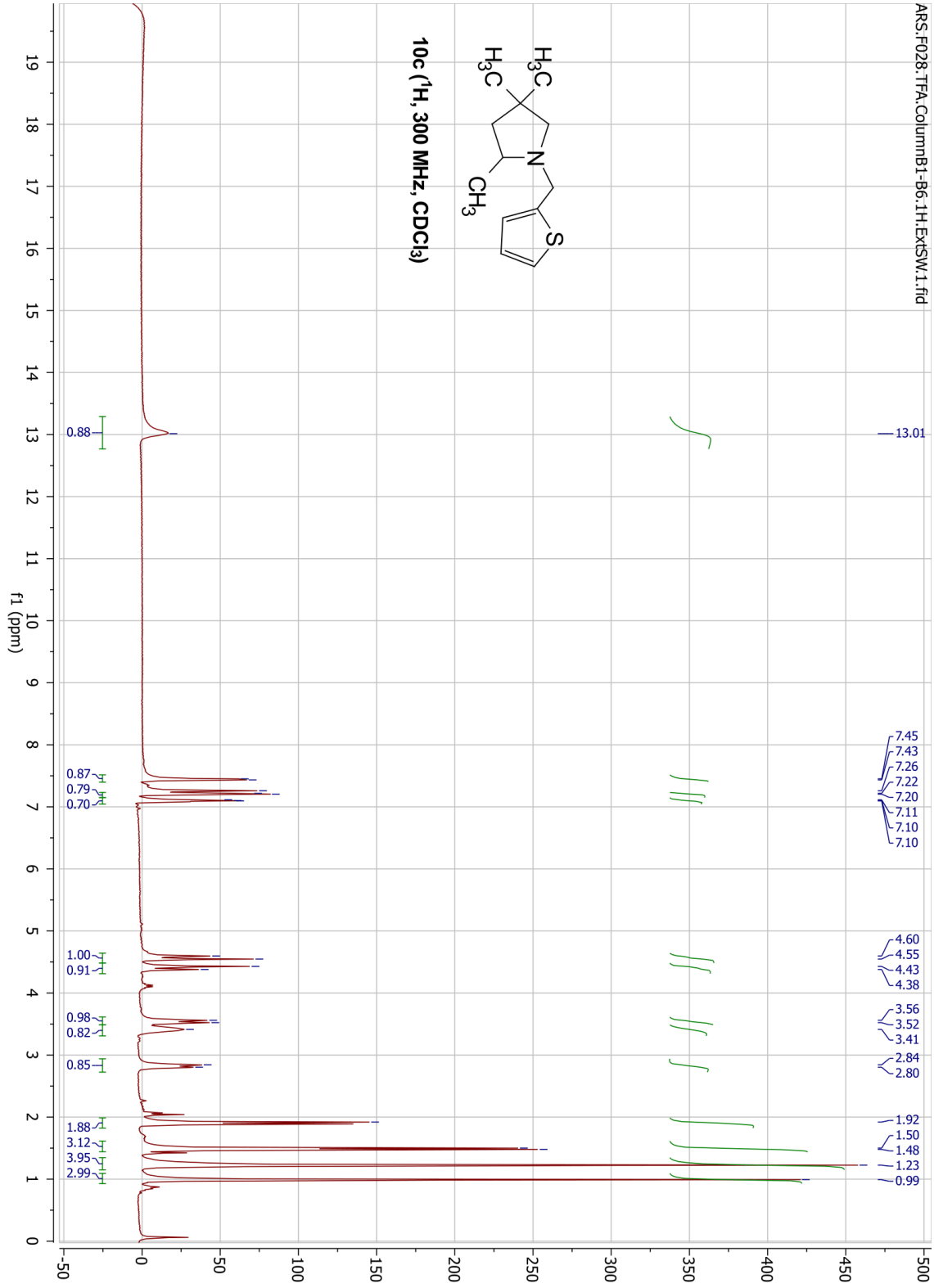

ARS.B289.13C.2.fid
9d (^{13}C, 126 MHz, CDCl$_3$)
158.62
138.63
135.54
129.36
114.44
113.79
77.23 CDCl3
76.97 CDCl3
76.72 CDCl3
55.25
51.92
50.53
35.92
30.23
20.01
f1 (ppm)

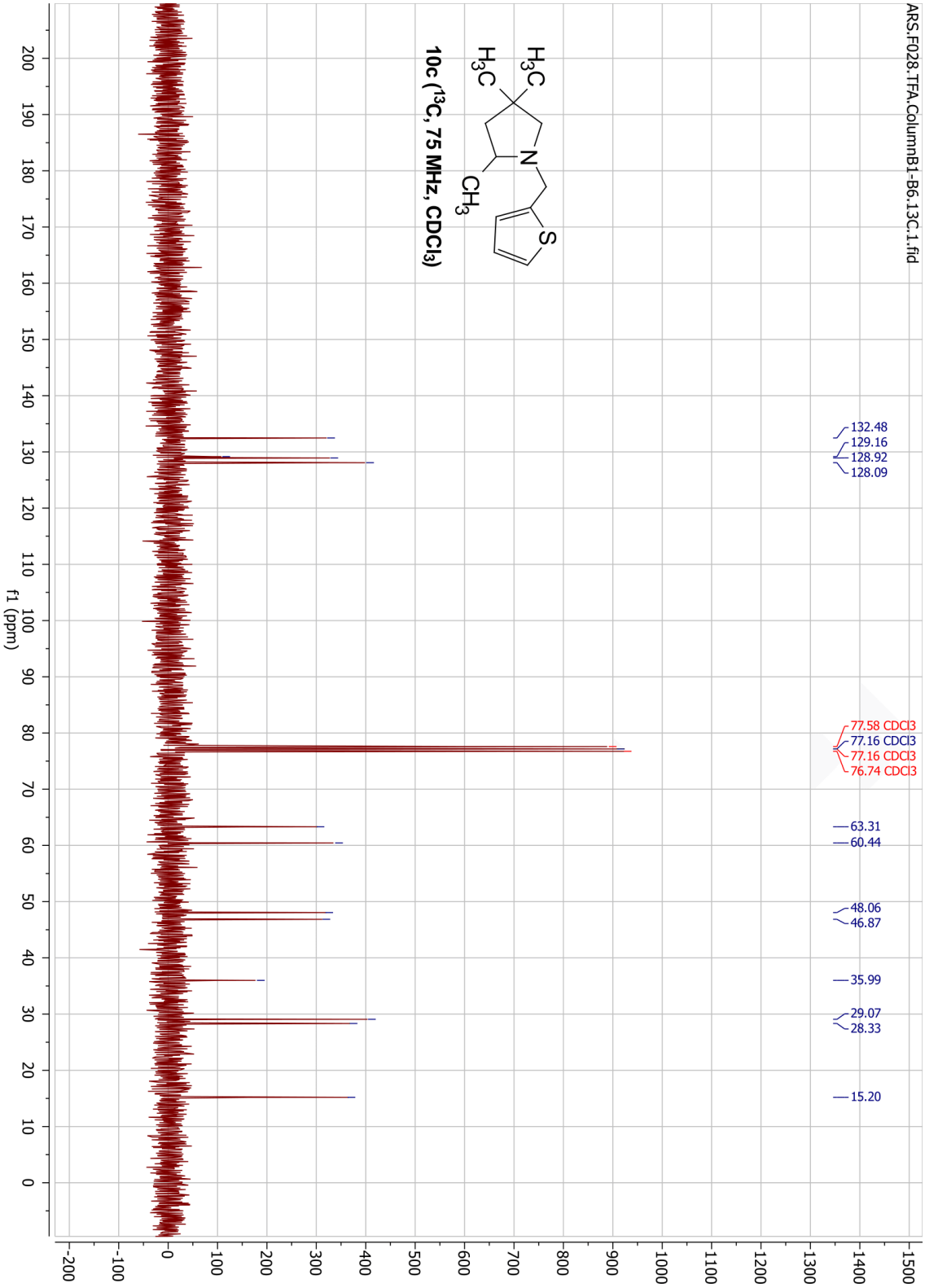

ARS.F022.ColF2retry.1H.1.fid
10a (1H, 500 MHz, CDCl3)
OCH3
N
7.24
7.22
7.21
6.83
6.81
3.94
3.91
3.78
3.05
3.02
2.60
2.58
2.50
1.92
1.90
1.71
1.69
1.68
1.67
1.29
1.13
1.04
0.95
f1 (ppm)

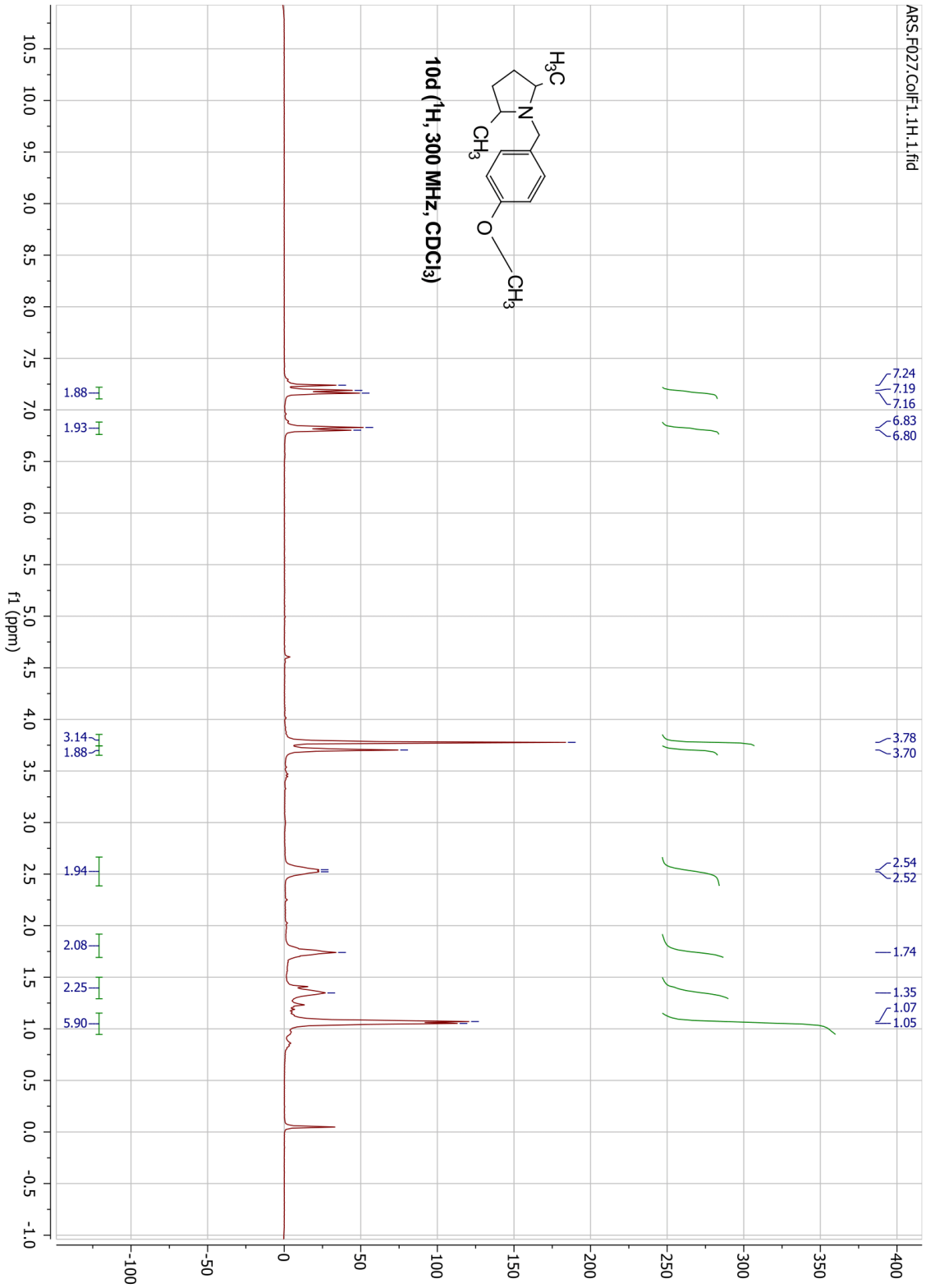

ARS.F022.ColF2.13C.1.fid
10a (^{13}C, 126 MHz, CDCl$_3$)
OCH$_3$
N
158.34
132.00
129.78
113.40
76.74
68.23
59.58
57.24
55.20
49.12
35.26
30.58
29.25
19.40
f1 (ppm)

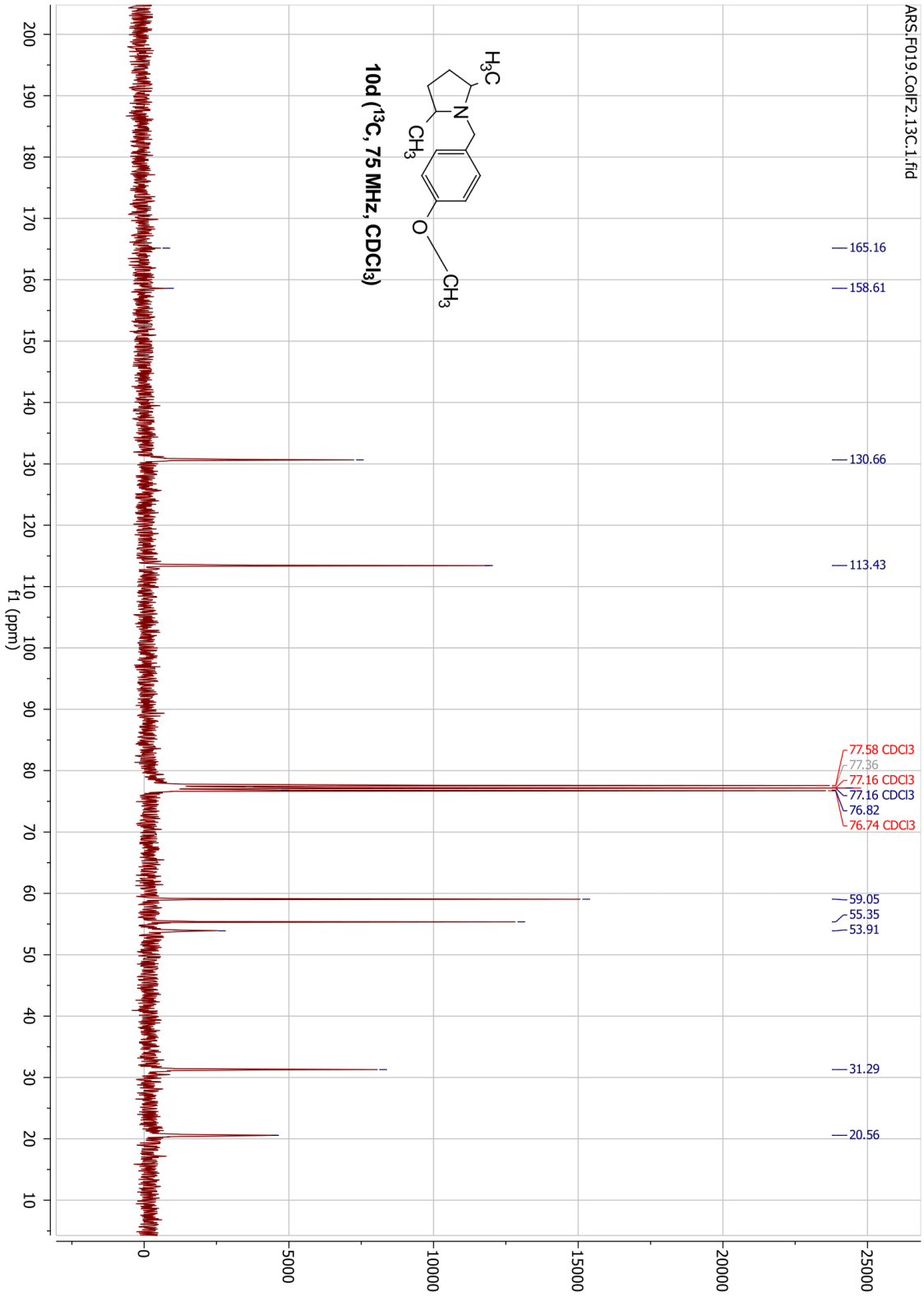

ARS.F030.TFA.ColumnA7-A12.SansVol.1H.ExtSW.1.fid
10b (1H, 300 MHz, CDCl3)
H3C
H3C
CH3
N
O
f1 (ppm)
1.00
0.90
1.10
1.00
1.21
0.99
1.06
1.13
1.09
2.09
3.19
3.50
3.03
12.90
7.48
7.24
6.56
6.43
4.36
4.31
4.27
4.22
3.55
3.51
3.36
2.84
2.80
1.87
1.84
1.47
1.45
1.18
0.93

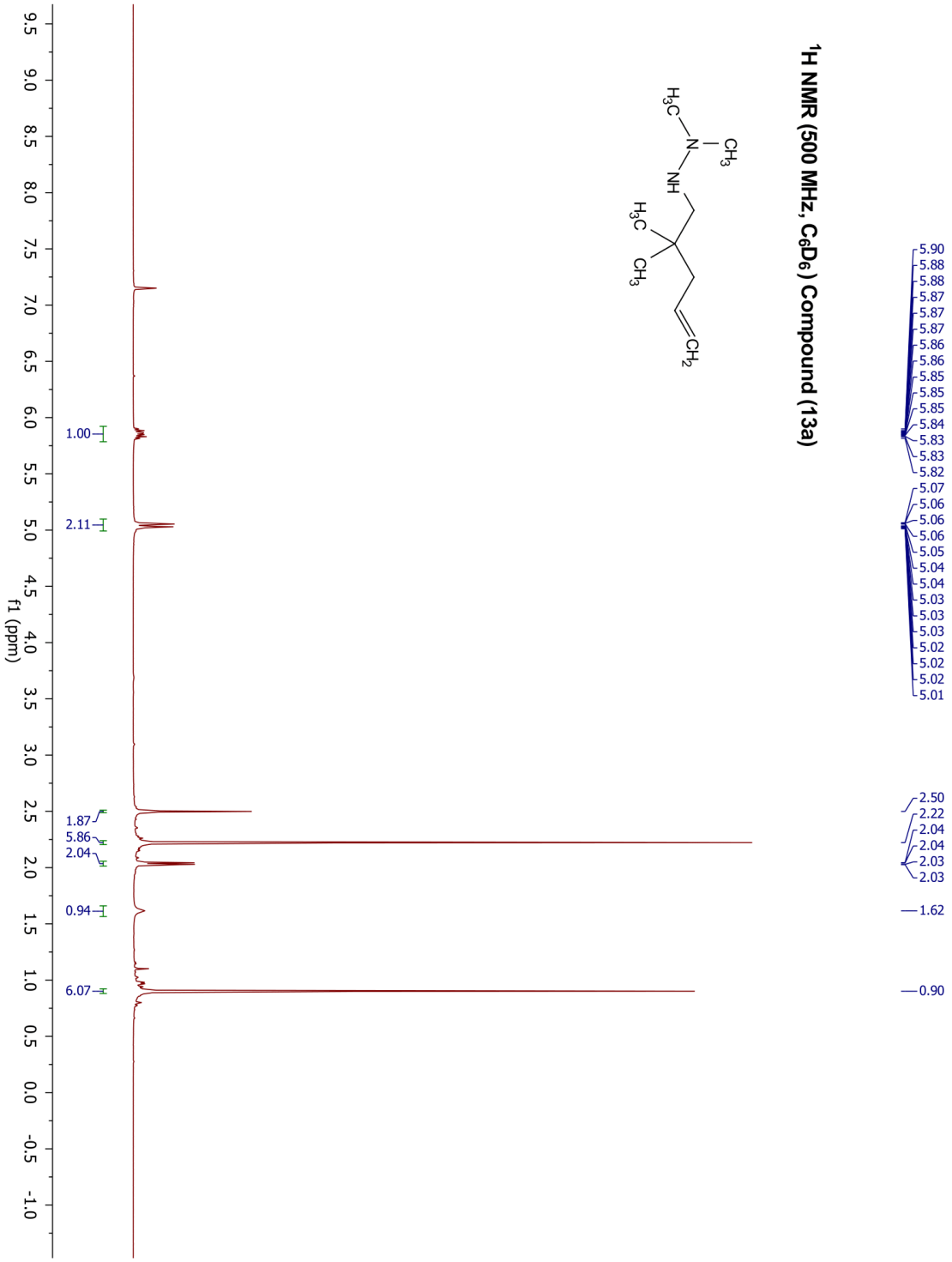

ARS.F030.TFA.ColumnA7-A12.SansVol.13C.1.fid
10b (^{13}C, 75 MHz, CDCl$_3$)
H3C
H3C
CH3
N
O
144.82
143.62
114.98
111.46
77.58
77.16
77.16 CDCl3
76.74
63.45
60.68
46.83
45.82
36.13
28.91
28.28
14.90
f1 (ppm)

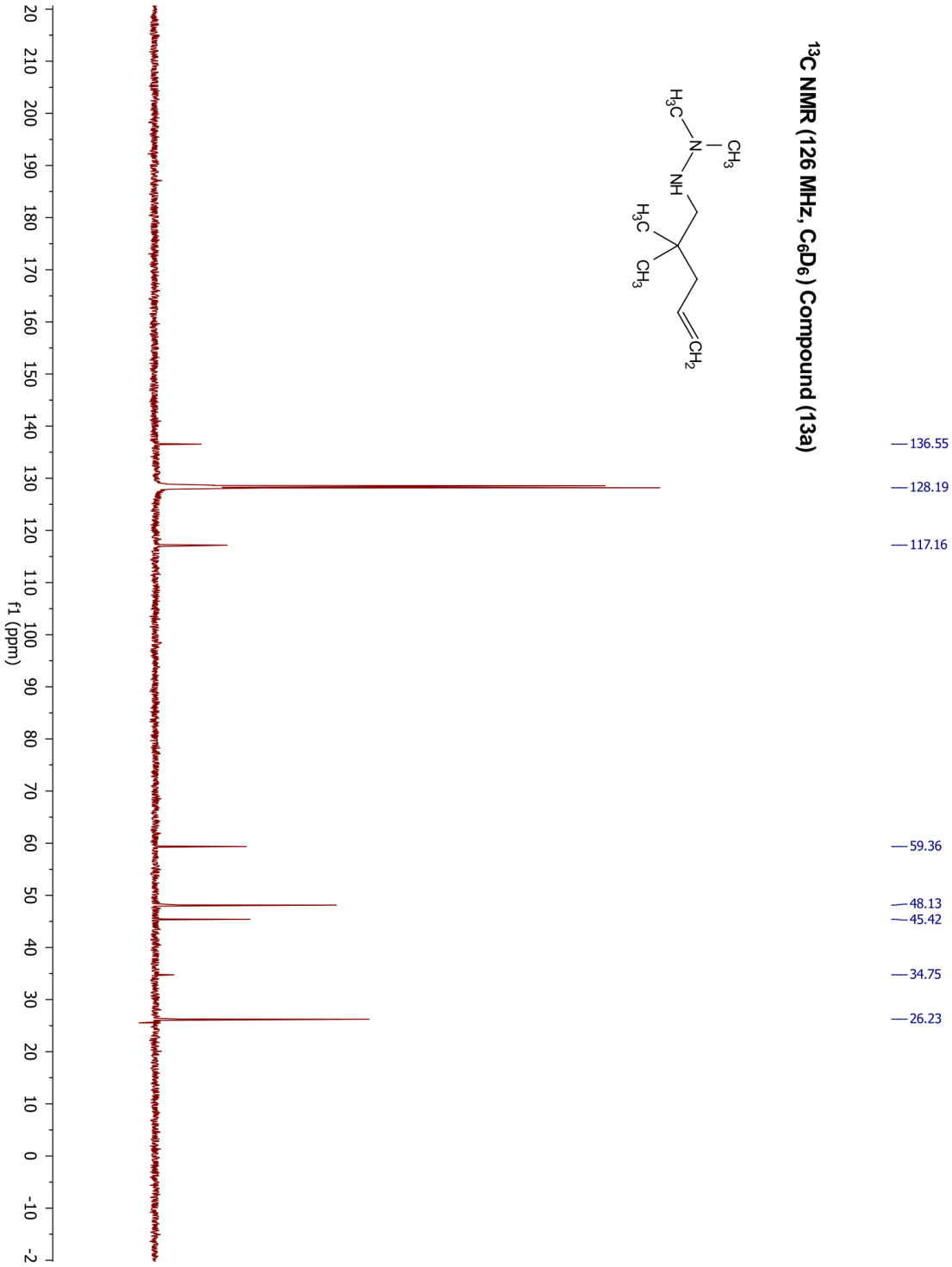

ARS.F028.TFA.ColumnB1-B6.1H.ExtSW.1.fid
10c (1H, 300 MHz, CDCl3)
H3C
H3C
CH3
N
S
f1 (ppm)
0.88
0.87
0.79
0.70
1.00
0.91
0.98
0.82
0.85
1.88
3.12
3.95
2.99
13.01
7.45
7.43
7.26
7.22
7.20
7.11
7.10
7.10
4.60
4.55
4.43
4.38
3.56
3.52
3.41
2.84
2.80
1.92
1.50
1.48
1.23
0.99

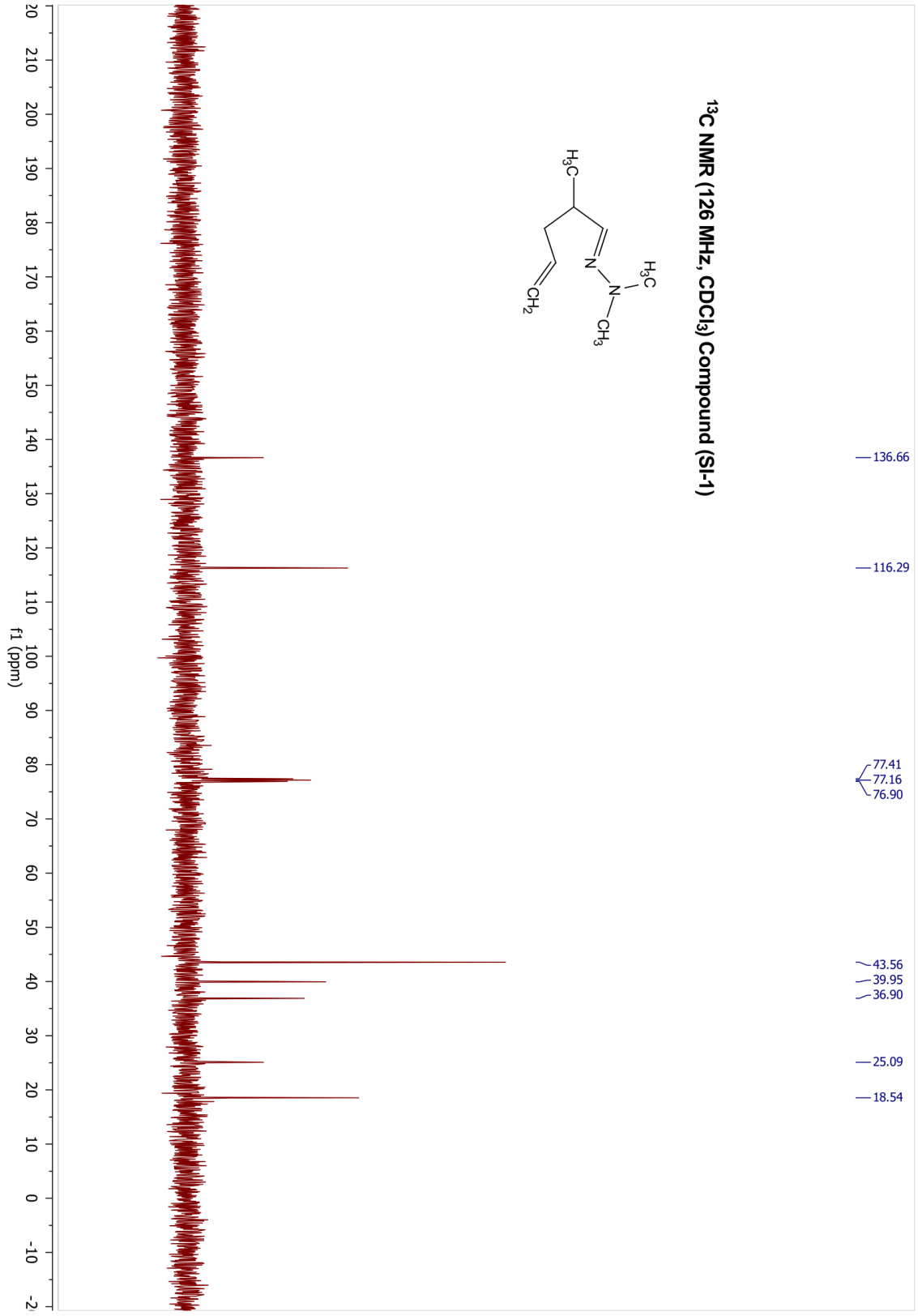

ARS.F028.TFA.ColumnB1-B6.13C.1.fid
10c (^{13}C, 75 MHz, CDCl$_3$)
H3C
H3C
CH3
N
S
132.48
129.16
128.92
128.09
77.58 CDCl3
77.16 CDCl3
77.16 CDCl3
76.74 CDCl3
63.31
60.44
48.06
46.87
35.99
29.07
28.33
15.20
f1 (ppm)

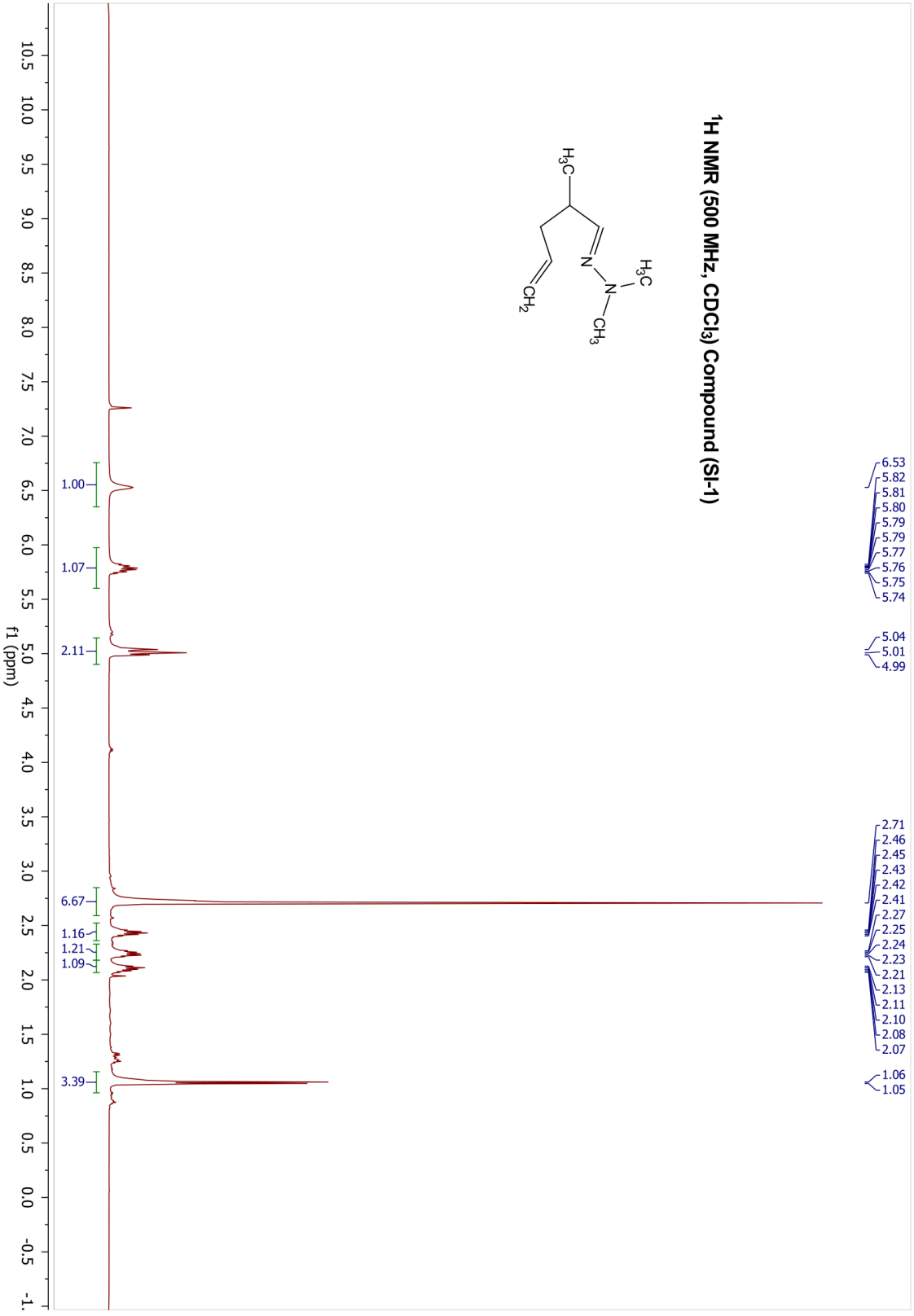

ARS.F027.Col1F1.1H.1.fid
10d (1H, 300 MHz, CDCl3)
H3C
CH3
N
O
CH3
f1 (ppm)
1.88
1.93
3.14
1.88
1.94
2.08
2.25
5.90
7.24
7.19
7.16
6.83
6.80
3.78
3.70
2.54
2.52
1.74
1.35
1.07
1.05

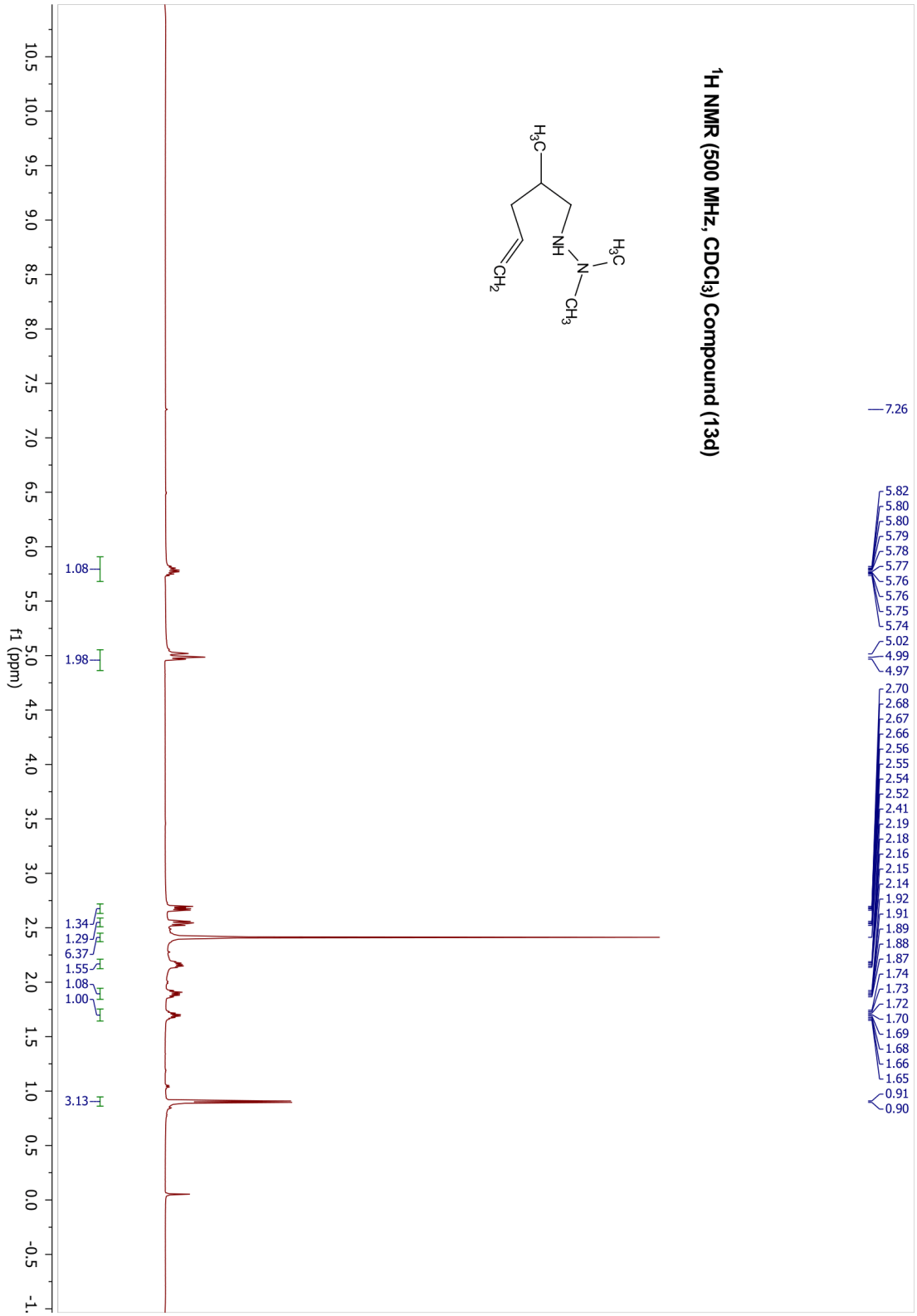

ARS.F019.Col F2.13C.1.fid
10d (^{13}C, 75 MHz, CDCl$_3$)
H$_3$C
CH$_3$
N
O
CH$_3$
165.16
158.61
130.66
113.43
77.58 CDCl3
77.36
77.16 CDCl3
77.16 CDCl3
76.82
76.74 CDCl3
59.05
55.35
53.91
31.29
20.56
f1 (ppm)
200
190
180
170
160
150
140
130
120
110
100
90
80
70
60
50
40
30
20
10
0
5000
10000
15000
20000
25000

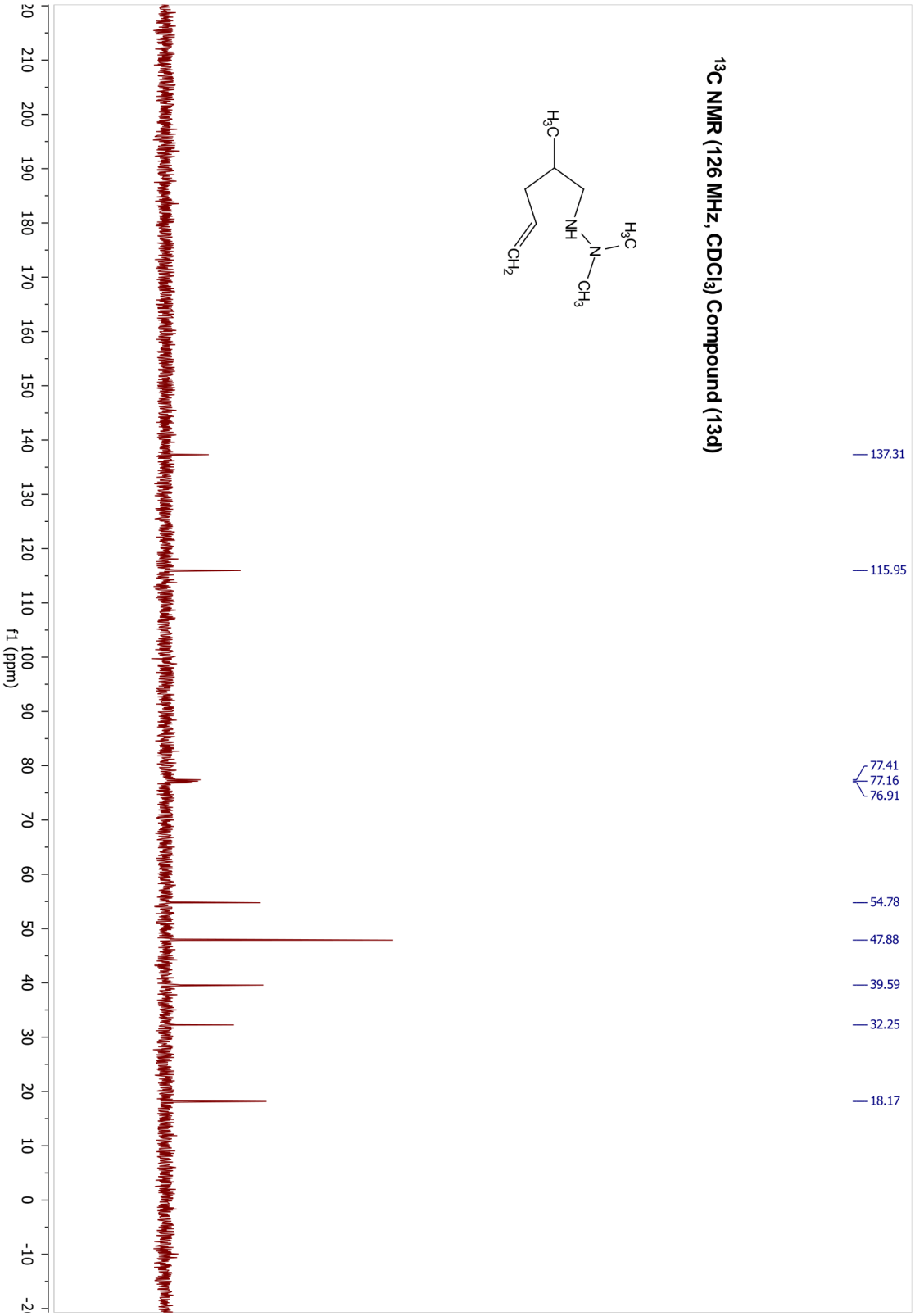

^{1}H NMR (500 MHz, C_6D_6) Compound (13a)
f1 (ppm)
1.00
2.11
1.87
5.86
2.04
0.94
6.07
5.90
5.88
5.88
5.87
5.87
5.87
5.86
5.86
5.85
5.85
5.85
5.84
5.83
5.83
5.82
5.07
5.06
5.06
5.06
5.05
5.04
5.04
5.03
5.03
5.03
5.02
5.02
5.02
5.01
2.50
2.22
2.04
2.04
2.03
2.03
1.62
0.90

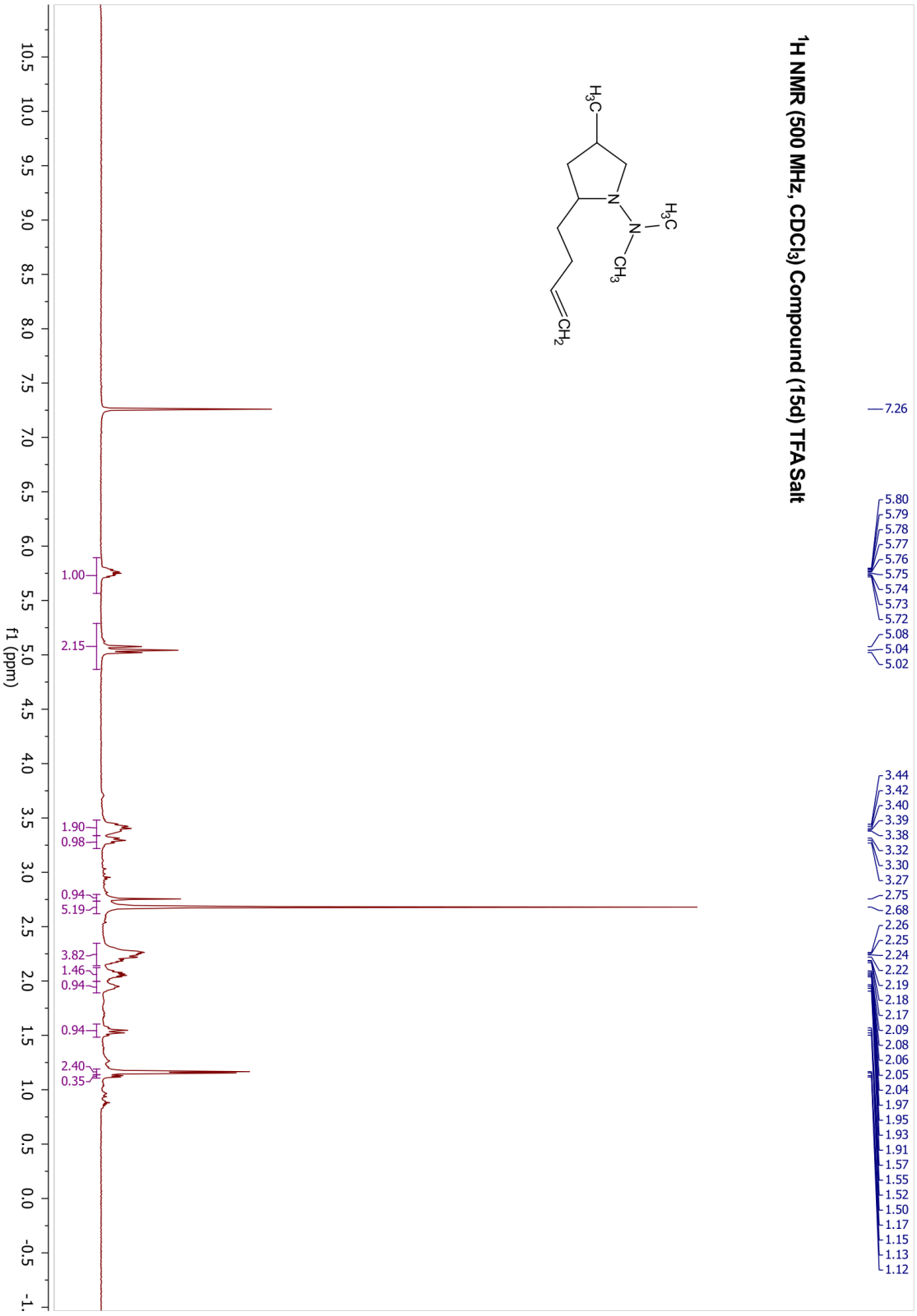

^{13}C NMR (126 MHz, C_6D_6) Compound (13a)
136.55
128.19
117.16
59.36
48.13
45.42
34.75
26.23
f1 (ppm)

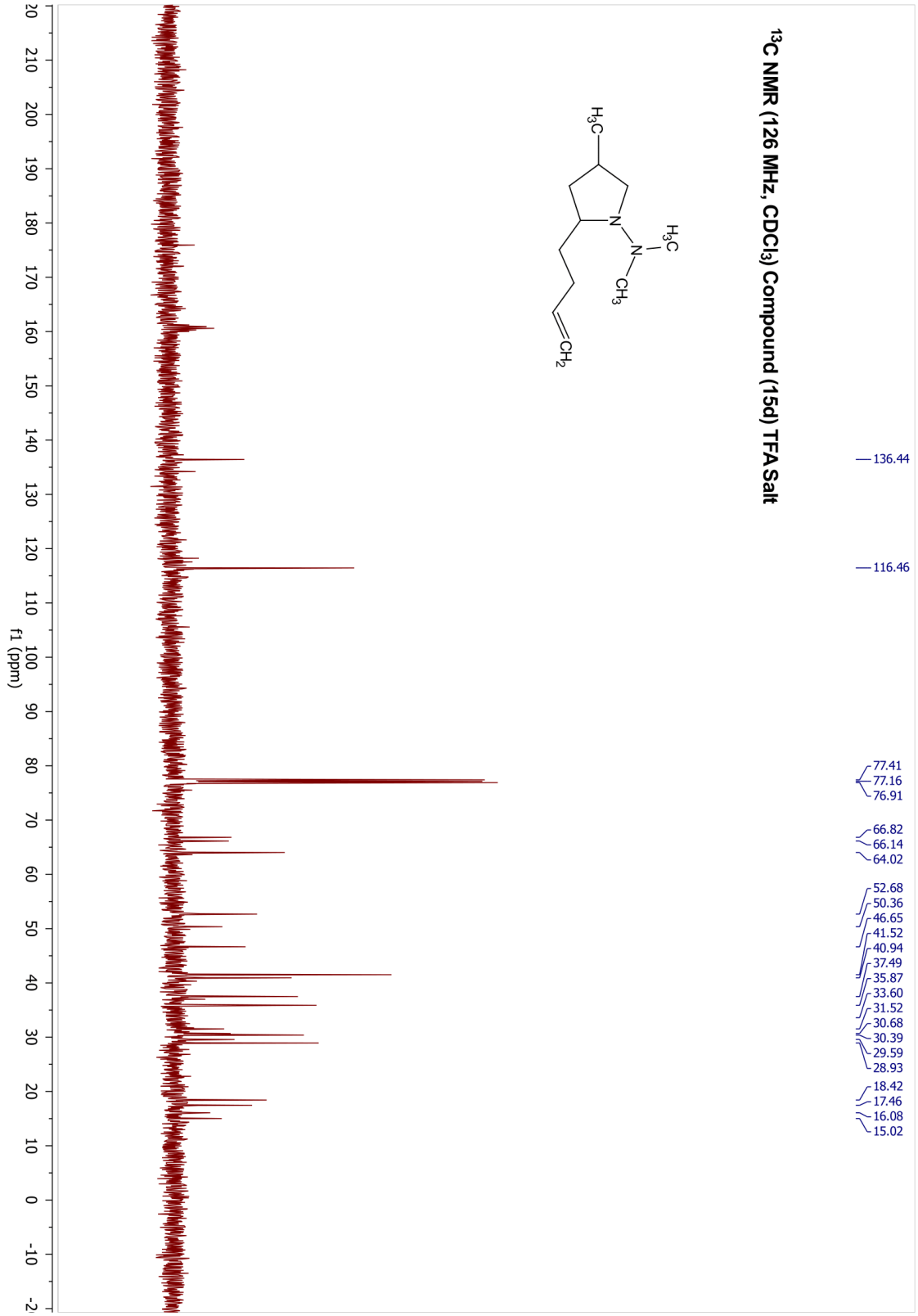

^{13}C NMR (126 MHz, CDCl$_3$) Compound (SI-1)
H$_3$C
N
N
H$_3$C
CH$_3$
CH$_2$
136.66
116.29
77.41
77.16
76.90
43.56
39.95
36.90
25.09
18.54
f1 (ppm)
220
210
200
190
180
170
160
150
140
130
120
110
100
90
80
70
60
50
40
30
20
10
0
-10
-20

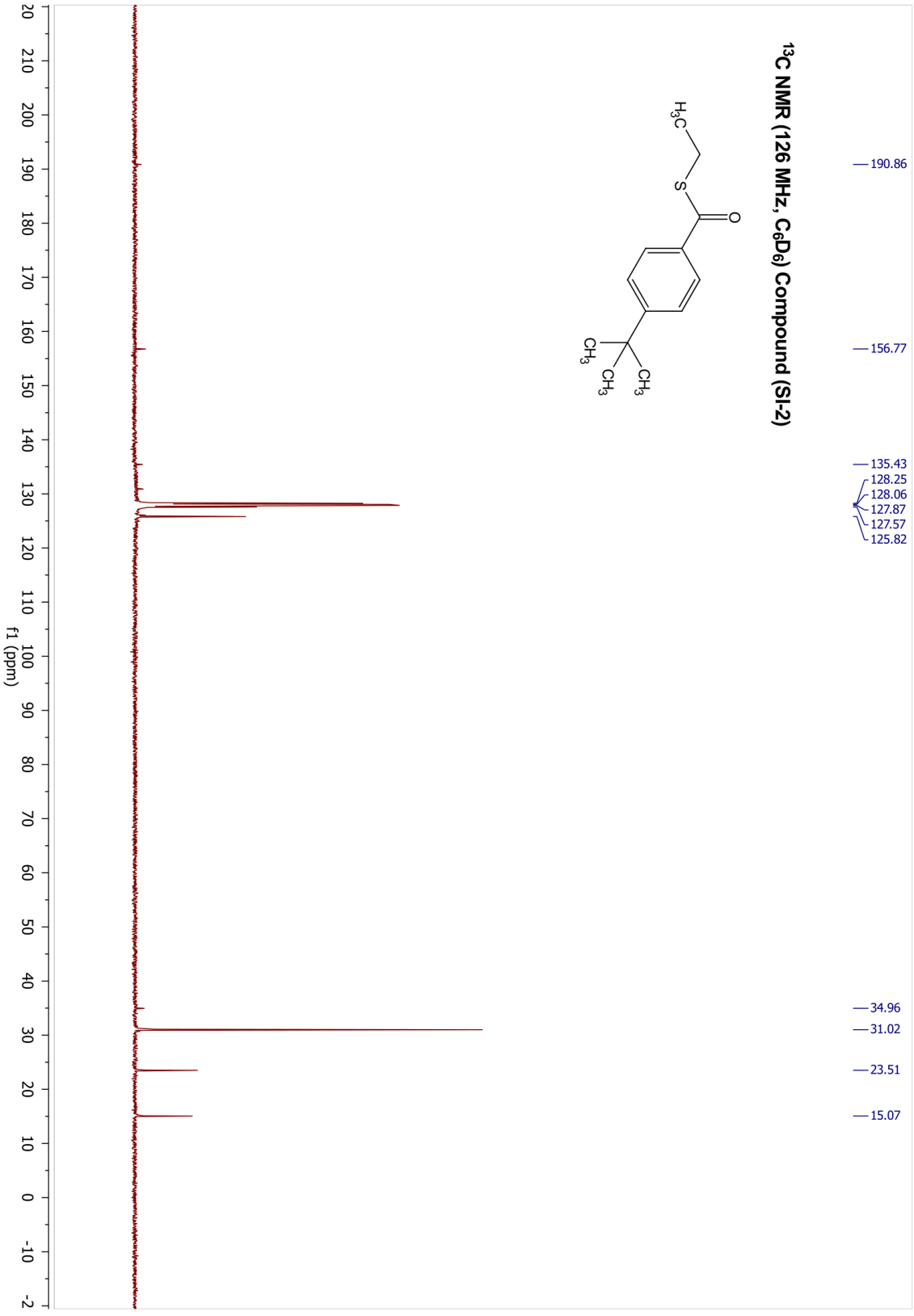

^{1}H NMR (500 MHz, CDCl$_3$) Compound (SI-1)
f1 (ppm)
1.00
1.07
2.11
6.67
1.16
1.21
1.09
3.39
6.53
5.82
5.81
5.80
5.79
5.79
5.77
5.76
5.75
5.74
5.04
5.01
4.99
2.71
2.46
2.45
2.43
2.42
2.41
2.27
2.25
2.24
2.23
2.21
2.13
2.11
2.10
2.08
2.07
1.06
1.05

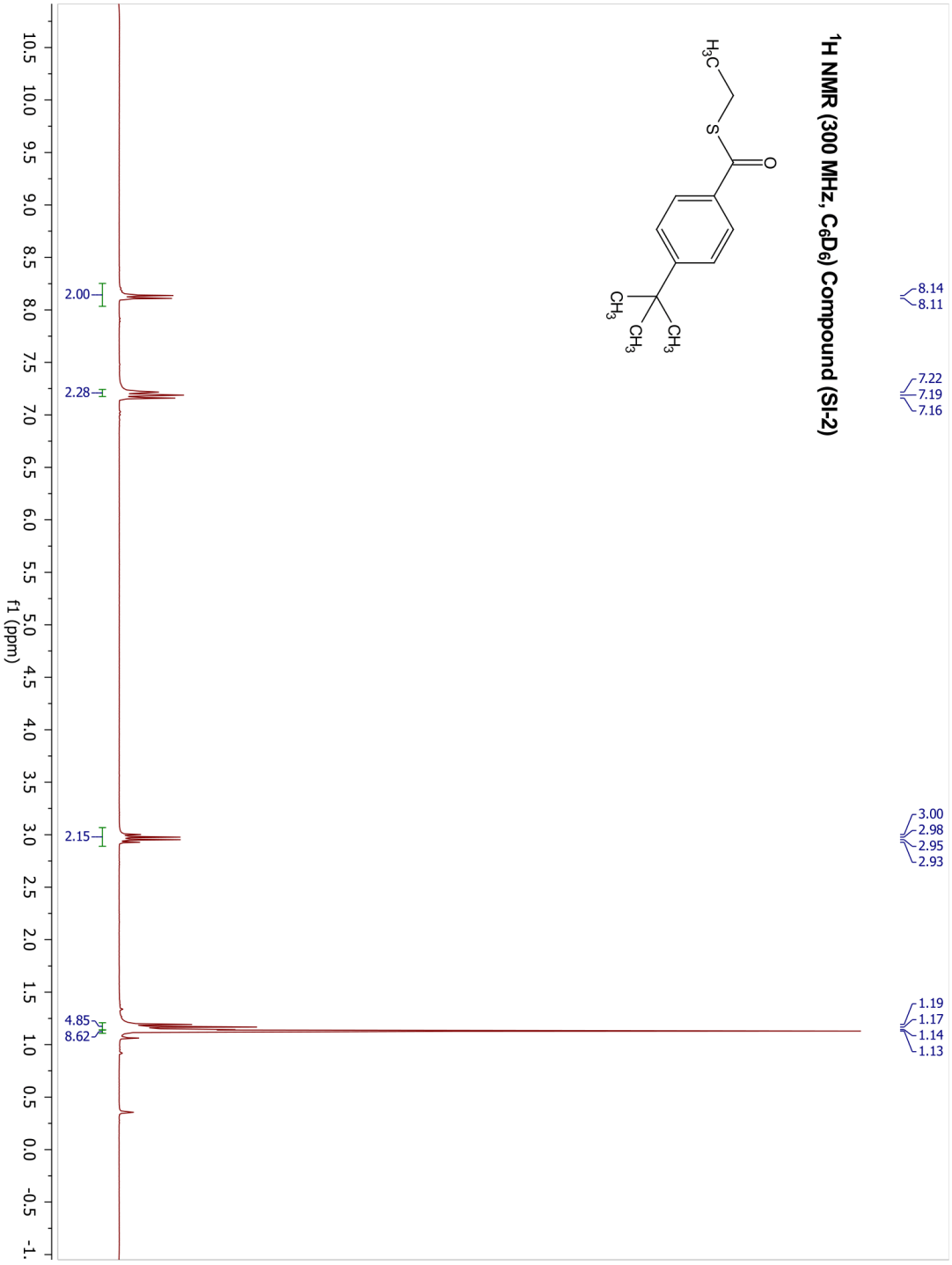

^{1}H NMR (500 MHz, CDCl$_3$) Compound (13d)
H$_3$C
NH
N
H$_3$C
CH$_3$
CH$_2$
7.26
5.82
5.80
5.80
5.79
5.78
5.77
5.76
5.76
5.75
5.74
5.02
4.99
4.97
2.70
2.68
2.67
2.66
2.56
2.55
2.54
2.52
2.41
2.19
2.18
2.16
2.15
2.14
1.92
1.91
1.89
1.88
1.87
1.74
1.73
1.72
1.70
1.69
1.68
1.66
1.65
0.91
0.90
1.08
1.98
1.34
1.29
6.37
1.55
1.08
1.00
3.13
f1 (ppm)

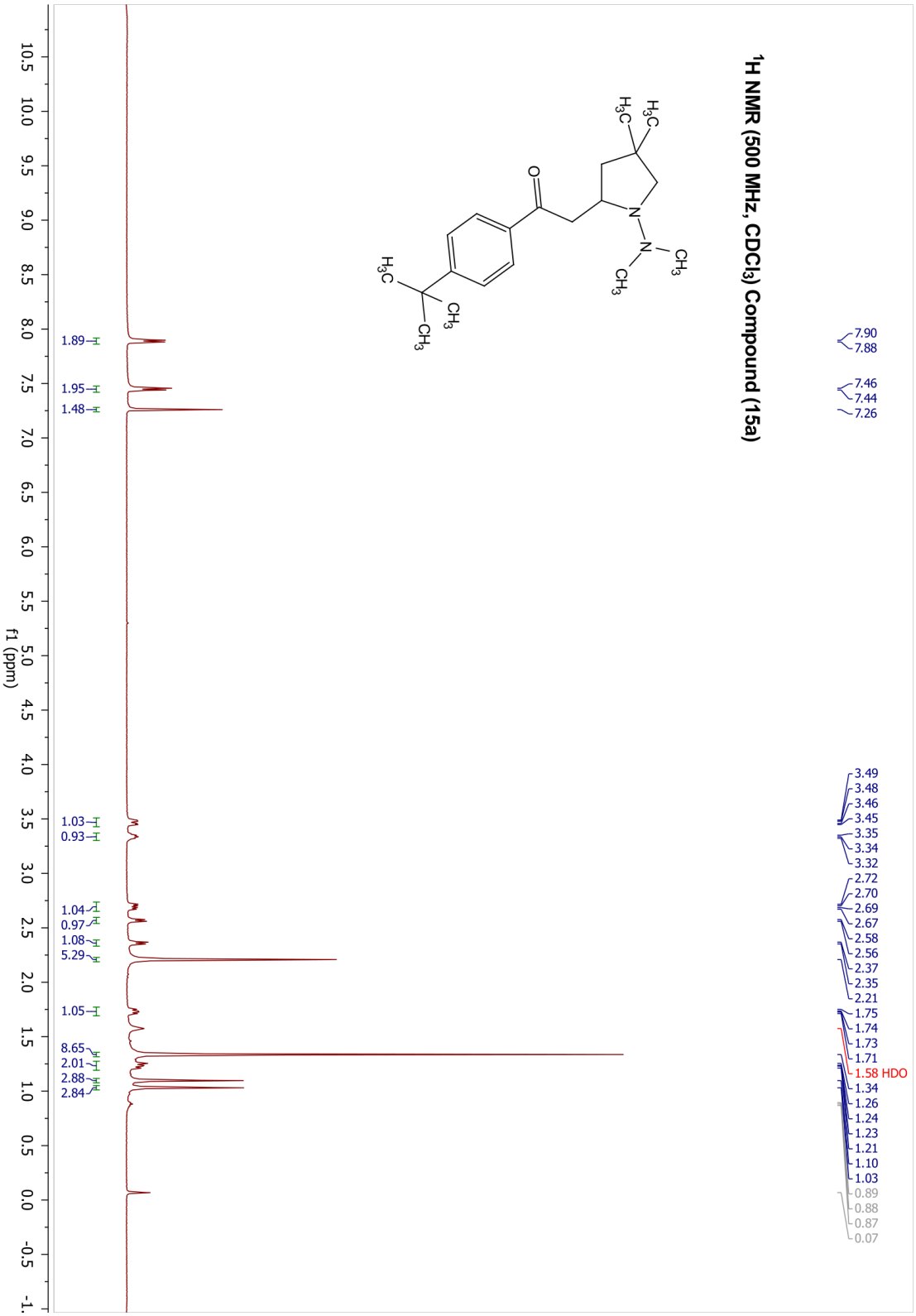

13C NMR (126 MHz, CDCl3) Compound (13d)
H3C
NH
N
H3C
CH3
CH2
137.31
115.95
77.41
77.16
76.91
54.78
47.88
39.59
32.25
18.17
f1 (ppm)

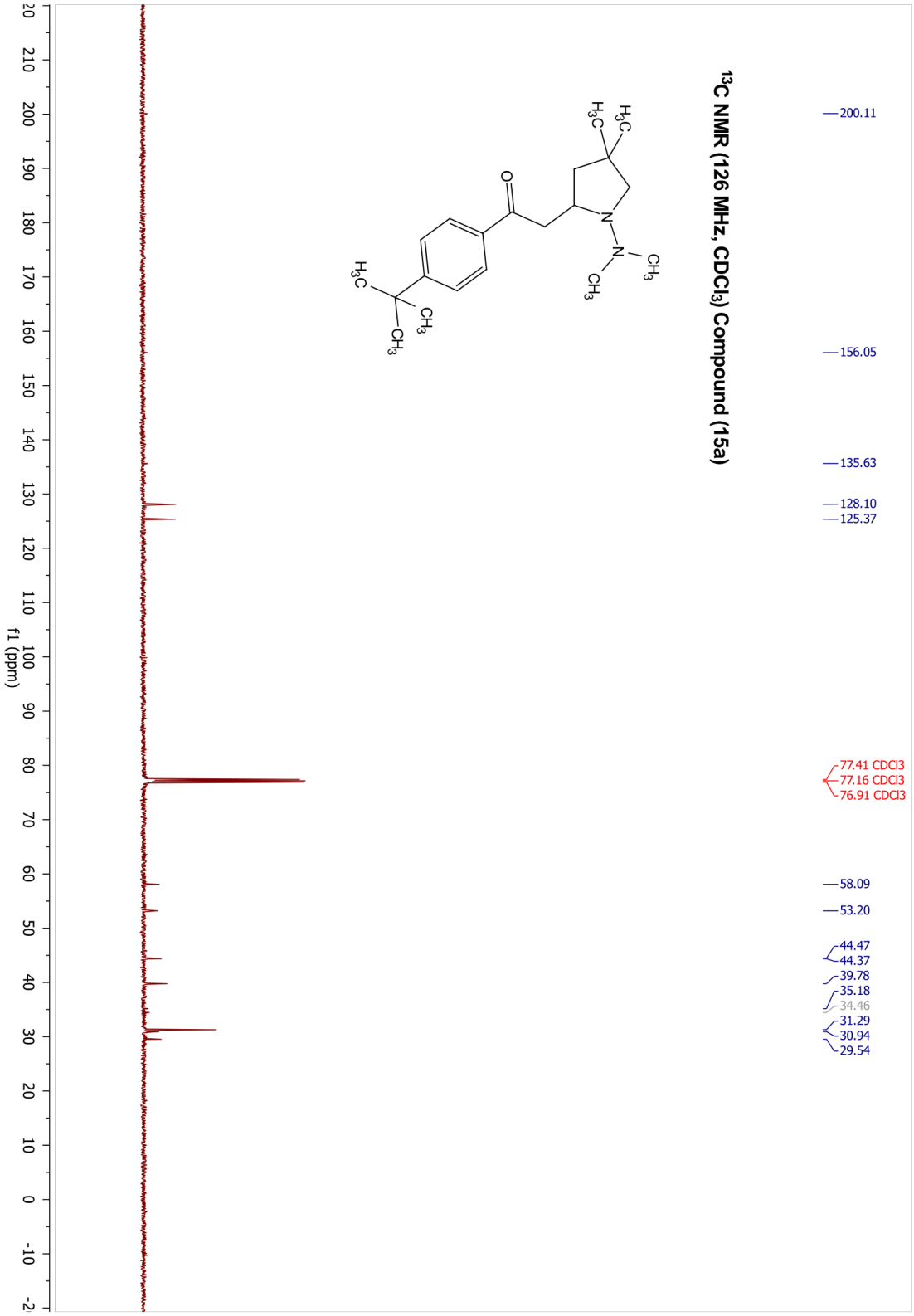

^{1}H NMR (500 MHz, CDCl$_3$) Compound (15d) TFA Salt
H3C
N
N
CH3
H3C
CH2
7.26
5.80
5.79
5.78
5.77
5.76
5.75
5.74
5.73
5.72
5.08
5.04
5.02
3.44
3.42
3.40
3.39
3.38
3.32
3.30
3.27
2.75
2.68
2.26
2.25
2.24
2.22
2.19
2.18
2.17
2.09
2.08
2.06
2.05
2.04
1.97
1.95
1.93
1.91
1.57
1.55
1.52
1.50
1.17
1.15
1.13
1.12
1.00
2.15
1.90
0.98
0.94
5.19
3.82
1.46
0.94
0.94
2.40
0.35
f1 (ppm)

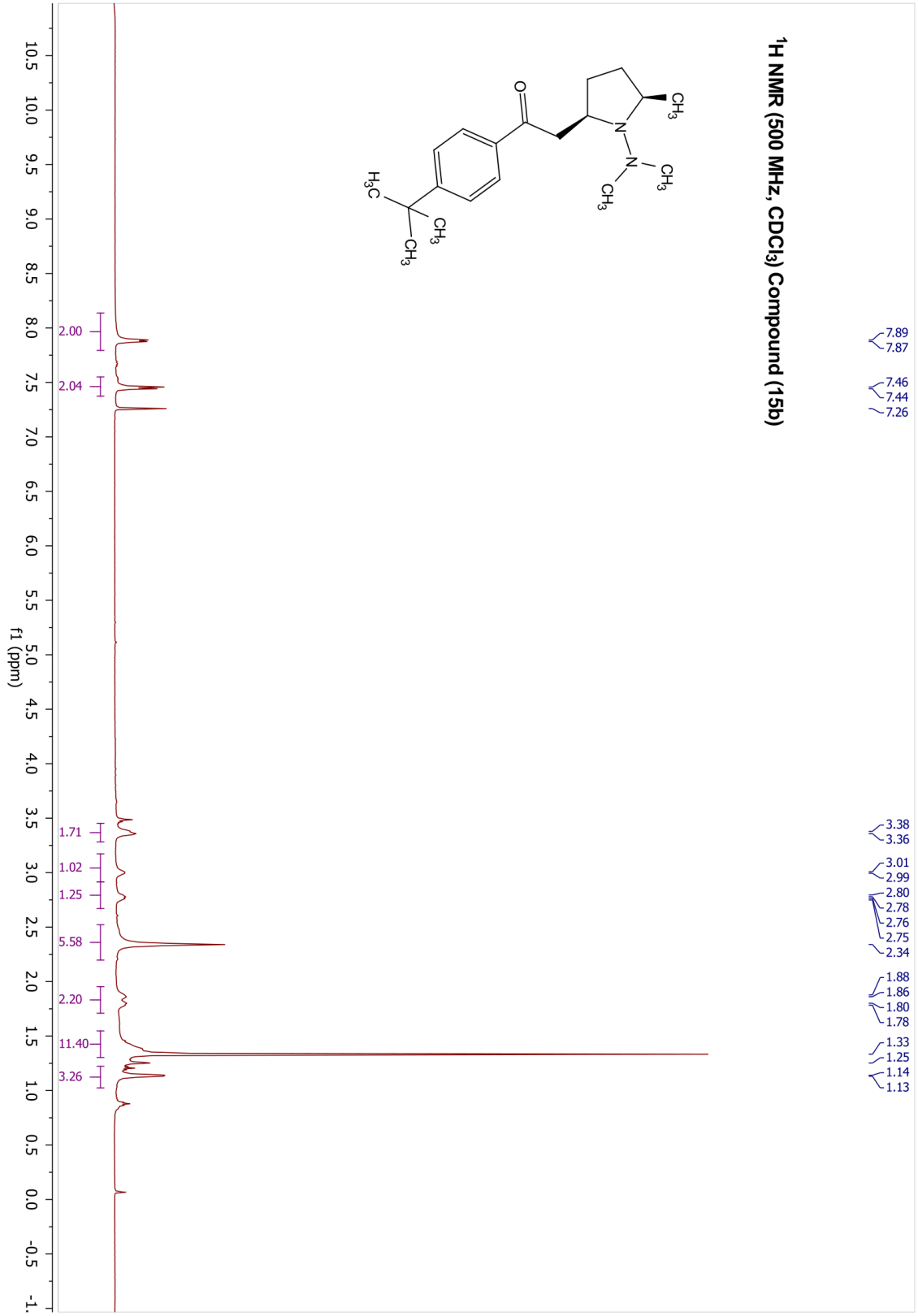

13C NMR (126 MHz, CDCl3) Compound (15d) TFA Salt
H3C
N
N
H3C
CH3
CH2
136.44
116.46
77.41
77.16
76.91
66.82
66.14
64.02
52.68
50.36
46.65
41.52
40.94
37.49
35.87
33.60
31.52
30.68
30.39
29.59
28.93
18.42
17.46
16.08
15.02
f1 (ppm)
20 210 200 190 180 170 160 150 140 130 120 110 100 90 80 70 60 50 40 30 20 10 0 -10 -2

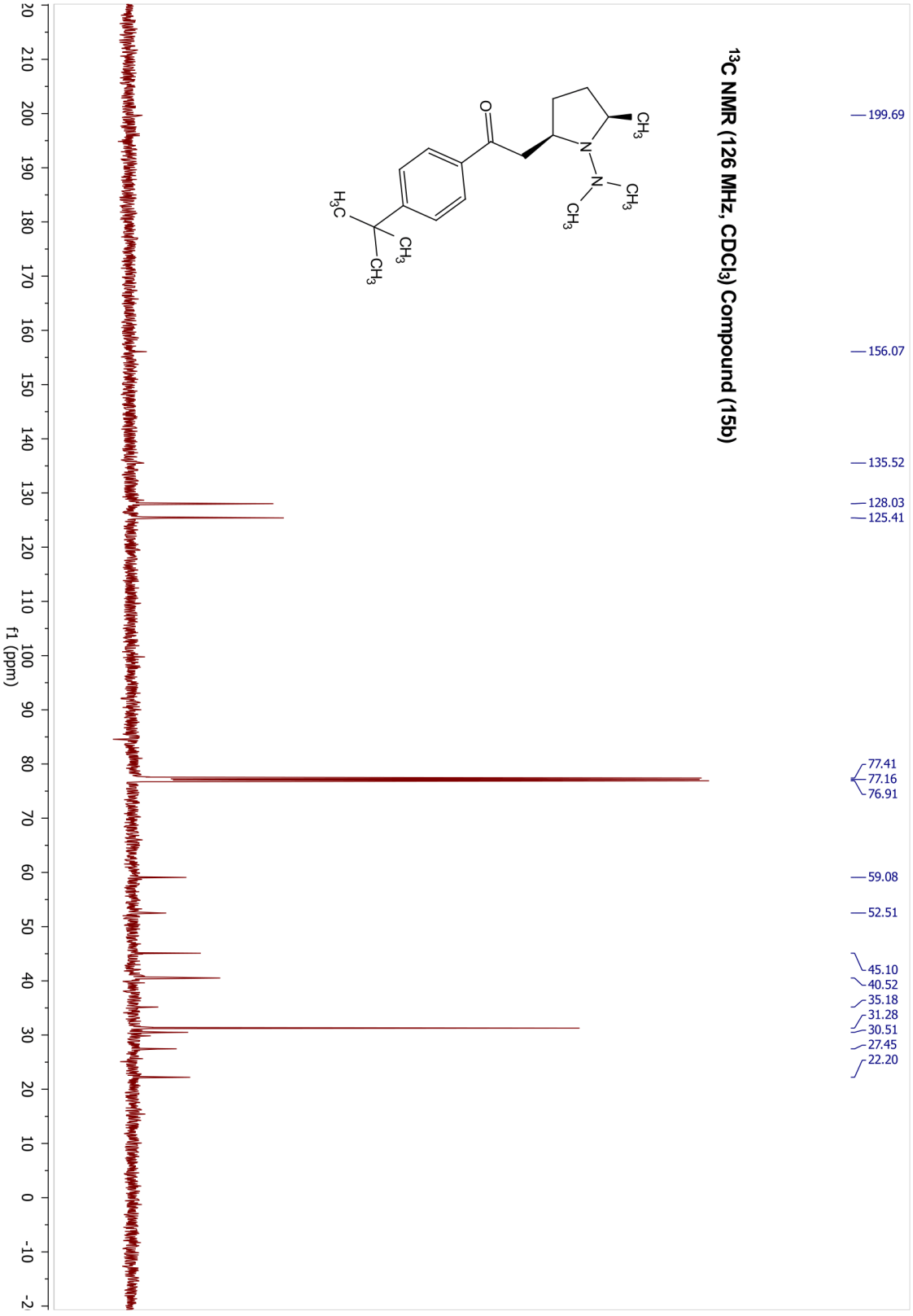

^{13}C NMR (126 MHz, C_6D_6) Compound (SI-2)
190.86
156.77
135.43
128.25
128.06
127.87
127.57
125.82
34.96
31.02
23.51
15.07
f1 (ppm)

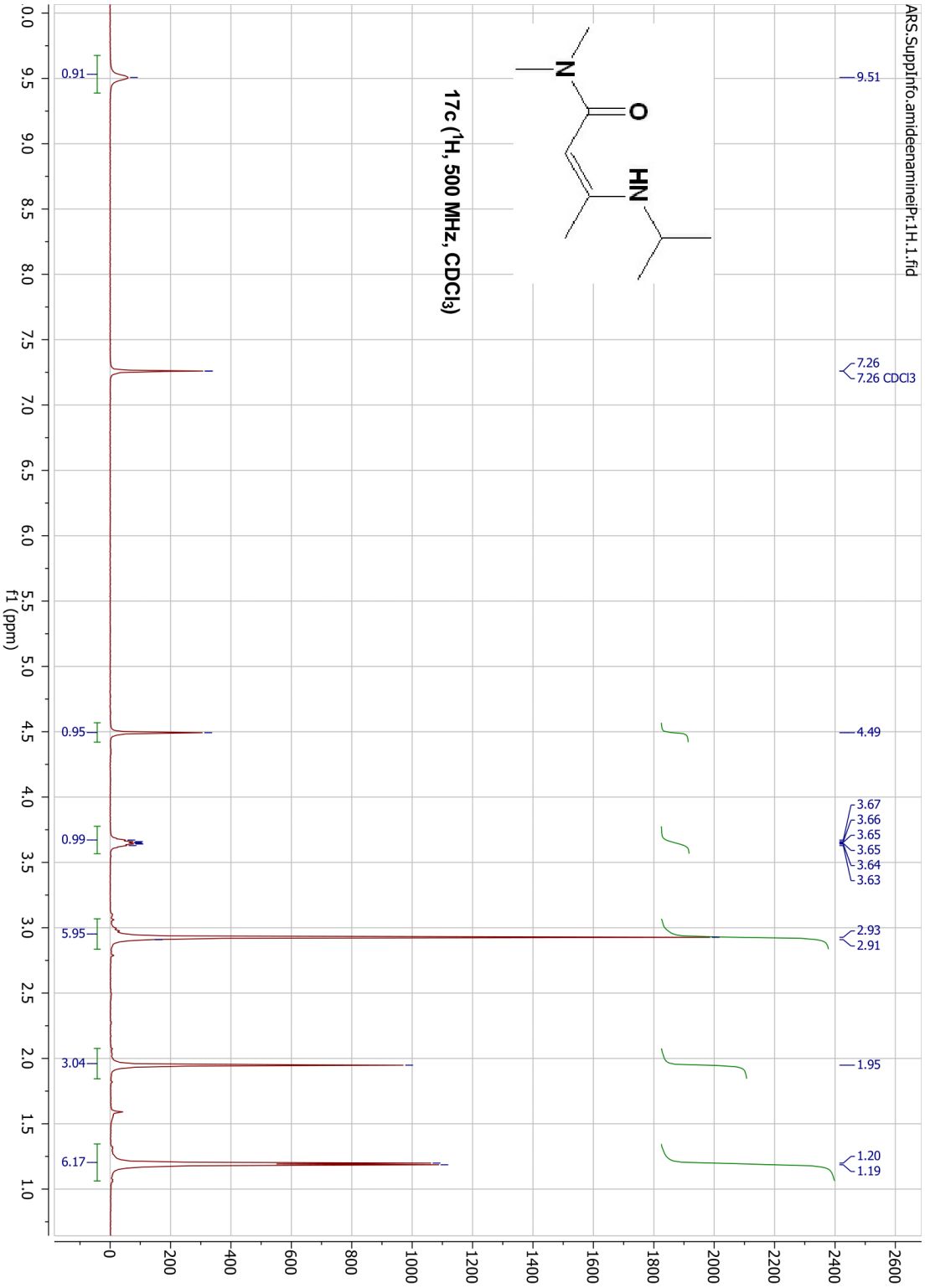

^{1}H NMR (300 MHz, C_6D_6) Compound (SI-2)
H_3C
S
O
CH_3
CH_3
CH_3
8.14
8.11
7.22
7.19
7.16
3.00
2.98
2.95
2.93
1.19
1.17
1.14
1.13
2.00
2.28
2.15
4.85
8.62
f1 (ppm)

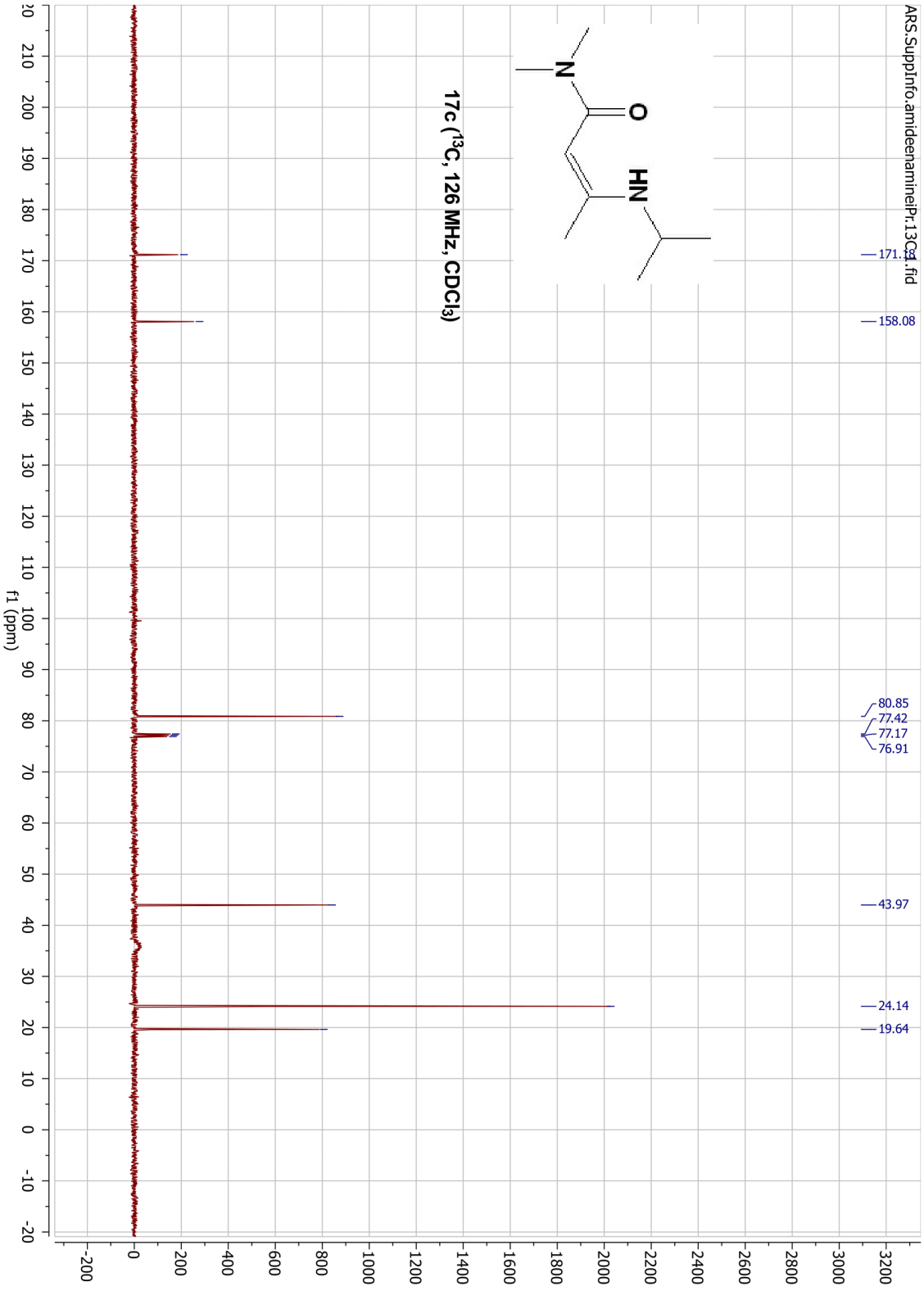

^{1}H NMR (500 MHz, CDCl$_3$) Compound (15a)
f1 (ppm)
1.89
1.95
1.48
1.03
0.93
1.04
0.97
1.08
5.29
1.05
8.65
2.01
2.88
2.84
7.90
7.88
7.46
7.44
7.26
3.49
3.48
3.46
3.45
3.35
3.34
3.32
2.72
2.70
2.69
2.67
2.58
2.56
2.37
2.35
2.21
1.75
1.74
1.73
1.71
1.58 HDO
1.34
1.26
1.24
1.23
1.21
1.10
1.03
0.89
0.88
0.87
0.07

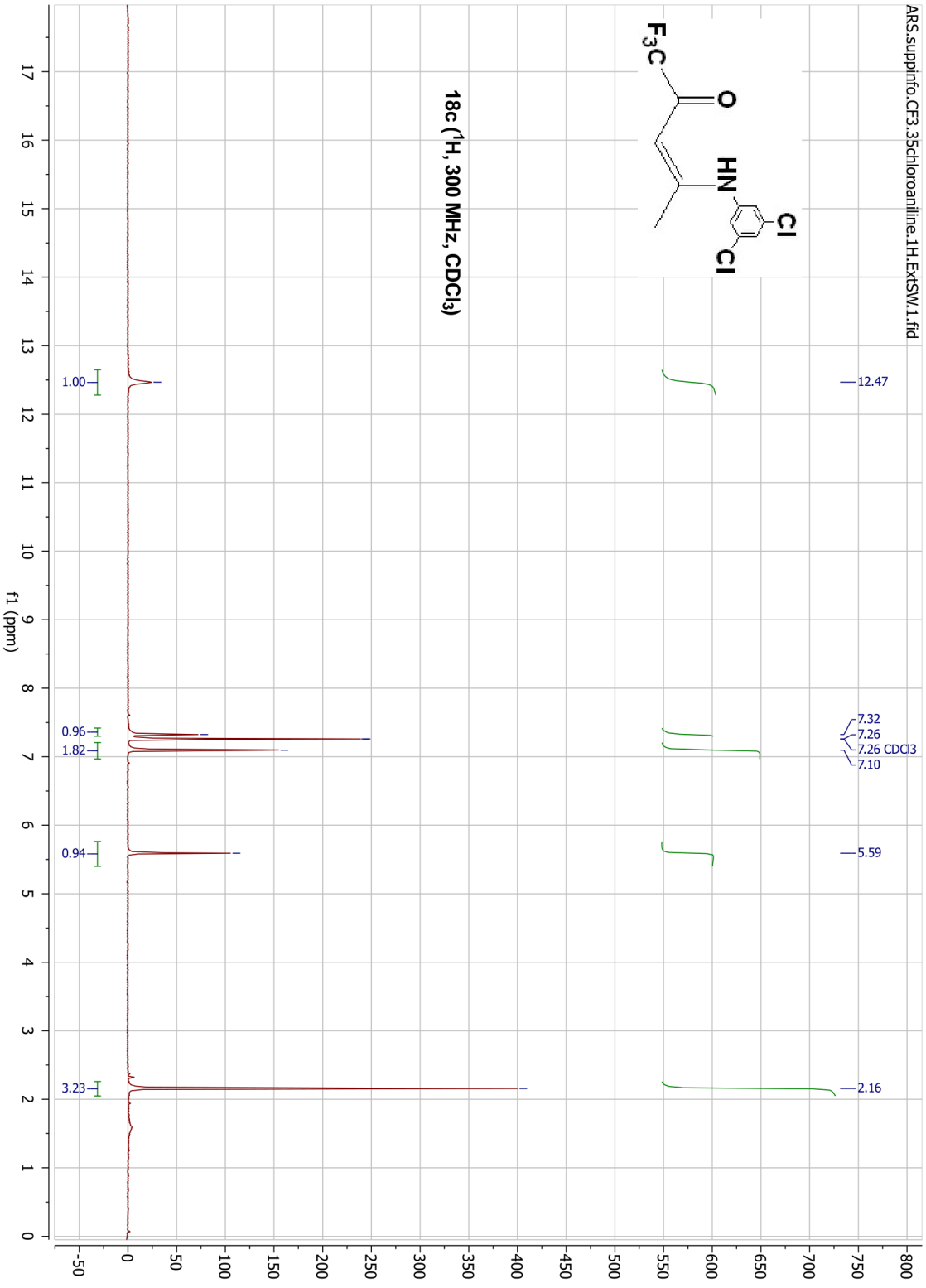

13C NMR (126 MHz, CDCl3) Compound (15a)
200.11
156.05
135.63
128.10
125.37
77.41 CDCl3
77.16 CDCl3
76.91 CDCl3
58.09
53.20
44.47
44.37
39.78
35.18
34.46
31.29
30.94
29.54
f1 (ppm)

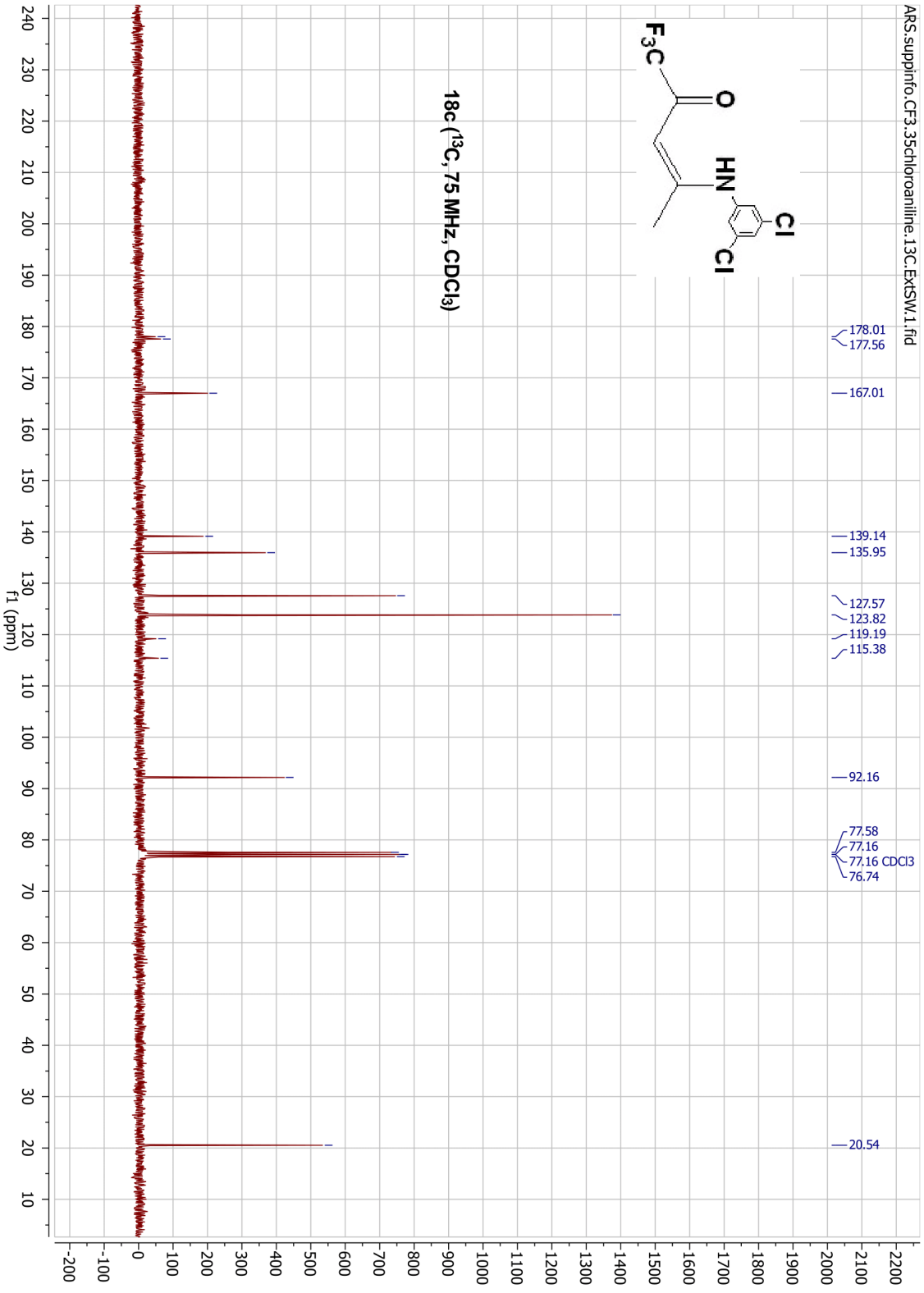

^{1}H NMR (500 MHz, CDCl$_3$) Compound (15b)
7.89
7.87
7.46
7.44
7.26
3.38
3.36
3.01
2.99
2.80
2.78
2.76
2.75
2.34
1.88
1.86
1.80
1.78
1.33
1.25
1.14
1.13
2.00
2.04
1.71
1.02
1.25
5.58
2.20
11.40
3.26
f1 (ppm)

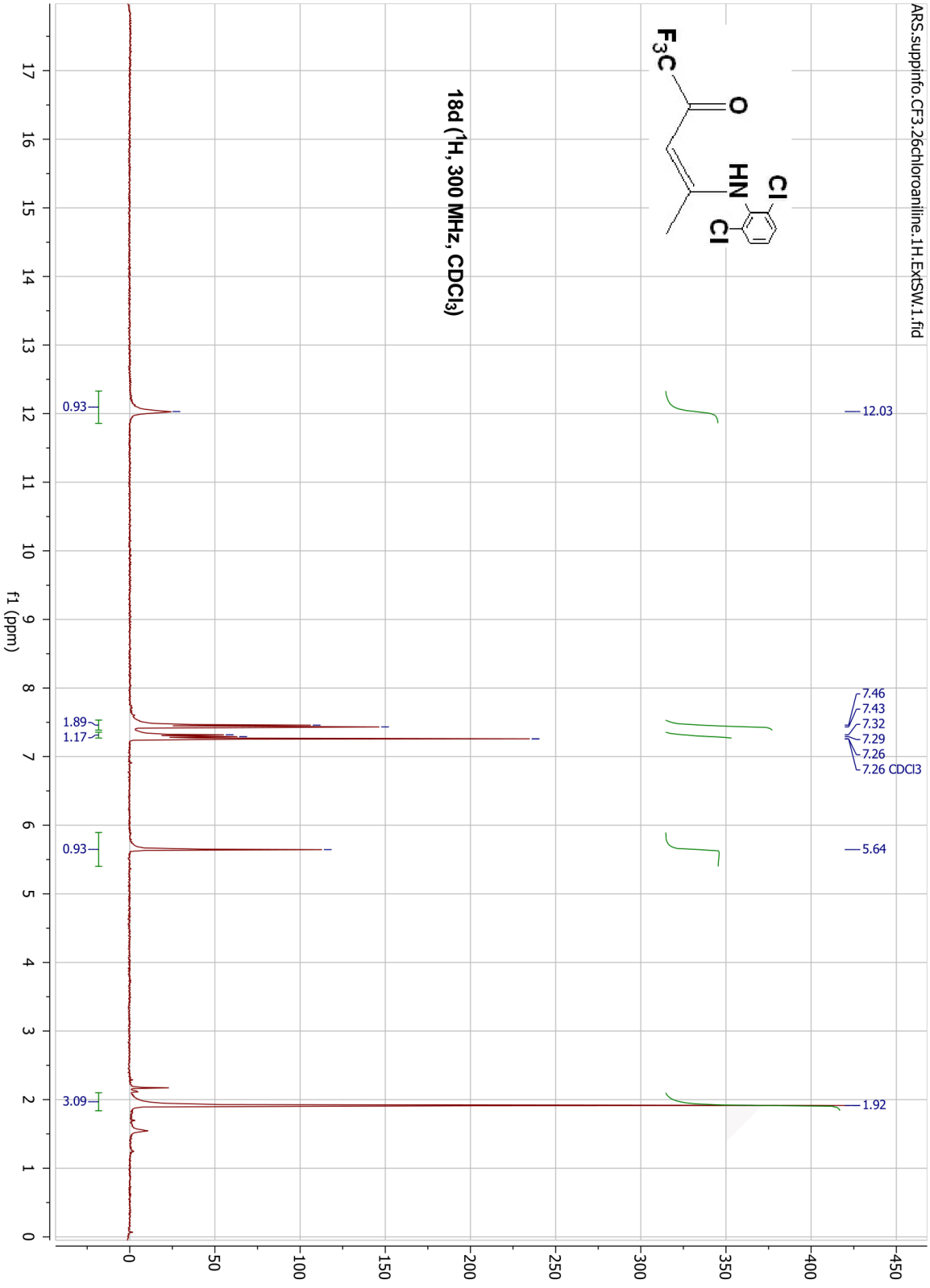

^{13}C NMR (126 MHz, CDCl$_3$) Compound (15b)
199.69
156.07
135.52
128.03
125.41
77.41
77.16
76.91
59.08
52.51
45.10
40.52
35.18
31.28
30.51
27.45
22.20
f1 (ppm)

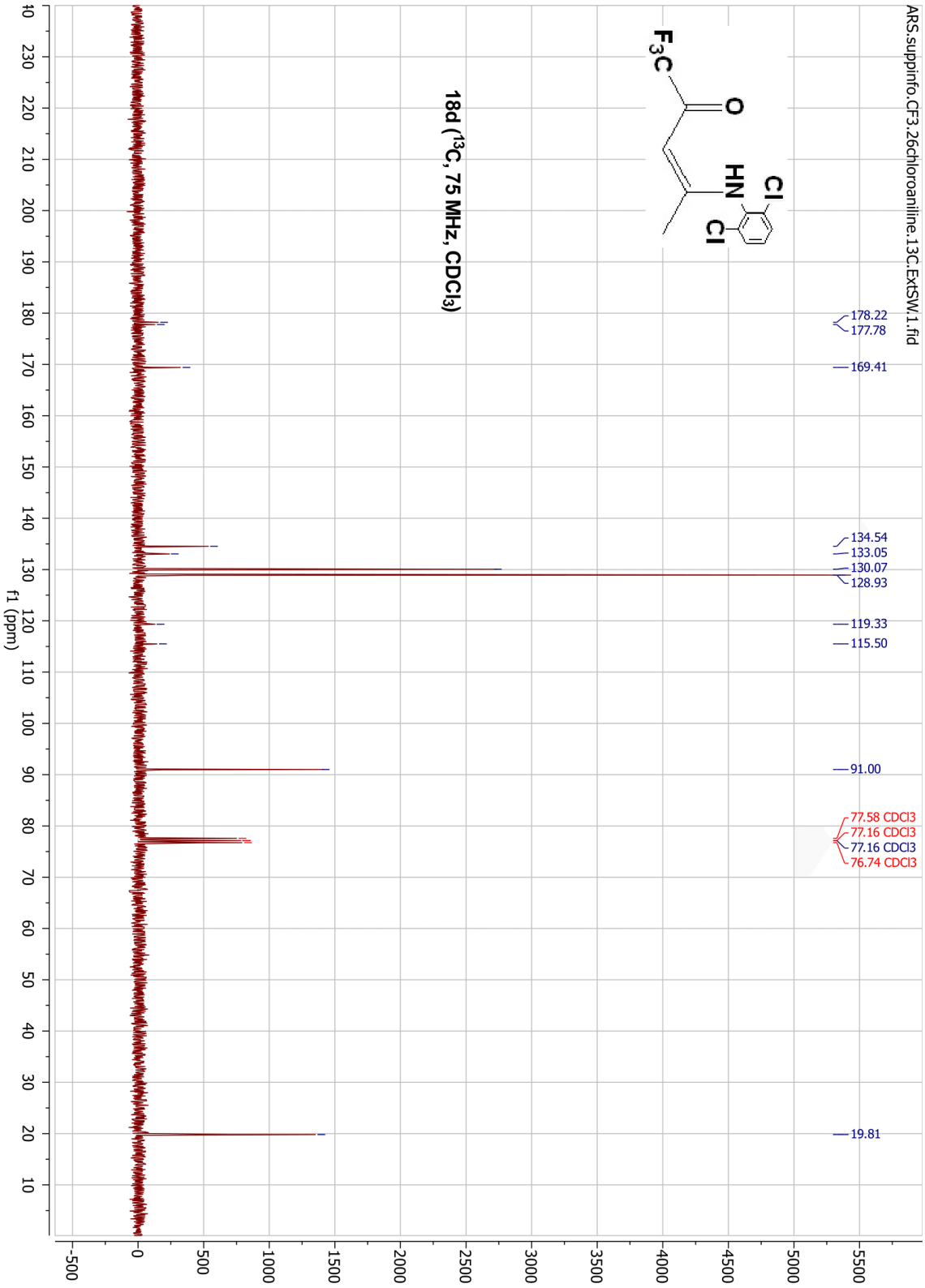

ARS.SuppInfo.amideenaminePr.1H.1.fid
17c (^{1}H, 500 MHz, CDCl$_3$)
f1 (ppm)
0.91
0.95
0.99
5.95
3.04
6.17
9.51
7.26
7.26 CDCl3
4.49
3.67
3.66
3.65
3.65
3.64
3.63
2.93
2.91
1.95
1.20
1.19

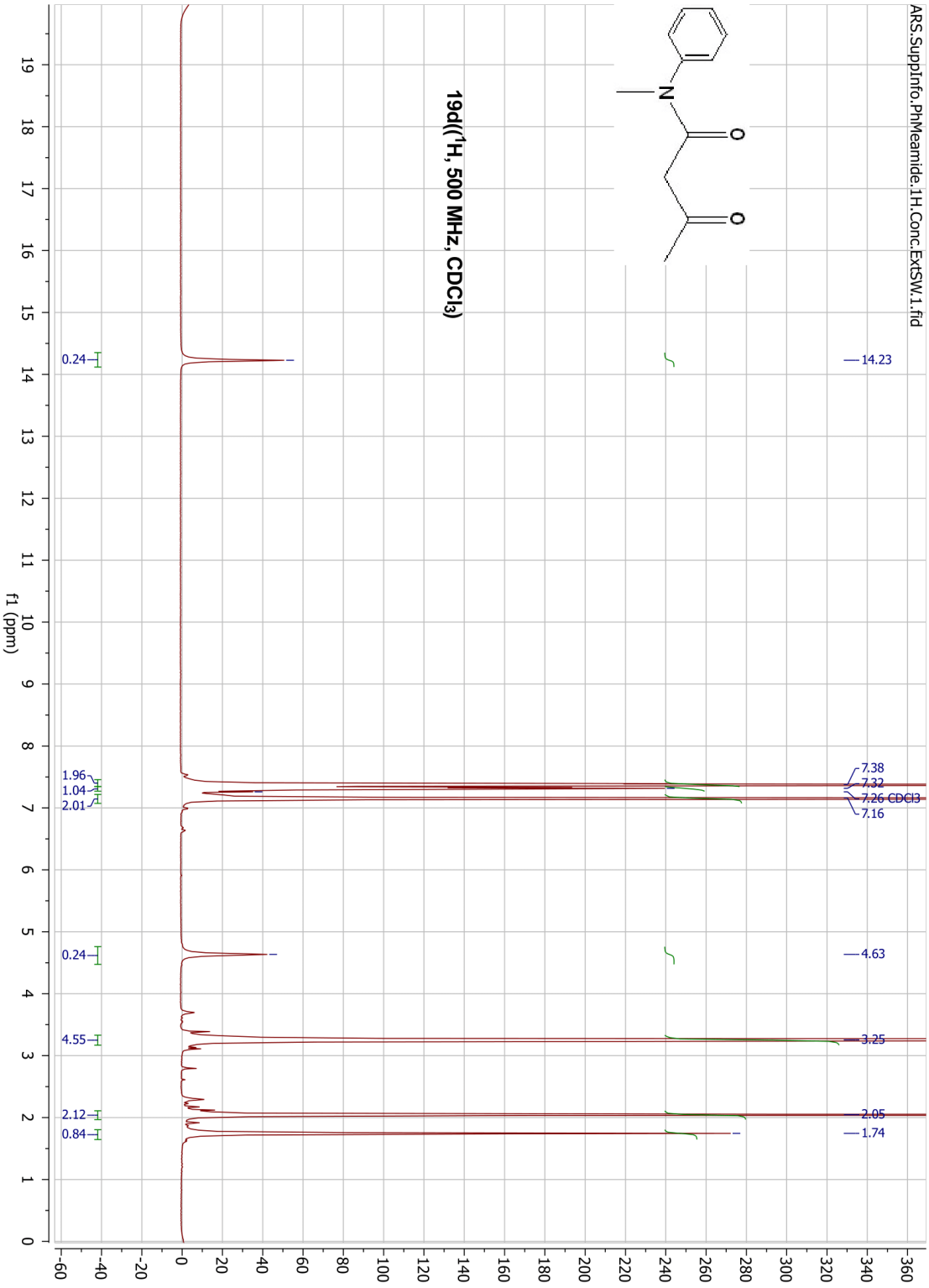

ARS.SuppInfo.amideenamineiPr.13C.1.fid
17c (^{13}C, 126 MHz, CDCl$_3$)
O
HN
171.23
158.08
80.85
77.42
77.17
76.91
43.97
24.14
19.64
f1 (ppm)

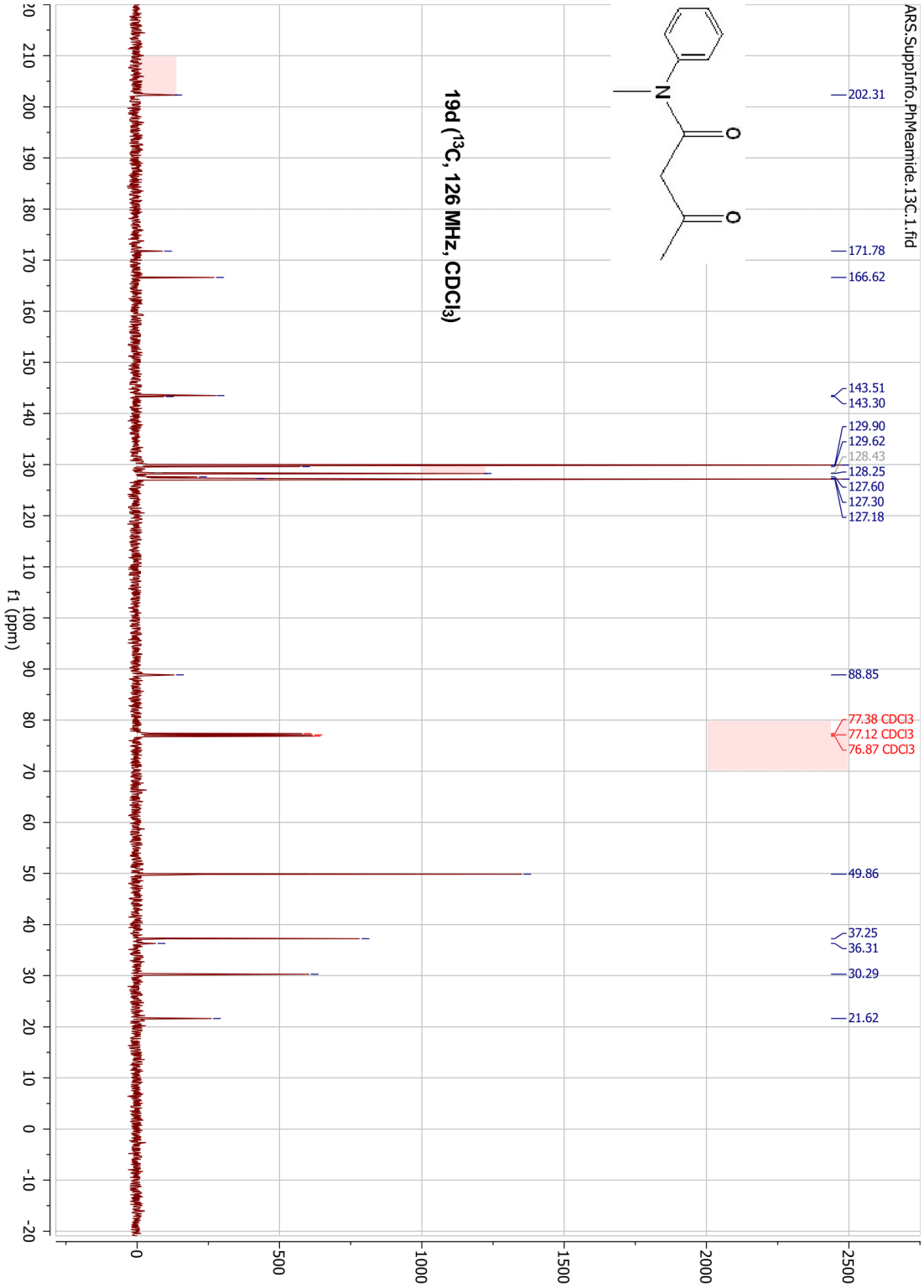

ARS.suppinfo.CF3.35chloroaniline.1H.ExtSW.1.fid
18c (^{1}H, 300 MHz, CDCl$_3$)
F3C
O
HN
Cl
Cl
1.00
0.96
1.82
0.94
3.23
12.47
7.32
7.26
7.26 CDCl3
7.10
5.59
2.16
f1 (ppm)

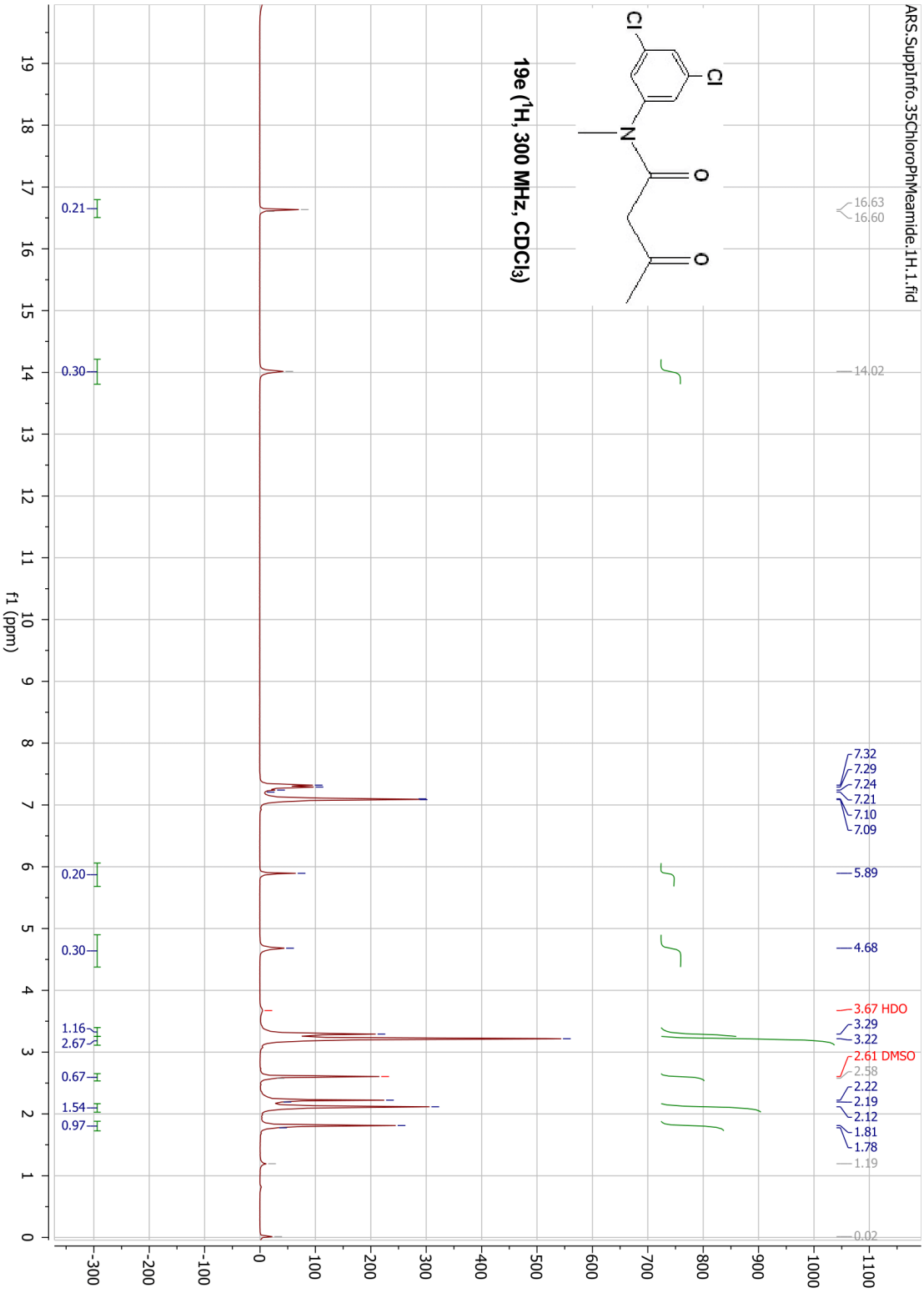

ARS.suppinfo.CF3.35chloroaniline.13C.ExtSW.1.fid
18c (^{13}C, 75 MHz, CDCl$_3$)
F3C
O
HN
Cl
Cl
178.01
177.56
167.01
139.14
135.95
127.57
123.82
119.19
115.38
92.16
77.58
77.16
77.16 CDCl3
76.74
20.54
f1 (ppm)

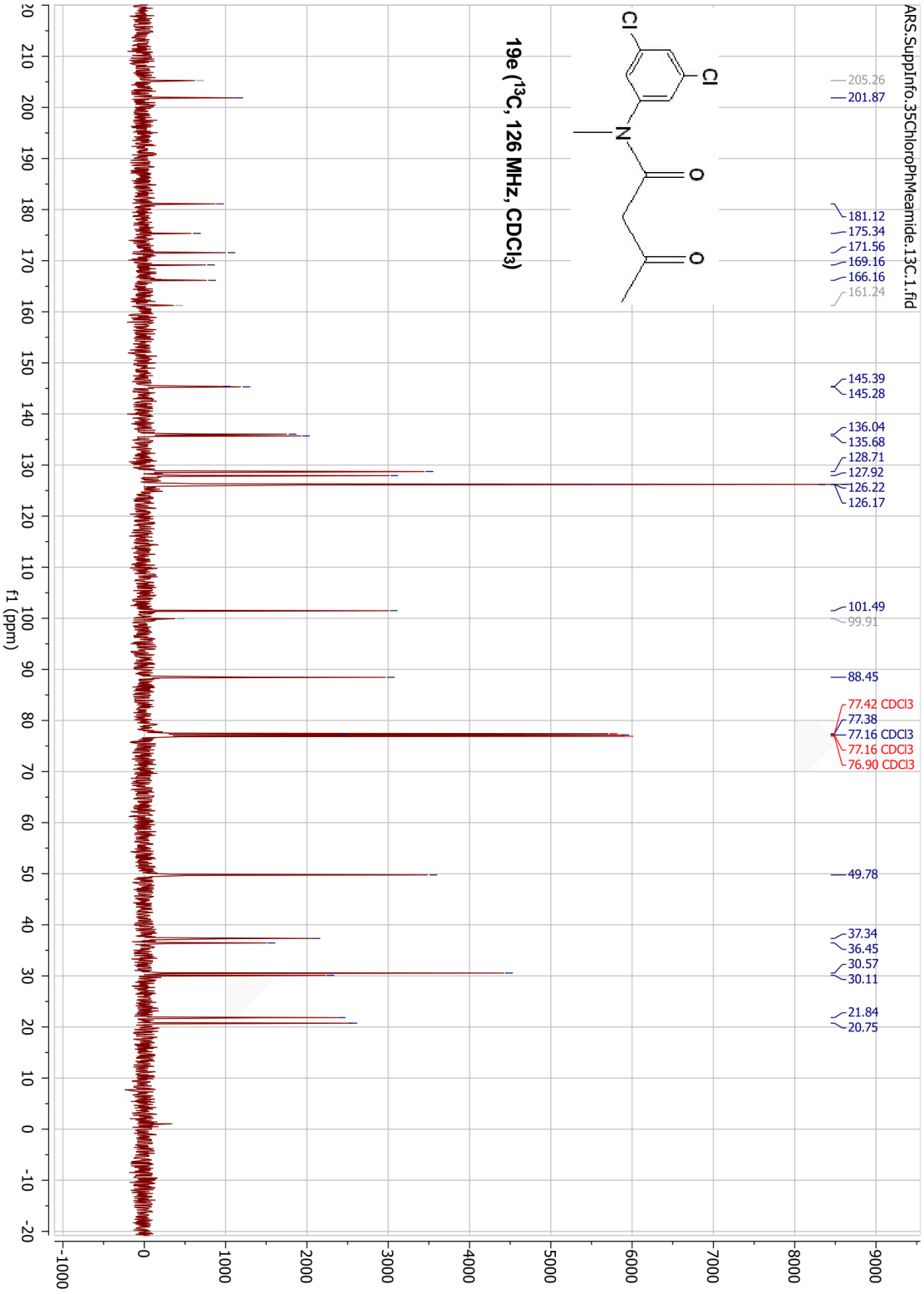

ARS.suppinfo.CF3.26chloroaniline.1H.ExtSW.1.fid
18d (^{1}H, 300 MHz, $CDCl_3$)
F_3C
O
HN
Cl
Cl
f1 (ppm)
0.93
1.89
1.17
0.93
3.09
12.03
7.46
7.43
7.32
7.29
7.26
7.26 CDCl3
5.64
1.92

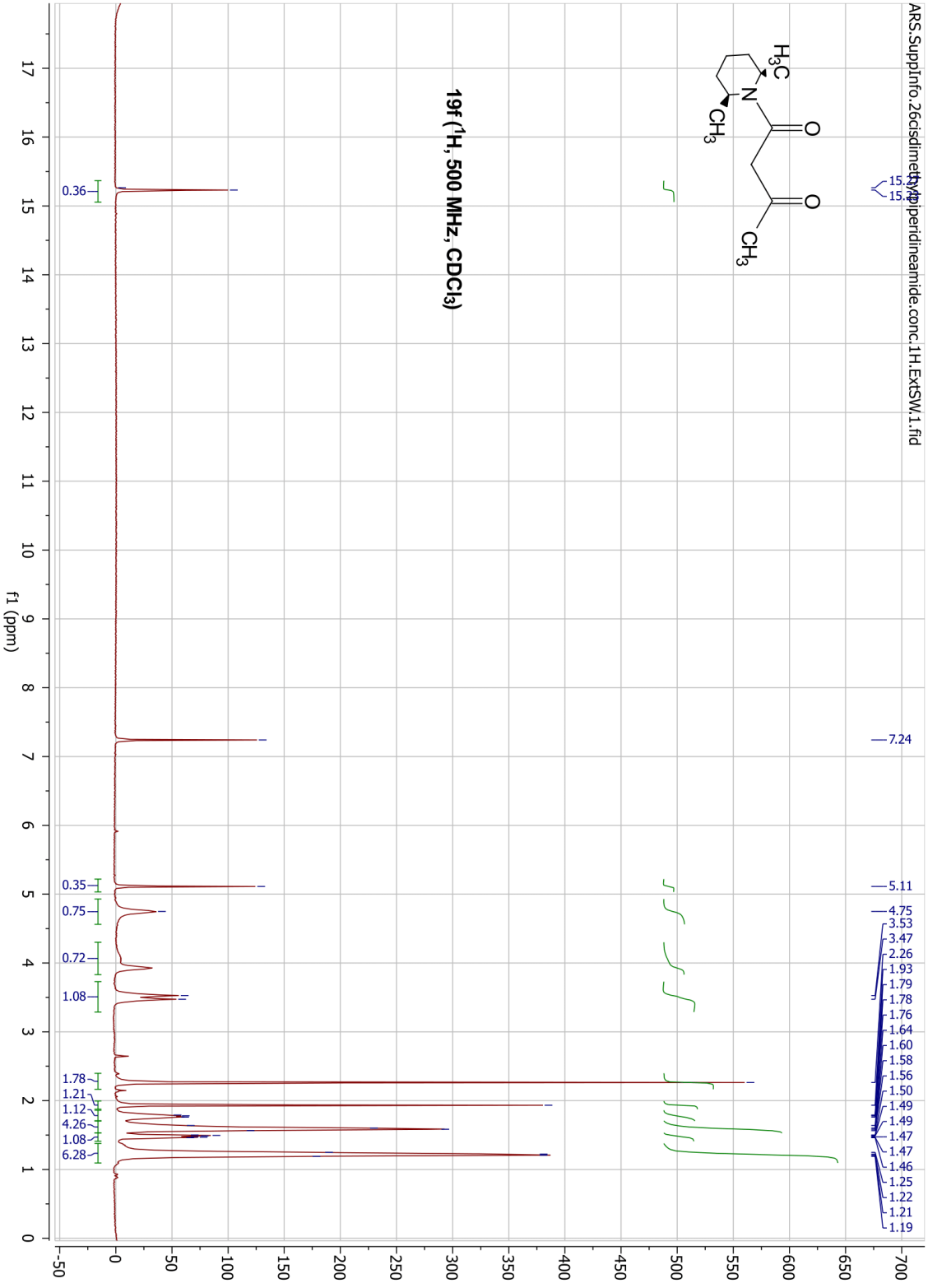

ARS.suppinfo.CF3.26chloroaniline.13C.ExtSW.1.fid
18d (^{13}C, 75 MHz, CDCl$_3$)
F3C
O
HN
Cl
Cl
178.22
177.78
169.41
134.54
133.05
130.07
128.93
119.33
115.50
91.00
77.58 CDCl3
77.16 CDCl3
77.16 CDCl3
76.74 CDCl3
19.81
f1 (ppm)

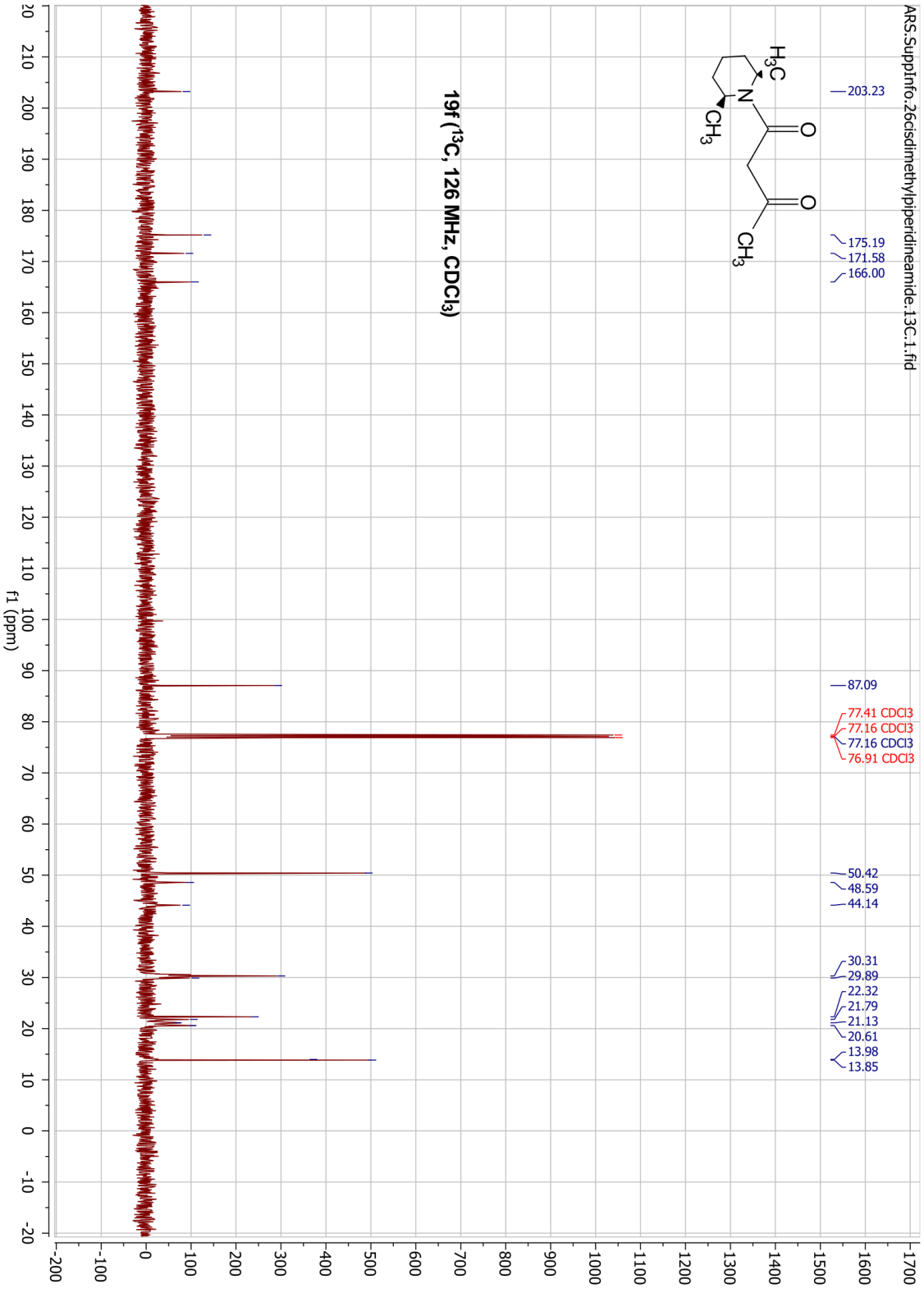

ARS.SuppInfo.PhMeamide.1H.Conc.ExtSW.1.fid
19d((1H, 500 MHz, CDCl3)
f1 (ppm)
0.24
1.96
1.04
2.01
0.24
4.55
2.12
0.84
14.23
7.38
7.32
7.26 CDCl3
7.16
4.63
3.25
2.05
1.74

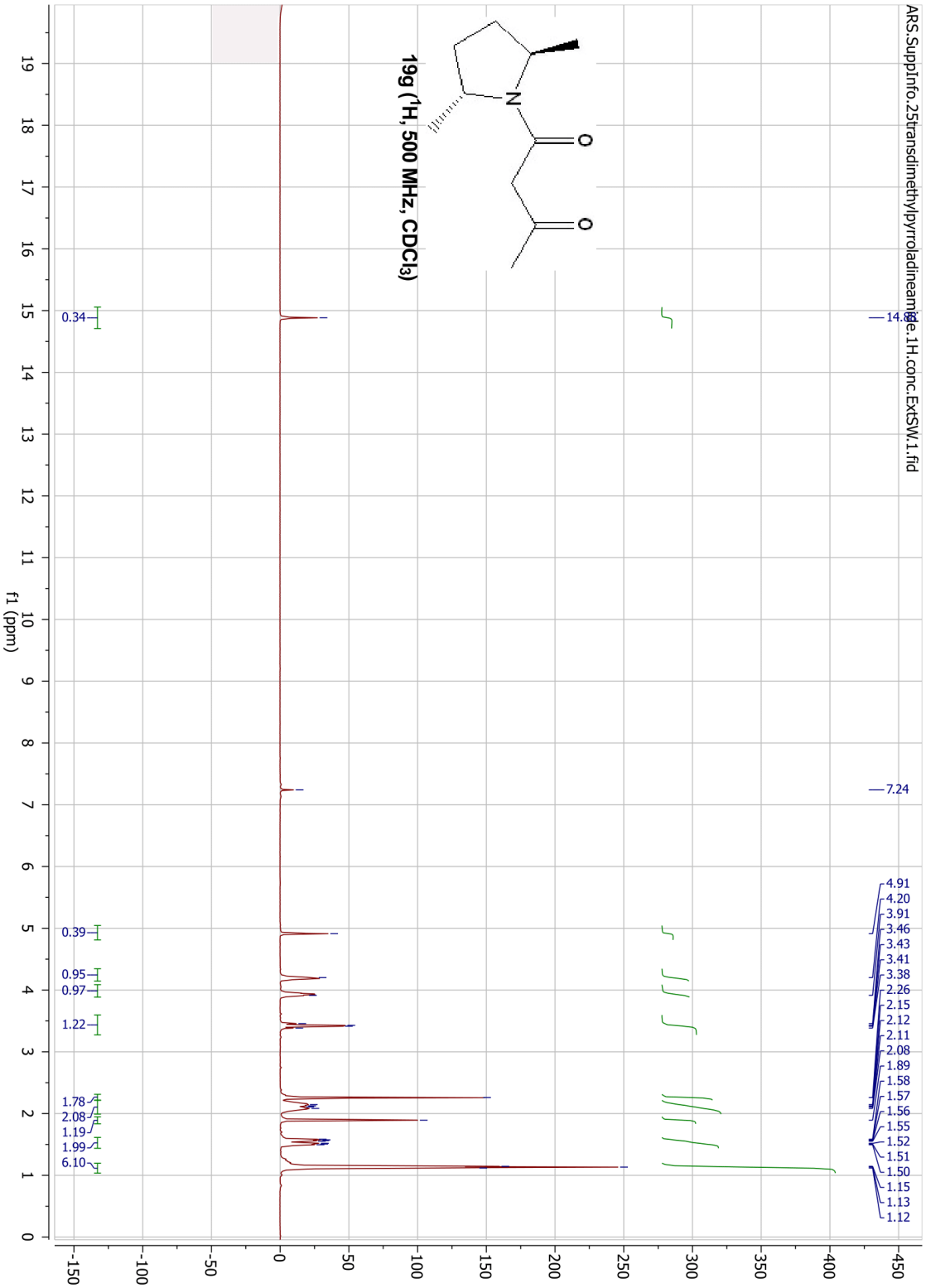

19d (^{13}C, 126 MHz, CDCl$_3$)
ARS.SuppInfo.PhMeamide.13C.1.fid
202.31
171.78
166.62
143.51
143.30
129.90
129.62
128.43
128.25
127.60
127.30
127.18
88.85
77.38 CDCl3
77.12 CDCl3
76.87 CDCl3
49.86
37.25
36.31
30.29
21.62
f1 (ppm)

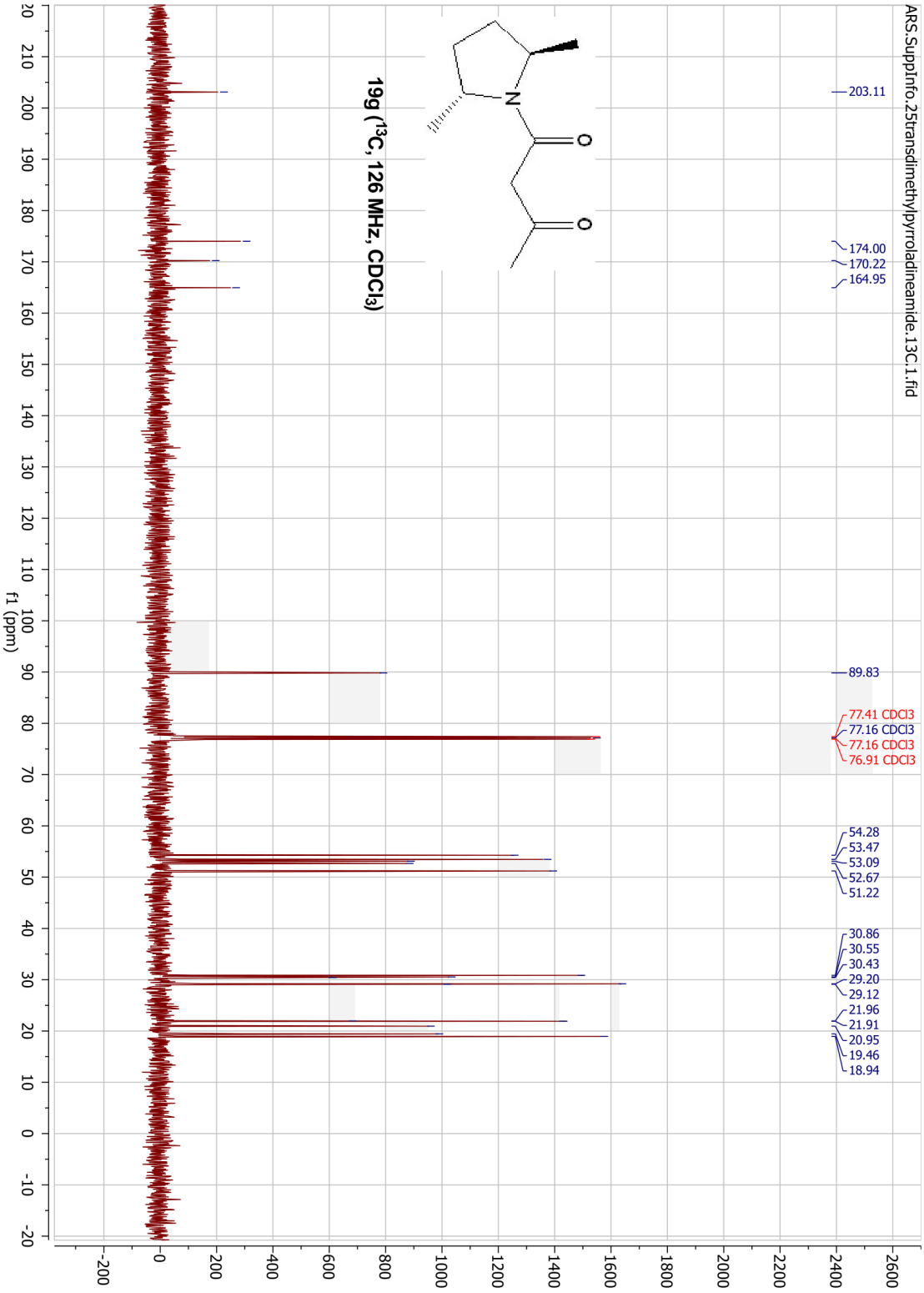

19e (^{1}H, 300 MHz, CDCl$_3$)
ARS.SuppInfo.35ChloroPhMeamide.1H.1.fid
f1 (ppm)
0.21
0.30
0.20
0.30
1.16
2.67
0.67
1.54
0.97
16.63
16.60
14.02
7.32
7.29
7.24
7.21
7.10
7.09
5.89
4.68
3.67 HDO
3.29
3.22
2.61 DMSO
2.58
2.22
2.19
2.12
1.81
1.78
1.19
0.02


19e (^{13}C, 126 MHz, CDCl$_3$)
ARS.SuppInfo.35ChloroPhMeamide.13C.1.fid
205.26
201.87
181.12
175.34
171.56
169.16
166.16
161.24
145.39
145.28
136.04
135.68
128.71
127.92
126.22
126.17
101.49
99.91
88.45
77.42 CDCl3
77.38
77.16 CDCl3
77.16 CDCl3
76.90 CDCl3
49.78
37.34
36.45
30.57
30.11
21.84
20.75
f1 (ppm)


19f (1H, 500 MHz, CDCl3)
ARS.SuppInfo.26cisdimethylpiperidineamide.conc.1H.ExtSW.1.fid
f1 (ppm)
0.36
0.35
0.75
0.72
1.08
1.78
1.21
1.12
4.26
1.08
6.28
7.24
5.11
4.75
3.53
3.47
2.26
1.93
1.79
1.78
1.76
1.64
1.60
1.58
1.56
1.50
1.49
1.49
1.47
1.47
1.46
1.25
1.22
1.21
1.19


ARS.SuppInfo.26cisdimethylpiperidineamide.13C.1.fid
19f (^{13}C, 126 MHz, CDCl$_3$)
203.23
175.19
171.58
166.00
87.09
77.41 CDCl3
77.16 CDCl3
77.16 CDCl3
76.91 CDCl3
50.42
48.59
44.14
30.31
29.89
22.32
21.79
21.13
20.61
13.98
13.85
f1 (ppm)


19g (^{1}H, 500 MHz, CDCl$_3$)
ARS.SuppInfo.25transdimethylpyrroladineamide.1H.conc.ExtSW.1.fid
f1 (ppm)
0.34
0.39
0.95
0.97
1.22
1.78
2.08
1.19
1.99
6.10
14.88
7.24
4.91
4.20
3.91
3.46
3.43
3.41
3.38
2.26
2.15
2.12
2.11
2.08
1.89
1.58
1.57
1.56
1.55
1.52
1.51
1.50
1.15
1.13
1.12


19g (^{13}C, 126 MHz, CDCl$_3$)
ARS.SuppInfo.25transdimethylpyrroladineamide.13C.1.fid
203.11
174.00
170.22
164.95
89.83
77.41 CDCl3
77.16 CDCl3
77.16 CDCl3
76.91 CDCl3
54.28
53.47
53.09
52.67
51.22
30.86
30.55
30.43
29.20
29.12
21.96
21.91
20.95
19.46
18.94
f1 (ppm)